Universitat Autònoma de Barcelona

HIV-1 Virus-Like Particles engineered to display a high antigen density
Preclinical development of a versatile vaccine platform

Ferran Tarrés i Freixas

HIV-1 Virus-Like Particles engineered to display a high antigen density

Preclinical development of a versatile vaccine platform

Ferran Tarrés i Freixas

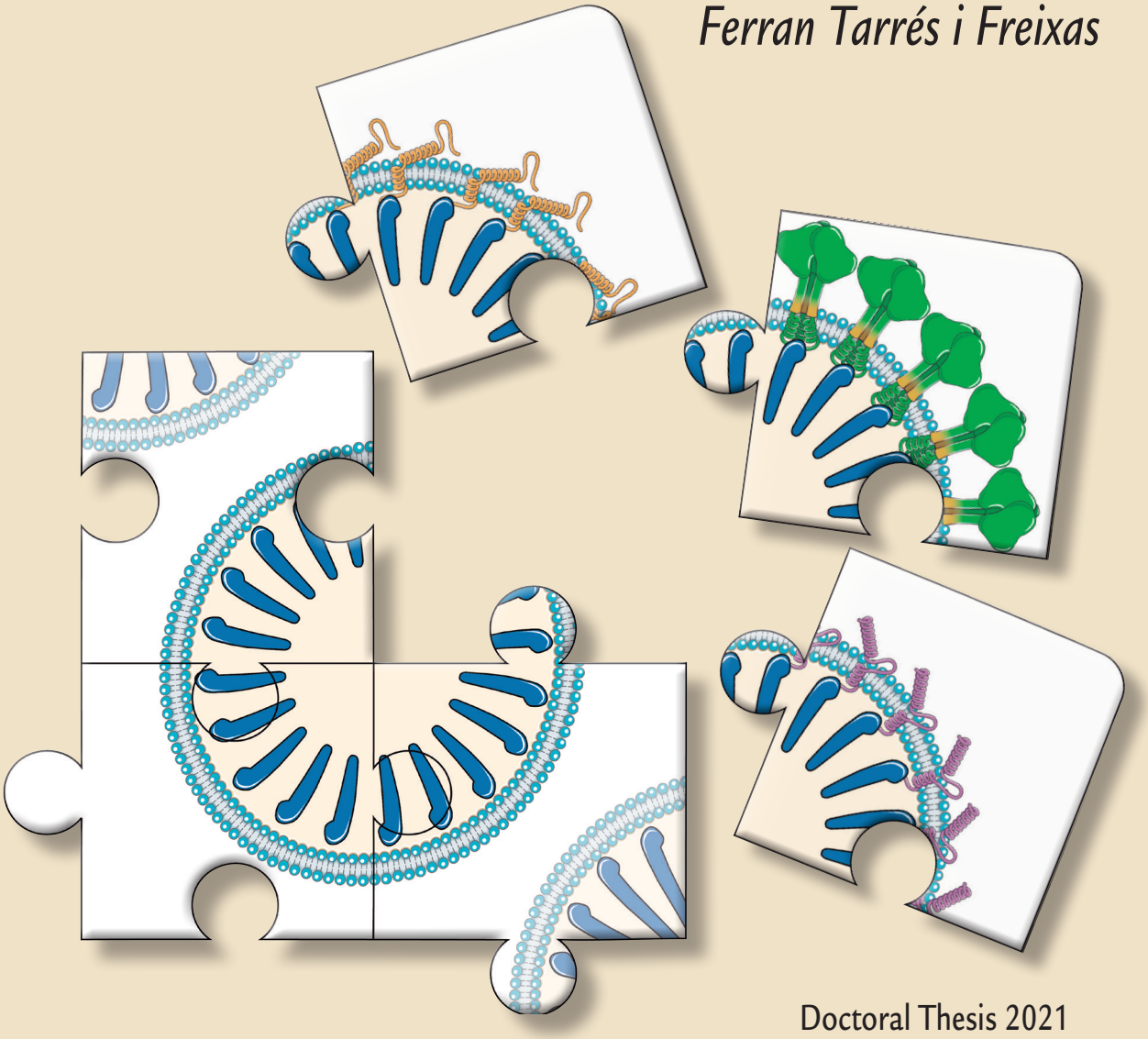

Doctoral Thesis 2021

HIV-1 Virus-Like Particles engineered to display a high antigen density

Preclinical development of a versatile vaccine platform

Ferran Tarrés i Freixas

DOCTORAL THESIS

Badalona, 15th October 2021

Thesis directors:

Jorge Carrillo Molina, PhD

Julià Blanco Arbués, PhD

IrsiCaixa
Institut de Recerca de la Sida

UAB
Universitat Autònoma de Barcelona

PhD programme in Advanced Immunology
Department of Cellular Biology, Physiology and Immunology
Universitat Autònoma de Barcelona

HIV-1 Virus-Like Particles engineered to display a high antigen density

Preclinical development of a versatile vaccine platform

Partícules similivíriques del VIH-1 modificades
per presentar una alta densitat d'antígens
Desenvolupament preclínic d'una plataforma versàtil per a vacunes

Partículas similares a virus del VIH-1 modificadas
para presentar una alta densidad de antígenos
Desarrollo preclínico de una plataforma versátil para vacunas

Thesis presented by Ferran Tarrés i Freixas to qualify for the
PhD degree in Advanced Immunology by the Universitat Autònoma de Barcelona.

The presented work has been performed in the Cell Virology and Immunology (VIC) group, at the IrsiCaixa AIDS Research Institute, and directed by Dr Jorge Carrillo Molina and Dr Julià Blanco Arbués.

Badalona, 15th October 2021

Ferran Tarrés i Freixas
PhD candidate

Jorge Carrillo Molina, PhD
Thesis director

Julià Blanco Arbués, PhD
Thesis director

This work has been funded by the *Ministerio de Economía y Competitividad* of the Spanish Government, co-financed with the European Regional Development funds (FEDER), by the *Instituto de Salud Carlos III* through the projects "Análisis de anticuerpos monoclonales contra la región MPER de la proteína de envuelta del VIH-1. Aplicación del diseño de inmunógenos" (PI14/01307) and "Desarrollo de una plataforma de vacunas contra el VIH basada en partículas similares a virus (VLP) envueltas y de alta densidad antigénica" (PI17/01518). This work has also been sponsored partly by Grífols.

The patent WO/2018/020324, related to the high-density VLPs described in this work, was developed at the IrsiCaixa AIDS Research Institute and has been published by Dr. Julià Blanco Arbués and Dr. Jorge Carrillo Molina (co-directors of this thesis project) and Dr. Luis M. Molinos Albert. Unrelated to this work, Dr. Julià Blanco Arbués and Dr. Jorge Carrillo Molina are founders and shareholders of the spin-off AlbaJuna Therapeutics S.L. Also unrelated to this work, Dr. Julià Blanco Arbués reports institutiontal grants from HIPRA and MSD. The author of this thesis declares no conflicts of interest.

The printing of this thesis was funded in part by the *Departament de Biologia Cel·lular, Fisiologia i Immunologia* of the Universitat Autònoma de Barcelona.

Cover design: *Piecing up the puzzle of high-density enveloped VLPs*, by Ferran Tarrés-Freixas (FT-F) and Vicente R. Bravo (VRB).
Infographics and layout by Vicente R. Bravo and Ferran Tarrés-Freixas.

IrsiCaixa
Institut de Recerca de la Sida

UAB
Universitat Autònoma de Barcelona

El Dr. Julià Blanco Arbués, investigador de la Fundació Institut d'Investigació en Ciències de la Salut Germans Trias i Pujol (IGTP) i professor de la Universitat de Vic-Universitat Central de Catalunya, i el Dr. Jorge Carrillo Molina, investigador de l'Institut de Recerca de la Sida-IrsiCaixa,

certifiquen

que el treball experimental i la redacció de la memòria de la Tesi Doctoral titulada "***HIV-1 Virus-Like Particles engineered to display a high antigen density***" han estat realitzats per en Ferran Tarrés i Freixas sota la seva direcció, i que

consideren

que és apte per a ser presentat i optar al grau de Doctor en Immunologia Avançada per la Universitat Autònoma de Barcelona.

I per a que quedi constància, signen aquest document a Badalona,
el 6 de setembre de 2021.

Dr. Julià Blanco Arbués

Dr. Jorge Carrillo Molina

A tota la meva família.
I en especial a tu, Silvia.

Vaccines are a revolutionary technology.
They save millions of lives.

Bill Gates

Table of Contents

Abbreviations

× g	Relative Centrifugal Force
aa	Amino acid
ADCC	Antibody-Dependent Cell Cytotoxicity
ADCF	Animal-Derived Component Free
ADCP	Antibody-Dependent Cell Phagocytosis
AEX	Anion Exchange Chromatography
AIDS	Acquired Immunodeficiency Syndrome
AMP	Antibody-Mediated Protection
AP	Alkaline Phosphatase
APC	Antigen-Presenting Cell
ART	Antiretroviral Therapy
BCA	Bicinchoninic Acid
BCR	B Cell Receptor
bNAb	Broadly Neutralising Antibody
BSA	Bovine Serum Albumin
CD4bs	CD4 Binding Site
CDC	Complement-Dependent Cytotoxicity
ChAdV	Chimpanzee Adenovirus
CO_2	Carbon Dioxide
ConA	Concanavalin A
COVID-19	Coronavirus Disease 2019
CRF	Circulating Recombinant Form
Cryo-TEM	Cryogenic Transmission Electron Microscopy
CTL	Cytolytic T Lymphocyte
D10	DMEM with 10% FBS
DC	Dendritic Cell
DDVV	2 DNA doses followed by 2 VLP doses (heterologous regimen)
dH_2O	Distilled Water
DMEM	Dulbecco's Modified Eagle Medium
DMSO	Dimethyl Sulfoxide
DNA	Deoxyribonucleic Acid

DRC	Democratic Republic of Congo
dsDNA	Double-Stranded DNA
dsRNA	Double-Stranded RNA
DZ	Dark Zone
EDTA	Ethylenediaminetetraacetic Acid
ELISA	Enzyme-Linked Immunosorbent Assay
ELISpot	Enzyme-Linked Immune Absorbent Spot
Env	Envelope Glycoprotein
eOD	Engineered Outer Domain
EV	Extracellular Vesicle
FBS	Foetal Bovine Serum
Fc	Crystallisable Fragment
FcγRIII	Fc γ receptor III
FDA	Food and Drug Administration
FDC	Follicular Dendritic Cell
FP	Fusion Peptide
Gag	Group-Specific Antigen
GC	Germinal Centre
GGGS	Glycine-Glycine-Glycine-Serine
Gp120/SU	Envelope Glycoprotein Gp120/Surface
Gp41/TM	Envelope Glycoprotein Gp41/Transmembrane
H_2O	Water
H_2SO_4	Sulfuric Acid
HEK293	Human Embryonic Kidney 293
HIV-1	Human Immunodeficiency Virus-1
HIV-2	Human Immunodeficiency Virus-2
HLA-I	Human Leukocyte Antigen class I
HLA-II	Human Leukocyte Antigen class II
HR1	Heptad Repeat 1
HR2	Heptad Repeat 2
HRP	Horseradish Peroxidase
HSC	Haematopoietic Stem Cell
IFN	Interferon
Ig/IgA/IgD/IgE/IgG/IgM	Immunoglobulin (A, D, E, G, M)
IMAC	Ion-Metal Affinity Chromatography
IN	Integrase
INSTI	Integrase Strand Transfer Inhibitors
IPTG	Isopropyl β-d-1-thiogalactopyranoside
ISH	Intrastructural Help
IU	International Unit

LB	Lysogeny Broth
LCC	Ligand-Activated Core Chromatography
LPS	Lipopolysaccharide
LRA	Latency Reversing Agent
LTR	Long Terminal Repeats
LZ	Light Zone
mAb	Monoclonal Antibody
mFcγRIV	Murine Fc γ receptor IV
$MgCl_2$	Magnesium Chloride
MHC-I	Major Histocompatibility Complex class I
MHC-II	Major Histocompatibility Complex class II
MPER	Membrane-Proximal External Region
MPLA	Monophosphorylate A
MRCA	Most Recent Common Ancestor
mRNA	messenger RNA
MSM	Men Who Have Sex with Men
MVA	Modified Vaccinia Ankara
MW	Molecular Weight
MWCO	Molecular Weight Cut-Off
NAb	Neutralising Antibody
NaCl	Sodium Chloride
NaH_2PO_4	Monosodium Phosphate
NFL	Native Flexibly Linked
NHP	Non-Human Primates
NK	Natural Killer
NNRTI	Non-Nucleoside Reverse Transcriptase Inhibitors
NOD	Non-Obese Diabetic
NRTI	Nucleoside Reverse Transcriptase Inhibitors
o/n	Overnight
OD	Optical Density
OLP	Overlapping Min Peptides
OPD	o-Phenylenediamine Dihydrochloride
ORF	Open Reading Frame
p17/MA	Matrix
p2/SP1 and p1/SP2	Spacer peptides 1 and 2
p24/CA	Capsid
p7/NC	Nucleocapsid
PBS	Phosphate Buffered Saline
PEP	Post-Exposure Prophylaxis
PI	Protease Inhibitors

PLWH	People Living with HIV
Pol	Polymerase
PR	Protease
PrEP	Pre-Exposure Prophylaxis
PRR	Pattern Recognition Receptor
R10	RPMI with 10% FBS
RNA	Ribonucleic Acid
RoA	Route of Administration
rpm	Revolutions per Minute
RPMI	Roswell Park Memorial Institute 1640 medium
RSC3	Resurfaced Stabilised Core 3
RT	Reverse Transcriptase
RTemp	Room Temperature
SARS-CoV	Severe Acute Respiratory Syndrome Coronavirus
SDS	Sodium Dodecyl Sulphate
SEC	Size Exclusion Chromatography
SF	Serum-Free
SFC	Spot-Forming Cells
SHIV	Chimaeric Simian-Human Immunodeficiency Virus
SHM	Somatic Hypermutation
SIV	Simian Immunodeficiency Virus
SIV_{cpz}	Chimpanzee's SIV
SIV_{gor}	Gorilla's SIV
SIV_{rcm}	Red-Capped Monkey's SIV
SIV_{smm}	Sooty Mangabey's SIV
SOSIP	Soluble stabilised gp40 I559P
SPF	Specific-Pathogen Free
ssRNA	Single-Stranded RNA
Tc	T cytotoxic
TCID50	50% Tissue Culture Infective Dose
TCR	T Cell Receptor
TFF	Tangential Flow Filtration
Tfh	T Follicular Helper
Th	T helper
TLR	Toll-like Receptor
TMB	3,3',5,5'-Tetramethylbenzidine
UC	Ultracentrifugation
UFO	Uncleaved Pre-fusion Optimised
VLP	Virus-Like Particle
VVVV	4 VLP doses (homologous regimen)
WB	Western Blot

Summary

Vaccines are one of the most successful achievements in the history of medicine. However, for some infectious agents, there still is a lack of an effective protective vaccine. Such is the case of the Human Immunodeficiency Virus (HIV-1), which is the causative agent of the acquired immunodeficiency syndrome (AIDS). HIV-1 has eluded nearly 40 years of vaccine research owing to its enhanced immune evasion mechanisms and the poor incorporation of the envelope glycoprotein (Env) at the viral surface, which is the main target for neutralising antibodies. HIV-1 vaccine candidates are based on nucleic acid strategies, subunit proteins or multivalent platforms that try to elicit potent and balanced humoral and cellular adaptive immune responses. The presentation of antigens within a multivalent platform induces a superior immune response compared to subunit proteins, and the combination of different vaccine strategies has been demonstrated to elicit more robust responses. One of these promising multivalent vaccine platforms are virus-like particles (VLPs), which mimic the structure of the virus. VLPs are non-infectious, non-replicative and highly immunogenic platforms that can be safely used as vaccines. HIV-1 based VLPs are produced by the cellular expression of the HIV-1 structural protein Gag, leading to the budding of lipid-enveloped VLPs that are structurally similar to HIV-1. The antigens can be easily expressed on the lipid membrane of the VLPs, but with poorly efficient incorporation. To bypass this limitation, our group designed a novel VLP-based platform yielding a high density of antigens at the VLP surface. This novel strategy consisted in fusing a small Env-derived immunogen (Min), which had a transmembrane domain, to Gag. This process resulted in high-density antigen-expressing MinGag-VLPs.

The hypothesis of this work was that the expression of a high density of antigens at the surface of VLPs would induce a robust immune response that could be beneficial for an HIV-1 vaccine candidate. To test that, we developed efficient production and purification protocols for our fusion-protein MinGag-VLPs. Additionally, antigen exposition on MinGag-VLPs was improved by the introduction of mutations at the transmembrane domain, resulting in an opti-

mised Min(RA)Gag-VLP candidate. Furthermore, the fusion-protein VLP vaccine platform could easily be formulated into nucleic acid-based vaccine strategies that were successfully delivered by *in vivo* DNA electroporation, favouring the development of combination heterologous DNA/VLP strategies that could lead to more potent responses. *In vivo* immunogenicity studies in mice demonstrated the superiority of heterologous DNA/VLP vaccination compared to homologous VLP regimens in most of the immune parameters assessed. Immune profiling of immunised mice showed how antibody titres in plasma were approximately 10-times higher with the heterologous regimen. Fusion-protein VLPs induced modest cellular responses and non-neutralising antibodies against HIV-1 pseudoviruses. However, these mouse anti-Min antibodies mainly displayed an IgG2c profile that could mediate antibody-dependent effector functions. This finding was relevant since these types of responses have been associated with modest correlates of protection against HIV-1 in human clinical trials. The absence of a relevant mouse model to study vaccine-mediated protection by vaccination led us to develop a mouse model where a Min-expressing tumour cell line acted as a surrogate of HIV-1 infected cells. Vaccination with Min(RA)Gag-VLPs efficiently impaired the progression of the Min-expressing tumour, hence demonstrating that fusion-protein-VLPs induced a full-fledged protective immune response. Finally, fusion-protein VLPs confirmed their versatility as a platform since they could present a wide diversity of immunogens on their surface, including a full HIV-1 Env trimer with preserved antigenicity.

Overall, our novel VLP platform demonstrated its potential and that merits further studies as potential HIV-1 vaccine candidates.

Resum

Les vacunes són un dels avenços científics més rellevants de la història de la medicina. Tot i així, encara no disposem de vacunes protectores per alguns agents infecciosos, com ara el Virus de la Immunodeficiència Humana (VIH-1), que és l'agent causant de la síndrome de la immunodeficiència adquirida (SIDA). El VIH-1 s'ha resistit al desenvolupament d'una vacuna protectora, degut a una alta capacitat d'evadir la resposta immunitària i també a la incorporació d'una baixa densitat de glicoproteïnes de l'envolta (Env) a la seva superfície, que és la principal diana de les respostes neutralitzants. Els candidats de vacuna pel VIH-1 consisteixen en estratègies basades en vacunes d'àcids nucleic, proteïnes recombinats o plataformes multivalents que intenten induir respostes immunitàries potents equilibrant la resposta humoral i cel·lular. La incorporació d'antígens en plataformes multivalents permet induir respostes més potents que les proteïnes recombinants per si soles. A més, la combinació de diferents estratègies de vacunes també indueixen respostes més robustes. Una d'aquestes plataformes multivalents prometedores són les partícules similivíriques (VLPs, per les sigles en anglès *Virus-like particles*), que mimetitzen l'estructura del virus. Les VLPs són partícules no infeccioses i altament immunogèniques que no poden replicar-se, per això són prototips de vacunes segurs. Les VLPs es produeixen a nivell cel·lular per l'expressió de Gag, la proteïna estructural del VIH-1, afavorint la seva formació amb un embolcall lipídic similar al virus. Diferents antígens es poden incorporar a la superfície de les VLPs, però la seva incorporació és poc eficient. Per evitar aquesta limitació, el nostre grup ha dissenyat una novedosa estratègia per augmentar la densitat d'antígens a la superfície de la VLP que consisteix en fusionar un petit immunogen derivat d'Env (Min) amb Gag a través d'un domini transmembrana.

La hipòtesi d'aquest treball és que l'expressió d'una alta densitat d'antígens a la superfície de les VLPs pot induir una resposta immunitària robusta que podria ser prometedora com a prototip de vacuna pel VIH-1. A més, aquesta plataforma de VLPs es pot adaptar fàcilment a una formulació de vacuna d'ADN administrada mitjançant electroporació *in vivo*, afavorint la generació d'un pro-

tocol de vacunació heteròleg que combini vacunes d'ADN i de VLPs. Els estudis d'immunogenicitat en ratolins van demostrar que el règim de vacunació heteròleg induïa una millor resposta immunitària en general. Els títols d'anticossos contra les proteïnes Gag i Min eren 10 vegades més elevats comparats amb un règim homòleg de VLPs, i les respostes cel·lulars eren marginalment superiors. Tot i que cap dels dos règims va ser capaç d'induir anticossos neutralitzants, els anticossos anti-Min eren de la subclasse IgG2c i per tant podrien ser capaços de generar respostes efectores dependent d'anticossos, fet rellevant ja que aquest tipus de respostes s'han associat amb una modesta protecció en assaigs clínics de vacunes pel VIH-1 en humans. La manca d'un model per a l'estudi de l'efecte protector de diferents candidats vacunals contra el VIH-1 en ratolins ens va portar a desenvolupar un model murí amb un empelt de cèl·lules de melanoma modificades per expressar la proteïna Min a la seva superfície i que actuaven de succedani d'una cèl·lula infectada pel VIH-1. La vacunació prèvia amb les VLPs va aconseguir frenar la progressió d'aquestes cèl·lules tumorals modificades, demostrant que aquestes VLPs van aconseguir induir una resposta immunitària completa i protectora. Finalment, vam demostrar la versatilitat de la nostra plataforma de VLPs amb alta densitat d'antígens expressant diferents immunògens a la seva superfície, fins i tot l'expressió de la proteïna Env trimèrica amb tota la seva complexitat antigènica.

En resum, la nostra plataforma de vacunes basada en VLPs que expressen una alta densitat d'antígens ha demostrat el seu potencial com a vacuna pel VIH-1.

Introduction

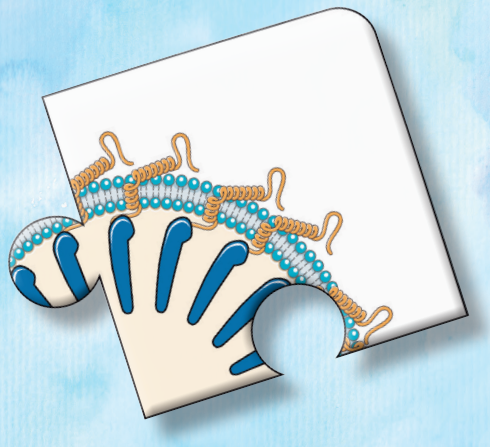

Vaccines are undoubtedly one of the most successful scientific achievements in the medical field. Since the description and implementation of vaccination by Edward Jenner more than 2 centuries back, vaccines have contributed to saving hundreds of millions of lives worldwide (Hinman, 1998; Vanderslott *et al.*, 2013). Massive vaccination programs, together with water sanitisation, better hygiene and the discovery of antibiotics, have had a huge impact on humanity, contributing decisively to increase, and nearly double, the life expectancy (Rappuoli *et al.*, 2014).

It is clear how infectious diseases have moulded history throughout the ages: from the black plague that profoundly impacted the European middle age history to the 1918 flu pandemics that resulted in a higher death toll than even the First World War (Goldstein and Lee, 2020). Also, tuberculosis caused by the bacteria *Mycobacterium tuberculosis* and malaria caused by different species of the protozoan *Plasmodium* led to millions of deaths throughout history (Holmes *et al.*, 2017). More recent examples include the Coronavirus Disease 2019 (COVID-19) caused by the Severe Acute Respiratory Syndrome Coronavirus 2 (SARS-CoV-2) or the acquired immunodeficiency syndrome (AIDS) caused by the Human Immunodeficiency Virus (HIV).

Although pathogens can dramatically impact our society, vaccines have the potential to mould history as well, the greatest example being SARS-CoV-2. COVID-19 was set to alter the lifestyle of a generation in 2020, but the rapid emergence of novel vaccines and global vaccination programs against SARS-CoV-2 in 2021 contributed to reverse the course of the disease (Hodgson *et al.*, 2021).

Unfortunately, the promise that vaccines embody is not yet attainable against all known pathogens. HIV is one of such examples, in which the development of a protective vaccine has proven elusive for more than 40 years (Zolla-Pazner *et al.*, 2021). And when conventional vaccine development strategies failed for HIV, new rational vaccine design approaches arose. These new strate-

gies could eventually lead to the successful development of a candidate that could help not only to prevent novel infections but also to ease the burden of people living with HIV (PLWH) (Gray *et al.*, 2016). A deeper understanding of the natural course of HIV infection, the immune response against the virus and the virus/host immune system adaptation is at the core of these rational vaccine strategies, and the knowledge gathered will be key to fight AIDS and help us deal with future emerging infections.

1. The Human Immunodeficiency Virus (HIV)

HIV infection is a major global health issue. HIV is a blood-borne virus that can infect CD4-expressing immune cells, especially $CD4^+$ T helper lymphocytes and destroys them during its life cycle, weakening the host's immune system (Sabin and Lundgren, 2013). If not treated properly with antiretroviral therapy (ART), HIV infection can lead to AIDS, during which many opportunistic diseases can arise and may prove fatal for the patient. ART effectively inhibits viral replication but is not able to clear the virus from latently infected $CD4^+$ T cells. Therefore, ART cannot be discontinued, making HIV a chronic and non-curable infection (Yoshimura, 2017).

HIV has a high mutational rate that translates into an extensive genetic diversity. Owing to this high diversity, HIV can be classified into multiple groups, types, and subtypes (Gartner *et al.*, 2020), and the development of cross-protective vaccines against the multiple variants is challenging (Gray and Walker, 2008).

Thus far, HIV stands as an infectious agent that has no preventive vaccine and no functional cure; however, the more we know about HIV and AIDS, the closer we are to bring this stigmatising disease to its end.

1.1. History of HIV

HIV has a relatively short but intense known history, since it has had a profound impact worldwide over the last 40 years. It was discovered as the causative agent of AIDS in 1983 by doctors Françoise Barré-Sinoussi and Luc Montagnier at Pasteur Institute (Barré-Sinoussi *et al.*, 1983), and since the beginning of the pandemics it is estimated that 79.3 million people have been infected with HIV-1 and 36.3 million people have died due to AIDS-related events (UNAIDS, 2021). However, HIV has a longer, albeit silent, history during which it latently established the pillars to become the pandemic agent it is nowadays.

1.1.1. From SIV to HIV

HIV birth can be traced back to Simian Immunodeficiency Virus (SIV) zoonotic infection in humans. SIV infection in humans is not rare in areas where humans and non-human primates (NHP) co-inhabit. It is estimated that 2.3 % of the population in Cameroon has been exposed by SIV, and this prevalence rises to 7.8-17.1 % in rural villages where poachers hunt NHP for bushmeat (Kalish *et al.*, 2005). Infection with SIV does not mean that the host will develop AIDS, nor that SIV will easily adapt to its host. The hypothesis suggests that poor equipment sterilisation during vaccination campaigns together with enhanced heterosexual transmissions may have played a role in helping SIV gain tropism for humans and establish itself as a human-to-human infection (Drucker *et al.*, 2001; de Sousa *et al.*, 2012).

Nowadays, HIV is a highly diverse virus. It has been classified into different types (HIV-1 and HIV-2) and groups; these groups are M, N, O and P from HIV-1 and groups A-I from HIV-2 (Sauter and Kirchhoff, 2019). Phylogenetic studies demonstrate that each one of these groups represents a single and different cross-species transmission from NHP to human (Van Heuverswyn *et al.*, 2007), meaning that there have been at least 13 known individual events in which SIV managed to cross the species barrier (Figure 1). For instance, HIV-1 group M

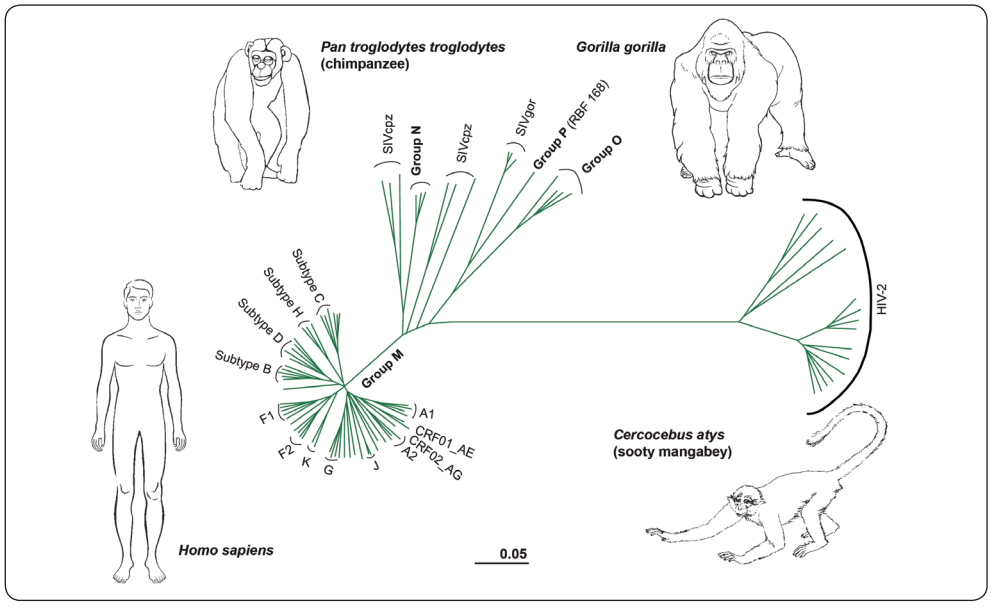

Figure 1. ***Phylogenetic tree of HIV-1 groups M, N, O and P, HIV-2 and SIV from chimpanzee (SIV_{cpz}), gorilla (SIV_{gor}) and sooty mangabey (SIV_{smm}).*** *HIV-1 group M is further divided into its clades or subtypes. Adapted from Tebit and Arts, 2011.*

("M" stands for "major") and group N most resemble chimpanzee's SIV (SIV_{cpz}) (Keele *et al.*, 2006), while HIV-1 groups O and P derive from SIV found in gorillas (SIV_{gor}) (D'arc *et al.*, 2015). Additionally, the HIV-2 virus, which is endemic in West Africa and less pathogenic than HIV-1, is closely related to sooty mangabey's SIV (SIV_{smm}) (Visseaux *et al.*, 2016).

HIV-1 group M accounts for more than 90% of HIV infections worldwide. Its increased pathogenicity and capability to expand beyond its endemic regions can be explained mainly, but not exclusively, by a better adaptation in humans than the other variants. SIV infection faces many host restriction factors such as tetherin, a host cell protein that "tethers" or anchors virions at the cell surface, impeding its release (Sauter *et al.*, 2010). SIV variants mostly block tetherin through Nef; however, human tetherin is resistant to Nef inhibition. SIV_{cpz} (HIV-1 group M ancestor) originated from the recombination in a chimpanzee co-infected with a red-capped monkey's SIV (SIV_{rcm}), which blocks tetherin through Nef, and a *Cercopithecus* SIV that blocked tetherin through Vpu (Sauter *et al.*, 2009). This preadaptation of SIV_{cpz} is thought to be one of the key factors for HIV-1 group M success in establishing itself as a pandemic agent in humans.

1.1.2. The origin of the pandemics

While HIV types (1 and 2) and groups (M, N, O and P) emerge from different cross-species transmissions, HIV subtypes or clades within a group derive from the same HIV common ancestor. Pandemic HIV-1 group M originated in the early 20^{th} century, likely when a hunter got infected with SIV_{cpz} in southeast Cameroon. The virus then travelled to Kinshasa in the Democratic Republic of Congo (DRC) through the Congo River in its host, where it settled as an epidemic agent (Sharp and Hahn, 2008).

Kinshasa is believed to be the focus of HIV-1 group M, since it houses the highest variability of this HIV group (Worobey *et al.*, 2008) (Figure 2). Evolutionary studies estimate group M's time and location of the most recent common ancestor (MRCA) to be around 1920 in Kinshasa (Faria *et al.*, 2014). In fact, the two oldest HIV samples conserved, ZR59 and DRC60 (subtypes D and A, respectively) were retrospectively obtained in Kinshasa. For 40 years HIV-1 group M stayed as an unidentified epidemic agent circumvented in Kinshasa and its neighbouring cities, where it diversified into multiple clades (namely subtypes A, B, C, D, F, G, H, J and K) and Circulating Recombinant Forms (CRFs) (*HIV Database*; Rhee and Shafer, 2018). Currently, these clades are globally distributed, but their prevalence differs across the distribution areas

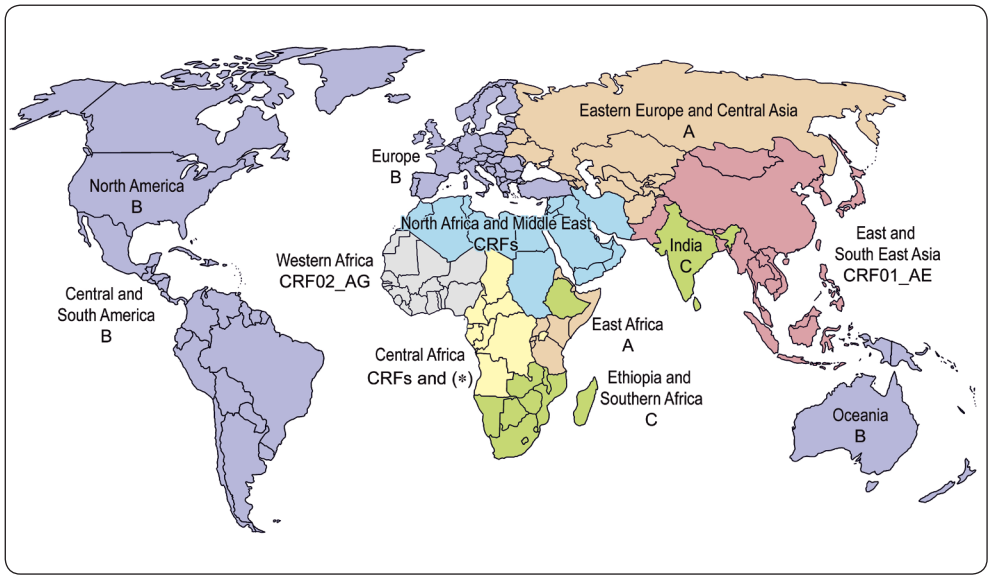

Figure 2. ***Global distribution of HIV-1 group M clades.*** *Colouring represents the predominant HIV-1 clade(s) in each geographic area (A, B, C or CRFs). CRF: circulating recombinant form. (*) indicates a high heterogeneity with no prevalent HIV-1 clade. Adapted from Gartner* et al.*, 2020.*

(Figure 2): subtype B is the predominant strain in Western Europe, America and Australia, clade C is the predominant clade in Southern Africa, CRF01_AE is the main subtype in Southeast Asia, while central Africa heterogeneously houses most variants, circumventing HIV-1 origin (Figure 2). Genetic diversity of HIV-1 group M within a clade represents up to 15% of variability, while it can reach up to 40% variability between different clades (Hemelaar, 2012).

Migration movements and changes in post-independence DRC helped HIV-1 group M to grow exponentially and expand worldwide (Faria *et al.*, 2014). Estimates indicate that HIV-1 arrived in Haiti around 1964 when professional workers returned from DRC, and from there the virus entered the United States of America (USA) through migratory movements (Korber *et al.*, 2000). By 1981 the Centre for Disease Control had reported in certain populations a series of unusual diseases such as *Pneumocystis carinii* pneumonia, Kaposi's sarcoma and opportunistic infections that were associated with cell-mediated immune deficiencies and, in 1982, the term AIDS was coined (Centre for Disease Control, 1981, 1982a, 1982b). By that time, AIDS diagnosis was a death sentence, but the discovery of HIV as the causative agent of AIDS in 1983 paved the way towards the development of antiretroviral therapies to tackle the virus (Barré-Sinoussi *et al.*, 1983).

1.1.3. Current state of the pandemics

In the last decades, the increased availability of antiretroviral drugs led to the development of highly active antiretroviral therapy, in which the antiretroviral drugs that better synergised were combined. This contributed to better viral control in PLWH, which resulted in less mortality, fewer escape variants and a reduction in secondary effects (Gulick *et al.*, 1997; Lederman *et al.*, 1998; Camacho and Teófilo, 2011), making HIV-1 infection a chronic infection but not a deadly one. The incidence of AIDS in patients that adhered to the treatment was severely reduced (Antiretroviral Therapy Cohort Collaboration, 2017). Moreover, the life expectancy of PLWH that strictly adhere to the treatment has caught up with the life expectancy of the non-infected population (Wandeler *et al.*, 2016).

The situation, though, is different in developing countries where access to ART is scarce. These countries experienced most of the 690,000 deaths from AIDS-related diseases and 1.5 million new HIV-1 infections in 2020. In spite of these alarming data, these numbers represent a 50% reduction in incidence and lethality compared to the peak of the pandemics in the late 1990s and early 2000s, consolidating the decreasing tendency of these past years and getting closer to the UNAIDS 90-90-90 objectives (Sohail *et al.*, 2020).

The UNAIDS 90-90-90 objectives aimed at having 90% of HIV-infected people diagnosed, of which 90% had to be on ART and, among those, 90% should be virally suppressed by 2020. Even though these objectives were not accomplished, currently they are standing at an 84-87-90 (UNAIDS, 2021). The reasoning behind these objectives was that, if achieved, 72.9% of all HIV-infected people would be virally suppressed, and since virally suppressed people cannot transmit the virus (*Undetectable=Untransmittable*), HIV-1 infections would be residual, and the pandemics would be more easily controllable (Bor *et al.*, 2021). However, it is not clear whether these objectives will sufficiently impact HIV-1 transmission, and prevention strategies such as vaccines will be essential to put an end to the HIV-1 epidemics (Corey and Gray, 2017).

Altogether, the current state of the pandemics is progressively improving, but until ART is available worldwide, PLWH can be functionally cured, and a preventive vaccine is approved for humans, prevention stands as the Rosetta stone to fight HIV. And despite no vaccine is yet available, pre-exposure prophylaxis (PrEP) and post-exposure prophylaxis (PEP) have proven effective at preventing HIV acquisition in high-risk populations (Riddell IV *et al.*, 2018).

1.2. The life cycle of HIV

HIV-1's particular pathogenesis and the hardship in generating protective vaccines and cure strategies can only be tackled with a deeper knowledge of its unique life cycle. HIV-1 is a retrovirus that has a lipid envelope containing the viral structural proteins and two positive chains of single-stranded ribonucleic acid (ssRNA) coding for HIV-1's genome (Figure 3).

The main HIV-1 target cells are the $CD4^+$ T helper (Th) cells, a particular subset of lymphocytes that orchestrate the adaptive immune response. HIV-1 engages the CD4 receptor on $CD4^+$ Th lymphocytes with the envelope glycoprotein (Env) displayed on the surface of the virus (Moss, 2013). Env is a complex heterotrimeric protein generated by the trimerisation of three gp160 molecules. Each gp160 monomer encompasses two different subunits (gp120 or SU for surface and gp41 or TM for transmembrane) joined non-covalently (Figure 3). Gp120 acts as the receptor recognising subunit, while gp41 harbours the fusion machinery (Chen, 2019). The CD4 binding site (CD4bs) on gp120 recognises CD4 and initiates a sequence of conformational changes that allows Env to bind a coreceptor, either CCR5 or CXCR4 (Deng *et al.*, 1996; Huang *et al.*, 2005). The coreceptor that each strain of HIV-1 binds to defines the tropism that each virus has (R5 or X4). Upon binding to the receptor and coreceptor, Env undergoes further conformational changes that expose the fusion machinery located in the gp41 subunit and allow the fusion peptide (FP) to be inserted into the host cell membrane, triggering the fusion process (Figure 4). The heptad repeats 1 and 2 (HR1 and HR2) and the

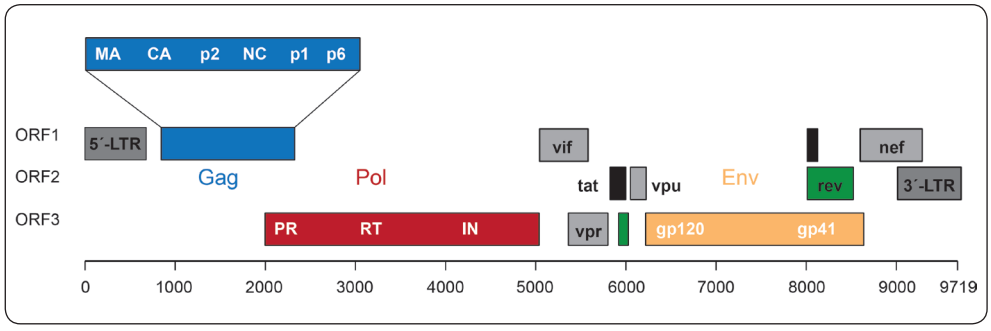

Figure 3. ***Schematic representation of HIV-1 genome with its 9 coding genes.*** *The genome is composed of 3 structural genes:* gag *(blue),* pol *(red) and* env *(yellow), 4 accessory genes in grey (*vif, vpr, vpu *and* nef*) and 2 regulatory genes in green (*tat *and* rev*) located throughout the 3 ORFs. Gag is further processed into 6 domains known as matrix (MA or p17), capsid (CA or p24), spacer peptide 1 (SP1or p2), nucleocapsid (NC or p7), spacer peptide 2 (SP2 or p1) and p6. ORF: open reading frame; PR: protease; RT: reverse transcriptase; IN: integrase. Adapted from Cervera* et al.*, 2019.*

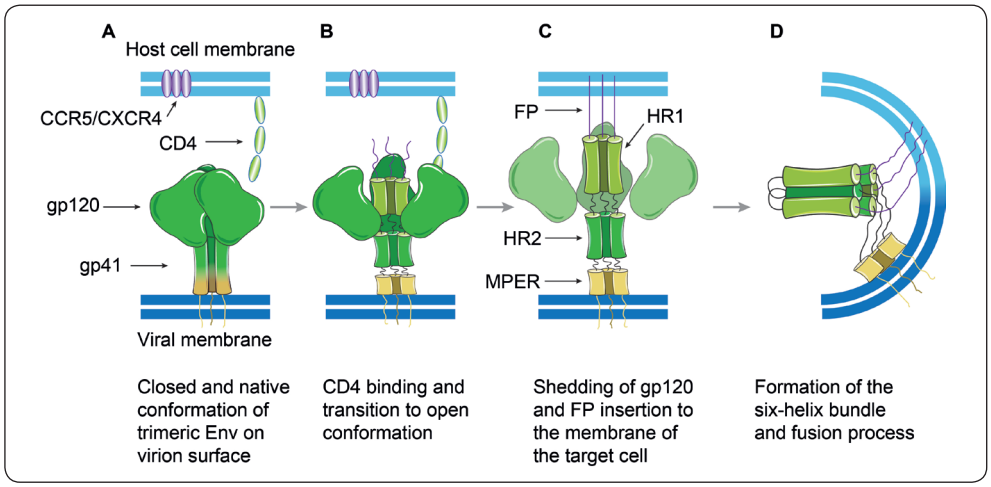

Figure 4. ***Conformational changes on HIV-1 Env to mediate fusion between the viral and the host cell membrane.*** **A)** *Closed conformation.* **B)** *Open conformation mediated by CD4 binding to gp120.* **C)** *Gp41 fusion peptide insertion to the host cell membrane (light blue).* **D)** *Membrane fusion mediated by the six-helix bundle formation between Gp41 HR1 and HR2 interaction. FP: fusion peptide of gp41; HR1: heptad repeat 1; HR2: heptad repeat 2; MPER: membrane proximal external region. Adapted from Kesavardhana and Varadarajan, 2014.*

Membrane Proximal External Region (MPER) play a pivotal role in this fusion process (Chen, 2019).

Once the virus has fused with the $CD4^+$ Th lymphocyte, the HIV-1 genome is released into the cytoplasm of the infected cell together with the viral enzymes: the reverse transcriptase (RT) and the integrase (IN) (Moss, 2013). Those enzymes are coded by *pol* and are responsible for the retrotranscription of the ssRNA to double-stranded deoxyribonucleic acid (dsDNA) and the integration of the retrotranscribed DNA into the host cell's DNA by the Long Terminal Repeats (LTR) that flank the HIV-1 genome (Figure 3). Since the RT is a low fidelity enzyme prone to mismatches and does not have proofreading activity, the mutational rate of HIV-1 is notably high (approximately 1.4 mutations/bp/cycle), resulting in the introduction of one mutation throughout the 10 kb every 3 cycles and hundreds of newly mutated viruses each time a cell is infected (Abram *et al.*, 2010). This high mutational rate combied with recombination results in a constellation of variants within one individual that comprise a quasispecies (Domingo and Perales, 2019), and leads to a quick evolution of the virus when it faces selective pressure by treatments or the immune system (Korber *et al.*, 2001).

Upon retrotranscription, viral DNA integrates into the host cell's genome. This proviral DNA has different potential outcomes that associate with the activation status of the infected cell: in non-activated cells, HIV-1 provirus can

remain silent for years allowing for the establishment of a pool of latently infected cells known as viral reservoir (Castro-Gonzalez *et al.*, 2018), while in activated cells, it can be efficiently transcribed resulting in the production and assembly of 10,000 to 100,000 viruses that will eventually lead to the cytopathic death of the infected cell (Chen *et al.*, 2007). To achieve this latter outcome, HIV-1 hijacks the cellular machinery, and its 10 kb genome is transcribed into mRNA via the RNA polymerase II, both for the synthesis of new viral proteins and for its packing into new virions (Figure 5).

The first HIV-1 genes synthesised in the cytoplasm are the regulatory genes *tat* and *rev*. Tat modulates the expression of the accessory proteins, which play a prominent role by altering the host cell responses against HIV-1 (Emerman and Malim, 1998). Tat and rev also promote the transcription of the structural protein p55Gag (Gag), the Pr160GagPol or Gag-Pol polyprotein, and Env. Even though Gag and Pol are coded in different Open Reading Frames (ORFs), the

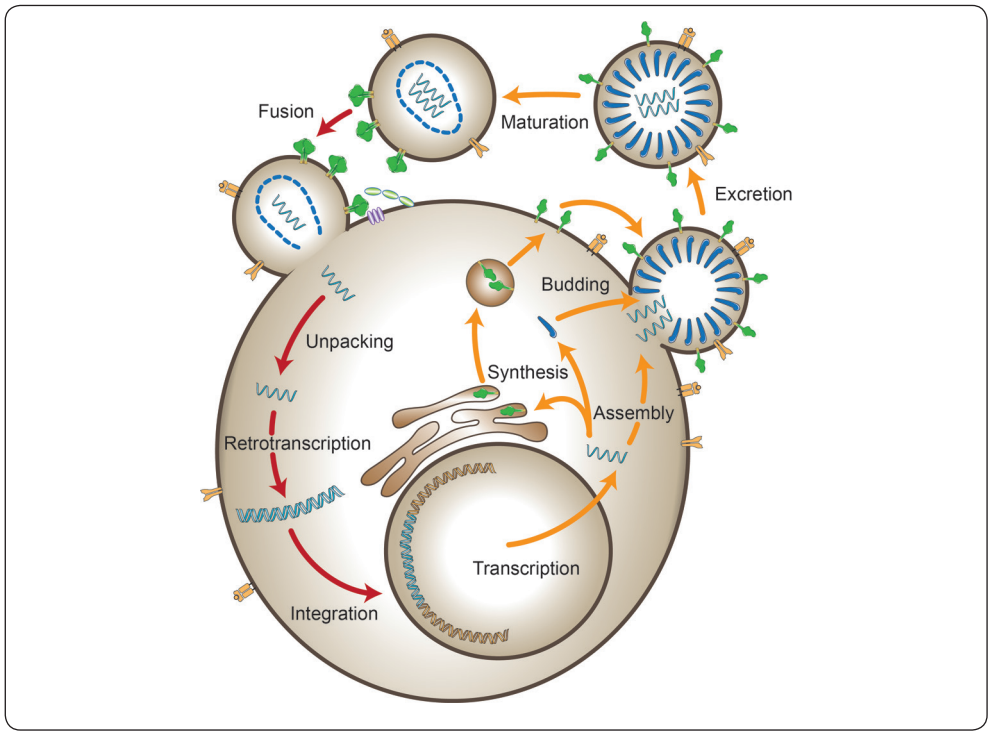

Figure 5. ***Schematic representation of the HIV life cycle inside a host CD4⁺ T lymphocyte.*** *Red arrows represent the first steps of host cell infection; yellow arrows represent the virus synthesis steps of the cycle. Dark blue: Gag and Matrix proteins; dark green: Env glycoprotein; light green: CD4; light purple: CCR5/CXCR4 coreceptor; light blue: viral ssRNA, dsRNA or dsDNA; dark brown: host cell or viral membrane; brown: endoplasmic reticulum and vesicles; yellow: host cell proteins. Adapted from Cervera* et al.*, 2019.*

presence of a slippery sequence promotes a ribosomal frameshift that allows for the synthesis of the Gag-Pol polyprotein (Biswas *et al.*, 2004). Gag and Gag-Pol are synthesised in the cytosol at a 20:1 ratio (Shehu-Xhilaga *et al.*, 2001). In parallel, Env is synthesised at the endoplasmic reticulum and migrates to the plasma membrane through the Golgi Apparatus. There, Gag and Gag-Pol interact with the phospholipids of the inner leaflet of the lipid bilayer and by protein-protein interactions they start oligomerising and budding into new virion particles (Sundquist and Kräusslich, 2012). At the same time, Gag interacts with the two chains of ssRNA that compose the HIV-1 genome, which are recruited and packed inside the newly forming virion (Jouvenet *et al.*, 2009), while Env is incorporated at a low density at the surface of the virion (Klein and Bjorkman, 2010). During that step, host cell proteins expressed at the surface of the cell acan be actively or passively incorporated in the virion (Izquierdo-Useros *et al.*, 2011). Finally, the virion buds from the plasma membrane of the host cell whilst the protease (PR) within Pol triggers a process of autocleavage that will lead to the proteolysis of the Gag and Gag-Pol polyproteins into the final functional structural elements (the matrix or MA, the capsid or CA and the nucleocapsid or NC) and the viral enzymes reverse transcriptase (RT) and integrase (IN), resulting in the maturation of the virion into a fully infectious HIV-1 particle (Freed, 2015). Viral replication can mediate a cytopathic effect on the host cell that may lead to a severe reduction of the $CD4^+$ Th lymphocyte compartment, among other mechanisms, until it compromises the efficiency of the immune system (Vidya Vijayan *et al.*, 2017).

1.3. Pathophysiology of HIV/AIDS

In absence of ART, HIV-1 pathophysiology could be unnoticeable until it reaches an irreversible point in which the host is in a deep immunosuppressive state and opportunistic infections easily arise. HIV-1 infection can be broadly divided into three main stages (Figure 6): i) acute infection; ii) chronic infection, and iii) AIDS.

During primoinfection, HIV-1 infects $CD4^+$ Th cells mainly present in the secondary lymphoid organs such as the Gut-Associated Lymphoid Tissue (Alcamí and Coiras, 2011). In these $CD4^+$ rich tissues, HIV-1 can multiply while latently infecting and establishing a notorious viral reservoir (Centlivre *et al.*, 2007). Viraemia during primoinfection can reach a peak of tens of millions of copies per millilitre (mL) of blood, which can result in a moderate drop in $CD4^+$ Th cell count due to HIV-1's cytopathic effect on $CD4^+$ Th lymphocytes (Sabin and Lundgren, 2013). This high viral load triggers the immune response

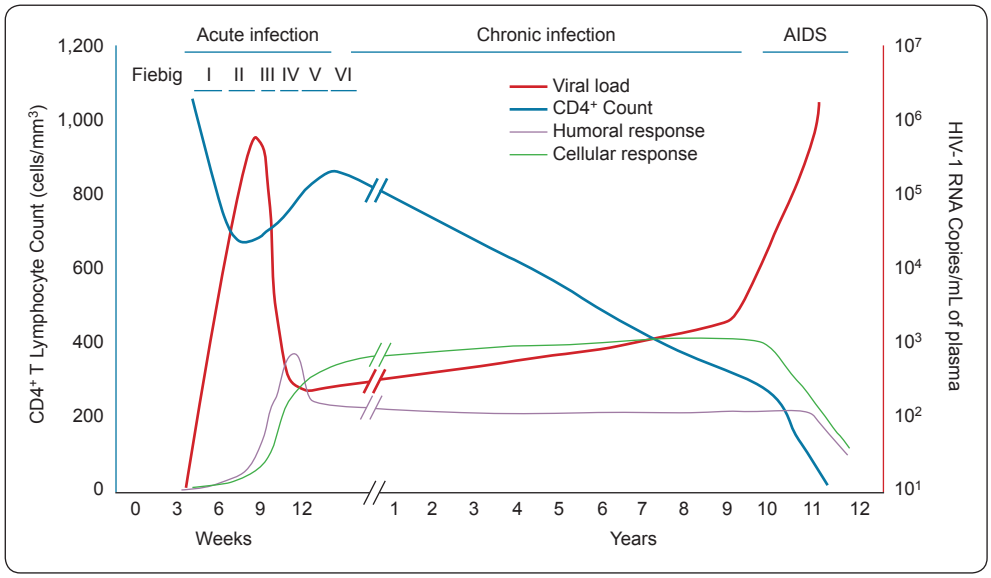

Figure 6. ***Schematic representation of the pathophysiology of HIV/AIDS.*** *Graphical representation of the cellular, virological and immunological parameters during HIV-1 infection in absence of ART. Red: HIV-1 viral load; blue: CD4⁺ T lymphocyte count; purple: anti-HIV-1 antibody titres; green: anti-HIV-1 specific T cells. Adapted from Redd* et al.*, 2013.*

which will try to control the viral replication. During this acute phase, which can be divided into 6 stages (Fiebig I-VI), the host can develop flu-like symptoms (Fiebig *et al.*, 2003). Eventually, cytotoxic CD8⁺ T lymphocytes (Tc) responses and neutralising antibodies produced by plasma cells, which are triggered by the virus, can partially control viral replication to reach a stable set point of viraemia defined by the individual balance between viral replication and immune responses (McMichael *et al.*, 2010).

Reaching a stable set point will mark the end of the acute phase and the beginning of the chronic phase. It is accepted that lower CD4⁺ cell counts result in faster disease progression, while higher CD4⁺ T cell counts generally lead to a slower progression of the disease (Sabin and Lundgren, 2013). The levels of CD4⁺ T cells and the viral load allow clinicians to categorise, broadly speaking, untreated patients into different groups: rapid progressors, long-term non-progressors and elite controllers. These groups are generally associated with the time it will take for them to develop AIDS in absence of ART (Gurdasani *et al.*, 2014). Long term non-progressors and elite controllers are a population worth characterising, since the immune responses they elicit are able to control the virus on their own, and can help to inform about the features associated with protective immune responses, which could be useful for the development of

better vaccines and immunotherapies (Lopez-Galindez *et al.*, 2019). However, HIV-1 can eventually escape control (Rosás-Umbert *et al.*, 2019) and, in the absence of ART, $CD4^+$ T cell count will slowly but steadily decrease until a point in which opportunistic pathogens can infect the host, leading to the final AIDS phase, which can take from months to several years to develop.

1.4. The era of antiretroviral drugs

In the past 30 years, major advances in HIV-1 care came by the hand of antiretroviral drugs, leading to the current situation in which people who have access to ART and adhere to the treatment do not develop severe complications associated with HIV-1 chronic infection, unless escape mutations arise.

The first antiretroviral drug against HIV arrived in 1987, when zidovudine (AZT) was approved by the FDA to treat AIDS. AZT was a big step forward in HIV treatment, since it targeted the HIV retrotranscriptase and reduced AIDS-related mortality of HIV-infected people (Fischl *et al.*, 1987). In the following years, similar treatments such as didanosine, zalcitabine and savudine were approved by the FDA, but escape mutants rapidly emerged (Fischl, 1994), and in 1995-1996 drugs targeting other viral pathways were developed (Pau and George, 2014), leading to better combination ARTs (Hammer *et al.*, 1997).

All the current therapies approved for HIV-1 treatment are mainly small molecules that target different elements of the virus (Kemnic and Gulick, 2021). These drugs are divided into several classes depending on their HIV-1 target: Protease Inhibitors (PI), Nucleoside Reverse Transcriptase Inhibitors (NRTI), non-nucleoside Reverse Transcriptase Inhibitors (NNRTI), Integrase strand transfer inhibitors (INSTI), fusion inhibitors and CCR5 antagonists. The standard of care for ART states that all HIV-1 infected individuals must be treated with a combination of three drugs using at least two different drug classes (Saag *et al.*, 2020). The greatest success of ART is that it achieves undetectable viral loads on the blood of PLWH, minimising the risk for the emergence of resistant mutated viruses and keeping the disease progression at bay, unless the therapy is discontinued. Notably, early treatment with ART also results in virological and immunological benefits, since the reservoir is smaller and $CD4^+$ Th cells are better preserved (Plana *et al.*, 2000).

Not only antiretroviral drugs have achieved a strict control of the viraemia in PLWH, but also have proven effective at preventing infection in populations at risk or already exposed to the virus by PrEP and PEP interventions, respectively (Riddell, Amico and Mayer, 2018). Truvada, a combination of emtricitabine and tenofovir (both reverse transcription inhibitors), has been approved

for its use as a PrEP agent. Currently, PrEP is approved in several countries, including Spain since 01/01/2020 (Schaefer *et al.*, 2021).

Despite all these major successes in the control and prevention of HIV-1 infection by antiretroviral drugs, no pharmaceutical intervention has yet succeeded in achieving a functional cure for PLWH. That is why new drugs that try to modulate or emulate the immune system are being extensively evaluated and developed.

2. The role of the immune system

The host immune system of PLWH plays a dual role both as a host for HIV replication and as a means of fighting HIV-1. $CD4^+$ Th lymphocytes, the main target for HIV-1, execute a pivotal function in the coordination of adaptive immune responses, which include the humoral and the cellular sides. Furthermore, the innate immune system has also a relevant role in prompting the adaptive immune response, which HIV-1 exploits to its benefit.

2.1. Innate immune responses in primoinfection

The first barrier against any kind of infection is the innate immune system, which surveils all the tissues identifying potential threats and pathogens. The innate immune system is composed of multiple layers of protection, starting from general aspects like anatomical barriers that act as a wall against pathogens, to the sentinel cells or innate leukocytes (Murphy *et al.*, 2017). These innate leukocytes are a diverse cell population composed of phagocytes such as macrophages, dendritic cells (DCs), and neutrophils, but also other cells with different roles like Natural Killer cells (NKs), mast cells, etc.

Myeloid professional antigen-presenting cells (APCs) like DCs and macrophages are the first to detect HIV-1 through pattern recognition receptors (PRR) such as Toll-like receptors (TLR) and Sialic acid-binding immunoglobulin-type lectins (Siglec) (Perez-Zsolt *et al.*, 2019b). These professional APCs become activated upon viral recognition and phagocytosis of the pathogen. Activated APCs secrete proinflammatory cytokines that recruit other immune cells at the site of infection, triggering a local pro-inflammatory response that further promote the production of antiviral proteins (Bertram *et al.*, 2019). Whereas DCs migrate to the lymph nodes and present HIV-1 derived antigens to lymphocytes via major histocompatibility complex class II (MHC-II) molecules in order to activate antigen-specific adaptive immune responses, macrophages remain at the site of infection maintaining the pro-inflammatory state

and further recruiting other immune cells. A central hypothesis is that HIV-1 could exploit both processes by using DCs as a vehicle to access areas enriched in $CD4^+$ Th lymphocytes such as the lymph nodes through a mechanism defined as "transinfection" (Perez-Zsolt *et al.*, 2019a), while also infecting the macrophages since they express CD4 (Cunyat *et al.*, 2016). Furthermore, myeloid APCs have been used as carriers of antigens in vaccine strategies to elicit potent responses against HIV-1 (Climent *et al.*, 2018).

Afterwards, NK cells are also recruited to the site of infection to scan the cells and trigger the death of HIV-1 infected cells. NK cells merit some attention since they can mediate a wide diversity of cytotoxic effects bridging between the innate and the adaptive immune systems. For instance, NKs recognise infected cells that have downregulated major histocompatibility complex class I (MHC-I) molecules by the effect of the virus, but they are also able to target cells that are expressing viral antigens through an antigen-specific mechanism known as antibody-dependent cell cytotoxicity (ADCC) (Murphy *et al.*, 2017). To induce ADCC, antibodies produced by B cells recognise surface-expressed viral antigens on infected cells and activate NK cells through binding of the fragment crystallisable (Fc) domain of the antibody to the Fc γ receptor III (FcγRIII), also known as CD16. NK cells can exert their cytotoxicity by either degranulation and release of perforin and granzymes that will lyse the target cell, or by induction of apoptosis on the target cell through the CD95/Fas pathway (Chua *et al.*, 2004).

2.2. Lymphocytes as a target for HIV

Even though innate immune cells play a prominent role in HIV-1 infection, $CD4^+$ Th lymphocytes stand as the main population targeted by HIV-1 and with which most of the HIV-1/AIDS pathophysiology can be associated.

As aforementioned, upon infection and integration of HIV-1's genome into $CD4^+$ T cells, a relevant portion of HIV-1 proviral genomes can remain silent, leading to the creation of a latent reservoir. This latency mechanism is the main reason why ART cannot lead to the cure of HIV-1 infected people, since latently infected cells are not affected by it and the virus can spontaneously reactivate once ART is discontinued, even decades after HIV-1 acquisition (Martinez-Picado and Deeks, 2016).

HIV-1 latent reservoir may grow even if PLWH strictly adhere to ART, since some tissues have been described as pharmacologic sanctuaries (Licht and Alter, 2016). These sanctuaries, such as the brain or secondary lymphoid tissues like the lymph nodes, may have low concentrations of antiretroviral

drugs that may allow the virus to replicate below the limits of detection and without apparent clinical impact, by infecting new cells through virological and immunological synapses (Bracq *et al.*, 2018). This viral replication is marginal, albeit significant, therefore it is important to develop efficient strategies capable of dealing with it, like treatment intensification (Buzón *et al.*, 2010), or the induction of potent cellular immune responses (Coiras *et al.*, 2009). Furthermore, the HIV-1 reservoir can grow through the clonal expansion of a $CD4^+$ T cell that harbours the HIV-1 proviral DNA within its genome. Activation and duplication of these cells may lead to an increase in the viral reservoir without the need for HIV-1's activation and the generation of new viral particles (Liu *et al.*, 2020).

The development of strategies that can activate and target the HIV-1 reservoirs or prevent their formation will be vital for defeating the virus, and the immune system itself can be a source of tools and mechanisms against it (Prado and Frater, 2020). To restore the compromised immune system or boost it, learning from situations in which the immune system has proven capable of controlling HIV-1 can pave the way towards the development of better approaches.

2.3. Lymphocytes as a means of fighting HIV

The adaptive immune response can be divided into two major components: the cellular response mediated by $CD4^+$ Th cells and $CD8^+$ Tc, and the humoral response composed of B cells and antibodies. Although differentiated, there is an intricate cooperation between these two types of immune response and also with the innate immune system, which can be exploited to fight HIV-1.

2.3.1. Weaponizing cellular adaptive immune responses

$CD4^+$ Th and $CD8^+$ Tc lymphocytes mediate two different aspects of the cellular adaptive immune response. $CD4^+$ T cells not only are the principal target of HIV-1, but also a major player in the control of the infection. These cells are responsible for the coordination of the adaptive immune response upon activation by professional APCs. Conversely, $CD8^+$ T cells can mediate cytotoxic effects upon engaging with their cognate antigen presented by MHC-I molecules. Both $CD4^+$ and $CD8^+$ T cells mediate their functions through the T cell receptor (TCR), which is assembled during the early stages of the T cell development in the thymus (Murphy *et al.*, 2017). There are 4 TCR genes that will be somatically assembled and rearranged in T cell precursors by variable (V), di-

versity (D) and joining (J) gene segments (VDJ) recombination to produce a near-infinite repertoire of TCRs (Krangel, 2009). Once the TCR genes have undergone recombination, thymocytes will go through a process of central tolerance where they will be positively selected if they can bind to MHC molecules with low affinity, and negatively selected if they bind to self-MHC/peptide complexes with high affinity. This process will also determine the specific lineage (CD4 or CD8) according to the TCR's affinity to either MHC-I or MHC-II molecules. Naïve T-cells will exit the thymus to seek activation signals.

The first step for the activation of immature $CD4^+$ T cells is to recognise its specific epitope presented by the MHC-II molecule of professional APCs (DCs, macrophages or B cells). Although this TCR-MHC-II interaction is pivotal in T cell activation, costimulatory molecules, as a second activation signal, also play a major role (Murphy *et al.*, 2017). Finally, the third signal is given by the cytokines that sentinel cells secrete, which will promote $CD4^+$ Th cell activation and proliferation. An active $CD4^+$ Th cell will then prompt and provide the necessary signals for the activation of $CD8^+$ Tc cells and B cells, but part of them will also differentiate into memory $CD4^+$ Th cells, in order to trigger faster responses when exposed to the pathogen again later on.

Activation of $CD4^+$ T lymphocytes is a double-edged sword in fighting HIV-1, since they are essential to coordinate the adaptive responses, but at the same time, their activation can lead to an increase of the HIV-1 targets that fuel the progression of the disease. For instance, HIV-specific activated $CD4^+$ T cells are the main target of HIV-1 (Douek *et al.*, 2002). Also, as aforementioned, resting infected T cells can harbour latent HIV-1 reservoirs that will remain silent until their activation years after infection. To achieve a functional cure, it will be vital to identify strategies that activate (or "shock/kick") latently infected $CD4^+$ Th cells, which can be later targeted (or "killed") by therapeutic interventions (i.e., vaccines, antibodies, etc.). Immune checkpoint receptors (such as PD-1) are associated with viral persistence and could be potentially targeted with immunomodulatory strategies for reactivation and viral clearance (Van der Sluis *et al.*, 2020).

Other $CD4^+$ Th cell features identified in the natural course of infection can be weaponised in a therapeutic setting to fight HIV-1. Some HLA-II molecules (such as DRB1*12:01) have been linked with lower viral loads and controller profiles (Oriol-Tordera *et al.*, 2017). Another feature associated with natural protection is a 32 bp deletion in the CCR5 coreceptor (CCR5Δ32), since coreceptor usage is essential for HIV-1 to infect a $CD4^+$ T cell (Moore *et al.*, 2004). Homozygous CCR5Δ32 individuals are naturally resistant to HIV-1 infection and have been used as donors of haematopoietic stem cells for PLWH that required a bone marrow transplant due to leukaemia, resulting in the three HIV-1

sterilising cures described to date: the Berlin Patient, the London Patient, and the Dusseldorf Patient (Kalidasan and Theva Das, 2020).

$CD8^+$ Tc cells are the other component of the cellular responses. $CD8^+$ Tc lymphocytes can recognise epitopes presented by somatic cells through MHC-I molecules. MHC-I in humans is composed of three Human Leukocyte Antigen (HLA) groups: A, B and C. Each group has many different alleles, and their combination results in the immense repertoire of HLA-I molecules in humans. Upon binding of the TCR to its complementary foreign cognate peptide presented by an MHC-I molecule, the activated $CD8^+$ Tc can engage the target cell. As $CD4^+$ Th cells, $CD8^+$ T cells need a second signal to carry out their function, which will be provided by the cytokines released by $CD4^+$ Th cells (Murphy *et al.*, 2017). After these second signals, $CD8^+$ Tc cells exert their cytotoxic functions through the same two mechanisms that NK cells use to induce cytotoxicity: i) CD95/Fas pathway; ii) secretion of perforins and granzymes. In any case, these processes will lead to the apoptosis of the target cell. After performing their function, subsets of $CD8^+$ Tc lymphocytes differentiate into memory $CD8^+$ Tc cells.

$CD8^+$ Tc cells are an effective mechanism against HIV-1, since they can target infected cells that are producing viral proteins and presenting them through MHC-I. In fact, some group B HLA alleles are the most notorious predictors of long-term non-progressor and elite controller profiles, namely HLA B*27, B*57, and B*58 (Payne *et al.*, 2010; Sundaramurthi *et al.*, 2017). Furthermore, effective $CD4^+$ Th and $CD8^+$ Tc responses against Gag have been clearly associated with a slower disease progression (Laher *et al.*, 2017; Pernas *et al.*, 2018). As a case in point, depletion of $CD8^+$ Tc cells results in loss of control in SIV-infected NHP (Jin *et al.*, 1999). All these parametres are informative for HIV-1 vaccine development.

2.3.2. *Humoral adaptive immune responses*

B cells constitute the humoral fighting arm of the adaptive immune response. They can act as APCs and internalise their target by specifically engaging pathogens through the B cell receptor (BCR), which is a non-secretable membrane-bound form of the specific immunoglobulin (Ig) they produce. Antibodies or Igs are homodimers formed by two identical heavy chains and two identical light chains. They are polarised molecules in which both light chains and the variable domain of both heavy chains form the two antigen-binding domains (Fragment antigen-binding or Fab) (Figure 7), while the two constant regions of the heavy chains form the fragment crystallisable that can engage immune cell receptors (Stanfield and Wilson, 2014).

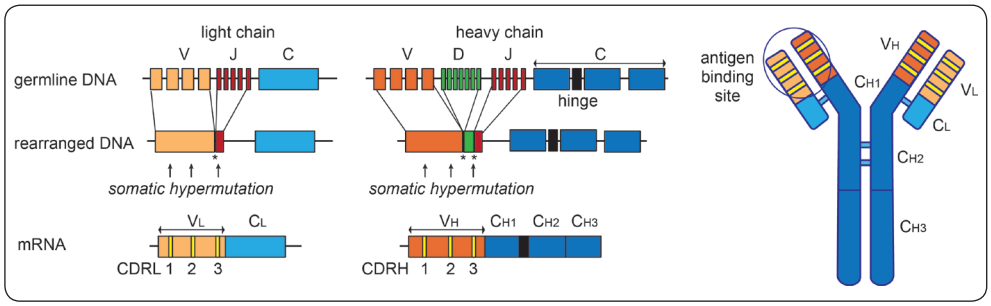

Figure 7. ***Antibody genes and structure.*** *The genome of antibody heavy and light chains are shown before and after somatic VDJ rearrangement in immature B cells. The final antibody structure is show in the left, and the antigen-binding site derived from the recombination is circled. V: variable; D: diversity; J: joining; V_H: variable domain of the heavy chain; $C_{H(1-3)}$: constant domains (1-3) of the heavy chain; V_L: variable domain of the light chain; C_L: constant domain of the light chain; $CDRH_{1-3}$: complementarity determining region 1-3 of the heavy chain; $CDRL_{1-3}$: complementarity determining region 1-3 of the light chain. Adapted from Feederle and Schepers, 2017.*

B cell development occurs in the bone marrow, where B cell precursors undergo a process of DNA recombination and rearrangement of the variable (V), diversity (D) and joining (J) gene segments (VDJ) in both variable regions of the heavy chain and the light chains to form the BCR, resulting in near-infinite specificities. After successful VDJ recombination of the heavy and light chains, two heavy chains and the two light chains (either λ or κ) pair with each other (Schatz *et al.*, 1989) (Figure 7). The initial antibody repertoire resulting from this process will be expressed at the surface of B cells in two different isotypes (IgM and IgD) as BCR. Before exiting the bone marrow, IgM^+ immature B cells will undergo a mechanism of central tolerance. Immature B cells will be positively selected when their heavy and light chains are properly paired and the BCR can trigger its signalling pathway. Additionally, immature B cells will be negatively selected if their heavy and light chains do not pair correctly or if they react against self-molecules, leading to apoptosis or another round of receptor editing (Nemazee, 2017). Positively selected immature B cells will become naïve B cells that will migrate to secondary lymphoid organs.

Naïve B cells will eventually find and bind their specific epitope through the BCR —the first activation signal—, and the antigen will be captured and degraded to be presented on MHC-II molecules, in order to seek the second activation signal that will mostly come by the hand of a $CD4^+$ Th lymphocyte (Murphy *et al.*, 2017). Alternatively, some foreign polysaccharide-specific B cells can be activated through T cell-independent pathways (Vos *et al.*, 2000). Upon activation, B cells will proliferate and follow different fates, both becoming early plasma cells that will produce the first batch of IgM antibodies that

target the foreign antigen, and also entering the germinal centre (GC) in lymph nodes to undergo somatic hypermutation (SHM) of the variable regions of Igs for affinity maturation and class switching (Wabl and Steinberg, 1996). Activation of naïve B cells and formation of plasma cells and antibodies can take up to 7-14 days, while affinity maturation takes longer. Affinity maturation by SHM in the lymph nodes spurs superior antibodies with an increased affinity for their antigen through a complex process in which B cells cycle around the dark zone (DZ) and light zone (LZ) of the GC. When B cells enter the DZ, mutations arise due to the expression of the activation-induced cytidine deaminase (AID), which deaminates cytidines in the variable Ig regions during cell division (Muramatsu *et al.*, 2000). Mutations during SHM tend to accumulate in the Complementarity Determining Regions (CDR) 1-3 of the heavy and light chains. Then, B cells migrate to the LZ to retest their affinity. Follicular dendritic cells (FDCs) in the LZ act as a long-term reservoir of antigens that the GC B cells will use to challenge their new BCRs, and T follicular helper cells (Tfh), a subset of $CD4^+$ T lymphocytes, will deliver the necessary secondary activation signals. B cells that have reduced affinity for their cognate antigen or that have developed mutations elsewhere will be signalled for apoptotic cell death or will return to maturation, while those B cells that have acquired BCRs with higher affinity can differentiate to plasma or memory B cells (Victora and Nussenzweig, 2012), which can also eventually return to affinity maturation.

Furthermore, during the affinity maturation process, antibodies also switch isotypes. In humans, there are 9 different heavy chain constant (C) loci in the following order from 5' to 3': μ, δ, γ_3, γ_1, α_1, γ_2, γ_4, ε and α_2. Ig C-chains μ and δ are the ones expressed in naïve B cells, producing IgM and IgD, respectively (LeBien and Tedder, 2008). Upon B cells entering the GC's DZ for affinity maturation, the constant chain can undergo class switching recombination, in which different Ig molecules can arise depending on the C-chain locus selected (IgG3 for γ_3, IgG1 for γ_1, IgA1 for α_1, IgG2 for γ_2, IgG4 for γ_4, IgE for ε and IgA2 for α_2). Class-switching recombination happens in an ordered 5' to 3' manner, meaning that if recombination leads to the production of IgA1 molecules, this B cell will not be able to switch Ig class to those loci that are upstream of α_1 (those being IgM, IgG3 and IgG1). The decision on which C-chain is selected will be based on the different cytokine inputs that the B cell is receiving (Kracker and Radbruch, 2004). Broadly speaking, each Ig class or isotype is responsible for a different function and compensate each other's function to mediate full-fledged protection. For instance, IgM molecules are the first to be produced during natural infection against pathogen-associated epitopes and have low affinity since they are generated before accessing the lymph nodes' GCs. Five IgM mol-

ecules oligomerise into a pentameric IgM that has a higher avidity, since it contains 10 antigen-binding domains per pentameric molecule, and its main function is to activate the complement system by engaging C1q (Murphy *et al.*, 2017). In comparison, IgA2 molecules are secreted as dimers in mucosal tissues and their main function is to mediate protection on site. Also, the four IgG isotypes (IgG1-4) are secreted as single molecules and are responsible for mediating a direct neutralising effect against the pathogens. IgG subclasses differ in their capability to engage FcγR on innate sentinel cells through their Fc fragment and mediate effector functions. In this sense, human IgG3 and IgG1 can promote antibody-dependent cell cytotoxicity or phagocytosis (ADCC and ADCP, respectively) (Vidarsson *et al.*, 2014); while IgG2 and IgG4 hardly bind to FcγR (Table 1). Finally, IgE binds to Fc ε receptors to sensitise mast cells and trigger the release of cytokines associated with allergies.

Different animal models, especially mice, have been used to study humoral immune responses against pathogens. Initially, the discovery that mice also had four IgG isotypes raised hopes that this model would be highly comparable to humans (Collins, 2016), but as any model, it has its limitations. That is why it is relevant to understand the differences between animal models to translate the experimental knowledge. Compared to humans, mice have 8 heavy chain constant loci, and ordered from 5' to 3' are: μ, δ, γ_3, γ_1, γ_{2b}, γ_{2a} (or γ_{2c}), ε and α. Although genetically equivalent to humans, Ig molecules behave slightly different in mice, especially IgG molecules. Additionally, some strain-specific differences have been detected in mice; for instance, C57Bl/6, non-obese diabetic (NOD) and SJL mice do not have the IgG2a isotype observed in BALB/c mice and other breeds, but IgG2c has an equivalent function instead. Furthermore, it is not clear that class switching in mice follows a 5' to 3' order like in humans, since an accumulation of SMH rates is not observed in Ig molecules containing the C-chains of the 3'-end loci (Collins *et al.*, 2015), and also SMH in mice is a less frequent event

Table 1. General comparative IgG isotype functions in mouse and human

	Human				Mouse			
	IgG1	IgG2	IgG3	IgG4	IgG1	IgG2a/c	IgG2b	IgG3
Neutralisation	++	++	++	++	++	++	++	++
ADCC	+++	+/–	++	+/–	–	+++	++	–
ADCP	++	+	+	–	–	+++	++	–
CDC	++	+	+++	–	+/–	++	++	++

ADCC: antibody-dependent cellular cytotoxicity; ADCP: antibody-dependent cellular phagocytosis; CDC: complement-derived cytotoxicity; IgG: immunoglobulin G. Based on Collins, 2016; Bruhns, 2012; Almagro et al., *2018 and Stewart* et al., *2014.*

compared to humans, in which anti-HIV1 bNAbs can accumulate up to 90 mutations or more, whereas antibodies from inbred mice rarely exceed 10 mutations (Scheid *et al.*, 2009; Hara *et al.*, 2015). Considering the functional effects, in humans, each IgG subclass tends to have a more distinguished or polarised function, while in mice, the four isotypes are believed to work more synchronised (Collins, 2016). Each isotype, however, mediates a different function: mouse IgG1 does not bind complement nor Fc receptors so it may have a direct effect on the pathogens, mouse IgG2a and IgG2c engage mouse FcγR and mediate antibody-dependent effector functions —similar to human IgG1 and IgG3— and are linked to viral infections, murine IgG2b is considered to be a T-dependent antibody that mediates similar, albeit weaker, functions as IgG2a, and mouse IgG3 mainly binds complement in a T-independent manner. Like human IgG isotypes, each murine isotype is induced by the effect of a different mix of cytokines on B cells.

Antibodies can mediate multiple effects, and direct neutralisation is one of such activities. Pathogen neutralisation is normally one of the most intensively sought immunological outcomes induced by vaccination. Neutralising antibodies (NAbs) against HIV-1 arise around two months after primoinfection with HIV-1. These NAbs mainly show autologous neutralisation against the Env expressed by the transmitter/founder virus, and rarely exhibit heterologous neutralisation against other clades; however, the selective immune pressure they exert on the virus will end up prompting the expansion of mutated escape variants (Bonsignori *et al.*, 2017). The immune system adapts in parallel to HIV-1's evolution, generating new antibodies and T cell responses, or improving by SMH the pre-existing antibody responses, generating an arms race between the host and the virus that the latter is bound to win due to its enhanced mutational rate, compared to a slowly adapting immune system. Remarkably, years after infection, around 1% of the PLWH develop exceptional elite neutralising responses against a wide range of HIV-1 variants (Simek *et al.*, 2009). These exceptional broadly neutralising antibodies (bNAbs) are highly somatically hypermutated antibodies, probably elicited by the long-term exposure to substantial HIV-1 viral loads and generally elicited due to exposure to a diversity of HIV-1 Env strains (Rusert *et al.*, 2016).

Structurally speaking, bNAbs display some general features shared by most of them independently of the Env epitope they target (Sadanand *et al.*, 2016). First, bNAbs target the most conserved regions of Env, that is why they can neutralise a wide diversity of viruses, namely the CD4bs, the V1V2 apex, the MPER, the FP or the gp120/gp41 interface (Figure 8). Additionally, these vulnerability regions have an important functional role in the infection process, and hence bNAbs can easily neutralise the virus by hindering viral infectivity (Lynch *et al.*, 2015). On the molecular level, bNAbs have been extensively described to have a considerably

high SHM rate, proofing how bNAbs undergo several cycles of affinity maturation at the GC throughout many years of being exposed to an evolving antigen. Compared to a standard antibody that has an average of 10-20 mutations in relation to its unmutated germline ancestor, bNAbs can present up to 40-100 mutations (Wang and Zhang, 2020), which means that they have 15-30% of mutated amino acids (aa) compared to the germline sequence. Furthermore, these mutations are more frequently located in the CDR3 antibody domain but also at the framework region of the variable domain, a region that generally is stringent to mutations (Klein *et al.*, 2013). Another exceptional feature of bNAbs is the unusually long CDRH3 fingers. CDRH3 loops in regular antibodies are 8-16 aa-long, while bNAbs on average have 21 aa-long CDRH3 fingers (Breden *et al.*, 2011), and may also be a consequence of the chronic antigen exposure and successive viral escapes or the selection of rare underrepresented B cell clones. Finally, a relevant feature of bNAbs is their polyreactivity, which is possibly induced by the process of broadening the antibody targets or by trying to increase the affinity against poorly expressed Env on the viral surface (Mouquet *et al.*, 2010).

Together with the high mutation rate or the low density of Env molecules at the viral surface to reduce antibody avidity, HIV-1 has a wide range of additional mechanisms to avoid the elicitation of NAbs and bNAbs or to evade their effect, such as exposure of highly immunogenic non-neutralising epitopes to divert the immune response, concealment of neutralizable functional epitopes in its pre-CD4 engagement state, infection of target cells by cell-to-cell transmission, and the presence of a glycan shield around Env to reduce its immunogenicity (Air and West, 2008; Zhou *et al.*, 2017; Amitai *et al.*, 2018; Landais and Moore, 2018; Ivan *et al.*, 2019). That is why elicitation of bNAbs is rare and only occurs in a small percentage of infected individuals later in the infection. Furthermore, even when broadly neutralising responses are induced, the virus can still evade them; and so, the presence of bNAbs does not correlate with an improvement on HIV-1 control in PLWH who elicit them (Subbaraman *et al.*, 2018).

Despite bNAbs are not able to control viral replication and infection progression in HIV-1 infected individuals (Euler *et al.*, 2010), they have recently proven as a potentially successful strategy to mediate a protective effect or to be used as a treatment by passive immunisation strategies.

2.4. The era of biopharmaceuticals

This last decade has seen a surge of biological-based strategies that try to emulate or stimulate immune responses to fight HIV-1, which derive from the accumulation of knowledge around HIV-1 infection and its interaction with the im-

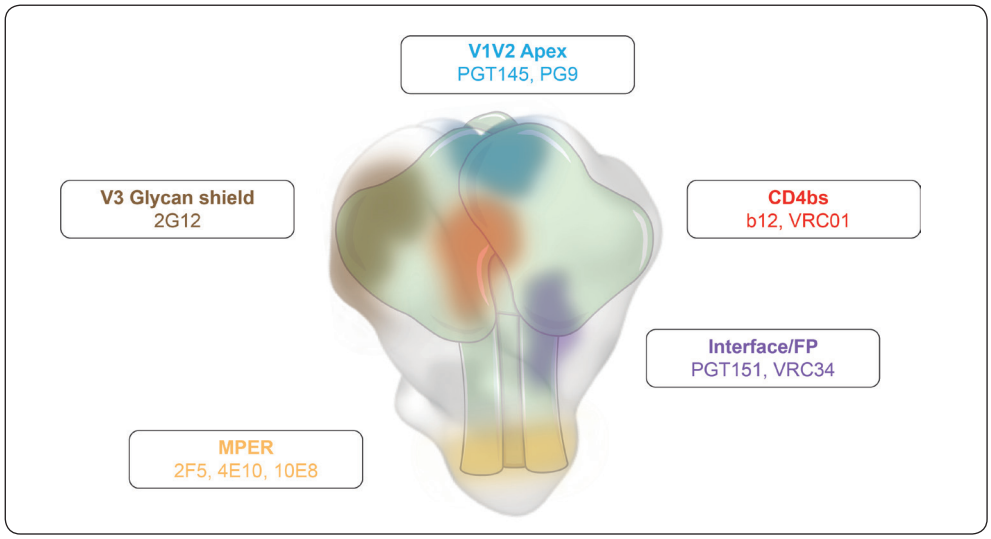

Figure 8. ***HIV-1 Env vulnerability map.*** *Native trimeric protein highlighting some of the principal areas targeted by broadly neutralising antibodies (bNAbs): CD4 binding site (CD4bs, red), V1V2 apex (blue), V3 (brown), gp120/gp41 interface and fusion peptide (FP, purple), membrane proximal external region (MPER, yellow). Adapted from West* et al.*, 2014.*

mune system. Owing to this knowledge gathered across 40 years of extensively studying HIV-1's pathophysiology, scientists are now harnessing the immune system's potential by Antibody-Mediated Protection (AMP) strategies, the development of better immunomodulators to reactivate latent HIV-1 reservoirs and the design of vaccine strategies to induce more potent humoral and cellular immune responses.

Since the identification and isolation of the first bNAb (b12), many groups have evaluated the feasibility of generating AMP by passive immunisation. Initial studies in animal models demonstrated the potential of this approach both in mice (Gauduin *et al.*, 1997) and macaques (Shibata *et al.*, 1999), especially when used in combination treatments of two or more bNAbs against different specificities (Mascola, 2002). The field of HIV-1 bNAbs was especially boosted from 2010 on, with the arrival of B cell cloning techniques, which allowed for the identification of more potent bNAbs targeting a wide range of Env epitopes (Figure 8), such as VRC01 or 10E8 (Wu *et al.*, 2010; Huang *et al.*, 2012). In parallel, further *in vivo* protection studies against SIV and chimeric Simian-Human Immunodeficiency virus (SHIV) infection in NHP demonstrated which considerations were important for AMP. For instance, potent *in vitro* neutralisation in a pseudovirus assay correlates with *in vivo* protection against a virus expressing the same Env molecule, while administration of a single bNAb

will not protect animals from challenge with a resistant strain (Moldt *et al.*, 2012). This issue can easily be overcome by the identification of broader and more potent bNAbs, or by the combination of 2-3 bNAbs with complementing sensitivities (Walker *et al.*, 2011; Julg *et al.*, 2017). Results derived from bNAbs' research are also informative for the development of better vaccine strategies.

AMP by bNAbs has also been tested in human clinical trials. VRC01, an anti-CD4bs bNAb was tested at two different doses (high: 30 mg/kg; or low: 10 mg/kg) for its capacity mediating PrEP protection in populations at risk in two different phase IIb clinical trials: HVTN703/HPTN081 and HVTN704/HPTN085. HVTN703 was directed to transgender people and men who have sex with men (MSM), while HVTN704 was directed to sub-Saharan heterosexual women. Preliminary results of both trials showed that VRC01 was safe and tolerable, but did not show significant protective effects on both VRC01 administered groups compared to the placebo control (8.8% protection for the HVTN703 and 26.6% protection for HVTN704) (Corey *et al.*, 2021). However, it is relevant to highlight that VRC01-treated people did get significantly more infected with VRC01 neutralisation-resistant viruses than placebo groups, suggesting that protection could be mediated by passive immunisation using a combination of broader and more potent bNAbs (Corey *et al.*, 2021).

In fact, bNAbs can be engineered to enhance their protective activities. The Fc region can be mutated to increase binding to the neonatal Fc receptor, which improves the plasma half-life (Ko *et al.*, 2014) and their biodistribution (Gaudinski *et al.*, 2018). Other mutations can increase their production or modulate their interaction with the FcγR (Kwon *et al.*, 2016). Interestingly, bNAbs can be formulated as a viral-vectored gene therapy for the treatment of PLWH (Mellins and Kay, 2015). Furthermore, bispecific and trispecific antibodies have been designed and have demonstrated their efficacy in preclinical models. The rationale behind these complex molecules is to incorporate multiple bNAb specificities at the same molecule, therefore administering a combination therapy with only one molecule (Montefiori, 2016; Xu *et al.*, 2017).

It is worth mentioning that bNAbs can mediate protection beyond the direct neutralisation on HIV-1 by inducing antibody-dependent effector functions. In fact, monoclonal bNAbs can be further engineered to incorporate mutations that increase binding to FcγR (Bournazos *et al.*, 2014). These receptor-associated functions not only are important for the immediate effect on the viral load by the role of innate immune leukocytes, but will also recruit the adaptive immune system and boost anti-HIV-1 immune responses, a property known as "vaccinal effect" (Naranjo-Gomez and Pelegrin, 2019). This vaccinal effect demonstrates the potential of bNAbs as a substitute of ART in PLWH. The benefits of these

sorts of biopharmaceutical therapies would be a longer effect upon administration, hence being more convenient since they do not need a daily administration, as classical ART drugs do. Further studies and clinical trials are still necessary to describe the exact posology and to avoid the rise of mutated escape variants (Caskey, 2020).

The antiviral effects of bNAbs are clear, and their potential is not only limited to AMP and treatment, but they could also play a key role in targeting HIV-1 reservoirs in the pursue of a functional cure (Ananworanich *et al.*, 2015). These types of approaches can also benefit from combination with other types of monoclonal antibodies (mAbs) to target latently infected cells, such as those targeting immune checkpoint receptors. Immune checkpoint inhibitors are candidate latency-reversing agents (LRAs), since their effect on latently infected $CD4^+$ Th cells can promote their activation and the induction of viral replication (Van der Sluis *et al.*, 2020), while also prompting $CD8^+$ Tc cells to exert their functions on infected cells (Boyer and Palmer, 2018). For instance, anti-PD1/PD-L1 leads to an activation of $CD8^+$ Tc cells and a decrease in viral reservoirs (Chen *et al.*, 2020), and clinical trials for their potential effect in humans are ongoing.

Besides mAbs that target immune checkpoint inhibitors, TLR agonists are immunomodulators that can also act as LRAs and stimulate anti-HIV-1 immune responses in infected people. TLRs are PRR that are mostly present in innate leukocytes both on the membrane and inside endosomes. TLRs can detect pathogen- or damage-associated molecular patterns (PAMPs and DAMPs), and their activation can lead to the production of pro-inflammatory cytokines (Kawasaki and Kawai, 2014). Among the TLR agonists that have been tested as LRA are CpG motifs, flagellin, vesatolimod, etc. A few of these TLR agonists have demonstrated their potential in NHP, with CpG and vesatolimod reaching clinical trials (Martinsen *et al.*, 2020). TLR agonists can also be used as preventive and therapeutic vaccine adjuvants, and direct administration of cytokines can also mediate the same adjuvating effect (Kula-Pacurar *et al.*, 2021). Altogether, the use of biopharmaceuticals is not limited to one aspect, since immunomodulators like TLR agonists can also be used as adjuvants and bNAbs can act as PrEP and therapeutic agents.

Owing to their flexibility, all these biopharmaceuticals can also be tested in combination to pursue a strategy for a functional HIV-1 cure, and bNAbs can also be a source of knowledge to generate better rational vaccine designs, which are one of the most intensely researched biopharmaceutical areas in the HIV-1 field. Initially, vaccines were designed with the intent to protect against the acquisition of HIV-1, but lately many efforts have also focused on developing HIV-1 therapeutic vaccines (Leal *et al.*, 2017). On the one hand, the main objective of preventive HIV-1 vaccines is to develop durable and broad immune responses that can

avoid primoinfection and the generation of HIV-1 reservoirs, with balanced humoral and cellular responses that can quickly clear initially infected cells (Graziani and Angel, 2016). On the other hand, therapeutic vaccines try to boost immune responses against HIV-1 capable of clearing the virus from latently infected cells in an already primed immune system, and as previously detailed, viral clearance is mainly mediated by the cellular arm of the adaptive immune response (Casazza *et al.*, 2013). The effect of preventive vaccines should ideally mediate life-long protection against a highly diverse virus, while therapeutic vaccines should exert a more potent effect in a shorter, but sufficient, time that allows for the elimination of a targeted reservoir. Therapeutic vaccines can also benefit from combined treatments with bNAbs and LRAs to kick the viral reservoirs, since the effect they must mediate is more circumscribed in time (Barouch *et al.*, 2020).

Despite these evident differences in the outcomes sought by preventive and therapeutic vaccines, advances in prevention approaches are also informative for the therapeutic strategies, and vice versa, since they are intimately intertwined. A deeper understanding of all the vaccine prototypes will help to pave the way towards a successful preventive vaccine strategy.

3. Preventive vaccine strategies for HIV-1

The year 2020 saw a quick rise of multiple effective vaccines against SARS-CoV-2 that reached clinical trials and commercialisation in less than a year, which is considerably faster than the 10-15 years average that vaccine development usually takes. While it is true that SARS-CoV-2 vaccine development benefited from technology that was generated owing to 40 years of basic and applied science in other fields, like HIV vaccine research (Pardi *et al.*, 2018; Sanders and Moore, 2021), it is still remarkable that vaccines with such a good efficiency could move from concept to approval within such a short time.

In comparison, many efforts have been invested in the development of HIV-1 vaccine candidates, but only modest correlates of protection have been achieved in humans so far. Even when facing these unfruitful results, hope is not lost, and many groups are still pursuing the development of ideal immunogens and vaccine strategies to elicit protective responses.

3.1. HIV-1 candidate immunogens for vaccine development

HIV-1 immunogens developed for vaccination can be categorised into two main groups: those designed for the induction of potent cellular responses, and those that aim at eliciting protective humoral responses. Considering cellular respons-

es, Env has been widely reported as a poor stimulator of protective $CD4^+$ Th and $CD8^+$ Tc lymphocytes, while Gag-Pol polyprotein and accessory proteins, like Nef, are better targeted by the cellular arm of the immune response (Masemola *et al.*, 2004). Gag-derived immunogens that cover most of the circulating HIV-1 variants were developed to be administered by DNA vaccination. Some examples of these immunogens are mosaic proteins —bioinformatically-designed Gag proteins made up of different fragments from multiple subtypes that covered most HIV-1 group M clades (Fischer *et al.*, 2007; Barouch *et al.*, 2010)—, HIV.consv —encoding only for the most conserved elements of Gag (Ondondo *et al.*, 2016)—, or HTI —encoding for immunogens that express conserved peptides that are targeted by effective cellular responses (Mothe *et al.*, 2015).

In comparison, Env is the main target of humoral responses, and has been modified in multiple ways to try to elicit potent neutralising antibodies. For instance, nucleic acid vaccines can encode the full gp160, resulting in Env trimers or monomers anchored to the host cell membrane, or can also encode gp140, which will be secreted as a soluble protein (Cao *et al.*, 2018). Other vaccines focus on the two Env subunits (gp120 and gp41). It is important to highlight how many of the bNAbs that target gp120 often recognise conformational epitopes or bind glycosylated residues and block receptor binding, while those targeting gp41 often bind to more linear and conserved epitopes hampering the fusion process (Wibmer *et al.*, 2015).

Since immunisation with unmodified Env proteins has proven to be insufficient to generate a protective response, more sophisticated immunogens have been engineered to present key epitopes targeted by bNAbs, such as the eOD-GT8, which displays CD4bs epitopes (Jardine *et al.*, 2016), or stable trimeric proteins displaying Env's native conformation, which can be key for the elicitation of bNAbs that target functional sites at the surface of infective viruses (Sanders *et al.*, 2015). Epitope-based vaccines try to elicit humoral responses against vulnerable regions while removing more immunogenic but irrelevant domains that can divert elicitation of protective responses against vulnerable domains like the FP or the MPER (Molinos-Albert *et al.*, 2017b).

All these immunogens have been tested in animal models to characterise their immunogenicity, but HIV-1 inherent properties hinder most attempts at generating protective vaccines, since it is a highly diverse virus that has multiple immune evasion mechanisms, such as a masking glycan shield or the concealment of vulnerable regions, both for B and T cell epitopes (Zhou *et al.*, 2017; Olvera *et al.*, 2020). Overcoming these difficulties is the main objective of current vaccine approaches that try to generate immunogen can-

didates through informed vaccine design, and, in that sense, animal models play an invaluable role.

3.2. Animal models for HIV-1 vaccine development

Various animal models have been employed throughout these 40 years of HIV-1 research in order to understand the virus and its pathogenicity, to test antiretroviral treatments and to develop vaccine strategies. NHP infection with SIV was the predominant preclinical model used to evaluate the first HIV-1 vaccine strategies, and SIV infection was later replaced by SHIV, which is a chimeric SIV engineered to express HIV-1's Env instead of SIV's (Chen, 2018). Additionally, other animal models are widely used as proof-of-concept for immunogenicity, like mice and rabbits.

Mice cannot get infected by HIV-1 nor have a virus closely related to it. Still, mice are the main model for the immunogenicity studies of any vaccine prototype at early preclinical phases. However, immunodeficient mice can be humanised by a $CD34^+$ human haematopoietic stem cell transplant. Some humanised mouse models include the NSG mice (NOD-SCID IL2R-γ_c-deficient mice) or the bone-marrow-liver-thymus transplanted (BLT) mice (Marsden and Zack, 2017). These models are extremely useful for testing antiretroviral therapies and for the study of the latent reservoir and biopharmaceutical therapies, but since they display an artificial immune system where mice elements, such as murine MHC, interact with human TCRs, they need to be further optimised to become a reliable vaccine model (Weichseldorfer *et al.*, 2020). Additionally, more complex mouse models have been employed to dig deeper into the immunological features that are essential for the induction of broad and potent neutralising responses, like the study of the GC, which directs the somatic hypermutation process that can lead to the development of bNAbs (Viant *et al.*, 2020), or the study of germline targeting in adoptive transfer models where transgenic mouse B cells expressing a desired BCR are injected to wild-type mice to evaluate how they are stimulated by different vaccine prototypes (Steichen *et al.*, 2019). All these models help to identify better immunogens and vaccine platforms before moving to NHP models.

3.3. Initial preclinical strategies to induce protective immune responses

Initial attempts at generating protection against HIV-1 by active immunisation focused on classical vaccine strategies, such as pathogen inactivation or attenuation (Daniel *et al.*, 1992), like a disrupted non-infectious SIV that mediated

protection in 2 out of 6 vaccinated macaques (Desrosiers *et al.*, 1989), or an inactivated and adjuvanted SIV that protected 8 out of 9 macaques (Murphey-Corb *et al.*, 1989). Despite this moderate demonstration of efficacy in macaques against SIV, these strategies were not translated into humans due to the threat derived from inefficient pathogen inactivation and presence of viral genetic material and other contaminants that probably interfered favouring the observed protection (Dowdle, 1986; Schild and Stott, 1993).

In parallel to the failure of classical vaccine strategies, advances in molecular biology and recombinant technologies allowed for the development of gp160 and gp120 subunit vaccines, which were safer since they did not contain the HIV-1 genome (Rusche *et al.*, 1987). Preclinical studies in NHP demonstrated how these vaccines were able to induce NAbs. Induction of neutralising responses was thought to be enough to control and prevent HIV-1 infection at that time, since challenging animals with SIV prevented infection and sera from vaccinated animals was able to neutralise some viral strains in *in vitro* neutralisation assays (Robey *et al.*, 1986; Berman *et al.*, 1990), but later it was demonstrated that the outcomes of these trials were highly dependent on the viral strains used and it did not properly recapitulate the real situation (Esparza, 2013). Gp160 subunits present the whole Env molecule, while gp120 vaccines contain the CD4bs and V3, some of the main neutralizable epitopes in HIV-1 (Steimer *et al.*, 1991). These were the initial attempts at rationalising the vaccine design to identify the best targets and epitopes, and it eventually led to the first wave of human vaccine efficacy trials; unfortunately, they did not take enough into consideration the high HIV-1 variability and eventually failed (Gallo, 2005).

Another vaccination strategy evaluated was the use of viral vectors encoding for HIV-1 genes. Among different vectors, poxviruses and adenoviruses have been preferentially tested. They induce a notable cellular response and have demonstrated to work synergistically in heterologous prime-boost strategies when combined with subunit proteins (Patterson and Robert-Guroff, 2008; Kim *et al.*, 2014). The initial viral vectors posed a risk for immunodeficient individuals, such as PLWH, that is why live attenuated viral vectors were developed (Picard *et al.*, 1991). The main attenuated viral vectors developed were derived from poxviruses, either from vaccinia viruses —like Modified Vaccinia Ankara (MVA) and NYVAC—, and canarypox viruses —like ALVAC (vCP1521)—, but can also derive from adenoviruses (García-Arriaza and Esteban, 2014). These vectors can code for various viral proteins, and in the first attempts, *Env* derivatives (gp160 or gp120) were predominantly selected, while later trials also incorporated *gag* and *pol*, alone or in combination (Cox *et al.*, 1993). These viral vectors

encoding for HIV-1 proteins demonstrated being highly immunogenic in laboratory and simian models, also exhibiting protection against HIV-2 infection when expressing HIV-2 antigens, and hence merited further studies in phase I clinical trials (Perkus *et al.*, 1995).

However, most studies that showed protection against SIV infection in NHP models failed in efficacy clinical trials, despite inducing NAbs, highlighting the need for improving the SIV model for HIV-1 vaccine development. One of the limitations of SIV infection in NHP was the use of laboratory-adapted strains, which are easily neutralizable compared to primary isolates from infected patients, and are not representative of circulating HIV-1 strains (Esparza, 2013).

Moreover, although HIV and SIV are closely related viruses, they still have their differences and infect different hosts. Therefore, in order to overcome this limitation, a chimeric SIV that expressed HIV-1 Env instead of SIV Env (SHIV) was developed (Shibata *et al.*, 1990). Additionally, low-dose intravaginal and intrarectal NHP challenge models were developed with the aim to better mimic the natural pathway of HIV-1 infection (McDermott *et al.*, 2004).

Failure of preclinical or clinical trials mostly meant that either the immunogen or the vaccine platform was not optimal and should not lead to the discontinuation of the strategy or vector, but to its further improvement. The main lessons learned from preclinical attempts were that better models and a more rationalised vaccine design had to be performed to reach clinical trials.

3.4. Lessons learned from efficacy clinical trials

Preclinical trials allowed for the identification of multiple tools that demonstrated to be safe in phase I clinical trials and progressed to phase II and finally to phase IIb/III double-blind, randomised, placebo-controlled clinical trials (Robinson, 2002). The first efficacy trial of an HIV-1 vaccine in humans started in 1998, 15 years after the identification of HIV-1 as the causative agent of AIDS. From that point, HIV-1 vaccine efficacy trials (Table 2) have been classically categorised in three different streams that were somewhat sequential: i) protein-based Env vaccines that induce NAbs; ii) viral vector-based vaccines coding for HIV-1 genes to induce cellular responses; iii) combined strategies that induce potent and balanced humoral and cellular responses (Esparza, 2013).

Protein-based Env vaccine trials to induce NAbs took place between 1998 and 2003 and ended with the publication of the results on the Vax003 and Vax004 clinical trials, in which no overall protection was observed in neither (Flynn *et al.*, 2005; Pitisuttithum *et al.*, 2006). Even though they were similar, Vax003 and

Table 2. **HIV-1 preventive vaccine efficacy trials (phase IIb/III)**

Name	Code	Phase	Immunogen	Formulation					Main finding	Study group	Status	Year	Location
				DNA	*Poxvirus*	*Ads*	*Protein*	*Adj.*					
Efficacy trials													
Vax 003	NCT00006327	III	Bivalent clade B&E gp120	—	—	—	AIDSVAX B/E	Alum	No protection	IDU	Complete	2003	Thai
Vax 004	NCT00002441	III	Bivalent clade B&B gp120	—	—	—	AIDSVAX B/B	Alum	No protection. Low Tier1 NAbs	MSM and high risk women	Complete	2004	USA Netherlands
STEP/ HVTN502	NCT00095576	IIb	Clade B *gag*, *pol* & *nef*	—	—	Ad5	—	—	Discontinued. Anti-vector Abs may increase risk of infection	High risk population	Stopped	2007	America Australia
Phambili/ HVTN503	NCT00413725	IIb	Clade B *gag*, *pol* & *nef*	—	—	Ad5	—	—		South-African population	Stopped	2007	South-Africa
RV144	NCT00223080	III	Clade B *gag-pro*; *env* AE Bivalent Clade B&E gp120	—	ALVAC	—	AIDSVAX B/E	—	31.2% protection	Thai population	Complete	2009	Thailand
HVTN505	NCT00865566	IIb	Clade B *gag*, *pol* & *nef* Clades A, B, C *env*	6 p.	—	rAd5	—	—	Stopped, futility. Anti-gp41 nNAbs.	MSM and transgenders	Stopped	2013	USA
UHAMBO/ HVTN 702	NCT02968849	III	Clade B/C *gag-pro* & *env* Clade C gp120	—	ALVAC	—	Cgp120 C	MF59	Stopped, futility. No protection	South-African population	Stopped	2020	South-Africa
IMBOKODO/ HVTN 705	NCT03060629	IIb	Mosaic gag, pol & env Clade C Env trimer	—	—	Ad26	Clade C gp140 trimer	Alum	No significant protection (25.2%)	Women at risk	Active	—	South-Africa
MOSAICO/ HVTN 706	NCT03964415	III	Mosaic *gag*, Clade C *pol* & *env* Mosaic gp120	—	—	Ad26	TV1.Cgp120 1086.Cgp120	Alum	—	MSM and transgenders	Recruiting	—	Europe America
IMBOKODO/ HVTN 705	NCT03060629	IIb	Mosaic *gag*, *pol* & *env* Clade C Env trimer	—	—	Ad26	Clade C gp140 trimer	Alum	—	Women at risk	N.Y.R.	—	Sub-saharan Africa
PrEPVacc	NCT04066881	IIb	Clade C *gag*, *env*, *pol-nef* Clade E *env*; Clade A *gag-pol* Clade B&E g120/Clade C gp140	3 p.	MVA	—	CN54gp140 AIDSVAX B/E	MPLA	—	High risk population	N.Y.R.	—	Uganda

MVA: modified vaccinia Ankara; Ads: adenoviruses; Adj.: adjuvants; MPLA: monophosphoryl lipid A; NAbs: neutralising antibodies; nNAbs: non-neutralising antibodies; IDU: intravenous drug users; MSM: men who have sex with men; N.Y.R.: not yet recruiting.

Vax004 differed in the countries where they were carried out and the target population. Vax004 was performed in developed countries and mainly recruited MSM (clinicaltrials.gov: NCT00002441), while Vax003 took place in Thailand and enrolled intravenous drug users. In these studies, a bivalent recombinant gp120 soluble protein named AIDSVAX adjuvanted with alum was studied, and in each trial the protein was adapted to the circulating strains the vaccinees would mainly face (clinicaltrials.gov: NCT00006327). For instance, Vax004 used AIDSVAX B/B, since subtype B is mainly found in developed countries, while Vax003 analysed the effect of AIDSVAX B/E (Billich, 2001). Despite no overall efficacy was achieved, some subgroups (women and non-whites) showed slight protection that could not reach statistical significance, and it was demonstrated that AIDSVAX constructs were capable of eliciting robust antibody responses (Gilbert *et al.*, 2005).

While these two efficacy trials that aimed at eliciting neutralising responses were finalising, two phase IIb trials (STEP study/HVTN502 and Phambili study/HVTN503) were initiated focusing on the induction of potent T cell responses. These studies delved into the fact that neutralising responses were not associated with slower HIV-1 progression in infected individuals, but cellular responses were (Harrer *et al.*, 1996), and hence could confer better protection against HIV-1. Similar to Vax003 and Vax004, these studies were carried out in two different contexts: the STEP study was performed in countries where the main circulating HIV-1 strain was subtype B and targeted MSM and heterosexual high-risk populations (clinicaltrials.gov: NCT00095576), while the Phambili trial took place in South Africa (clinicaltrials.gov: NCT00413725), where subtype C was the prevalent HIV-1 strain, and the targeted population were individuals with high-risk heterosexual behaviour (Dhesi and Stebbing, 2011). These trials used an adenoviral vector (MRK Ad5) coding for subtype B *gag*, *pol* and *nef* genes that were not adapted to the main circulating HIV-1 clades, the rationale being that T cell responses induce broader responses and can more easily display cross-clade cytotoxic profiles (Coplan *et al.*, 2005). The STEP study initiated vaccination in early 2007, and was halted in late 2007 due to concerns about a higher incidence in the vaccinated group than the placebo group; and, in consequence, so was the Phambili trial (Sekaly, 2008). Further analysis indicated how increased HIV-1 incidence could be associated with pre-existent high anti-Ad5 antibodies, showing how anti-vector antibodies play a crucial role and are a relevant aspect to consider in future vaccine designs (Buchbinder *et al.*, 2008; Gray *et al.*, 2011). Some authors theorised about how anti-vector responses played no role in enhancing HIV-1 infection, but inducing a $CD4^+$ T cell response, the very same cells that HIV-1 infects, was the root of the problem (Barry, 2018).

Additionally, in 2009 the HVTN505 trial was performed in the US and tested in MSM a combination strategy to potentiate cellular responses priming with a DNA mix of 6 vectors coding for subtype B *gag*, *pol*, *nef*, subtype A, B and C *env* and as a boost a mix of 4 rAd5 vector coding for subtype B *gag-pol* and subtype A, B and C *env* (clinicaltrials.gov: NCT00865566). HVTN505 was stopped due to futility in 2013 (Hammer *et al.*, 2013), and despite it induced good humoral and cellular immune responses in most of the patients, only anti-Env $CD8^+$ responses seemed to be enhanced in vaccinated and non-infected individuals (Janes *et al.*, 2017).

In parallel to phase IIb trials that evaluated the effect of inducing potent cellular responses, a trend to develop combination strategies using a priming viral vector that elicited cellular and humoral responses and boosting with soluble proteins to enhance humoral responses gained a lot of focus. That is why, in 2003, the RV144 Trial —also known as "Thai Trial"— was initiated (clinicaltrials.gov: NCT00223080). In this study, a canarypox vector (vCP1521), named ALVAC-HIV, coding for a subtype B *gag-pol* and a membrane-bound CRF01_AE gp120 linked to a subtype B gp41 was administered four times, and alum-adjuvanted AIDSVAX B/E was administered twice together with the third and fourth ALVAC-HIV doses (Rerks-Ngarm *et al.*, 2006). Despite a wave of criticism for choosing vaccine components that did not demonstrate *in vivo* efficacy in previous human trials separately (Burton *et al.*, 2004), RV144 started immunisations in late 2003 and results were published in 2009, demonstrating overall protection of 31% in vaccinated people over placebo controls (Rerks-Ngarm *et al.*, 2009). Even if this protection was considered too low to merit further commercial development, it still is the highest protection ever achieved with a vaccination strategy to date (Russell and Marovich, 2016). Deeper analysis to determine correlates of protection identified that antibodies targeting the V1V2 apex correlated with protection, while anti-Env IgAs were associated with increased risk of infection (Haynes *et al.*, 2012). These anti-V1V2 antibodies were not able to neutralise the virus and it was hypothesised that their protective effect was mediated by ADCC (Wren and Kent, 2011). Further phase II trials on the RV144 vaccinated group tried to elucidate the capacity to recall vaccine-induced immune responses by a late boosting with AIDSVAX 6-8 years after the vaccination (clinicaltrials.gov: NCT01435135, NCT01931358) (Rerks-Ngarm *et al.*, 2017; Pitisuttithum *et al.*, 2020).

RV144 results reignited the HIV-1 vaccine field demonstrating that protection was achievable and led to the design of more combined strategies aiming at eliciting protective responses. The Uhambo/HVTN702 phase IIb/III trial (clinicaltrials.gov: NCT02968849) tried to reproduce the RV144 results while

adapting the vaccine components to clade C, the main circulating strain in South Africa, where it took place (Bekker *et al.*, 2018). Unfortunately, HVTN702 was halted due to futility detected in an interim analysis in early 2020 (Gray *et al.*, 2021).

Overall, the results obtained from clinical trials published to date have demonstrated that protective responses can be achieved, albeit only a modest effect has been elicited with current strategies (Table 2). Combination strategies eliciting both arms of the adaptive response must be pursued, since certain anti-Env antibodies correlated with protection, while cellular mechanisms are vital to prevent latent reservoir formation and cell-to-cell transmission. Furthermore, pre-existing anti-vector immune responses must be carefully considered before choosing a viral vector, since they can hamper the effect of the vaccine leading to counterproductive responses.

Among the three HIV-1 vaccine efficacy trials currently ongoing, there are two using the same strategy adapted to different populations (IMBOKODO/HVTN705 and MOSAICO/HVTN706). HVTN705 is a phase IIb trial being performed in women from sub-Saharan Africa and recently published an interim analysis that demonstrated no significant protectio among vaccinees (25.2%) (Cohen, 2021) (clinicaltrials.gov: NCT03060629), while HVTN706 (clinicaltrials.gov: NCT03964415) is a phase III trial that is still recruiting MSM from North and South America and Europe, including Spain, and is expected to publish the results in 2024. Despite the negative results in Imbokodo, Mosaico will continue as planned (Janssen Vaccines, 2021). Both trials will assess the effect of priming with four doses of 4 Ad26 viral vectors that code 4 mosaic constructs —Mos1.Gag-pol, Mos2.Gag-pol, Mos1.Env and Mos2S.Env—, and boosting with a soluble protein (mosaic gp120 for Imbokodo and clade C Env trimer for Mosaico) with the third and fourth Ad26 mosaic dose. In preclinical and phase I/II trials (clinicaltrials.gov: NCT02315703, NCT02788045) preceding the phase IIb/III assays, Ad26 mosaic vaccines were safe and showed an induction of ADCP-mediating anti-Env antibodies and induction of T cell responses in vaccinees (Baden *et al.*, 2020), a response that was able to mediate protection against SHIV infection in macaques (Barouch *et al.*, 2018).

The remaining phase IIb active clinical trial, which has not yet started recruiting, is known as PrEPVacc (clinicaltrials.gov: NCT04066881). In this study, two vaccinations will be tested against a placebo group. The vaccine components in this study are a DNA vaccine (DNA-HIV-PT123) encoding for clade C *gag*, *env* and *pol-nef*, a bivalent clade C gp140, an MVA coding for a subtype E *env* and subtype A *gag-pol* and also AIDSVAX B/E (Moodie *et al.*, 2020; Hosseinipour *et al.*, 2021). The groups will be distributed so as one group re-

ceives DNA-HIV-PT123 and AIDSVAX on weeks 0, 4, 24 and 48, while the other group receives DNA-HIV-PT123 in combination with the clade C gp140 (weeks 0 and 4) and Clade C gp140 with the MVA vector on weeks 24 and 48. The novelty of this trial is that all groups will be administered PrEP treatment for the duration of the immunisations (Laher *et al.*, 2020).

The main conclusion that these 10 HIV-1 vaccine efficacy trials (7 finished and 3 ongoing) have taught the scientific community is that the final goal of eradicating HIV-1 through the means of prevention will only be achieved with an extremely rational, biologically informed, and highly collaborative vaccine. To generate superior strategies, a deeper understanding of the vaccine candidates and vector repertoires available is key.

3.5. Current platforms in HIV-1 vaccinology

Nearly forty years of vaccine research have yielded a diverse armamentarium of vaccine platforms to fight HIV-1. Either by adapting pre-existent technologies or by creating new platforms, scientists have generated an extensive array of strategies that have proven safe and potentially effective in preclinical trials and are making their way up to early clinical trials. These strategies can come formulated as soluble proteins or multivalent platforms that directly stimulate APCs, or as nucleic acid vaccines encoding for the pathogen-derived antigens that will be produced by the host cells of the vaccinee (Figure 9). Whether the vaccine is directly administered or produced by the cells of the immunised individual, the immunogens will be recognised by APCs and will stimulate the different components of the adaptive response leading to the production of antibodies and cytotoxic responses to train the immune system. Each strategy has its own benefits and drawbacks, which will be summarised below.

3.5.1. Nucleic acid vaccines and delivery

Nucleic acid vaccines were an extensively researched and promising field in the last decades that, however, produced scarce commercially available products until recently, when the SARS-CoV-2 pandemic accelerated the need for readily accessible vaccines (Bezbaruah *et al.*, 2021). Immunogen-encoded nucleic acid vaccines have mainly been developed as a strategy to fight infectious diseases, but they have also been tested as a platform for cancer vaccines and autoimmunity (Yang *et al.*, 2014; Serra and Santamaria, 2019). The main advantage of these types of vaccines is the easiness of producing and adapting —or pseudotyping— the platform to express different immunogens, since the modifications are per-

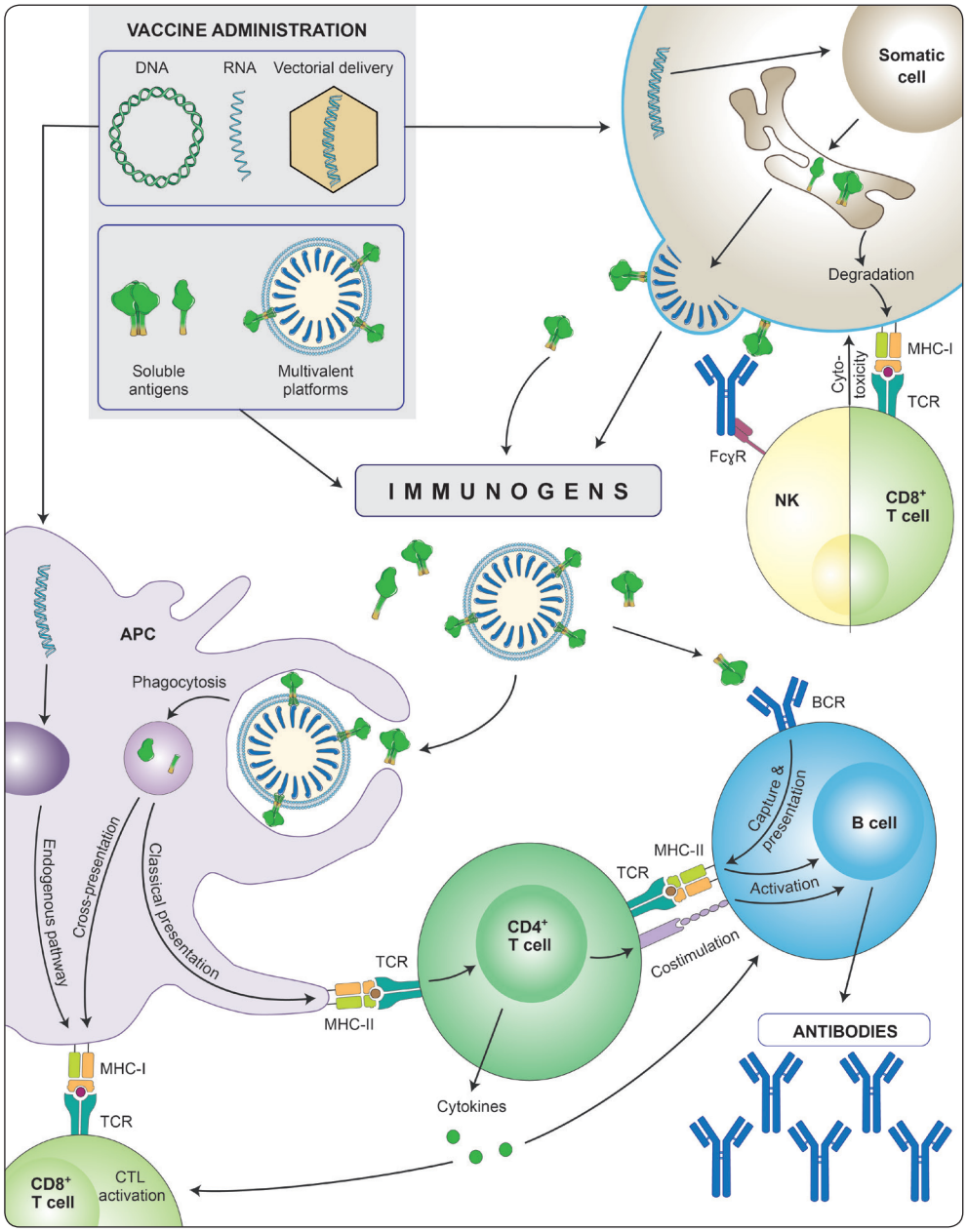

Figure 9. ***Schematic representation of the pathways to immune stimulation by nucleic acid vaccines, subunit antigens and multivalent platforms.*** *Nucleic acid vaccines will be uptaken by somatic cells and produce the immunogen. Alternatively, APCs can also uptake the DNA and produce the antigen, that will be presented by MHC-I molecules, stimulating more potent cellular responses. In any case, antigens produced by somatic cells or directly administered as soluble proteins or multivalent platforms will stimulate the adaptive immune response. Cells: somatic cell (brown), innate antigen-presenting cells (purple), CD4⁺ T lymphocyte (dark green), CD8⁺ T lymphocyte (light green), B lymphocyte (blue), Natural Killer cell (yellow). Green: monomeric/trimeric Env; blue: antibody; grey area: vaccine formulation.*

formed on the DNA level. This situation facilitates vaccine production, purification and quality control, since all the downstream processes will be similar independently of the antigenic content (Hobernik and Bros, 2018).

Nucleic acid vaccines can be categorised into three major groups: viral vectored vaccines, messenger (mRNA) vaccines and DNA vaccines. This field has evolved in parallel with gene therapy, in which the necessity to deliver genes for genetic engineering prompted research and improvements with viral vectors (Ertl, 2016). In the HIV-1 field, the main viral vectors used, as previously detailed in the efficacy trials section, have been adenoviruses and poxviruses, despite a wider arsenal of attenuated viral vectors is available: lentiviral, adenoviral and adeno-associated vectors (AAV), Sendai vectors, poxvirus and vaccinia viruses, among others (Hokello *et al.*, 2021).

Viral vectored HIV-1 vaccines have proven their potential efficacy in humans in the Thai trial, in which ALVAC-HIV —canarypox vector vCP1521— demonstrated protection in combination with the bivalent gp120 soluble protein AIDSVAX. In comparison, the STEP study raised concerns about a high prevalence of anti-vector antibodies in vaccinees and their elicitation in naïve individuals (Gray *et al.*, 2011). Anti-vector immune responses have been one of the main concerns in the gene therapy field, since they can hamper its applicability and, after a single administration, anti-vector responses will be elicited, limiting further administrations (Sasso *et al.*, 2020). Many efforts have been dedicated to developing non-replicating viral vectors for which humans are naïve, and hence no immune response has been previously elicited, like chimpanzee adenoviruses (ChAdV), or rarer adenovirus subtypes (Ad26 or Ad35) (Barry, 2018). Also, attenuated versions of smallpox vaccine strains or *vaccinia* viruses, such as NYVAC, MVA or Tiantan, were developed as poorly immunogenic vectors that potently stimulate immune responses against the encoded extrinsic antigens, and have been extensively assayed in preclinical settings as preventive and therapeutic vaccines (Jacobs *et al.*, 2009). The advantage of using poxvirus vectors is that younger generations have not been exposed to them, since smallpox vaccination was stopped in the late 1970s and the virus was declared eradicated in 1980, hence the immune systems of those born from 1980 on are naïve to smallpox (García-Arriaza and Esteban, 2014).

RNA vaccines have currently drawn all the enthusiasm in the vaccine field owing to their pivotal role in dealing with the SARS-CoV-2 pandemic (Pilkington *et al.*, 2021). Many years of basic research and resources were invested in generating a synthetic mRNA that was not immunogenic and rejected by the host cells (the Karikó paradigm) (Karikó *et al.*, 2008). Additionally, the development of safe and effective delivery systems was key for the success of RNA vaccines,

since RNA is very susceptible to degradation and needs to be encapsulated for better protection (Reichmuth *et al.*, 2016). In the HIV-1 vaccine field, attempts at generating RNA-based vaccines were slowly moving towards clinical trials (Leal *et al.*, 2018; Esteban *et al.*, 2021), but they were facing a certain degree of reluctancy caused by their novelty (Pardi *et al.*, 2018; Jones *et al.*, 2020). However, the rapid approval of BNT162b2 and mRNA-1273 SARS-CoV-2 vaccines and their proven efficacy in a global setting will pave the way for many more RNA-based vaccines to reach advanced clinical trials shortly (Dolgin, 2021), with some attempts at developing HIV-1 vaccines using mRNA strategies currently reaching clinical trials (clinicaltrials.gov: NCT05001373) and surely more to come in the future.

In comparison, DNA vaccines are also starting to display their potential globally by reaching phase I and II clinical trials for HIV-1 vaccines (Table 3), for SARS-CoV-2 (Momin *et al.*, 2021) and other infectious and non-infectious diseases (Lee *et al.*, 2018). Similar to other nucleic acid-based vaccines, the main advantage of DNA vaccines is the straightforwardness at the production, purification and modification levels, and for DNA and RNA vaccines the anti-vector response issue is bypassed (Hobernik and Bros, 2018). However, DNA vaccines are controversial for the risk of inducing anti-DNA antibodies that can lead to systemic autoimmune diseases, which has ignited some mistrust for their use. Additionally, the integration of DNA inside the host cell's nucleus after vaccination is also debated (Langer *et al.*, 2013).

DNA vaccines are often administered in the context of a plasmid DNA vector that encases the gene of interest within a promoter and a poly-adenylation site. These plasmid vectors may also contain an antibiotic resistance gene for selection in prokaryotes during production. One of such vectors is pVAX1, which follows the FDA Recommendations for DNA vaccines (Klinman *et al.*, 2010). pVAX1 is a reduced version of the pcDNA3.1 vector that contains a CMV promoter and a BGH polyadenylation site, while having a kanamycin resistance gene for selection.

The main hurdle that DNA administration faces is its poor incorporation inside host cells, since DNA cannot easily cross the plasma and nuclear membranes. That is why multiple physical and chemical delivery systems to enhance *in vivo* "transfection" of host cells have been described (Jorritsma *et al.*, 2016). Some of these techniques are also shared by RNA vaccination, especially chemical delivery systems such as liposomes, cationic polymers, and other nanoparticles that can encapsulate the nucleic acids and enhance the target cell uptake (Qin *et al.*, 2021). For DNA internalisation, physical techniques are also attractive, especially *in vivo* electroporation, which consists in applying an electrical

Table 3. Clinical trials for HIV-1 DNA vaccines in the last 5 years

Name	Code	Immunogen	Combination	No	Adjuvants	Delivery	RoA	Phase	Main finding	Date
DNA-HIV-PT123	NCT04066881	Clade C *env*, *gag*, *pol-nef*	Subunit/MVA	3	Alum	—	IM	IIb	Ongoing	—
DNA-HIV-PT123	NCT04842682	Clade C *env*, *gag*, *pol-nef*	Subunit protein	3	CD40 mAb	—	IM	I	Ongoing	—
Env-C DNA	NCT04826094	Clade C *env*	Subunit protein	1	Alum/ALF43	—	IM	I	Ongoing	—
Env/Gag DNA vaccine	NCT03409276	Clades A, B, C, A/E *env* Clade C *gag*	Subunit protein	5	—	—	IM	I	Safe & tolerable, immunogenic & broader IRs	2021
p24CE1/2 & p55_DNA	NCT03181789	CE of p24*gag* & full p55*gag*	—	2	IL-12	EP (Ichor)	IM	I	Safe, 50% RR for Th&Tc, EP induced high IRs	2020
DNA Nat-B/ Con-S/ mosaic	NCT02296541	Clade B, Cons. M and Mosaic *env*	MVA	3	—	—	IM	I	N.Y.R	2020
HIV DNA-C CN54ENV	NCT02654080	Clade C *env*	Subunit protein	1	—	EP (Ichor)	IM/ID	I		2019
Pennvax-GP Pennvax-B	NCT02431767	Cons. A&C *env*	—	1	IL-12	EP (Cellectra)	ID/IM	I	Robust Ab and cellular IR	2018
GEO-D03 DNA	NCT01571960	Clade B *env*, *gag*, *pol*	MVA	1	GM-CSF	—	IM	I	Safe, good for priming	2017
pSG2.HIVconsv	NCT01151319	HIV.consv construct	ChAdV or MVA	1	—	—	IM	I	Safe, high Tc	2017
MAG-pDNA	NCT01578889	Clade B *env*, *gag*, *pol*, *nef*, *tat* & *vif*	rVSV	2	IL-12	EP (Ichor)	IM	I	Safe, primes Tc/Th IR	2016

No: number of plasmids; RoA: Route of administration; IM: intramuscular: ID: intradermal; MVA: modified vaccinia Ankara; mAb: monoclonal antibody; IRs: immune responses; CE: conserved element; RR: response rate; Th: T helper lymphocyte; Tc: T cytotoxic lymphocyte; EP: electroporation; N.Y.R.: not yet recruiting; ChAdV: Chimpanzee adenovirus; GM-CSF: granulocyte-monocyte colony stimulating factor; rVSV: replicating vesicular stomatitis virus

field at the site of injection. This procedure serves a double purpose, since it destabilises the plasma and nuclear membranes, generating pores through which the DNA can enter the cell, while it creates an electrical field that will ease DNA migration *in situ* through electrophoresis (Satkauskas *et al.*, 2002). *In vivo* DNA electroporation does not only enhance transfection efficiency, it also destabilises the cells at the electroporation site, which prompts recruitment of innate immune system cells, and hence it indirectly acts as an immune potentiator, having a similar effect as adjuvants (Sällberg *et al.*, 2015). Other physical delivery mechanisms are high-pressure DNA injection and gene gun, but these are less standardised than *in vivo* electroporation.

Overall, nucleic acid strategies are an extremely useful tool as vaccine platforms, that not only have demonstrated a relevant effect in preclinical models, but their efficacy has also been globally challenged in a context of a pandemics situation and have displayed superior characteristics than more classical vaccine strategies. Undoubtedly, these strategies will become essential platforms for the development of vaccines in the HIV-1 field and beyond.

3.5.2. Soluble subunit proteins

Subunit vaccines attracted a lot of interest in early HIV-1 vaccine development, owing to the introduction of recombinant technologies that successfully yielded vaccine prototypes for other infectious diseases in the market (Valenzuela *et al.*, 1982), in parallel to the first years of the HIV/AIDS pandemic. Their safety profile compared to whole vaccines and subunit vaccines isolated from infected patients was an asset, and lead to the first HIV-1 vaccine phase I-III clinical trials.

Initial gp120 subunits prototypes aimed at eliciting neutralising responses, but these strategies faced two major drawbacks: i) the wide diversity and major differences between HIV-1 strains, which makes heterologous or cross-neutralisation a rare event, and ii) immune evasion by virus mutations in individuals with incomplete protection (Bonsignori *et al.*, 2017), leading to an impasse when gp120 subunits AIDSVAX B/B and AIDSVAX B/E did not induce protection in phase III trials (Pitisuttithum *et al.*, 2006). Even when administering a strain-tailored vaccine matched to the most prevalent circulating subtype, no effect was observed.

Currently, one of the most promising prototypes of subunit vaccines are native Env trimers, which present trimeric Env in a stable native conformation, a strategy that has thrust the research on bNAb-like response induction (Klasse *et al.*, 2020). Env trimers are mainly categorised into three groups: NFL trimers

—native flexible linked—, UFO trimers —uncleaved pre-fusion optimised— and SOSIP —soluble-stabilised gp140 with I559P— (Thalhauser *et al.*, 2020). SOSIP trimers contain multiple stabilising mutations: disulphide bridges between gp120 and gp41, a stabilising I559P point mutation, and a truncation at amino acid 664, which confers them similar antigenicity as membrane-bound viral trimeric Env (Sanders *et al.*, 2002). SOSIP trimers were generated using different sequences of HIV-1 Env, starting with primary isolates like JRFL (Sanders *et al.*, 2002), then adapting the platform to BG505 a subtype A transmitter/founder strain (Julien *et al.*, 2015), and more recently, based on ConS and ConM that contain consensus HIV-1 sequences (Sliepen *et al.*, 2019), or GT1.1 that was designed to specifically elicit VRC01-like responses (Whitaker *et al.*, 2019). SOSIP trimers have demonstrated their potential in NHP preclinical experiments, where protection against a Tier2 SHIV was achieved in macaques (Pauthner *et al.*, 2019), and are now steadily reaching phase I clinical trials, with five active trials ongoing (clinicaltrials.gov: NCT03699241, NCT04224701, NCT04177355, NCT03961438, NCT03816137).

Despite their promise and flexibility, most subunit vaccines, including gp120 subunits or SOSIP trimers, are normally adjuvanted since their immunogenicity is lower compared to whole vaccines or nucleic acid vectored strategies.

3.5.3. Multivalent platforms

Another strategy to increase the immunogenicity of subunit proteins is their administration formulated or conjugated with a multivalent platform. These platforms rely on nanotechnology-based strategies like polymeric carriers and liposomal formulations, but also include biological approaches that aim at mimicking the virus morphology, such as Virus-Like Particles (VLPs).

Multivalent platforms come in a wide range of sizes, structures and compositions, and all these properties are key for their increased immunogenicity and better kinetics of immune responses (Thalhauser *et al.*, 2020). Size is a pivotal aspect of these platforms, playing a major role in the half-life of the immunogen and determining the way in which they will interact with their cognate B and T cells (Reddy *et al.*, 2006). Nanoparticle stability is also an important aspect of their immunogenicity, since it will extend bioavailability in the lymph nodes and increase the chances of stimulating B cells while helping with affinity maturation (Tokatlian *et al.*, 2018). Finally, antigen orientation and density are especially important for Env presentation, since they will promote the exposure of relevant epitopes while cross-linking multiple BCRs and triggering potent responses (Hennig *et al.*, 2014).

Synthetic nanoparticles can either be inorganic particles or organic lipidic or protein-based molecules (Brinkkemper and Sliepen, 2019). Self-assembling protein nanoparticles are an attractive strategy since they are easily produced and tailored to incorporate a determined quantity of immunogens per particle. Such is the case of the lumazine-based eOD-GT8 prototype, a vaccine formed by 60-mers of an Env engineered Outer Domain (eOD) immunogen that was designed to trigger VRC01-like germline ancestors, an anti-CD4bs bNAb precursor, and which has been tested in phase I clinical trials achieving the expected outcomes (clinicaltrials.gov: NCT03547245). Other protein-based nanocarriers are ferritin nanoparticles, which can accommodate SOSIP trimers and demonstrated superior neutralising responses in rabbits when compared to the soluble protein (Sliepen *et al.*, 2015).

Liposomes have also been extensively assessed as vehicles for a wide range of applications, such as drug delivery (Bulbake *et al.*, 2017), tolerance induction in autoimmune diseases (Rodríguez-Fernández *et al.*, 2021), nucleic acid vaccine delivery (Jorritsma *et al.*, 2016), or as a vehicle for immunogens (Gao *et al.*, 2018). In these last few years, liposomes have been engineered to accommodate Env SOSIP trimers, and to do so multiple strategies have been followed, like Ni-NTA chelation (Pejawar-Gaddy *et al.*, 2014) or by Michael addition reaction (Pauthner *et al.*, 2017). These liposome-conjugated trimers have proven potent at inducing neutralising responses, and some of them are currently being evaluated in phase I clinical trials (clinicaltrials.gov: NCT03816137, NCT03961438).

Additionally, liposomes have also been engineered to express smaller poorly immunogenic antigens, like gp120 molecules (clinicaltrials.gov: NCT03856996) or the MPER (clinicaltrials.gov: NCT03934541) and are being tested in phase I trials. This strategy to boost the antigen's immunogenicity by presenting it at the surface of a multivalent platform was also previously evaluated by our group, by expressing a MPER-containing gp41 miniprotein (Min) at the surface of different proteoliposomal formulations (Molinos-Albert *et al.*, 2017a). In this study, Molinos-Albert *et al.* identified that more complex membranes containing cholesterol and complex lipids led to better elicitation of 2F5-like NAb responses.

VLPs are a vaccine platform as heterogeneous as viruses themselves, since VLPs are produced with viral structural and/or capsid proteins (Fuenmayor *et al.*, 2017). HIV-1 VLPs are produced by the expression of Gag, the main HIV-1 structural protein. Upon synthesis, Gag migrates to the host cell membrane, where it buds producing enveloped VLPs. This process is similar to HIV-1 virion production (Figure 5) and leads to the formation of non-infectious and non-replicative immature VLPs that will mimic the HIV-1 virion's size and morphology (Cervera *et al.*, 2019).

HIV-1 Gag-VLPs have been used as immunogens to elicit potent cellular responses against Gag or Gag-Pol proteins by vaccination (Paliard *et al.*, 2000; Chege *et al.*, 2013), but also as multivalent immunogen carriers since they can accommodate immunogens at the surface of their lipid membrane. The benefit of using Gag-VLPs as immunogen carriers is that balanced humoral and cellular responses against the immunogen and Gag, respectively, can be elicited. Furthermore, immunogen presentation at VLPs' surface faithfully mimics viral proteins at the surface of a virus, and presents the immunogens in the right orientation, and hence it induces responses that will better engage the virus (Thalhauser *et al.*, 2020).

However, one of the main drawbacks faced by HIV-1 VLPs is that, since VLPs mimic the HIV-1 structure, immunogens are incorporated at a low density at the surface of VLPs. HIV-1 has evolved to evade the immune system by poorly incorporating Env molecules on its surface to reduce antibody avidity, and that stands as a main hurdle in strategies in which high-density is vital to induce potent responses (Klein and Bjorkman, 2010). Therefore, multiple strategies have aimed at increasing immunogen density at the surface of a VLP by modifying the transmembrane or intracellular domains of the immunogen (Deml *et al.*, 1997; Wang *et al.*, 2007). Other groups have tried to enhance VLPs immunogenicity by promoting maturation of VLPs conserving their non-infectious and non-replicative characteristics (Ellenberger *et al.*, 2005; Gonelli *et al.*, 2021).

A relevant aspect of HIV-1 Gag-VLPs is that they can be produced *in vitro* in a wide diversity of platforms with different properties (Cervera *et al.*, 2019), but they can also be produced *in vivo* upon nucleic acid vaccination (Buchbinder *et al.*, 2017). For nucleic acid vaccination, upon co-administration of a Gag-coding vector (either from SIV or HIV-1) and an immunogen (full Env, gp120, SOSIP-trimers, etc.), transfected cells will produce and secrete VLPs with immunogens on their surface that will stimulate B cells similarly to direct administration of VLPs (Figure 9).

The immunogenicity of multivalent VLP platforms presenting various Env-derived immunogens has been assessed in multiple animal models (Table 4). In these preclinical trials, VLPs have been administered as *in vitro* produced VLPs, as nucleic acid vectored vaccines or as combined DNA/VLP strategies. Overall, these studies have demonstrated that VLPs can induce potent cellular responses against Gag and elicit superior antibody levels compared to subunit proteins, owing to multivalent presentation, better immunogen orientation, synergic combinations, right adjuvant selection and/or intrastructural help (ISH). ISH is a phenomenon in which the immunogen will bind to its cognate BCR and trigger internalisation of the whole multivalent platform, which will lead to the pres-

Table 4. Immunogenicity studies of VLPs as vaccine candidates for HIV-1

Immunogen	Adj.	Aim	Production	Model	Regimen	RoA	Major findings	Authors
HIV-1 Gag VLPs								
Subtype B Env	—	CFA, IFA	Insect cells	BALB/c mice	Homologous	N.D	Strong anti-Gag weak anti-Env responses	Turong *et al.*, 1996
Subtype B gp120	—	Test Gag VLPs in models w/ and w/o gp120	Insect cells	BALB/c, rabbits and macaques	Homologous	IP and IM	Induction of both arms of the IR	Wagner *et al.*, 1996
Subtype B gp120	—	Test surface Env or recombinant Gag-Env	Insect cells	Macaques	Homologous	IM	No protection against SHIV	Wagner *et al.*, 1998
Subtype B gp120	Alum	Test surface Env or recombinant Gag-Env	Insect cells	Macaques	Homologous VLP or heterologous SFV/VLP	IV/SC and IM	Reduced SHIV viral oad in macaques	Notka *et al.*, 1999
Subtype B Env	CpG	Compare Env-VLP, nude VLP & Env	COS cells	BALB/c mice	Homologous (VLP vs Prot)	IN	Superior Ab & cellular response in Env-VLP	McBurney *et al.*, 2005
Subtype B Env	CpG	Immunogenicity of VLPs w/ & w/o inactive RT	COS cells	BALB/c mice	Homologous	IN	Similar immunogenicity	McBurney *et al.*, 2006
Clade B gp160	CCL28	Test effect of CCL28	HEK293T cells	BALB/c	Homologous	IM	Enhanced NAbs in CCL28-VLP group	Rainone *et al.*, 2011
Truncated gp41	—	Generate anti-MPER bNAbs	Insect cells	Guinea pig	Homologous DNA vs VLP	IM	Higher induction of anti-MPER antibodies	Ye *et al.*, 2011
Clade B gp120/ gp41	TLR ligands	Induce bNAbs	HEK293 cells	C57BL/6J	Only VLP	IN	TLR3 agonist promotes NAbs induced by VLPs	Poteet *et al.*, 2016
SIVmac239 Env	Alum or TLR ligands	Test adjuvant NPs with VLPs	HEK293F cells	Macaques	VLP or protein w/ or w/o adjuvant.	Hock	Long-lasting response by adjuvanted VLPs	Kasturi *et al.*, 2017
Clade B gp160	MPLA, Adjuplex	Induce bNAbs	HEK293T cells	Rabbit (NZW)	Only VLP or heterologous	IM	Promote CD4bs NAbs w/ moderate breadth by VLPs	Crooks *et al.*, 2017
Consensus Group M gp145	CCL20	Induction of mucosal IR	Insect cells	BALB/c	Only VLP	IM/IN/ IV	CCL20 enhances mucosal immunity induced by VLPs	Sun *et al.*, 2017
Clade B Env	Adjuplex	Induce bNAbs	HEK293F cells	Rabbit	Heterologous (DDVVV)	—	Enhanced Ab response by 4E10-selected VLPs	Beltran-Pavez, *et al.*, 2018
Clade A gp120/140	Eurocine	Induction of mucosal Abs	Insect cells	Rhesus macaque	Heterologous (D/V)	IN/IM	Higher Ab with IN VLP prime + IM VLP boost	Buonauguro *et al.*, 2018
MPER-V3	—	Evaluation high-copy MPER	—	BALB/c	Homologous or heterologous VLP	—	Th2-like responses in heterologous	Tohidi *et al.*, 2019
Subtype B (AD8) SOSIP Env	CpG	Evaluation of mature VLPs	HEK293T cells	BALB/c	Homologous	IP and SC	Broader NAbs in mVLPs, but anti-Expi response	Gonelli *et al.*, 2021

Adj.: adjuvant; RoA: route of administration; CFA: complete Freund adjuvant; IFA: incomplete Freund adjuvant; N.D.: not determined; VLPs: virus-like particles; w/: with; w/o: wiithout; IP: intraperitoneal; IM: intravenous; SC: subcutaneous; IN: intranasal; IR: immune response; SHIV: chimaeric simian-human immunodeficiency virus; Semliki Forest virus; Ab: antibody; RT: reverse transcriptase; Prot: protein; bNAbs: broadly neutralising antibodies; TLR: Toll-like

Table 4. *Continued*

Table 4. Immunogenicity studies of VLPs as vaccine candidates for HIV-1 *(Continued)*

Immunogen	Adj.	Aim	Production	Model	Regimen	RoA	Major findings	Authors
Nucleic acid HIV-1 Gag VLPs								
Subtype B Env	—	Test DNA/MVA vaccine forming VLPs	*In vivo*	Macaques	Heterologous (DMM)	IM	Superior Ab response in VLP constructs	Smith *et al.*, 2004
CRF02_AG Env	—	Test DNA/MVA CRF02_AG in mVLPs	*In vivo*	Macaques	Heterologous (DDDM)	IM	Better immune responses in mVLPs	Ellenberger *et al.*, 2005
Clade B Env	GM-CSF	Safety and immunogenicity	*In vivo*	Humans	MVA	IM	Safe, good regimen for priming	Buchbinder *et al.*, 2017
Clade C gp145	—	Compare combine Gag-Pol-Env vs MVAs	*In vivo*	BALB/c	MVA	IM	Superior Ab & CTL in the combined MVA	Perdiguero *et al.*, 2019
Subtype C gp160	—	Increase Env density at VLP surface	*In vivo*	Rabbit	Heterologous (DDMMPP)	IM	No high-density Env Tier 2 autologus NAb	Chapman *et al.* 2020
Combined Nucleic acid VLPs and Gag-VLPs								
Subtype B Env	QS21	Assess immunogenicity	Vero cells *In vivo*	Macaques	Heterologous (D/V/A)	IM	Autologous NAbs and CTL	Montefiori *et al.*, 2001
Subtype B Env	—	Evaluate VLP as a boost for D/Fpox	Vero cells *In vivo*	Rabbits	Heterologous (D/Fpox/V)	ID	VLP boosting elicits potent Ab	Radaelli *et al.*, 2003
Subtype B Env	—	Compare heterologous immunisation	Vero cells *In vivo*	BALB/c mice	Heterologous (3xD/Fpox+VV)	IM/ SC	NAbs & CTLs control env-tumour cells	Radaelli *et al.*, 2007
Clade A Gp120	Eurocine	Compare mucosal immunisation	Insect cells *In vivo*	BALB/c mice	VV vs DV	IN	Superior Ab & CTL with DV	Buonauguro *et al.*, 2007
Clade B gp160 and Gp120	—	Check VLPs produced in S2 cell platform	S2 cells *In vivo*	BALB/c	Heterologous (DDVVV)	SC	Antibody induction and modest neutralisation.	Yang *et al.*, 2012
Gp41 variants	—	Induce anti-MPER bNAbs	HEK293T *In vivo*	BALB/c	Heterologous (DDDVVV)	SC	Trimeric MPER increases Ab titres.	Toukam *et al.*, 2012
Clade B gp140	—	ISH testing	HEK293T *In vivo*	C57BL/6J	Heterologous (Ad/DNA+VLP)	Foot-pad	Gag boosts Env via ISH	Nabi *et al.*, 2013
Clade B Env	Alum or CpG	To test mixing PrEP and vaccine	COS cells *In vivo*	Rhesus macaque	Heterologous (DDVVV)+PrEP	IM/IN	PrEP+vaccine induce higher protection	Ross *et al.*, 2014
Truncated gp41	Carbo-pol974	Induce anti-MPER bNAbs	HEK293F *In vivo*	Rabbit (NZW)	Heterologous (DDVV)	IM	Anti-MPER Ab and low NAbs by gp41-DDVV	Benen *et al.*, 2014
Clade B and C Env	—	Test CT on VLP immunogenicity	Insect cells *In vivo*	Guinea pig	Heterologous (DDVV)	IM	Modified Env CT enhances VLP IR	Vzorov *et al.*, 2016
SIV239 Env	CD40L, MPLA, R848	Induce protective IR in rhesus	—	Rhesus macaque	Heterologous (DDMMV)	Hock	Partial protection in DDMMV group	Iyer *et al.*, 2016
Subtype B gp140	IL-12, IL-28	Induce balanced response by ISH	293T cells *In vivo*	BALB/c mice	DD vs DDV	IM	Higher Ab & CTL by heterologous ISH-based vaccine	Storcksdieck genannt Bonsmann *et al.*, 2016
Subtype B gp120	c-di-GMP	Test *in vivo* EP in an heterologous regimen	Insect cells *In vivo*	BALB/c mice	Heterologous (DDVV)	SC	Th1-like response in DDVV w/ NAb & CTL	Huang *et al.*, 2017
Subtype B Env	R848	Test PIV vector as a prime	FreeStyle 293 *In vivo*	Macaques	Heterologous (PIV/VLP)	IN/IM	Potent IR, previous anti-PIV exposition no major effect	Xiao *et al.*, 2021

receptors; NP: nanoparticle; CD4bs: CD4 binding site; mVLPs: mature virus-like particles; MVA: modified vaccinia Ankara; GM-CSF: granulocyte-monocyte colony stimulating factor; CTL: cytotoxic T lymphocyte; FPox: fowlpox; MPER: membrane proximal external region; PrEP: pre-exposure prophylaxis; ISH: intrastructural help; MPLA: monophosphoryl lipid A; EP: electroporation; PIV: parainfluenza virus.

entation of immunogen-derived epitopes and other epitopes within —like Gag— through MHC-II molecules, seeking $CD4^+$ Th validation, and thus increasing the chances of $CD4^+$ Th costimulation (Elsayed *et al.*, 2018; Klessing *et al.*, 2020).

Despite these notable improvements in immunogenicity, none of the strategies induced a bNAb-like response, indicating that both the VLP platform and the immunogen still need to be improved.

3.6. Adjuvants

Vaccine adjuvants are an essential tool to enhance the immunogenicity of subunit proteins and less potent vaccines, but also can help to skew humoral and cellular responses towards more beneficial $CD4^+$ Th and $CD8^+$ Tc profiles (Shah *et al.*, 2017). The role of adjuvants is to trigger and stimulate innate cells that will help to assemble a superior adaptive response at the site of injection, mostly by PRR activation and recruitment of APCs. In HIV-1 vaccine strategies, multiple adjuvants have been tested in combination with immunogens and vectors and demonstrated their safety and favourable immune response induction (Ratnapriya *et al.*, 2021).

Adjuvants can be broadly divided into different groups according to their composition: pathogen-derived adjuvants —Freund adjuvant, thermolabile toxins or lipopolysaccharide (LPS)—, alum salts, lipid emulsions —squalene, monophosphorylate A (MPLA), liposomal formulations—, co-receptors and cytokines —CD40L, GM-CSF, IL-2, IL-12, IL-15, IL-28, CCL20, CCL28— and TLR agonists —TLR4 [LPS, MPLA, AS01B (MPLA/QS-21)], TLR5 (flagellin), TLR7/8 (ssRNA and 3M-052) and TLR9 (CpG)— (Rao and Alving, 2016; Liu and Ostrowski, 2017). Some of the main adjuvants that have been tested in clinical trials for HIV-1 vaccines are alum phosphate in combination with AIDSVAX gp120 proteins in the Vax003/Vax004 and in the RV144 efficacy trials (clinicaltrials.gov: NCT00002441, NCT00006327, NCT00223080), as adjuvant to gp140 trimers in HVTN705 and HVTN706 (clinicaltrials.gov: NCT03060629, NCT03964415), and in some trimeric Env trials (clinicaltrials.gov: NCT03878121, NCT03783130). Also, MF59 emulsion was tested as an adjuvant in HVTN702, and is being further tested as a subunit protein adjuvant in phase I/II trials like HVTN107, HVTN120 and HVTN108 (clinicaltrials.gov: NCT03284710, NCT03122223, NCT02915016). AS01B, a complex adjuvant containing MPL and QS-21, is being evaluated in trials for its ability to skew immune responses towards Th2 profiles and elicit better neutralising responses (Nielsen *et al.*, 2021). And for DNA vaccines, IL-12 coding plasmids are also being tested in phase I HIV-1 clinical trials (Eusébio *et al.*, 2021; clini-

caltrials.gov: NCT01578889, NCT02431767, NCT03181789). Finally, many lipid-based adjuvants are included in liposome formulations to deliver immunogens (Wang *et al.*, 2019).

3.7. Immunisation strategies

The vaccine armamentarium available to generate preventive vaccination strategies for HIV-1, as previously detailed, is diverse and key to developing better immunisation strategies. However, many groups have reported that a successful HIV-1 vaccine will not only come from the identification of immunogens and platforms that elicit potent responses, but also from the characterisation of which platforms, immunogens and adjuvants synergise better to induce superior neutralising and effector-mediating antibodies together with effective cellular responses (Excler and Kim, 2019). The RV144 trial is a clear example of that, since AIDSVAX, a component that did not elicit protecting responses on its own, managed to induce moderate protection in combination with ALVAC-HIV (Kim *et al.*, 2014).

Another paradigm on the relevant role of sequential immunisation strategies is the elicitation of bNAbs, where three sequential steps may be essential for bNAb induction: i) germline targeting with a priming immunogen, ii) shepherding with another immunogen that helps antibodies undergo affinity maturation, and iii) polishing with a native Env molecule (Burton, 2019).

Overall, combining novel platforms and immunogens with pre-existing technologies into a rational and informed strategy aiming at eliciting balanced humoral and cellular responses will be the keystone to achieve HIV-1 prevention by vaccination. In this regard, our work has focused on the development of new high-density antigen exposing VLPs using a previously described prototype of Env-based immunogen (gp41-Min) that is immunogenic in proteoliposomal formulations (Molinos-Albert *et al.*, 2017a).

Hypothesis and Objectives

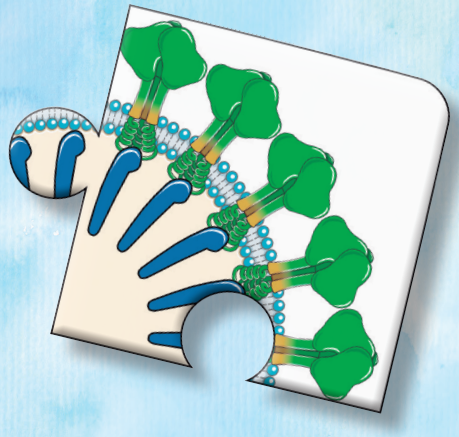

Hypothesis

HIV-1 has developed several strategies to avoid the induction of potent and protective immune responses and to evade their effect. Among them, the low incorporation of Env on the viral surface reduces antibody avidity and may hamper the elicitation of NAbs. To date, no preventive HIV-1 vaccine has shown a significant efficacy at inducing protective responses.

HIV-1 Gag-based VLPs are a safe vaccine platform that mimic HIV-1 structure, which results in poor incorporation of immunogens on their surface. Gag is the only protein needed for the formation of HIV-1 derived VLPs, which buds to the host cell membrane and incorporates 2,500 Gag proteins/VLP. To overcome the limitation of poor incorporation of immunogens on the VLP surface, we hypothesised that fusing an immunogen of interest to Gag through the gp41 transmembrane domain would enforce a high density of immunogens at display, thus potentially inducing a robust and protective humoral immune response. The selected immunogen was a previously described gp41-based immunogen (gp41-Min) (Molinos-Albert *et al.*, 2017a).

Objectives

The main aim of this project is to fully characterise the potential of our fusion-protein HIV-1 Gag-based enveloped VLP platform and test *in vivo* its immunogenicity and capacity to mediate protection in animal models. The specific objectives to fulfil this aim are:

1. To characterise and optimise the antigenicity, the production and the purification of MinGag-VLPs.
2. To adapt Gag-VLPs and MinGag-VLPs into DNA-based vaccine strategies.
3. To test the immunogenicity of MinGag-VLPs in homologous and heterologous vaccine regimens using DNA-based and/or purified VLPs.
4. To develop an *in vivo* mouse model for the assessment of immune-mediated protection and test MinGag-VLPs in said model.
5. To assess the versatility of high-density antigen enveloped Gag-based VLPs to present other relevant HIV-1 immunogens at its surface.

Materials and Methods

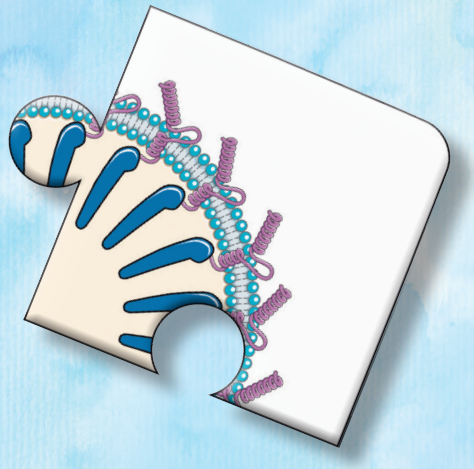

1. Virus-Like Particle design

HIV-1 Gag fusion-protein Virus-Like Particles (VLPs) were designed as a means of displaying a dense array of antigens on a surface that simulates a viral envelope and with the objective of inducing potent immune responses capable of mediating protective immunity. These fusion-protein based retroviral VLPs were protected by intellectual property rights (Patent WO/2018/020324; PCT/IB2017/001101) and further optimised in this project.

1.1. Fusion-protein based VLP strategy

HIV-1 Gag-based VLPs are enveloped particles that have a cell-derived lipid membrane. The fusion-protein based VLP strategy was designed to have four different structural elements according to its enveloped structure (Figure 10). From N- to C-terminus, these main structural domains were: i) an immunogen of interest accommodated at the VLP lipid surface; ii) a transmembrane domain that crosses the lipid VLP envelope; iii) a linker between the transmembrane domain and HIV-1 p55Gag, and iv) p55Gag as the main VLP structural protein (Figure 10D).

The initial fusion-protein VLP design *mingag* was generated with a codon optimised HIV-1 subtype B gp41 miniprotein ("*gp41-min*"), which contained the extracellular domains Heptad Repeat 2 (HR2), the Membrane Proximal External Region (MPER) and the transmembrane domain [HXB2: 8057-8345, (*HIV Database*)] (Figure 10). *Gp41-min* was fused with a codon optimised HIV-1 subtype B gag_{HXB2} (Molinos-Albert *et al.*, 2017a). HIV-1 group M subtype B is the most extensively studied variant, since it is the most prevalent variant in developed countries, and therefore HXB2 has been established as an HIV-1 consensus or reference strain, even though it only represents 12% of global HIV-1 infections. A flexible GGGS (3 glycines and 1 serine) linker was introduced between the C-terminus of the transmembrane domain

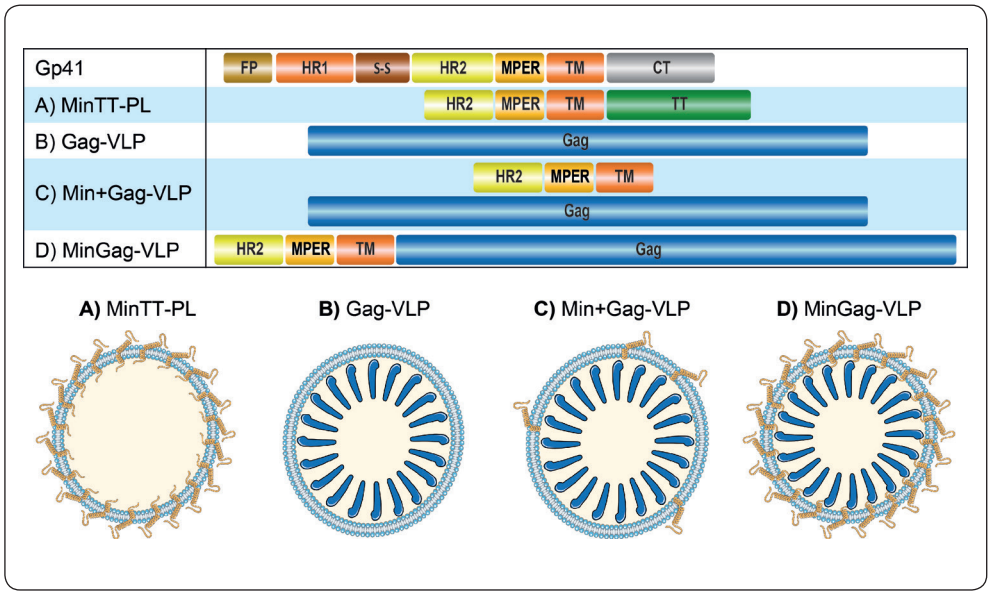

Figure 10. ***Schematic representation of proteoliposomes and nude, low- and high-density Virus-Like Particles (VLPs).*** *Gp41-Min is a gp41 miniprotein that contains the Heptad Repeat 2 (HR2), the Membrane Proximal External Region (MPER) and the transmembrane domain (TM) without the cytoplasmic tail (CT), the fusion protein (FP) and the Heptad Repeat 1 (HR1).* **A)** *Proteoliposomes were chemically produced with a Gp41-Min recombinant protein with a tetanus toxoid tail (TT) and a mix of lipids.* **B)** *Nude Gag-VLPs were generated by transfection of only* gag. **C)** *Low-density VLPs are produced by co-transfection of* gp41-min *and* gag. **D)** *High-density VLPs were produced by transfection of a fusion protein* mingag *construct.*

and the N-terminus of Gag to allow for independent movements in both domains. The initial methionine of Gag was removed.

1.2. Cloning of immunogens and vectors

The *mingag* VLP construct was generated with the GeneArt service (ThermoFisher Scientific, Waltham, MA, USA) into a pcDNA3.1 vector. The *mingag* construct included various restriction enzyme sites to facilitate the cloning of different immunogens and the use of different vectors (Figure 11). The sequence starts with a *KpnI* restriction site (GGTACC) at the 5' end of the gene of interest, immediately followed by a Kozak sequence (GCCACC) and the start codon (ATG). Then, a *BamHI* restriction site (GGATCC) was included within the GGGS-linker sequence (GGCGGAGGATCC) between the transmembrane domain and gag_{HXB2}. Finally, at the 3' end of gag_{HXB2} a pair of stop codons was included followed by a *XhoI* restriction site (TGATGACTCGAG).

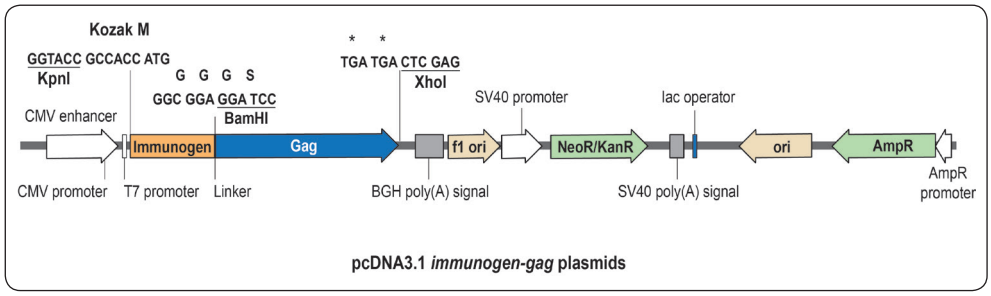

Figure 11. ***Linear diagram of pcDNA3.1* immunogen-gag *plasmids***. *Each* immunogen-gag *construct had a* KpnI *restriction site upstream of the Kozak sequence (GCCACC), a* BamHI *target inserted in the GGGS linker, and a* XhoI *target after the stop codons (**). The construct was regulated by a Cytomegalovirus (CMV) promoter and enhancer and had a Bovine Growth Hormone (BGH) polyadenylation signal. The plasmid had an antibiotic resistance gene for eukaryotic selection (NeoR/KanR: neomycin resistance) and an antibiotic resistance gene for prokaryotic selection (AmpR: ampicillin resistance).*

1.2.1. Transformation, cryopreservation and DNA purification of VLP plasmids

To generate large quantities of *mingag* plasmids or *immunogen-gag* constructs (Table 5 and Table 6) in a pcDNA3.1 vector, OneShot™ TOP10 Chemically Competent *E. coli* were transformed with pcDNA3.1-*mingag* according to the manufacturer's protocol (ThermoFisher Scientific). Briefly, the plasmid was re-suspended in 50 microlitres (µl) of nuclease-free H_2O (ThermoFisher Scientific); meanwhile, the cells were thawed on ice. One µl of DNA was transferred into the vial of TOP10 cells which were then incubated for 20 minutes (min) on ice. The cells were heat-shocked at 42 °C for 30 seconds (s) and transferred immediately on ice. Super Optimal Broth medium was added to the cells at a 1:5 ratio and the mix was incubated for 1 hour (h) at 37 °C and horizontal shaking at 225 revolutions per minute (rpm). After that, 100 µl of the bacteria were seeded on a Lysogeny Broth (LB) agar plate containing 100 micrograms/millilitre (µg/mL) ampicillin (ThermoFisher Scientific) and grown overnight (o/n) at 37 °C. The day after, a single colony was picked and seeded into a 13 mL culture tube (Sarstedt, Nümbrecht, Germany) with 3 mL of LB + 100 µg/mL of ampicillin, and was grown o/n at 37 °C and 225 rpm agitation. Once grown, 0.5 mL of the medium were collected for long-term freezing at –80 °C in a 30% glycerol solution, while the rest was used for plasmid extraction.

For plasmid DNA extraction, a NucleoSpin Mini kit (Macherey-Nagel, Bethlehem, PA, USA) was used. For that, the remaining 2.5 mL of bacteria culture from the previous step were centrifuged at 3,000 relative centrifugal forces (× g) for 15 min and the supernatant was discarded. The pellet was resuspended in 150 µl of buffer A1, followed by the addition of 250 µl of lysis A2 buffer. The

lysate was mixed by inversion and incubated for 2 min at room temperature (RTemp). Then, 350 µl of neutralising A3 solution was added and homogenised by inversion. The mix was centrifuged for 5 min at 11,000 × g and 750 µl of the supernatant were transferred to a Nucleospin column, which was then centrifuged for 2 min at 2,000 × g. The flowthrough was discarded, and the column was washed with 450 µl of buffer AQ for 3 min at 11,000 × g. Finally, the plasmid was incubated for 1 min with 50 µl of elution AE buffer and the column was centrifuged at 11,000 × g for 1 min. The eluted plasmid was quantified by absorbance determination at 260 nm using a Nanodrop One (ThermoFisher Scientific).

1.2.2. Digestion, ligation and sequencing

To optimise the expression of Min on the surface of VLPs, Min variants with different transmembrane and linker domains were generated by gene synthesis (ThermoFisher's GeneArt Synthesis platform) (Table 5) and cloned into the pcDNA3.1-*mingag* plasmid by cutting out *min* with *KpnI* and *BamHI* restriction enzymes.

To clone *min* variants in the pcDNA3.1-*mingag* vector, the plasmid was sequentially digested using FastDigest *KpnI* and *BamHI* restriction enzymes (ThermoFisher Scientific) according to the manufacturer's protocol. Briefly, the reaction mix was prepared in a final volume of 35 µl with 1X FastDigest Green Buffer and 3 µg of DNA. The mix was incubated with 1.5 µl of the first restriction enzyme for 15 min at 37 °C and heat-inactivated for 5 min at 80 °C. A

Table 5. List of transmembrane and linker *mingag* variants for immunogen optimisation

Vector	Construct name	Min prot. seq.	Transmembrane prot. seq.	Linker	Gag
pcDNA3.1 & pVAX1	*gag*	—	—	—	✔
	mingag	MWLQSLLLL-GTVACSISIWN-HTTWMEW-DREINNYTSLI-HSLIEESQN-QQEKNEQEL-LELDKWASL-WNWFNITNWL-WYIKL	FIMIVGGLVGL**R**IVFAVLSIVNR	GGGS	✔
	min(gp41RAtm)gag		FIMIVGGLVGL**A**IVFAVLSIV	GGGS	✔
	min(CD22tm)gag		VAVGLGSCLAILILAICGL	GGGS	✔
	min(CD36tm)gag		LLGLIEMILLSVGVVMFVAFMI	GGGS	✔
	min(CD44tm)gag		WLIILASLLALALILAVCIAV	GGGS	✔
	min(NL)gag		FIMIVGGLVGLRIVFAVLSIVNR	—	✔
	min(AEA)gag		FIMIVGGLVGLRIVFAVLSIVNR	AEAAAKAGS	✔
	min(APA)gag		FIMIVGGLVGLRIVFAVLSIVNR	APAPAPAGS	✔
pcDNA3.1	*min(tm)*		FIMIVGGLVGLRIVFAVLSIVNR	—	—

min(gp41RAtm)gag or *min(RA)gag*: R→A substitution at the transmembrane domain (tm).

second round of digestion was performed after the addition of the second restriction enzyme. Then, the digested plasmid sample was directly loaded into a 1% agarose gel with 1X SYBR® Safe DNA gel stain (ThermoFisher Scientific) and run for 20 min at 135 volts (V). The agarose gel was exposed to UV light in a GelDoc-It® Gel documentation system (Analytik Jena, Jena, Germany) and the bands of interest were cut with a scalpel.

For the recovery of the digested DNA, Zymoclean™ Gel DNA Recovery Kit (Zymo Research, Irvine, CA, USA) was used according to the manufacturer's protocol. Shortly, excised bands were incubated at 50 °C for 10 min with 3 volumes (vol) of ADB buffer. The mix was transferred into a Zymo-Spin™ column and centrifuged for 30 s at 11,000 × g. The column was washed twice with 200 µl of DNA wash buffer 30 s at 11,000 × g. Finally, the column was incubated for 1 min with 15 µl of DNA elution buffer and centrifuged for 1 min at 11,000 × g. DNA yield and purity were assessed with Nanodrop One (ThermoFisher Scientific).

The various *KpnI* and *BamHI*-digested *min* constructs (Table 5) were ligated into a *KpnI*- and *BamHI*-digested pcDNA3.1-*mingag* plasmid with the T4 DNA Ligase (ThermoFisher Scientific) following the manufacturer's protocol. In short, 50 nanograms (ng) of the purified digested vector were mixed at a 3:1 ratio (insert:vector) with the digested insert plus 2.5 international units (IU) of T4 Ligase and 1X Ligation buffer in a total of 10 µl. The mix was incubated o/n at RTemp and dialysed for 20 min in distilled water (dH_2O) with a "Series V" dialysis membrane (Merck & Co., Kenilworth, NJ. USA). The full dialysed material was transformed into OneShot™ Chemically Competent *E. coli* (ThermoFisher Scientific) following the aforementioned protocol.

The same cloning protocol was used to generate new VLP constructs coding for other *env*-related immunogens (Table 6).

Table 6. List of *immunogen-gag* constructs designed in this project

Construct name	Signal peptide	Immunogen Size	Main epitopes targeted by bNAbs
RedMinGag	CD5	91 aa	2F5, 4E10, 10E8
MinGag	CD5	103 aa	2F5, 4E10, 10E8
RSC3-MPER-Gag	CD5	392 aa	b12, 2G12, 2F5, 4E10, 10E8
RSC3(V1V2)-MPER-Gag	CD5	459 aa	b12, 2G12, PG9, PGT145, 2F5, 4E10, 10E8
V1V2-RSC3-MPER-Gag	CD5	478 aa	b12, 2G12, PG9, PGT145, 2F5, 4E10, 10E8
Env-B41(ΔHR1)-MPER-Gag	H5	604 aa	All targets
Env-B41(SOSIP)-MPER-Gag	H5	705 aa	All targets

bNAbs: broadly neutralising antibodies; RSC3: Resurfaced Stabilised Core 3; MPER: Membrane Proximal External Region; Env: envelope glycoprotein; SOSIP: soluble stabilised I559P Env trimer.

All constructs were cloned into a pVAX1 vector (ThermoFisher Scientific) using two FastDigest *KpnI* and *XhoI* restriction enzymes (ThermoFisher Scientific) and following the same previously detailed cloning protocol. pVAX1 is an FDA-approved vector used in the generation of DNA vaccines. It has the same backbone as pcDNA3.1 but it lacks the eukaryotic selection antibiotic resistance gene (*neomycin*), and instead of having an ampicillin-resistance gene for prokaryotic selection, it has a kanamycin-resistance gene, to avoid allergic reactions against ampicillin contaminants from plasmid production.

All plasmids were sequenced by Sanger at IrsiCaixa's Sequencing Platform. All inserts were amplified using a T7 sense primer (5'-TAATACGACTCAC TATAGGG-3') and a BGH antisense primer (5'-TAGAAGGCACAGTCG AGG-3'). Sequencing PCR master mix contained 200 ng of the plasmid, 500 ng of either T7 sense or BGH antisense primer, 1% dimethyl sulfoxide (DMSO), 0.5X Sequencing buffer and 2X BigDye™ Terminator v3.1 (ThermoFisher Scientific) in a total reaction of 10 µl. PCR amplification cycles were: i) 1 cycle of 3 min at 94 °C; ii) 25 cycles of 1 min at 94 °C, 25 s at 52 °C and 2 min at 60 °C, and iii) samples were held at 4 °C. After amplification, DNA precipitation was performed. First, DNA was pelleted at 2,000 × g for 20 min with 8.3 millimolar (mM) of ethylenediaminetetraacetic acid (EDTA) (ThermoFisher Scientific) and 80% ethanol. The supernatant was removed, and the DNA was washed in 70% ethanol and centrifuged for 5 min at 2,000 × g. Finally, the pellet was dried and resuspended with 15 µl of formamide. Samples were run in an ABI PRISM 3100 Genetic Analyzer (Abbott, Chicago, IL, USA) and analysed with Sequencher 5.1 (Gene Codes Corporation, Ann Arbor, MI, USA).

1.2.3. Production of plasmids for transfection and vaccination

All plasmids coding for the different MinGag variants and immunogen-Gag constructs were purified for transfection with the HiSpeed Plasmid Maxi Kit (QIAGEN, Hilden, Germany). For any plasmid, the protocol consisted in growing 250 mL of bacteria culture in LB + 100 µg/mL of ampicillin (pcDNA3.1 plasmids) or in LB + 30 µg/mL of Kanamyicin (pVAX1 plasmids) o/n at 37 °C and 225 rpm orbital shaking. Following the manufacturer's protocol, cells were pelleted at 3,000 × g for 20 min and resuspended in 10 mL of buffer P1. Cells were lysed by the addition of 10 mL of buffer P2 and, after 5 min of lysis, the reaction was stopped by adding 10 mL of pre-chilled neutralising P3 buffer. The lysate was transferred into a QIAfilter Cartridge and incubated for 10 min at RTemp, after which a plunger was inserted in the Cartridge to transfer the cleared lysate into a QBT equilibrated HiSpeed Tip. Once the whole lysate

had flown through the HiSpeed Tip, the tip was washed with 60 mL of QC Wash buffer and eluted with 15 mL of QF elution buffer. The DNA was precipitated by adding 10.5 mL of isopropanol to the eluate and incubated for 5 min. After that, the sample was drawn through a QIAprecipitator Module and it was washed twice with 70% ethanol. Finally, the sample was eluted with a TE buffer. Samples were sterilised with a 0.2 µm UltraFree-MC filter (Merck & Co.) at 10,000 × g for 5 min. The plasmid's yield and purity were quantified by absorbance determination at 260 nm with a Nanodrop One (ThermoFisher Scientific).

All pVAX1 plasmids coding for the different MinGag variants and immunogen-Gag constructs were purified under endotoxin-free conditions for vaccination with the HiSpeed Plasmid Mega and Giga EF Kit (QIAGEN). For all plasmids, the protocol followed consisted in growing 1.5 L of the bacteria in LB + 30 µg/mL of Kanamycin o/n at 37 °C and 225 rpm orbital shaking. The procedure was a scaled-up version of the HiSpeed Plasmid Maxi Kit (QIAGEN), with an extra endotoxin-removal step (ER buffer) after the lysate had been drawn through the QIAfilter Cartridge. Additionally, the plasmid was eluted from the QIAprecipitator Cartridge with physiological saline solution instead of TE buffer, and sterilised. Yield and purity were quantified with Nanodrop One (ThermoFisher Scientific) and the plasmid DNA was adjusted at 1 milligram (mg)/mL under strict sterile conditions.

2. Virus-Like Particle production and purification

VLP production and purification were performed in serum-free (SF) and animal-derived component free (ADCF) conditions and most of the work was performed under a sterile environment using class II biosafety cabinets (Type B2) at IrsiCaixa's Biosafety Level 3 (BSL3) Laboratory, to ensure the best quality possible of the product to be injected in animals for testing.

2.1. Transfection and harvesting in Expi293F cells

VLPs were produced using the Expi293F cell system (ThermoFisher Scientific). Expi293F is a cell line derived from the Human Embryonic Kidney (HEK293) line adapted to grow at high concentration in SF and ADCF conditions. These cells were grown in suspension and continuous orbital shaking (125 rpm) at 37 °C and 8% CO_2 conditions. Cells were subcultured twice a week at 0.3×10^6 cells/mL in Expi293F medium. The day before transfection, cells were seeded at 2×10^6 cells/mL and, on the day of transfection, reseeded at 2.5×10^6 cells/mL.

Expifectamine (ThermoFisher Scientific) was used as the transfection reagent according to the manufacturer's indications. For a 150 mL transfection, 400 µl of Expifectamine were mixed with 7.5 mL of OptiMEM (ThermoFisher Scientific) and incubated for 5 min at RTemp before mixing it with 150 µg of DNA (1 µg of DNA per mL of transfection) that were diluted in 7.5 mL of OptiMEM. The 15 mL transfection mix was incubated for 20 min at RTemp before addition to the Expi293F cells. Enhancers 1 and 2 were added to the transfected cells 18 h post-transfection. Cells were harvested 48 hours post-transfection and centrifuged for 5 min at 400 × g. The supernatant was clarified by a 10 min centrifugation at 1,000 × g and filtered at 0.22 µm with a Nalgene™ Rapid-flow™ Vacuum Filter (ThermoFisher Scientific).

2.2. VLP purification from the supernatant

Protein purification protocols often consist of multiple steps: clarification, capture, intermediate purification, polishing and sterilisation. In this project, a full purification protocol was optimised for the purification of fusion protein-based high-valency MinGag-VLPs and compared to the sucrose-cushion ultracentrifugation (UC), which is the gold-standard protocol for VLP purification.

2.2.1. Tangential Flow Filtration on harvested supernatants

The first purification protocol, which worked as an intermediate purification step, prior to either the sucrose-cushion UC or the optimised chromatography protocol was a tangential flow filtration (TFF) or crossflow filtration. In TFF the sample runs parallel or "tangential" to the filtering membrane, as opposed to dead-end filtration where the sample runs perpendicular to the membrane. That way the sample can recirculate multiple cycles across the membrane and increase its concentration while removing those contaminating molecules that have a smaller size than the Molecular Weight Cut-Off (MWCO) of the membrane pores (Figure 12).

To purify and concentrate harvested VLPs by TFF, a 300,000 MWCO Minimate™ TFF Omega Membrane Cassette (Pall Laboratories, Port Washington, NY, USA) was connected to a Masterflex L/S Economy Peristaltic Pump System (Cole-Parmer, Vernon Hills, IL, USA). Clarified VLP supernatant was loaded in the TFF reservoir and run through the cassette at a speed that did not exceed a 2.5 bar pressure. Once the sample reached 1:10 of the initial volume, the buffer was exchanged to Phosphate Buffered Saline (PBS; ThermoFisher Scientific) with the same cassette (Figure 12B). Once the buffer exchange proce-

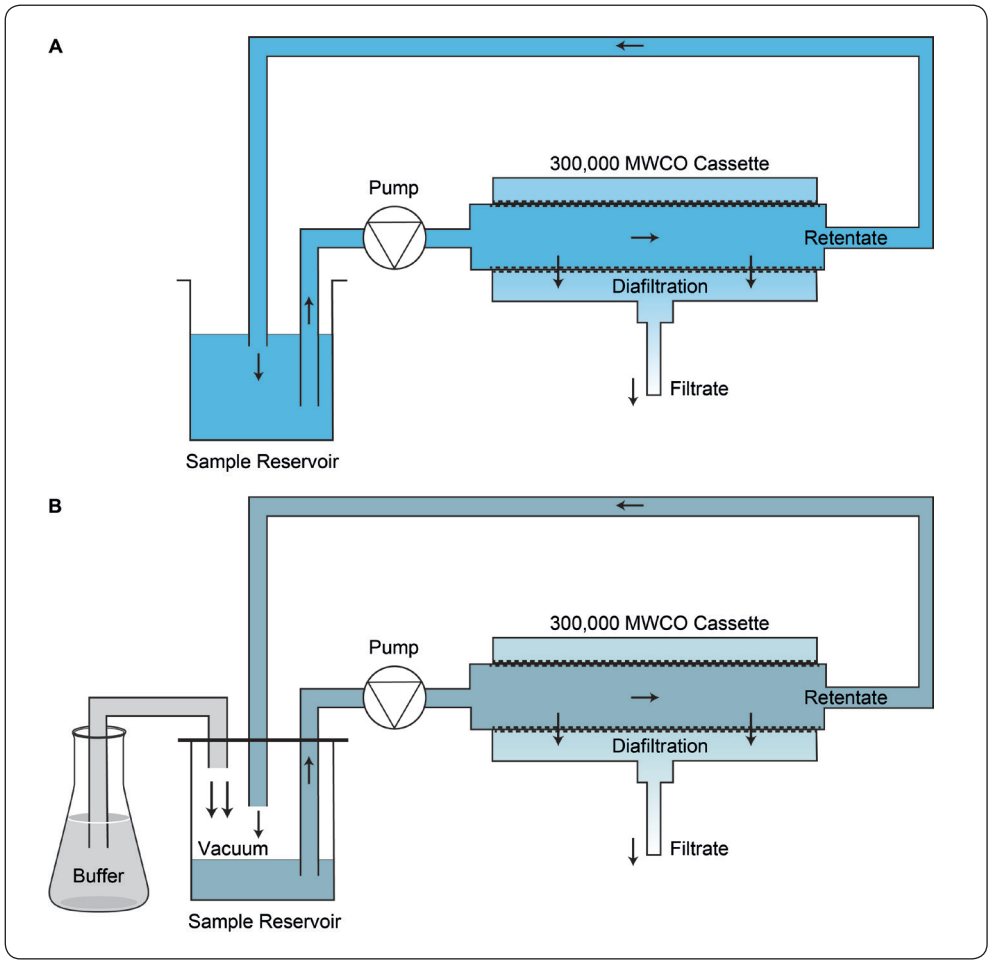

Figure 12. ***Diagram of tangential flow filtration (TFF) or crossflow filtration where a peristaltic pump drives the sample through a filtering cassette and the sample recirculates back to the reservoir.*** **A)** *Concentration and purification of a sample by TFF;* **B)** *Buffer exchange by TFF where the reservoir is sealed, and the buffer is slowly incorporated so the sample volume is constant; circulation of 5 volumes of the buffer is enough to change 96% of the sample solvent.*

dure was complete, 10 mL of PBS were run through the cassette to recover as much material as possible and improve the final yield.

2.2.2. Sucrose-cushion ultracentrifugation

Concentrated and buffer exchanged VLP preparations were purified by a 35% sucrose-cushion UC. First, the T-1270 Titanium Fixed-Angle UC rotor (ThermoFisher Scientific) and the Sorvall™ WX Ultra 100 ultracentrifuge (ThermoFisher Scientific) were cooled at 4 °C. Meanwhile, the sample was loaded on top

of a 35% sucrose cushion at a 3:1 volume in an OptiSeal Polypropylene Tube (Beckman Coulter, Brea, CA, USA). Samples were run for 70 min at 35,000 rpm. All the fractions were removed for quantification and the pellet was resuspended with PBS.

2.2.3. *Ligand-activated Core Chromatography and Anion Exchange Chromatography*

For a capture purification step, two complementary chromatography protocols were run sequentially. The first step consisted of a Ligand-activated Core Chromatography (LCC) and the second one in an Anion Exchange Chromatography (AEX). LCC is a hybrid technique between size exclusion chromatography (SEC) and AEX (Figure 13A). LCC resins have a dual property: they have an inactive porous surface that excludes molecules bigger than the pores' MWCO, while smaller molecules, that can enter the resin, can be trapped by the positively charged ligand-activated cores (Figure 13B). Anion exchange chromatography was selected over cationic exchange chromatography since VLPs, as all extracellular vesicles, have a negative net charge derived from the membrane potential from the producing cells (Steppert *et al.*, 2016).

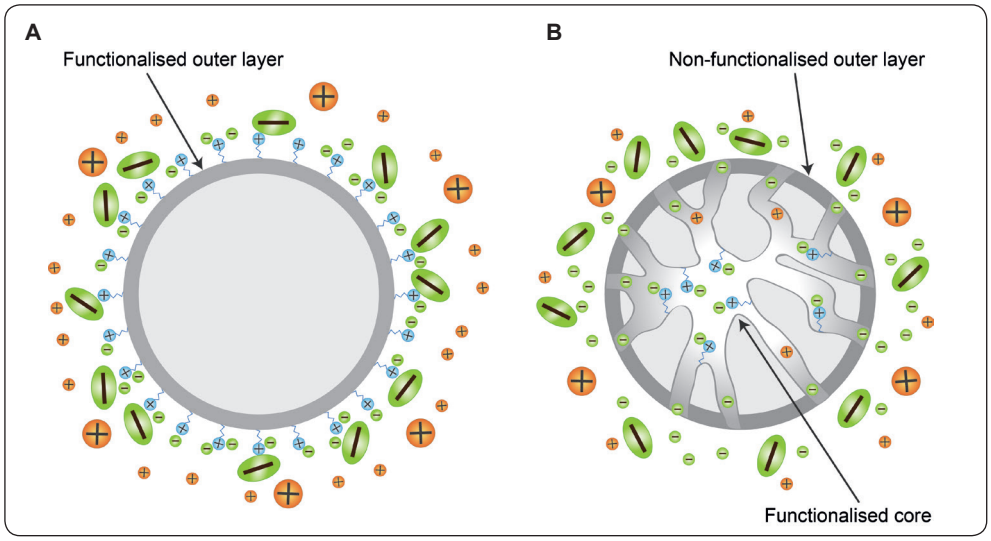

Figure 13. ***Graphical representation of the physical properties of resins used for chromatography protocols.*** **A)** *Anion Exchange (AEX) chromatography, where the resin beads' surface is positively charged to capture negatively-charged molecules;* **B)** *Ligand-activated Core Chromatography (LCC) where the beads have an inactive surface but a positively-charged functionalised core only accessible to those molecules smaller than the pores' Molecular Weight Cut-Off (MWCO).*

Theoretically, LCC would capture all negatively charged contaminants that were smaller than the MWCO, while VLPs that have a negative charge, but a bigger size, would not enter the pore (Weigel *et al.*, 2014). That way, contaminants that would compete with VLPs in an AEX chromatography, where the positively charged resin interacts with negatively charged substances, would have been removed in the previous LCC purification step (Figure 13B). That is why concentrated and buffer exchanged VLP preparations were loaded into a PBS-equilibrated HiTrap® Capto™ Core 700 (Cytiva, Marlborough, MA, USA) LCC column coupled to an Äkta Start Chromatograph (Cytiva). Capto™ Core 700 resins have a 700,000 MWCO pore and the core has positively charged octylamine groups. The flowthrough was recovered and loaded into a PBS-equilibrated 5 mL HiTrap® Q XL (Cytiva) AEX Column also connected to an Äkta Start Chromatograph (Cytiva). The column was washed with 4 column volumes (CV) of 200 mM sodium chloride (NaCl) PBS buffer and eluted with 2 CV of 400 mM NaCl PBS buffer.

2.2.4. Polishing and sterilisation

AEX eluted samples were sterilised with a Millex-GP 0.22 µm filter unit (Merck & Co.) plugged into a 10 mL syringe. After filtration, VLP samples were concentrated and adjusted at 1 mg/mL of total protein with a 300,000 MWCO Vivaspin™ 20 Centrifugal Concentrator (Cytiva) at 3,000 × g. Vivaspin™ 20 centrifugal concentrators were sterilised with a 70% ethanol solution, blocked with a 0.1 M Glycine solution, and thoroughly washed with PBS beforehand.

3. Virus-Like Particle characterisation

Multiple techniques were performed to characterise the fusion-protein high-valency VLPs. Among those, flow cytometry was used to analyse VLP-producing cells, while p24Gag specific Enzyme-Linked ImmunoSorbent Assay (ELISA), Bicinchoninic Acid (BCA) protein assay, Western Blotting (WB) and Coomassie gels were used to evaluate the yield and purity of VLPs throughout all the purification steps.

3.1. Flow cytometry analysis of VLP-producing cells

For the characterisation of the orientation of the fusion protein in the VLP-producing cells, transfected Expi293F cells were co-stained with an anti-p24Gag antibody and an antibody that targeted the specific immunogen. VLP plasmids

were designed to produce the fusion protein so that the immunogen was exposed on the cell surface, while Gag remained inside the cell connected to the immunogen through the transmembrane domain (Figure 14). That way Gag would oligomerise at the plasma membrane and bud, producing VLPs.

The staining protocol consisted first in washing the cells with staining buffer [PBS + 10% foetal bovine serum (FBS; ThermoFisher Scientific)] and then extracellularly staining them with an anti-Env bNAb (Table 7) for 30 min at RTemp. Cells were washed with staining buffer and incubated with an APC Affinipure goat anti-human IgG (Jackson ImmunoResearch, West Grove, PA, USA) (Table 8) for 15 min at RTemp. Then, cells were washed with PBS and fixed with FIX&PERM Fixation and Cell Permeabilization Medium A (ThermoFisher Scientific) for 15 min at RTemp. Cells were washed again with PBS and intracellularly stained, for 15 min, with the anti-p24Gag antibody KC57-PE (Beckman Coulter) diluted 1:200 in permeabilizer FIX&PERM Medium B. Cells were washed with PBS and run in a BD FACSCelesta™ Flow Cytometer (BD, Franklin Lakes, NJ, USA). Analysis was performed with FlowJo v10.6.1 (Tree Star, Ashland, OR, USA).

3.2. Quantification of p24Gag and total protein

VLP production and purification efficiency was assessed by quantification of p24Gag and total protein. The ratio between these two elements was an indica-

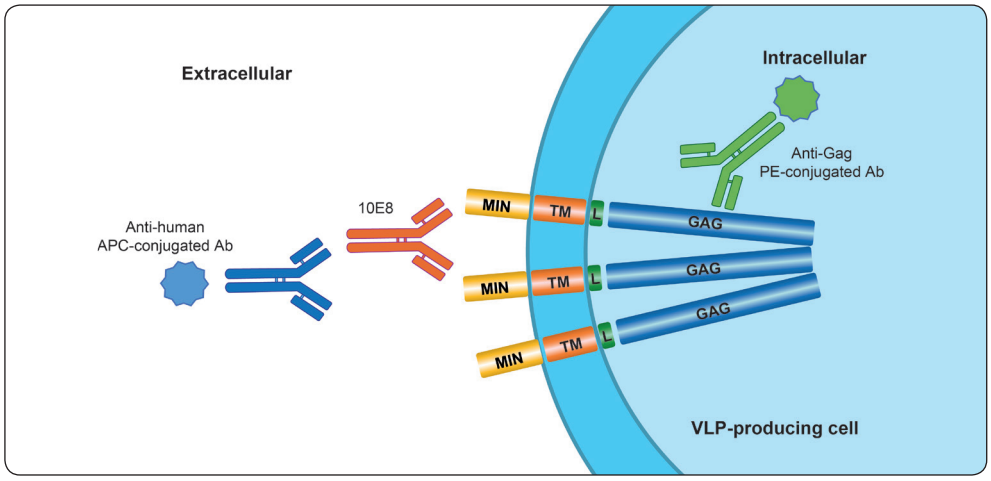

Figure 14. ***Schematic representation of VLP-producing cells staining protocol.***
VLP-producing cells were extracellularly stained with a broadly neutralising antibody (bNAb) and an anti-human APC-conjugated antibody, and intracellularly stained with a PE-conjugated anti-Gag antibody.

Table 7. Human bNAbs used for Flow Cytometry

Target	Name	Epitope	Isotype		Work. dil.	Provider
MPER	2F5	ELDKWA	IgG1 (κ)	AB001	4 µg/mL	Polymun
	4E10	NWFDIT	IgG1 (κ)	AB004	2 µg/mL	Polymun
	10E8	NWFDITNWLWYIK	IgG1 (λ)	ARP-12294	1 µg/mL	NIH
CD4bs	b12	Conformational	IgG1 (κ)	AB011	1 µg/mL	Polymun
	2G12	N-linked glycans (295, 332, 386, 392 & 448)	IgG1 (κ)	AB002	1 µg/mL	Polymun
V1V2 loops	PG9	Quaternary trimer dependent (Glycans N156 and N160)	IgG1 (λ)	AB015	1 µg/mL	Polymun
	PGT145	Quaternary trimer dependent (Glycan N160)	IgG1 (κ)	ARP-12703	1 µg/mL	NIH

Work. dil.: working dilution; MPER: Membrane Proximal External Region; CD4bs: CD4 binding site; NIH: National Institute of Health AIDS Reagent Repository.

tor for the grade of purity, while total p24Gag was used to determine the yield and the purification efficiency.

For p24Gag quantification, INNOTEST® HIV Antigen mAb (Fujierbio, Tokyo, Japan) was employed according to the manufacturer's protocol. Briefly, samples were diluted in the range of $1/10^2$ to $1/10^6$ and mixed with the Working Solution 1 at a 1:1 ratio in the provided ELISA plates and incubated for 1 h at 37 °C. The plate was washed 5 times with 300 µl of 1X Wash Buffer and incubated for 1 h at 37 °C with Working Solution 2. Then, the plate was washed again and incubated with 200 µl/well of substrate solution for 30 min at RTemp. Finally, the reaction was stopped with 50 µl of a 2 molar (M) sulfuric acid (H_2SO_4) solution. Absorbance was read at 450 nm with background subtraction at 620 nm using an Ensight Multimode Plate Reader (Perkin Elmer, Waltham, MA, USA).

For total protein quantification, Pierce™ BCA Protein Assay (ThermoFisher Scientific) was employed following the manufacturer's instructions. In short, samples were diluted in the range of 1 to 1/10 and 25 µl were incubated for 30 min at 37 °C with 200 µl of BCA working reagent. Absorbance was read at 550 nm with Ensight Multimode Plate Reader (Perkin Elmer).

3.3. Identification of proteins by Western Blot and mass-spectrometry

To qualitatively assess the composition and purity of the different VLP preparations, Coomassie staining on protein gels and WB was performed. Briefly, 15 µg of the sample were loaded into a NuPAGE™ 4 to 12%, Bis-Tris, 1.0mm, Mini Protein Gel, 12 wells (ThermoFisher Scientific) assembled with 1X MES

Buffer (ThermoFisher Scientific) in a Novex Mini-Cell (ThermoFisher Scientific). Before loading, the samples were prepared in 1X NuPAGE™ LDS Sample Buffer (ThermoFisher Scientific), 1X NuPAGE™ Sample Reducing Reagent (ThermoFisher Scientific) and heat-denatured at 95 °C for 5 min. Bluestar prestained protein marker (NIPPON Genetics, Tokyo, Japan) was used as a protein ladder size reference. Samples were run at 180 V, 110 mA and 50 W for 45-90 min. Once the running was finished, proteins for WB were transferred to a Trans-Blot Turbo Mini 0.2 µm PVDF Membrane (Bio-Rad, Hercules, CA, USA) with the Trans-Blot Turbo Transfer System (Bio-Rad). Membranes were then blocked with 5% skimmed milk (Regilait, Saint-Martin-Belle-Roche, France) and 0.05% Tween-20 PBS solution for 1h at RTemp on a rocker platform. Then, membranes were incubated o/n with the primary antibody (Table 8) at 4 °C on a roller. After primary antibody incubation, membranes were washed twice with PBS + 0.05% Tween-20 for 20 min at RTemp and incubated with the secondary antibody (Table 8) for 1h at RTemp on a rocker. Samples were washed again twice with PBS for 20 min at RTemp and then incubated with Pierce™ ECL Western Blotting Substrate (ThermoFisher Scientific) at RTemp on a roller. Chemiluminescence was detected with Chemidoc™ MP Imaging System (Bio-Rad).

Protein gels, destined for Coomassie Blue staining were rinsed with dH_2O and fixed with a 40% ethanol + 10% acetic acid solution for 15 min at RTemp and washed thrice with dH_2O for 5 min. Fixed gels were incubated in SimplyBlue™ Safe Stain (ThermoFisher Scientific) Coomassie Blue for 45 min at RTemp on a rocker. Then, excess Coomassie was washed twice with dH_2O for 30 min and o/n at RTemp. A picture of the Coomassie Blue stained gel was taken with the Chemidoc™ MP Imaging System (Bio-Rad).

MALDI-TOF protein determination was performed at the Proteomic Service of Vall d'Hebron Institute of Oncology (VHIO, Barcelona, Spain) in a MALDI-TOF/TOF Mass Spectrometer (Bruker Daltonics, Billerica, MA, USA). Sample preparation for mass spectrometry consisted in staining an unfixed protein gel with SimplyBlue™ Safe Stain (ThermoFisher Scientific) and cutting the bands of interest with a scalpel. Further preparations before determination and subsequent analysis were performed at VHIO.

3.4. Cryogenic Transmission Electron Microscopy of purified VLPs

Morphology assessment of purified VLPs was performed by cryogenic transmission electron microscopy (Cryo-TEM). VLPs were prepared with a Leica EM GP Workstation (Leica) and were deposited on a carbon-coated copper

Table 8. Antibodies employed in all the immunodetection assays performed in this project

Antibody	Reference	Work.dil.	Technique	Provider
Unconjugated				
Anti HIV-1 gp41 mAb D50	ARP-11393	2 µg/mL	ELISA, FACS	NIH AIDS Reagent Program
Anti-HIV1 p24 antibody	ab9071	1 µg/mL	ELISA, WB	Abcam
Anti-HIV1 p55+p24+p17	ab63917	1:5,000	WB	Abcam
6-His Tag mAb (HIS.H8)	MA1-21315	1 µg/mL	ELISA, WB	ThermoFisher Scientific
Anti-mouse IFN-γ (AN18)	517901	1:250	ELISpot	Biolegend
Biotinylated				
Biotin-AffiniPure goat anti-mouse IgG1	115-065-205	1:5,000	ELISA	Jackson ImmunoResearch
Biotin-AffiniPure goat anti-mouse IgG2b	115-065-207	1:5,000	ELISA	Jackson ImmunoResearch
Biotin-AffiniPure goat anti-mouse IgG2c	115-065-208	1:5,000	ELISA	Jackson ImmunoResearch
Biotin-AffiniPure goat anti-mouse IgG3	115-065-209	1:5,000	ELISA	Jackson ImmunoResearch
Biotin-anti-mouse IFN-γ (R4-6A2)	505701	1:2,000	ELISpot	Biolegend
Peroxidase-conjugated				
HRP-Afifnipure Goat anti-human IgG	109-036-098	1:10,000	ELISA, WB	Jackson ImmunoResearch
HRP-AffiniPure Goat anti-mouse IgG	115-036-071	1:10,000	ELISA, WB	Jackson ImmunoResearch
HRP-AffiniPure Donkey anti-rabbit IgG	711-036-071	1:20,000	WB	Jackson ImmunoResearch
HRP-conjugated streptavidin	N100	1:6,000	ELISA	ThermoFisher Scientific
Other				
Streptavidin-AP	3310-8	1:2,000	ELISpot	Mabtech
KC57-RD1	6604667	1:200	FACS	Beckman Coulter
AlexaFluor647 goat anti-mouse IgG Fc	115.605-071	1:500	FACS	Jackson ImmunoResearch
APC AffiniPure Goat anti-human IgG	109-136-098	1:500	FACS	Jackson ImmunoResearch

mAb: monoclonal antibody; ELISA: Enzyme-Linked Immunosorben Assay; WB: Western Blot, FACS: Fluorescent-Activated Cell-Sorting; ELISpot: Enzyme-Linked Immune-absorbent Spot; IFN-γ: interferon-γ; IgG: Immunoglobulin G; HRP: Horseradish Peroxidase; AP: Alkaline Phosphatase; APC: allophycocyanin; Fc: crystallisable fragment.

grid. VLP observation was carried out in a Jeol JEM-2011 Electron Microscope (JEOL Ltd, Tokyo, Japan) coupled to a CCD895 USC4000 Camera (Gatan, Pleasanton, CA, USA) at the Electron Microscopy Service of the Universitat Autònoma de Barcelona (UAB, Bellaterra, Spain). VLP diameter was analysed using the ImageJ software and the 200 nm scale bar.

4. Animal procedures

In this project, a C57Bl/6 mouse substrain, C57Bl/6JOlaHsd (Envigo, Indianapolis, IN, USA) mice were used as the animal model for the characterisation of VLP-induced immune responses. C57Bl/6 substrains are inbred mice whose immune system has been extensively studied. C57Bl/6 mice are characterised by a bias towards a Th1 profile of T helpers, which means that they have weaker Th2-driven humoral immune responses, compared to other mouse strains (Watanabe *et al.*, 2004). Also, the same group described that NK cells in C57Bl/6 mice have higher activity.

4.1. Ethics statement and animal welfare

All animal experiments performed in this project were evaluated by the Ethical Committee on Animal Experimentation (CEEA) of the Germans Trias i Pujol Research Institute (IGTP, Badalona, Spain) and were approved by the Ministry of Territory and Sustainability of the *Generalitat de Catalunya* (DAAM 9525 and 9943). All procedures strictly followed the Guide for the Care and Use of Laboratory Animals of the *Generalitat de Catalunya*, the Principles of Laboratory Animal Care of the National Institute of Health (NIH, Bethesda, MA, USA) and the Declaration of Helsinki for animal experimental investigation. All the experiments consisted of animal groups that had a 50% distribution of males-females, to account for sex-based variability, since sex bias has been described in the immunology field (Lee, 2018).

C57Bl/6JOlaHsd animals were purchased at the age of 7 weeks (Envigo) and quarantined for at least 7 days before experiment initiation. Animals were housed at a Specific-Pathogen Free (SPF) facility for the whole duration of the experiment and were fed *ad libitum*. Temperature and humidity were kept at a constant range (21-22 °C and 30-40% humidity), and light/dark cycles that lasted 12 h, with a progressive light change. Animals were housed in groups of 2-5 animals/cage with environmental enrichment; cages were cleaned twice a week. All procedures were performed cautiously, and animals underwent periodic veterinary inspection.

4.2. *In vivo* DNA electroporation

For DNA immunisation, animals were injected with 20 µg of DNA intramuscularly at the posterior hind leg. Before the procedure, mice were anaesthetised with 5% isoflurane (Baxter, Deerfield, IL, USA) at 1 L/min using the Veterinary Anaesthesia Workstation (Minerve Equipement Veterinaire, Esternay, France) and maintained during the procedure with 3% isoflurane. Immediately after DNA inoculation, the muscle was electroporated at the site of injection with a NEPA21 *in vivo* electroporator (NepaGene, Chiba, Japan) using variable gap tweezers with 2 round-shaped SS Plate Electrodes (Sonidel, Dublin, Ireland). We used two different electroporation protocols. The first one was optimised in-house for maximal expression and consisted of 8 positive pulses of 60 Volts (V) and 20 milliseconds (ms) separated by a 1 s interval (Figure 15A). The second electroporation protocol consisted of a combination of 2 high-voltage poring pulses (200 V and 0.1 milliseconds (ms) positive pulses with a 20% decay separated by a 10 ms interval) followed by 6 low-voltage transfer pulses (3 pulses of 60 V, 20 ms and positive polarity with a 20% decay separated by a 50 ms interval, followed by 3 pulses with the same parameters but inverted polarity) (Figure 15B). The latter was a more humane electroporation protocol since it was notably shorter in time.

4.3 *In vivo* bioluminescence

Electroporation efficiency was assessed with an *in vivo* bioluminescence assay. Animals were electroporated using the in-house protocol optimised for maximal expression with 20 µg of both a 1:1 ratio mix of pVAX1-*Fluc* and pVAX1 (empty) plasmids on the right hind limb and a mix at a 1:1 ratio of pVAX1-*FLuc* and pVAX1-*min(RA)gag* plasmids on the left hind limb. Once electroporated, bioluminescence fading was assessed once a week with an IVIS Lumina III *In Vivo* Imaging System (Perkin Elmer). To do so, animals were injected with 150 mg/kg of D-luciferin (Biovision, Milpitas, CA, USA) and then anaesthetised with 5% isoflurane at 1 litre (L)/min and maintained inside the imaging system with 3% isoflurane. Images were taken with 30 s of exposure time and medium binning.

4.4. VLP immunisation and vaccination regimens

VLP immunisation in mice was performed using two different strategies. On the one hand, mice were immunised subcutaneously by directly injecting purified VLPs produced *in vitro* in the hock. On the other hand, DNA was injected and electroporated intramuscularly at the posterior hind limb using the protocol that combines high and low voltage pulses, to transfect muscle cells in a way

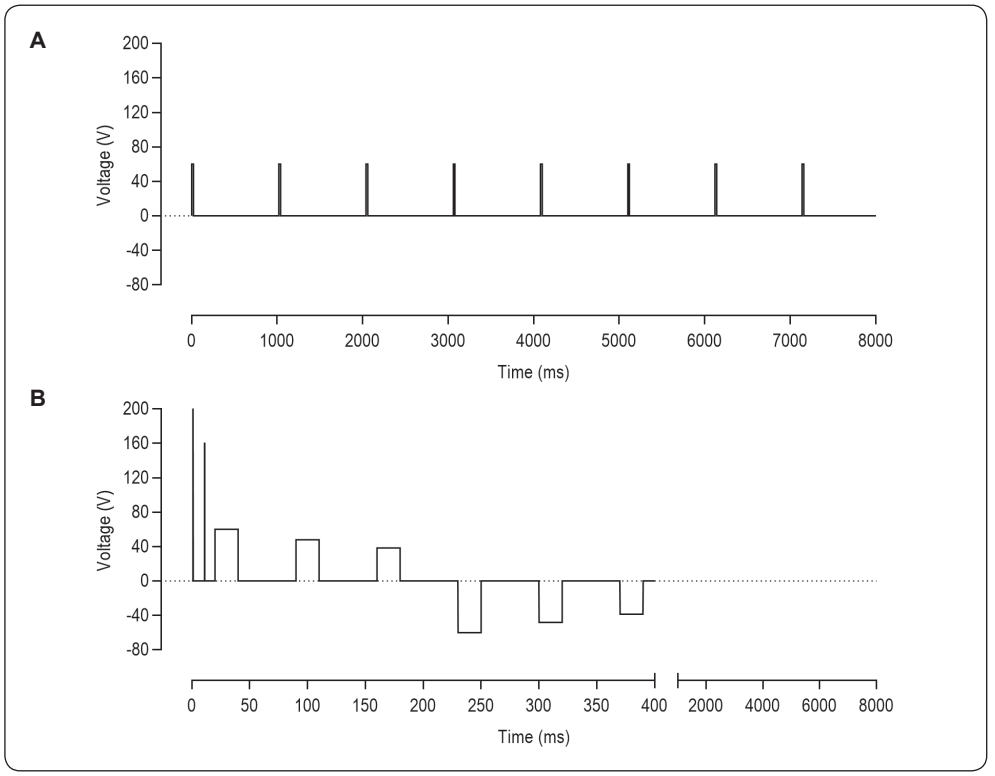

Figure 15. ***Schematic representation of the* in vivo *electroporation protocols.*** **A)** *This protocol that lasted 8 seconds consisted of the application of 8 positive middle voltage constant pulses with a 1 s interval.* **B)** *This protocol lasted 400 ms and consisted of the application of 2 short and high voltage poring pulses with the same polarity (+/+) and a 20% decay, followed by 6 longer and lower voltage-transfer pulses with inverted polarity (+/-; 3 pulses of each polarity) with a 20% decay.*

that they produce *in vivo* the VLPs that will stimulate the immune system. Overall, mice were vaccinated with the same VLPs displaying the same immunogens but using two different formulations.

Purified VLPs were injected in the hock at a dose of 0.004 mg/kg (approximately 0.1 µg of p24Gag per animal). Before injection, animals were anaesthetised with 5% isoflurane at 1 L/min and maintained during the procedure with 3% isoflurane.

C57Bl/6JOlaHsd mice were immunised with two different vaccination regimens using the two immunisation strategies (DNA or VLP): i) a homologous vaccination regimen where 4 doses of VLPs (VVVV) were administered with a 3-week interval, or ii) a heterologous vaccination regimen where 2 doses of DNA were followed by 2 doses of purified VLPs (DDVV), with a 3-week interval as well (Figure 16).

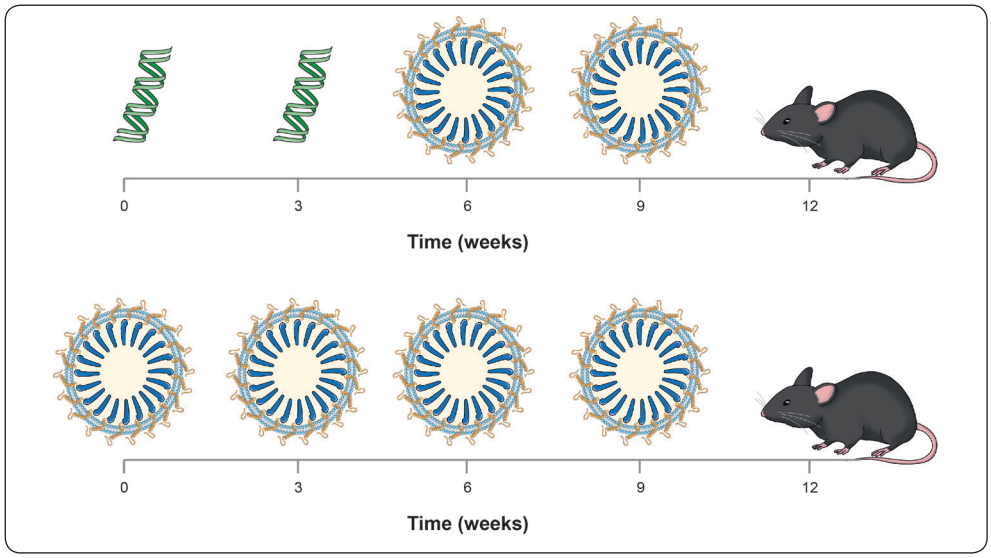

Figure 16. ***Schematic representation of the immunisation regimens.*** *In the heterologous regimen (top) mice were immunised with 2 doses of DNA electroporated intramuscularly, followed by 2 doses of purified VLPs injected subcutaneously (hock) and separated by a 3-week interval between each dose. In the homologous regimen (bottom), mice were immunised 4 times, every 3 weeks, with purified VLPs administered subcutaneously at the hock.*

4.5. *In vivo* protection assay

Demonstrating the efficaccy of HIV-1 vaccines in *in vivo* models is difficult. NHPs are the ideal model since they can be infected by HIV-related viruses, like SIV and SHIV. In compariosn, humanised mouse models are useful tools to test HIV treatments but they are not not ideal for vaccine testing, since their immune system induces suboptimal immune responses. Here, we developed an indirect method in which a poorly immunogenic syngeneic tumour cell line was engineered to express Min on the surface. This cell line would act as a proxy for an infected cell that expresses HIV-related proteins when implanted in mice. If tumour-inoculated mice were able to halt tumour progression, it would mean that the vaccine is able to induce an effective immune response.

4.5.1 Generation of a Min-expressing B16F10 cell line

B16F10 (ATCC, Manassas, VA, USA) is a mouse melanoma cell line with a C57Bl/6 genetic background. B16F10 cells are a useful tool for the study of melanoma cancer treatments in mice, since this cell line is poorly immunogenic, and in particular, it does not induce potent cellular immune responses. Once implanted into the mice these cells grow exponentially, since the host's immune system

cannot control it. B16F10 cells were stably transfected with pcDNA3.1-*min(tm)* (Table 5), to make them express Min at their surface.

B16F10 cells were transfected with pcDNA3.1-*min(tm)* (1 µg of DNA per mL of transfection) using X-tremeGENE™ 9 DNA Transfection Reagent (Sigma Aldrich, St. Louis, MO, USA). Briefly, B16F10 cells were seeded in glutamine-supplemented Dulbecco's Modified Eagle Medium (DMEM; ThermoFisher Scientific) and complemented with heat-inactivated 10% FBS (ThermoFisher Scientific) (D10) at 30% confluence the day before transfection. Half an hour before transfection, the medium was replaced with fresh D10, and the DNA and transfection reagents were equilibrated at RTemp. Next, X-tremeGENE was mixed with the DNA preparation at a 3:1 ratio and incubated for 15 min at RTemp. The day after, media was supplemented with 2 mg/mL of Geneticin® (ThermoFisher Scientific) for selection and replenished every 2 days.

After culturing the cells for 10 days in antibiotic-supplemented selection media, Min-positive B16F10 cells were single-cell sorted. In short, B16F10Min cells were stained with 2F5 (Table 7) for 30 min at RTemp. After that, cells were washed and incubated with an APC-conjugated Affinipure goat anti-human IgG (Jackson ImmunoResearch) for 15 min at RTemp. Cells were washed again and resuspended in PBS + 1% FBS + 2 mM EDTA. APC-positive events were single-cell sorted in a 96-well plate with a BD FACSAria™ II Cell Sorter (BD). Min expression and stability on sorted clones was assessed by periodically staining the cells with 2F5.

4.5.2. B16F10Min melanoma cell line injection to C57Bl/6

To determine if Gag-VLP induced a functional immune response, C57Bl/6JOlaHsd mice were immunised twice with purified Gag- or Min(RA)Gag-VLPs with a 3-week interval. Two weeks after the second immunisation, mice were implanted subcutaneously with B16F10Min cells (Figure 17). Prior to implantation, B16F10Min cells were washed with PBS and detached with Versenne (ThermoFisher Scientific). Cells were counted using Perfect-Count™ Microspheres (Cytognos, Salamanca, Spain) beads in a BD FACSCelesta (BD). For inoculation, cell concentration was adjusted in PBS at 2×10^6 cells/mL with 2 mM EDTA. Vaccinated animals were shaved on the right flank and were injected subcutaneously with a total of 100,000 B16F10Min cells per animal.

After tumour inoculation, mice were supervised 4 times a week for monitorisation of tumour growth and welfare. Tumour width and length were measured with a calliper and tumour volume was calculated according to the equation: $0.52 \times \text{length} \times \text{width}^2$ (Mei *et al.*, 2016). Animals were euthanised when tumours reached a size bigger than 1 cm^3 or at the end of the follow-up period.

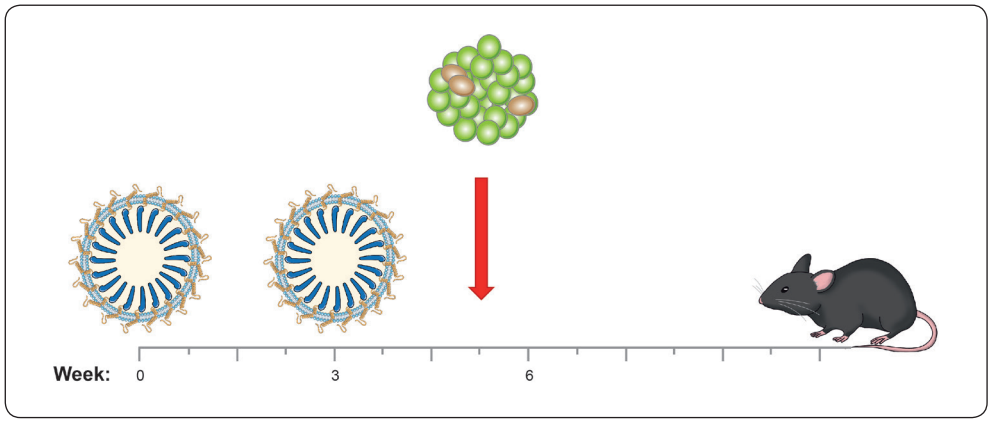

Figure 17. ***Schematic representation of the* in vivo *protection assay procedure.*** *Mice were vaccinated twice with either Gag-VLPs or Min(RA)Gag-VLPs subcutaneously at the hock with a 3-week interval. Two weeks after the last immunisation, mice were injected with 100,000 B16F10Min tumour cells subcutaneously at the flank. Mice were followed up for a maximum of 80 days after tumour injection and they were euthanised after reaching a tumour size bigger than 1 cm^3.*

4.6. Sample collection and processing

Blood sampling was periodically performed before starting a procedure and before each immunisation or tumour inoculation. To do so, animals were punctured with a 25G needle (Novico Medica, Barcelona, Spain) at the facial vein to collect approximately 100 µl of blood in a 1.5 mL tube (Sarstedt). After collection, hemostasia at the draining site was performed to stop the bleeding.

At the end of the follow-up periods or once a humane endpoint was reached, animals were euthanised with 5% isoflurane and blood draining was performed by intracardiac puncture. Immediately after, cervical dislocation was performed as a secondary method to confirm euthanasia. Tissues were harvested in accordance with the objectives of the study. In the immunisation assays with the homologous and heterologous regimens, spleen and lymph nodes were harvested, while in the *in vivo* protection assay, the spleen and the tumour were collected.

Serum was recovered from whole blood by centrifugation at 4,000 × g centrifugation for 10 min. A second centrifugation at 10,000 × g for 5 min was performed to maximise the serum recovery while removing all cell debris. Serum was heat-inactivated at 56 °C for 30 min. After heat-inactivation, serum was centrifuged again at 10,000 × g for 5 min, aliquoted and frozen at –80 °C until analysis.

After harvesting, spleens were kept on ice until sample processing. Spleens were mechanically disaggregated with a syringe plunger and a 70 µm Easystrainer (Greiner bio-one, Kremsmünster, Germany) on a 50 mL falcon (Corning Inc.,

Corning, NY, USA) in PBS. Disaggregated spleens were washed at 400 × g for 5 min and splenocytes were resuspended in freezing medium (10% DMSO FBS) for storage in a liquid nitrogen tank. Tumours were frozen by immersion in isopentane and stored solid-frozen at –80 °C.

5. Analysis of vaccine-induced immune responses

The level and profile of humoral and cellular immune responses induced in vaccinated mice were characterised by various assays: ELISA, Flow Cytometry, neutralization assay, CD16-2 binding assay and ELISpot. For the determination of humoral responses, recombinant Gag and Min antigens, that would be used as target antigens were produced in prokaryotic cells in-house.

5.1. Production and purification of soluble recombinant antigens

Soluble recombinant forms of Min (Gp41-MinTT) and Gag (rGag) were produced in BL21 *E. coli*. These proteins had the same protein sequence as Min and Gag proteins used in VLP production but lacked glycosylations and had a 6-histidine tail tag for ion-metal affinity chromatography (IMAC) purification.

Both Gag and Gp41-MinTT constructs were cloned into a pET21(d+) vector (Merck & Co.) and transformed in OneShot™ BL21(DE3) Chemically Competent Cells (ThermoFisher Scientific). All chemical reagents in this section were purchased from Sigma Aldrich (Merck & Co.) unless stated otherwise. For protein production, positive clones were grown o/n at 37 °C and 225 rpm orbital shaking in 400 mL LB + 100 µg/mL ampicillin. The day after, 400 µl of 1 M Isopropyl β-D-1-thiogalactopyranoside (IPTG) were added to the culture and incubated for 4 h at 37 °C and 225 rpm orbital shaking. After that, cells were centrifuged at 3,000 × g for 20 min and the supernatant was discarded. The cells were lysed in 50 mL of a lysis buffer (pH=8) containing 50 mM Tris-HCl, 100 mM NaCl and 10 mg/mL of lysozyme for 1 h at 4 °C with end-over-end mixing. In the final 15 min, 1% of Triton-X100 was added to the lysate. The lysate was frozen at –80 °C and thawed on ice. After thawing, 250 µl of Protease Inhibitor Cocktail (Cat num. P8849, Sigma Aldrich), 20 µg/mL of DNase I (cat. num. DN25, Sigma Aldrich) and 2 mM of magnesium chloride ($MgCl_2$) were added and incubated for 1 h at 4 °C with end-over-end mixing. The lysate was centrifuged at 15,000 × g for 30 min and the pellet was resuspended with 50 mL of a pH=8 solubilising buffer containing 500 mM NaCl, 100 mM monosodium phosphate (NaH_2PO_4), 10 mM Tris-Cl and 8 M urea. Solubilised protein was centrifuged again at 15,000 × g for 30 min and the pellet was discarded. The supernatant was incubated with 1 mL of Ni^{2+}-Sepharose® High Performance beads

(Cytiva) and 20 mM imidazole for 1 h at RTemp with end-over-end-mixing and transferred into a 10 mL PolyPrep® Chromatography Column (Bio-Rad). Once the Sepharose beads settled and all the depleted sample had been drawn by gravity, the column was washed twice with solubilising buffer supplemented with 50 mM imidazole. Next, protein was eluted from the column with the solubilising buffer with 500 mM imidazole. Samples were concentrated and washed with the solubilising buffer first to remove excess of imidazole with a 3kDa or a 10 kDa Amicon Ultra-15 Centrifugal Unit, for Gp41-MinTT or Gag, respectively. The same centrifugal units were used to replace 8 M urea solubilising buffer for a PBS + 0.1% Sodium Dodecyl Sulphate (SDS) buffer. The yield and purity of each protein were analysed with NanoDrop One (ThermoFisher Scientific).

5.2. Humoral immune response analysis on mouse sera

Humoral response against Min and Gag proteins, IgG subclass and mapping of the targeted epitopes were characterised by ELISA. The level of binding of anti-Min antibodies to B16F10Min and the concentration of anti-human antibodies generated against Expi293F proteins on the surface of purified Gag-VLPs and MinGag-VLPs were determined by Flow Cytometry.

5.2.1. Characterisation of anti-Gag and anti-Min humoral responses by ELISA

For anti-Min and anti-Gag antibody quantification, Nunc MaxiSorp™ 96-well ELISA plates (ThermoFisher Scientific) were coated with 50 ng/well of the antigen of interest (rGag or Gp41-MinTT) in PBS o/n at 4 °C in a wet chamber. The following day, the plate was washed 3 times with 300 µl of wash buffer (PBS + 0.05% Tween20) and the wells were blocked with 300 µl of blocking buffer (PBS + 1% bovine serum albumin (BSA) + 0.05% Tween-20) for 2 h at RTemp. After that, plates were washed 5 times with 300 µl of wash buffer and loaded with the serum samples from VLP-vaccinated animals at the appropriate dilution (1:100-1:10,000) in blocking buffer. As standard, we used the following mAbs: mouse anti-p24 (ab9071, abcam) and mouse anti-gp41 (clone D50M NIH) for anti-Gag and anti-Min response quantification, respectively (Table 8). The standard curve consisted in 7 dilutions of 1/3 starting at 333 ng/mL. The samples were incubated o/n at 4 °C in a wet chamber. Next, samples were washed 5 times with 300 µl of wash buffer and incubated with 100 µl of horseradish peroxidase (HRP)-conjugated Affinipure Goat anti-mouse IgG (Jackson ImmunoResearch) (Table 8) at 1:10,000 dilution in 0.1% BSA and 0.05% Tween20 PBS

buffer for 1 h at RTemp. Then, each ELISA plate was washed 5 times with 300 µl of wash buffer, while one tablet of o-Phenylenediamine dihydrochloride (OPD) HRP-substrate (Sigma Aldrich) was diluted in 11 mL of Phosphate-Citrate Buffer with Sodium Perborate (pre-equilibrated at RTemp), and 100 µl/well of the substrate solution were added and incubated for 10 min. The reaction was stopped with 100 µl of 2 M H_2SO_4 and the absorbance was read at 492 nm and at 620 nm for background subtraction using the Ensight Multimode Plate Reader (Perkin Elmer).

The same ELISA protocol was performed for the identification of the IgG subclass profile of anti-Gag and anti-Min antibodies in vaccine-induced mice serum, but instead of an HRP-conjugated Affinipure Goat anti-mouse IgG secondary antibody (Jackson ImmunoResearch), biotin-conjugated IgG subclass-specific secondary antibodies were employed (Table 8). After the incubation with these secondary antibodies, the plate was washed 5 times with 300 µl of wash buffer and incubated for 30 min with HRP-conjugated streptavidin (ThermoFisher Scientific) diluted at 1:6,000 in blocking buffer. The plate was washed again, the signal was revealed with OPD and absorbances were measured as previously detailed.

To identify which epitopes targeted vaccine-induced anti-Min antibodies, a mapping with 12 overlapping Min peptides (OLP; synthesised by Covalab, Bron, France) (Table 9) was performed by ELISA. In that case, instead of coating the plates with recombinant antigens, plates were coated with 500 ng of each Min OLP diluted in a 0.2 M carbonate/bicarbonate buffer at pH=9. Then, the protocol was performed as described above.

5.2.2. Determination of humoral responses by Flow Cytometry

Mouse antibodies induced against human proteins expressed on the surface of purified VLPs were analysed by flow cytometry. To do so, 0.2×10^6 cells were washed with staining buffer and labelled with each mouse sera at a 1:1,000 dilution in staining buffer for 30 min at RTemp. After that, cells were washed twice by diluting in staining buffer and at 400 × g for 5 min. Then, stained cells were incubated for 15 min at RTemp with an AlexaFluor647-conjugated goat anti-mouse IgG Fc (Jackson ImmunoResearch) (Table 7) at a 1:500 dilution. Cells were washed with PBS and acquired with a BD FACSCelesta™ Flow Cytometer (BD). Analysis was performed with FlowJo v10.6.1 (Tree Star).

The ability of vaccine-induced anti-Min antibodies to engage Min presented at the surface of B16F10Min cells was also assessed by Flow Cytometry. The protocol was the same as described above, but the target cells were B16F10 and B16F10Min cells.

Table 9. List of overlapping Min peptide and Gag pools' Peptide sequence

	Code		Domain	Seq	Epitope
Min overlapping peptides	155		HR2	NMTWMEWEREIDNYT	
	156		HR2	MEWEREIDNYTSLIY	
	157		HR2	REDINYTSLIYTLIE	
	158		HR2	NYTSLIYTLIEESQN	
	159		HR2	LIYTLIEESQNQQEK	
	160		HR2	LIEESQNQQEKNEQE	
	161		HR2-MPER	SQNQQEKNEQELLEL	
	162		HR2-MPER	QEKNEQELLELDKWA	2F5
	163		MPER	EQELLELDKWASLWN	2F5
	164		MPER	LELDKWASLWNWFDI	
	165		MPER	KWASLWNWFDITNWL	4E10
	166		MPER	LWNWFDITNWLWYIK	4E10, 10E8
Gag pools	6	36	p24	APGQMREPRGSDIAGTTS	
		37	p24	GSDIAGTTSTLQEQIGWM	
		38	p24	TLQEQIGWMTNNPPIPVG	
		39	p24	TNNPPIPVGEIYKRWIIL	
		40	p24	EIYKRWIILGLNKIVRMY	
		41	p24	GLNKIVRMYSPTSILDIR	
		42	p24	SPTSILDIRQGPKEPFRD	
		43	p24	QGPKEPFRDYVDRFYKTL	
		44	p24	YVDRFYKTLRAEQASQEV	
		45	p24	RAEQASQEVKNWMTETLL	
	7	46	p24	KNWMTETLLVQNANPDCK	
		47	p24	VQNANPDCKTILKALGPA	
		48	p24	TILKALGPAATLEEMMTA	
		49	p24	ATLEEMMTACQGVGGPGH	
		50	p24-p2	CQGVGGPGHKARVLAEAM	
		51	p24-p2	KARVLAEAMSQVTNSATI	
		52	p2	SQVTNSATIMMQRGNFRN	
		53	p2-p7	MMQRGNFRNQRKIVKCFN	
		54	p7	QRKIVKCFNCGKEGHTAR	
		55	p7	CGKEGHTARNCRAPRKKG	

HR2: Heptad Repeat 2; MPER: Membrane Proximal External Region; p24: Matrix; p2: Spacer Peptide 1 (SP1); p7: nucleocapsid.

5.2.3. In vitro *pseudovirus neutralisation assay*

The neutralising activity of vaccine-induced antibodies was analysed by an *in vitro* pseudovirus neutralisation assay. In this assay, a HeLa cell line engineered to produce luciferase regulated by a tat-inducible promoter —TZM-bl cells

(NIH)—, emit bioluminescence when infected with HIV-1 pseudoviruses and incubated with luciferin (Montefiori, 2009).

As described elsewhere (Sánchez-Palomino *et al.*, 2011), pseudoviruses were produced by cotransfection of Expi293F cells with a pSG3ΔEnv backbone and various Env-coding plasmids (Table 10). Pseudoviruses were harvested 48 h post-transfection and clarified by centrifugation at 400 × g for 5 min and filtration with a syringed-plugged Millex-GP 0.22 µm filter unit (Merck & Co.). Pseudoviruses were kept at –80 °C until use. For titration, pseudoviruses were incubated for 48 h at a starting 1:10 dilution and serial 1:5 dilutions with 10,000 TZM-bl cells. After that, cells were incubated for 2 min with BriteLite plus Reporter Gene Assay System (Perkin Elmer) and bioluminescence was analysed by luminometry with the Ensight Multimode Plate Reader (Perkin Elmer).

For the *in vitro* neutralisation assay, 100 µl of the sera samples from vaccinated mice were diluted 1:40 in D10 and incubated with 50 µl of each pseudovirus at a concentration of 4,000 50% Tissue Culture Infective Dose (TCID50)/mL for 45-90 min with at 37 °C and 5% CO_2. Meanwhile, TZM-bl cells were detached with Versenne and counted. TZM-bl cells were diluted at 0.1×10^6/mL with D10 and a 1:400 dilution of dextran was added to the cells. Then, 10,000 cells/well were plated and incubated for 48 h at 37 °C and 5% CO_2. Finally, BriteLite plus Reporter Gene Assay System (Perkin Elmer) was added to the cells, incubated for 2 min and bioluminescence was analysed with the Ensight Multimode Plate Reader (Perkin Elmer).

5.2.4. Mouse CD16-2 binding to anti-Min antibodies

Binding to mouse Fc γ Receptor IV (mFcγRIV) is a prerequisite of vaccine-induced antibodies to exert ADCC. Therefore, the binding of vaccine induced IgG antibodies to CD16-2 was determined by ELISA. The protocol was similar

Table 10. Panel of 6 subtype pSG3ΔEnv pseudotyped HIV-1 pseudoviruses with control and subtype B HIV-1 envelope glycoproteins

	Tier	Subtype	Backbone
pNL4-3	Tier1A	Subtype B	pSG3 ΔEnv
BaL.01	Tier1B	Subtype B	
TRO.11	Tier2	Subtype B	
AC10.0.29	Tier2	Subtype B	
7312A	HIV-2 wildtype	HIV-2	
7312A C1	HIV-2 with HIV-1's MPER	Subtype B (MPER)	
VSV-G	Negative control		

to a standard in-house ELISA (see above), but in the last step, a biotin-conjugated CD16-2 recombinant protein was used instead of a conjugated secondary antibody. First, 500 ng/well of Gp41-MinTT, diluted in a carbonate/bicarbonate buffer, were coated o/n at 4 °C in a wet chamber. Wells without coating were also added to determine the background. Next, plates were washed 3 times with 300 µl of wash buffer and blocked with blocking buffer for 2 h at RTemp. After that, the plates were washed again 5 times and sera samples at 1:100 dilution in blocking buffer were added to the plates and incubated o/n at 4 °C in a wet chamber. The next day, the plate was washed 5 times and 100 ng of Biotinylated mFcγRIV / CD16-2 Protein (AcroBiosystems, Newark, DE, USA) per well were added and incubated o/n at 4 °C in a wet chamber. On the fourth day, the plate was washed again 5 times and incubated for 30 min at RTemp with HRP-conjugated streptavidin (Table 8; ThermoFisher Scientific) while 1-Step™ Ultra TMB-ELISA (ThermoFisher Scientific) 3,3′,5,5′-Tetramethylbenzidine (TMB) substrate was equilibrated at RTemp. After this last incubation, the plate was washed 5 times and incubated with 100 µl of TMB substrate for 15 min at RTemp, and the reaction was stopped with 100 µl of 1 M H_2SO_4. Absorbance was read at 450 nm with background subtraction at 620 nm with Ensight Multimode Plate Reader (Perkin Elmer).

5.3. Cellular immune responses (ELISpot) on splenocytes

To measure cellular responses induced by VLP vaccination, mouse splenocytes were tested by Enzyme-linked Immune absorbent spot (ELISpot). The 0.45 µm white and sterile MultiScreen$_{HTS}$ plates (Merck & Co.) were coated with 0.2 µg/well of the anti-mouse IFN-γ (AN18) antibody (Biolegend, San Diego, CA, USA) and incubated o/n at 4 °C in a wet chamber. The following day, splenocytes from vaccinated animals were thawed and washed with Roswell Park Memorial Institute 1640 medium (RPMI1640; ThermoFisher Scientific) supplemented with 10% FBS (R10). Cells were incubated at 37 °C and 5% CO_2 for 4 h. Meanwhile, plates were washed 6 times with PBS + 1%FBS and blocked for 1 h at RTemp with R10. Next, R10 was removed and 40 µl of a pool of Min OLPs (12 Min OLPs; Table 9) or a pool of Gag peptides (15 p24Gag peptides; Table 9), each peptide at a concentration of 14 µg/mL, were added together with 400,000 splenocytes/well. Three negative controls (0.5% DMSO) and two positive controls using 7 µg/mL of Concanavalin A (ConA; Sigma Aldrich) per animal were included. Samples were incubated o/n at 37 °C and 5% CO_2. On the final day, plates were washed 5 times with PBS and incubated with a biotinylated anti-mouse IFN-γ antibody (Biolegend) for 1 h at RTemp. Then, plates

were washed again with PBS and incubated with Streptavidin-conjugated Alkaline Phosphatase (AP) (Mabtech, Augustendalstorget, Sweden) for 1 h at RTemp. Finally, the plate was washed again and incubated for 12 min with the AP Conjugate Substrate Kit (Bio-Rad) by mixing 100 µl of colour reagents A and B with the 25X buffer in 10 mL of dH_2O and adding 100 µl per well. After that, the colouring AP solution was aspirated, the plate was washed with PBS + 0.05% Tween20, and finally washed thrice with dH_2O. The plate was left to dry for 2 days and then spots were counted with the automated ImmunoSpot S6 Versa Reader System (Cellular Technology Ltd, Shaker Heights, OH, USA) and expressed as Spot-Forming Cells (SFC) per million cells.

6. Statistical analysis

Statistical analyses were performed using Prism 7.0 (GraphPad Software Inc., CA, USA) and R-3.6.3 (R Foundation for Statistical Computing). Unpaired data was compared using a non-parametric Mann-Whitney test. Multiple comparisons were performed using Kruskal-Wallis tests with Dunn's comparison or Tukey's multiple comparison test. Survival in a Kaplan-Meier table was analysed using a Mantel-Cox test. Finally, for the bioluminescence assay, curves were compared using linear mixed models with a likelihood ratio test. A p-value below 0.05 was considered statistically significant.

Results

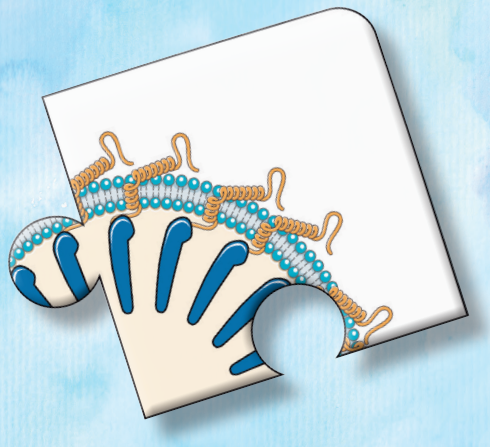

SECTION 1: CHARACTERISATION AND OPTIMISATION OF VLP PRODUCTION AND ANTIGENICITY

In this first section, MinGag-VLPs, which are HIV-1 Gag-based VLPs displaying a high density of a gp41 miniprotein called "Min" (Molinos-Albert *et al.*, 2014, 2017a) on the VLP surface, were characterised, and a protocol for their production and purification was developed and optimised. The VLP-generating *mingag* construct is a fusion protein that contains a signal peptide followed by the Min protein and the HIV-1 transmembrane domain fused to Gag with a protein linker in-between (Figure 10). Theoretically, MinGag fusion protein should be produced in the endoplasmic reticulum and then migrate to the cell membrane, where budding occurs, generating new VLPs that harbour as many immunogens as Gag molecules are needed to produce a VLP.

1. Production of fusion-protein VLPs by transient transfection with pcDNA3.1 and pVAX1 VLP-encoding constructs

To produce MinGag-VLPs, the *mingag* construct was cloned into two different plasmids, a pcDNA3.1 vector and a pVAX1 vector. pcDNA3.1 are vectors developed for expression in mammalian cells *in vitro*, while pVAX1 is an FDA-approved plasmid that can be used as a vector for DNA vaccine administration in humans. pVAX1 has the same backbone as pcDNA3.1 but has no antibiotic resistance gene for eukaryotic selection. Also, to avoid ampicillin contaminants in the final DNA product that could trigger allergic reactions in vaccinees, pVAX1 vector has a kanamycin resistance gene for prokaryotic selection instead of ampicillin. *Gag* constructs were used as a control and were also cloned into both types of plasmids.

Transfection of Expi293 with pVAX1-*mingag* and pcDNA3.1-*mingag* vectors resulted in the production of the MinGag protein, as determined by WB (Figure 18A). Gag and MinGag from supernatants of transfected cells were both recognised by an anti-p24 mAb in a WB, but only MinGag was recognised by

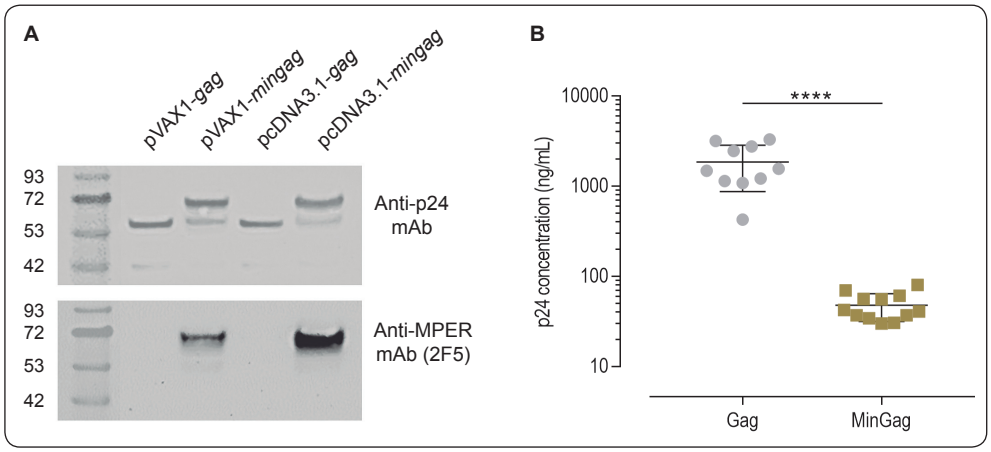

Figure 18. ***Characterisation of VLP production on Expi293F-transfected cells' supernatant.*** **A)** *WB of supernatant of Expi293F cells transfected with* gag- *or* mingag-*expressing plasmids cloned into a pcDNA3.1 or a pVAX1 vector and stained with both an anti-p24 monoclonal antibody (top panel) or an anti-MPER bNAb (2F5, bottom panel).* **B)** *Quantification of p24 concentration by ELISA on harvested supernatants from* gag-*transfected and* mingag-*transfected cells using both pVAX1 and pcDNA3.1 vectors. Data represented as mean±SD. Significant differences were found between Gag and MinGag productions (*****p*<*0.0001, Mann-Whitney test).*

an anti-MPER bNAb (2F5). They both had the expected molecular weight (MW), 55 and 70 kDa respectively. A second band was detected in the supernatant of MinGag-transfected cells when staining with the anti-p24 mAb, which was probably generated by processing or degradation of the MinGag fusion protein (Figure 18A, top panel). However, these truncations were not cleaved at the linker between Min and Gag, since the supernatant of Gag-transfected cells also had truncations with a similar size (10-15 kDa). Furthermore, MinGag truncations were positively stained by 2F5, demonstrating that the protein was cleaved at the C-terminus end of the protein (Figure 18A, bottom panel).

Although Gag and MinGag proteins were successfully produced by transient transfection of Expi293F cells, the production yield of MinGag was consistently lower than that of Gag (Figure 18B). p24 concentration of MinGag-transfected cells on the supernatant was 10 to 20 times lower compared to Gag (p<0.0001), and Gag-VLP production reached a concentration of 1 µg/mL of p24Gag.

2. Optimisation of Min antigenicity at the surface of VLP-expressing cells

Antigen conformation is important for epitope display and recognition by B cells. Min disposition at the surface of the VLPs was optimised to better expose the MPER and hence the whole Min protein, and to increase immunogenicity. To

do so, several Min variations on the *mingag* constructs at the transmembrane and linker domains were generated by cloning.

The original MinGag construct had a flexible GGGS linker between Min and Gag and the transmembrane was from the wild-type HXB2 sequence (Table 6). In the transmembrane variants, the original wild-type HXB2 transmembrane was substituted for those of human CD22, CD36 and CD44 proteins. Additionally, Min(RA)Gag had the wild-type HXB2 sequence with an arginine-to-alanine substitution at position 696. In the linker variants, the GGGS linker was substituted for AEAAAKAGS in the Min(AEA)Gag construct, for APAPAPAGS in the Min(APA)Gag construct and for no linker in the Min(NL)Gag constructs.

Min antigenicity was assessed at the surface of VLP-producing cells by flow cytometry using the anti-MPER 10E8 bNAb (Figure 19). Among these new variants, Min(CD22tm)Gag, Min(NL)Gag and Min(APA)Gag had similar antigenicity to the original MinGag construct; Min(CD44tm)Gag and Min(RA)Gag had better antigenicity and in Min(CD36tm)Gag and Min(AEA)Gag, antigenicity worsened.

A deeper characterisation was performed among the variants that displayed better antigenicity properties. The binding of 10E8 to MinGag, Min(RA)Gag, Min(NL)Gag and Min(CD44tm)Gag was further on VLP producing Expi293F cells (Figure 20A). A trend for superior binding to MPER by 10E8 was detected against Min(RA)Gag and Min(CD44)Gag, compared to MinGag and Min(NL)Gag. Additionally, the production of Min(RA)Gag seemed to be slightly higher as detected by p24 ELISA on the supernatants of VLP-producing cells (Figure 20B).

3. Development and optimisation of the purification protocol for fusion-protein VLPs

The gold-standard technique for the purification of HIV-1 VLPs and other viral particles is the sucrose cushion UC (Cervera *et al.*, 2019). However, this technique is difficult to scale up to large productions. Therefore, we developed an alternative purification strategy based on chromatography and we optimised it for the purification of MinGag-VLPs. Both approaches were compared head-to-head considering the yield and purity of the final product.

Clarified supernatants from *gag*- and *mingag*-transfected Expi293F cells were first concentrated by crossflow filtration (TFF; see methods). A 300,000 MWCO cassette was used for the retention of viral particles, while smaller soluble proteins that will pass through the pores were removed. This step increased

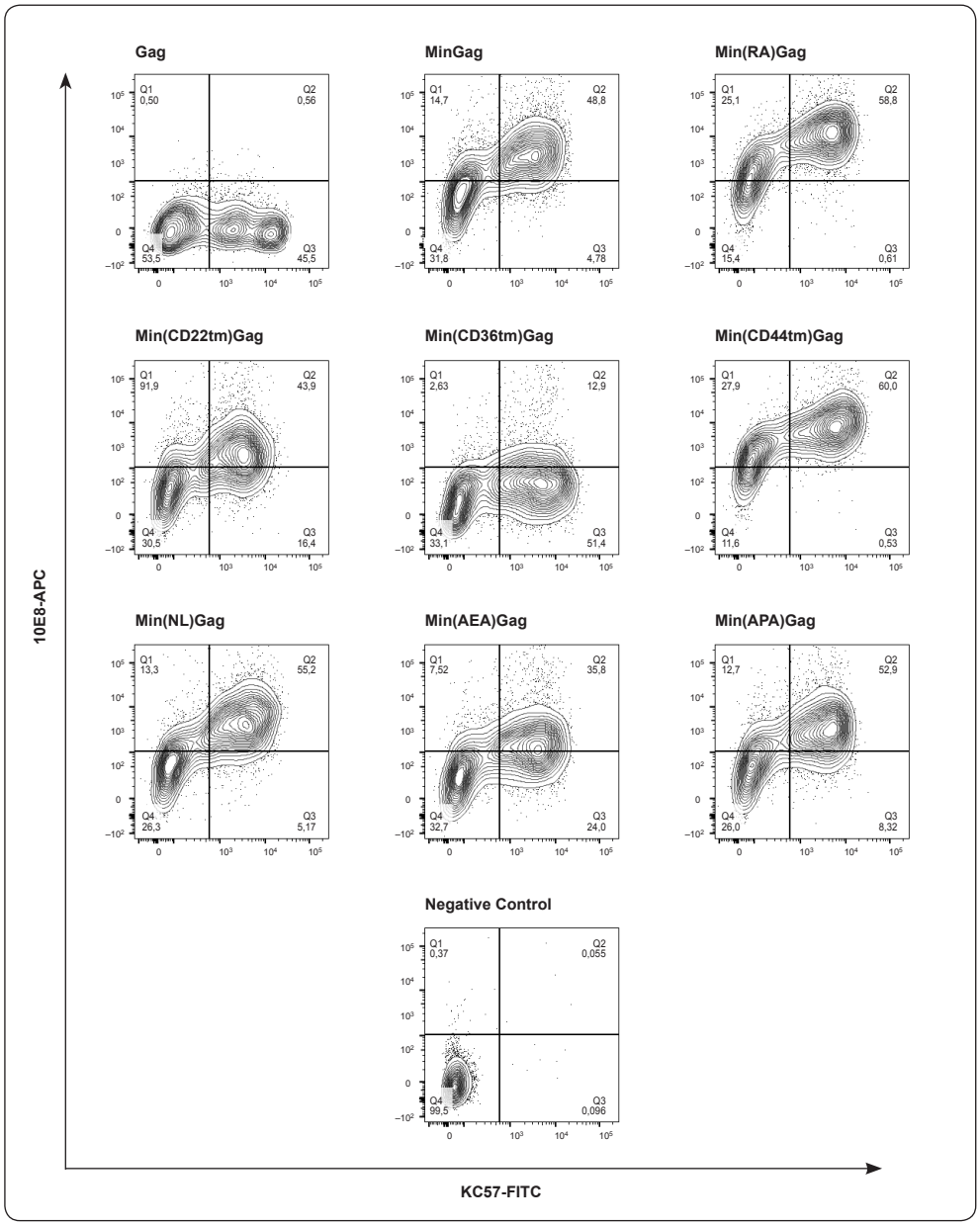

Figure 19. ***Optimisation of antigen presentation at the surface of Expi293F VLP-producing cells by FACS****. Cells were stained extracellularly with an anti-MPER bNAb (10E8) plus a secondary APC-conjugated anti-human IgG (Y-axis) and intracellularly with KC57-FITC (X-axis), a FITC-conjugated anti-p24 mAb. Different MinGag constructs with variations at the transmembrane and linker domains were transfected in Expi293F cells. Gag-transfected cells and untransfected cells were used as controls.*

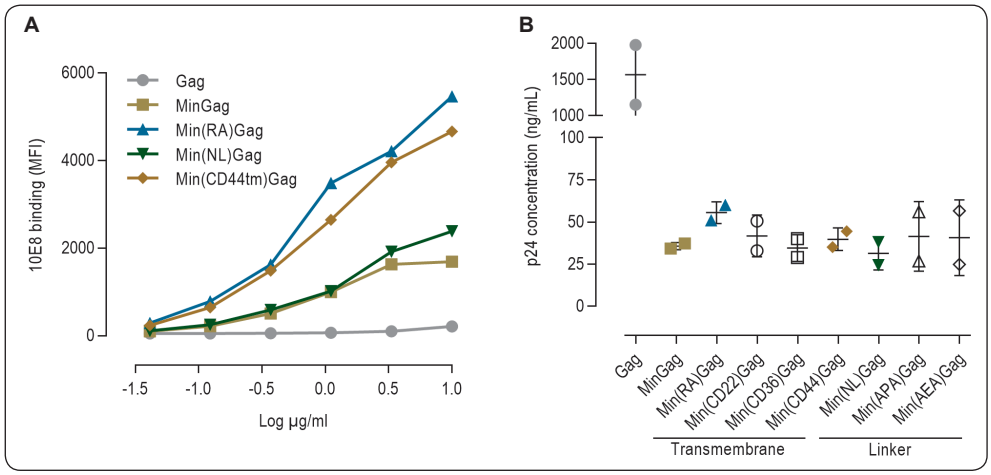

Figure 20. ***Optimisation of antigen presentation and VLP production in VLP-transfected cells with Min variants****. Variants have substitutions at the transmembrane and linker domains of the* mingag *fusion protein construct. Transmembrane variations were gp41(R696A) mutant (Min(RA)Gag), CD22, CD36 and CD44; linker variations were no-linker (NL), AEA and APA.* **A)** *Dose-response curve of 10E8-binding to Min variants on the surface of VLP-transfected cells analysed by Flow cytometry.* **B)** *p24 concentration in the supernatant of Expi293F cells transfected with each of the Min variants analysed by p24 ELISA. Data represented as mean±SD.*

the concentration of p24Gag 5-10 times (Table 11), and reduced 10-fold the initial volume, making the following UC or chromatography steps more manageable. Furthermore, removal of soluble proteins below the 300,000 Da threshold resulted in an increase of purity by a magnitude of 10 to 50-fold for both Gag-VLPs and MinGag-VLPs, as seen by comparing the final and initial ratios of p24 *vs*. total protein. The recovery by TFF for both VLP types was around 60%.

3.1. Sucrose-cushion ultracentrifugation of VLPs

After an initial TFF purification step, Gag-VLPs and MinGag-VLPs were purified by a sucrose-cushion UC procedure. The TFF retentate fraction was loaded on top of a 35% sucrose layer, ultracentrifuged, and resuspended in PBS. After

Table 11. Concentration, yield, and purity ratios of Gag-VLPs and MinGag-VLPs produced in Expi293F cells and purified by TFF

TFF	Supernatant		Retentate		Ratio p24:protein			Recovery (%)
Concentration (µg/mL)	*p24*	*Protein*	*p24*	*Protein*	*Initial (%)*	*Final (%)*	*Increase*	
Gag-VLPs	1.75	2,927.97	9.55	1,388.09	0.06	0.69	11.53	60.72
MinGag-VLPs	0.08	2,970.59	0.44	361.53	0.00	0.12	47.43	64.14

UC, the final p24 concentration was around 100 times higher compared to the p24 concentration on the clarified supernatant of Gag-VLP and MinGag-VLP transfected cells (Table 12), and the volume was reduced 250 times. Despite the increase in p24 concentration, MinGag-VLP purity did not increase compared to TFF alone, while Gag-VLP purity increased by a factor of 8 compared to purification by TFF only (Table 11). Approximately, 60-80% of the p24 that was UC was recovered in the pelleted fraction, showing that the full protocol (TFF + UC) had an overall recovery of around 50% of the loaded sample.

3.2. Ligand-core capture and anion exchange chromatography purification of VLPs

Alternatively, a two-step chromatography protocol was developed and optimised to improve MinGag-VLP purity at the end of the purification procedure. The first step of the chromatography-based purification was an LCC column (see methods). The sample was run through the column and the flowthrough recovered, while the column-bound fraction was discarded. There was no p24 loss in this step and purity increased by 2-fold (data not shown). Immediately after that, the sample was loaded to an AEX chromatography column and eluted with NaCl. To determine the ideal NaCl concentration suited for the elution of MinGag-VLPs, a gradient elution ranging from 150 mM to 850 mM of NaCl was performed. The elution of MinGag-VLPs peaked at a concentration of 250-320 mM of NaCl (Figure 21), and hence 300 mM of NaCl was used for subsequent purifications.

The full chromatography-based purification protocol, including a final step of sterilisation and adjustment of total protein concentration, delivered highly pure MinGag-VLPs and Min(RA)Gag-VLPs ready for mouse immunisation. The purity ratios of MinGag-VLPs and Min(RA)Gag-VLPs obtained with these chromatography methods were comparable to the purity ratio of Gag-VLPs (Table 13). MinGag and Min(RA)Gag purity ratio increased by a factor of 300-400 compared to the purity in the harvested supernatants, and the p24 concen-

Table 12. Concentrations, yields and purity ratios of Gag-VLPs and MinGag-VLPs produced in Expi293F cells and purified by TFF + UC

TFF + UC	Supernatant		Final product		Ratio p24:protein			Recovery (%)
Concentration (µg/mL)	*p24*	*Protein*	*p24*	*Protein*	*Initial (%)*	*Final (%)*	*Increase*	
Gag-VLPs	1.25	3,456.89	142.29	4,941.53	0.04	2.88	79.79	50.69
MinGag-VLPs	0.10	2,190.03	9.58	5,591.40	0.00	0.17	36.52	41.43

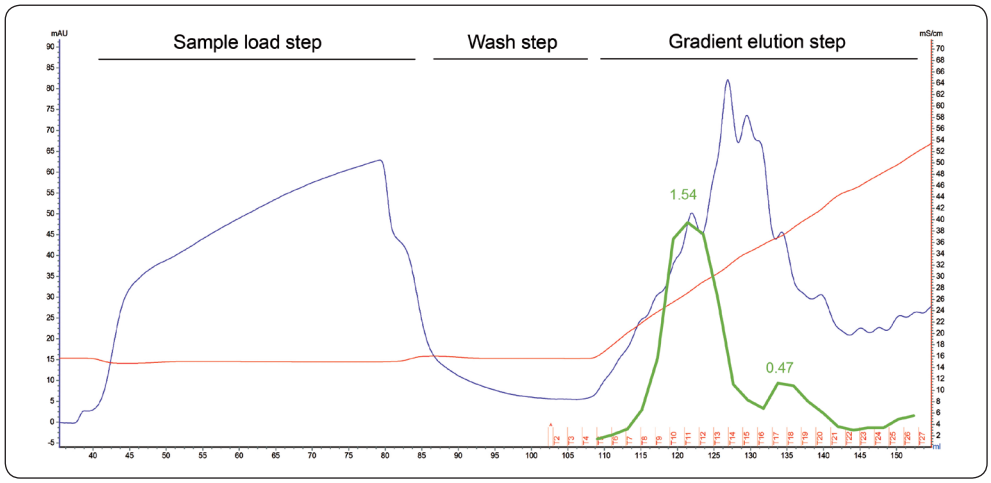

Figure 21. ***Chromatographic profile of an Anion Exchange purification of MinGag-VLPs.*** *The sample was eluted with a linear NaCl gradient starting at 150 mM NaCl and finishing at 850 mM NaCl. VLPs were eluted at 300 mM NaCl. Left axis: absorbance (mAU) at 280 nm. Right axis: conductivity (mS/cm). Green line: p24 concentration (ng/mL) determined by p24 ELISA. Green values indicate maximal concentration at each peak.*

tration increased 100 times. Although high purity levels for MinGag-VLPs and Min(RA)Gag-VLPs were achieved, the overall performance of the protocol was low since the recovery was around 10%.

Gag-VLP purity ratios were consistent across the different techniques (Table 11, 12 and 13) and did not benefit much from the chromatography based-purification protocol. The buffer conditions used for the elution of Gag-VLPs bound to AEX columns were the same as the ones decided for the optimal elution of MinGag-VLPs. This allowed for the homogenisation of physicochemical properties between constructs, when testing the VLP immunogenicity *in vivo*, and hence the reduction in confounding factors (Table 13).

Gel analysis by Coomassie Blue staining and WB using an anti-p24 mAb and an anti-MPER bNAb (2F5) confirmed the results seen by p24 ELISA and

Table 13. Concentrations, yields and purity ratios of Gag-VLPs, MinGag-VLPs and Min(RA)Gag-VLPs produced in Expi293F cells and purified by TFF + AEX

TFF + AEX	Supernatant		Final product		Ratio p24:protein			Recovery (%)
Concentration (µg/mL)	*p24*	*Protein*	*p24*	*Protein*	*Initial (%)*	*Final (%)*	*Increase*	
Gag-VLPs	1.48	2,748.30	19.77	1,399.31	0.05	1.41	26.28	5.95
MinGag-VLPs	0.04	2,089.74	4.98	804.91	0.00	0.62	317.86	13.60
Min(RA)Gag-VLPs	0.08	1,461.18	12.35	520.68	0.01	2.37	431.02	8.53

total protein quantification by BCA: several protein contaminants were removed in the filtrate fraction of the TFF step (Figure 22A, FT fraction), while having very few losses of VLPs (Figure 22B & 22C, FT fraction). VLPs mostly attached to the AEX column (Figure 22B & 22C, L&D fractions) and were eluted at an approximate concentration of 300 mM of NaCl (Figure 22B & 22C, 10-12 fractions). Those contaminants detected in the eluted 10-12 fractions were likely proteins associated with or dragged along the production and release of VLPs, such as cytoskeletal proteins. Probably, the structural Gag or MinGag protein represented less than 5% of the total protein content of a VLP, that is why repeated purifications with different VLPs (Gag, MinGag and Min(RA) Gag) and different techniques consistently yielded a purity ratio ranging 0.5-3% (Table 11, 12 and 13).

A direct comparison of both purification protocols (TFF followed by UC or TFF followed by AEX) by a Coomassie Blue stained gel and WB with an anti-p24 and an anti-MPER (2F5) antibody corroborated what had been previously described by p24 ELISA and BCA. For Gag-VLPs, both purification strategies resulted in products with similar contaminants (Figure 23A, Gag-VLPs TFF + UC and TFF + AEX lanes) but TFF + UC yielded higher p24 contents (Figure 23B, Gag-VLPs). However, for MinGag-VLPs, AEX chromatography-based purification resulted in a better product, both for the number of contaminants (Figure 23A, MinGag-VLPs TFF + UC and TFF + AEX lanes) and for the amount of the MinGag fusion protein (Figure 23B & 23C). The results were also comparable to previous WB results (Figure 18A and Figure 22B & 22C) and Coomassie Blue stained gels (Figure 22A).

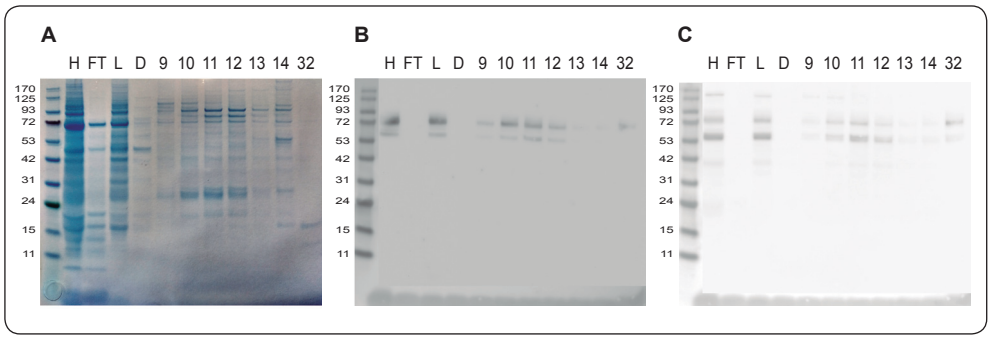

Figure 22. ***Characterisation of Min(RA)Gag-VLPs produced in transfected Expi293F cells and purified by TFF and AEX.*** **A)** *Coomassie Blue staining of each purification step and fraction;* **B)** *anti-p24 mAb WB;* **C)** *anti-2F5 bNAb Western blot. H: harvest. FT: filtrate from TFF. L: retentate from TFF and loaded to an AEX column. D: depleted fraction from AEX. 9-14: eluted fractions from AEX. 32: elution at 2 M NaCl.*

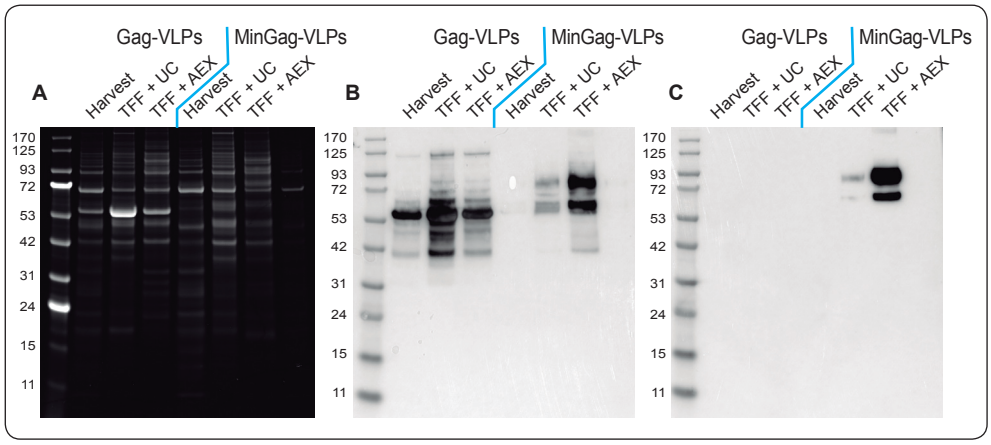

Figure 23. ***Characterisation of HIV-1 Gag-VLPs and MinGag-VLPs purified by different methods***. *Samples from harvest and purified VLP preparations by TFF plus sucrose-cushion ultracentrifugation (TFF + UC) or by TFF plus chromatography (TFF + AEX).* **A)** *Coomassie blue staining,* **B)** *anti-p24 Western blot, and* **C)** *anti-2F5 Western blot.*

4. Characterisation of purified Gag-VLPs and MinGag-VLPs

The morphology of both Gag-VLPs and MinGag-VLPs were characterised by Cryo-TEM. Cryo-TEM images of Gag-VLPs and MinGag-VLPs purified by TFF and AEX showed how both VLPs had the typical morphology of HIV-1 Gag-based VLPs, consisting of a round-shaped particle with a lipid membrane at the outer-most part of the particle that contained an electrodense Gag core surrounding the inner side of the plasma membrane (Figure 24A). MinGag-VLPs had a similar morphology (Figure 24B), but their mean size was significantly smaller (124.7±13.6nm vs. 62.9±13.0nm; $p<0.0001$) (Figure 24C).

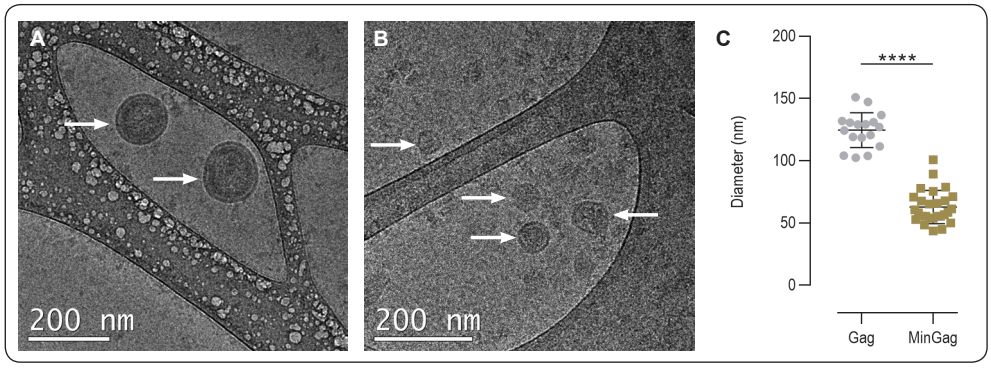

Figure 24. ***Cryogenic transmission electron microscopy images of purified VLPs***. **A)** *Cryo-TEM of purified Gag-VLPs;* **B)** *Cryo-TEM of purified MinGag-VLPs.* **C)** *Comparison of Gag-VLP (n=17) and MinGag-VLP (n=27) diameters, data represented as mean±SD. Significant differences were found between Gag-VLP and MinGag-VLP sizes (****p<0.0001, Mann-Whitney test).*

Beyond HIV-1 Gag, some host-cell proteins are also incorporated in the VLPs. Such proteins are often associated with the cytoskeleton (actin and myosin), vesicle transport (ALIX, Tsg101), protein folding (PDIA4), etc. (Cervera *et al.*, 2019). Other authors described how extracellular vesicle (EV) associated proteins can be incorporated into virions and VLPs (Izquierdo-Useros *et al.*, 2011; Steppert *et al.*, 2016). Here, the purified MinGag-VLPs were run on a Coomassie Blue stained gel, and the three main bands were excised and identified by mass spectrometry (Table 14). The main band on purified MinGag-VLPs had a size of 90 kDa and contained a mix of proteins related to the Heat shock protein 90 complex (Hsp90), such as HS90A, HS90B, H90B4, HS90, ENPL. The Hsp90 complex is involved in protein folding in the endoplasmic reticulum and has also been associated with EVs. The second most intense band, which

Table 14. Proteomic analysis of the three main bands detected in Coomassie Blue staining of MinGag-VLP products

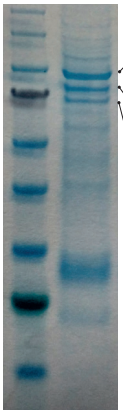

Band	Code	Name	Species	EV*	Counts
Band 1 90kDa	Hsp90[a]	Heat shock protien 90 (Hsp90) family	Human	yes	1098
	PDIA4	Protein disulfide Isomerase	Human	yes	39
	LG3BP	Galectin-3-binding protein	Human	yes	33
	Hsp70[b]	Heat shock protein 70 (Hsp70) family	Human	yes	26
	SYTC	Threonine-tRNA ligase	Human	no	25
	Gag	*Gag polyprotein*	*HIV*	—	*23*
	Env	*Envelope glycoprotein (gp41)*	*HIV*	—	*8*
Band 2 75kDa	PDIA4	Protein disulfide Isomerase	Human	yes	179
	Hsp90[a]	Heat shock protien 90 (Hsp90) family	Human	yes	81
	ACPH	Acylamino-acid-releasing enzyme	Human	no	37
	Hsp70[b]	Heat shock protein 70 (Hsp70) family	Human	yes	36
	Gag	*Gag polyprotein*	*HIV*	—	*32*
	Env	*Envelope glycoprotein (gp41)*	*HIV*	—	*2*
Band 3 65kDa	Hsp70[b]	Heat shock protein 70 (Hsp70) family	Human	yes	2013
	Plastin[c]	Plastin family	Human	act*	200
	LKHA4[d]	Leukotriene A-4 hydrolase	Human	no	88
	TKT	Transketolase	Human	no	52
	MOES	Moesin	Human	act*	44
	PGM2	Phosphoglucomutase	Human	no	44
	Gag	*Gag polyprotein*	*HIV*	—	*52*
	Env	*Envelope glycoprotein (gp41)*	*HIV*	—	*6*

EV* Proteins closely related to extracellular vesicles (EV markers)
act* Proteins related to the actin cytoskeleton
Hsp90[a] Hsp90 superfamily includes: HS90A, HS90B, H90B4, HS90, ENPL
Hsp70[b] Hsp70 superfamily includes: HS71A, HS71L, HSP76, HSP7C, GRP78, STIP1
Plastin[c] Plastin FAMILY includes PLST-I(1), -L(2) and -T(3)
LKHA4[d] LKHA4 includes Aminopeptidase B, with similar function and homology

had a size of 75 kDa, was mainly Protein disulfide Isomerase (PDIA4). PDIA4 has a similar function to Hsp90, protein folding in the endoplasmic reticulum and is an EV-marker. Finally, the band with a 65 kDa size mainly contained proteins associated with the Hsp70 (HS71A, HS71L, HSP76, HSP7C, GRP78, STIP1), which also plays a role in protein transport and folding in the endoplasmic reticulum and acts as an EV-marker. In those three bands, less predominant proteins, such as ALIX, Na^+/K^+ ATPase pump, actin, PDCD6IP, EF2, etc. were also detected (data not shown). Additionally, Gag and Min sequences were also identified throughout the three bands.

Altogether, Cryo-TEM and mass spectrometry confirmed that *gag* and *mingag* constructs were able to produce complete and intact particles that were not altered by the purification process.

To summarise, VLP fusion protein was characterised and adapted into a DNA-based vaccine strategy and the purification of VLPs *in vitro* were optimised. The VLPs selected for *in vivo* immunogenicity testing were the original MinGag-VLPs and the Min(RA)Gag-VLPs that were optimised for better antigen exposure. Also, nude Gag-VLPs were included as a control.

SECTION 2: VLP IMMUNOGENICITY AND IMMUNE RESPONSE PROFILING

In this second section, VLP immunogenicity was assessed *in vivo* in C57Bl/6JOlaHsd mice. Vaccines were tested in a homologous VLP formulation or in a heterologous DNA/VLP combination strategy. Before starting with the immune response profiling using different vaccine regimens, vaccine administration and immunogenicity of DNA and VLP formulations were evaluated to improve delivery and establish a vaccination calendar.

5. Evaluation of vaccine posology

The main challenge that DNA vaccines face is the poor uptake of plasmidic DNA into the target cells (Langer *et al.*, 2013). Many delivery strategies have been devised, but electroporation is a promising delivery system since it does not require any further downstream process and avoids the issue of anti-vector immune response induction. *In vivo* electroporation is applied at the site of injection, generally intramuscularly, where it promotes the destabilisation of the target cells' plasma membrane and the internalisation of the DNA vaccine.

5.1. Electroporation of DNA to improve *in vivo* VLP production

Injection of a firefly luciferase encoding pVAX1 plasmid (pVAX1-*FLuc*) allowed for the determination of *in vivo* transfection efficiency of DNA injection with and without electroporation by *in vivo* bioluminescence. Injection of 20 µg of pVAX1-*FLuc* was performed at both posterior hind limbs of an animal and only the left limb was electroporated (Figure 25A). After injection of luciferin 48 h post-electroporation, it was clear how *in vivo* electroporation improved the transfection efficiency of muscle cells resulting in a 3 log higher production of luciferase as demonstrated by analysis of the RLUs. Furthermore, the animals tolerated well the electroporation and did not manifest any secondary effects after awakening, other than a temporary limping that spontaneously resolved in a few seconds.

5.2. Determination of the optimal vaccination schedule

Additionally, in a second *in vivo* bioluminescence experiment, five C57Bl/6JOlaHsd mice were injected and electroporated with 20 µg of two different

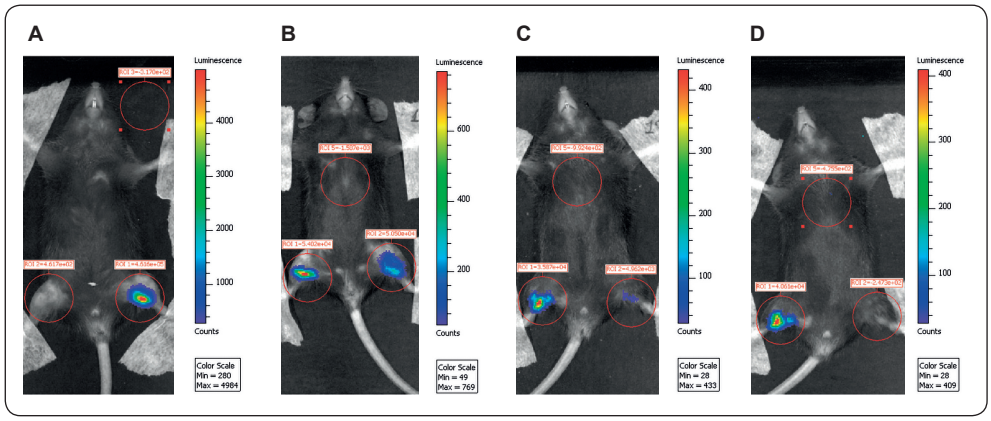

Figure 25. In vivo *bioluminescence analysis of DNA electroporation in C57Bl/6JOlaHsd mice*. A) *C57Bl/6JOlaHsd mouse injected with 20 µg of a pVAX1*-FLuc *plasmid at the posterior hind limbs with (left limb) and without (right limb) electroporation after injection.* **B)** *Mouse injected with 20 µg of DNA and electroporated with both a 1:1 mix of pVAX1:pVAX1*-FLuc *at the right limb and a 1:1 mix of pVAX1*-FLuc:*pVAX1*-min(RA)gag *at the left limb. Representative bioluminescence images of animals 48 h after co-electroporation.* **C)** *Bioluminescence of the same animal in (B) 7 days after co-electroporation.* **D)** *Bioluminescence of the same animal in (B) 14 days after co-electroporation.*

1:1 mixtures of plasmids. On the one hand, animals were intramuscularly administered with a 1:1 mix of a pVAX1 empty vector and pVAX1-*FLuc* at the posterior of the right hind limb (Figure 25B-25D). On the other hand, mice were injected with a 1:1 mix of pVAX1-*min(RA)gag* and pVAX1-*FLuc* at the posterior of the left hind limb. *In vivo* bioluminescence analysis 48 h, 7 days and 14 days post-electroporation showed how luciferase expression at the right hind limb (co-electroporated with pVAX1:pVAX1-*FLuc*) remained constant, while bioluminescence at the left hind limb (electroporated with pVAX1-*FLuc*:pVAX1-*min(RA)gag*) steadily decreased over time (Figure 25B-25D).

Longitudinal analysis of bioluminescence in animals co-electroporated at both limbs further confirmed that bioluminescence was completely eliminated 5 weeks after the DNA administration at the left limb, where firefly luciferase was co-electroporated with Min(RA)Gag (Figure 26). However, bioluminescence at the right limb remained constant, demonstrating that luciferase expression was not toxic for the muscle cells and that no clear immune response against firefly luciferase was induced. The luciferase decay observed in the left limb, where luciferase was electroporated with Min(RA)Gag, could have two explanations: i) Min(RA)Gag-VLP expression was toxic for the muscle cells; ii) muscle cells silence the expression of Min(RA)Gag-VLPs, and iii) Min(RA)

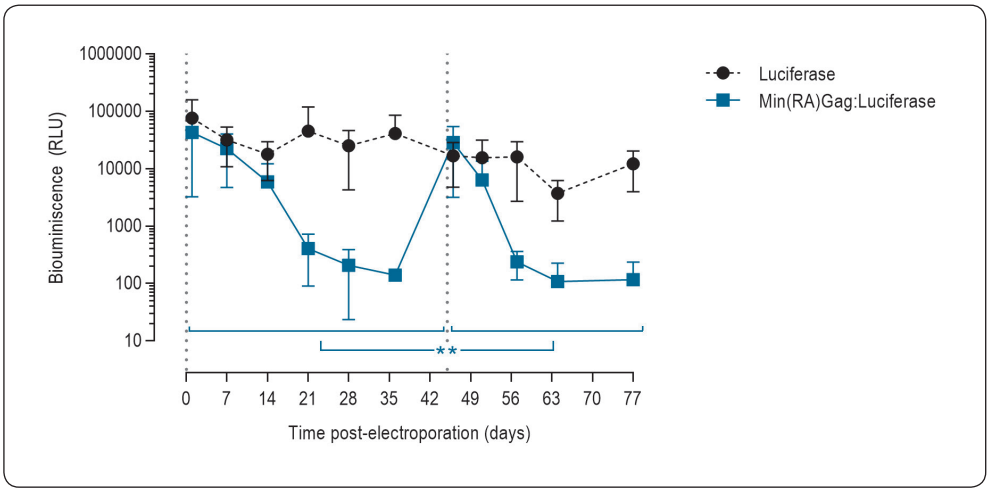

Figure 26. In vivo *bioluminescence follow-up of electroporated C57Bl/6JOlaHsd mice*. *Animals were electroporated with both pVAX1/pVAX1-*FLuc *plasmids (1:1 ratio) at the right limb and a 1:1 mix of pVAX1* FLuc:min(RA)gag *plasmids at the left limb (n=5, mean±SD of BLI). pVAX1/pVAX1-*FLuc *was electroporated at day 0 (vertical line) and pVAX1-*FLuc:*pVAX1-*min(RA)gag *mix was electroporated at day 0 and day 45. Significant differences were found using a linear mixed model analysis between the first and second slope of pVAX1-*FLuc:*pVAX1-*min(RA)gag *co-electroporated animals (**p=0.0012; likelihood ratio test).*

Gag-VLP expression in the muscle cells induced an immune response that led to the clearance of transfected cells. These three theories were not mutually exclusive.

To identify the cause of this decay, 45 days after the first co-electroporation, the left hind limb of the 5 animals was co-electroporated again with a 1:1 mix of pVAX1-*FLuc*:pVAX1-*min(RA)gag*. Bioluminescence was determined again for 1 month after the second co-electroporation. Here, the results indeed showed how bioluminescence decayed faster (Figure 26), reaching statistical significance with a linear mixed model analysis (p=0.0012; likelihood ratio test). It is important to highlight that this linear mixed model analysis considered a normal distribution of the values, but the sample size was not large enough to determine that. Despite that, these results clearly point towards a faster clearance of muscle cells after the second luciferase and Min(RA)Gag co-electroporation. This faster clearance could be immune-mediated, since a primary immune response against Min(RA)Gag-VLPs would be elicited after the first co-electroporation and, upon the second electroporation, a faster secondary immune response would arise to clear Min(RA)Gag-transfected muscle cells (Figure 26). Anti-Gag and anti-Min antibody detection in the sera of electroporated animals further supported this observation (data not shown).

These results also validate that a 3-week interval was the ideal period between each immunisation since most of the electroporated cells had been cleared by the third week after the first DNA administration (Figure 26).

5.3. Identification of immune response magnitude and antibody fading

Next, purified Gag-VLP and MinGag-VLP immunogenicity and the duration of the immune response were tested in mice. VLPs were administered at the hock, which is a subcutaneous/intradermal route of administration (RoA). This RoA represents a more humane alternative to footpad administration, while draining to similar sites, such as the popliteal and the iliac lymph nodes (Kamala, 2007). Two doses of Min(RA)Gag-VLPs (0.1 µg of p24Gag/dose without adjuvating) with a 3-week interval induced potent anti-Gag and anti-Min responses that were detectable in serum by ELISA for more than 20 weeks (Figure 27).

Overall, these pilot studies demonstrated how both DNA-based and purified VLP formulations of the *mingag* constructs induced potent humoral responses both against the Gag and the Min proteins. Furthermore, we could establish a vaccination schedule of 3-week periods that could induce potent, long-lasting responses.

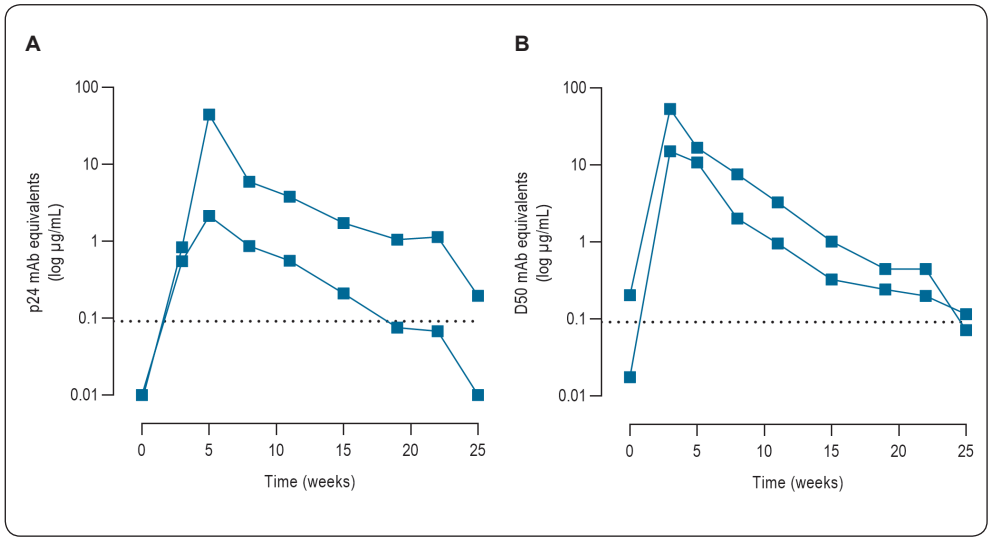

Figure 27. ***Min(RA)Gag-VLP induced antibody concentration over 25 weeks in C57Bl/6JOlaHsd mice.*** *Mice were vaccinated twice with purified MinGag-VLPs (n=2) at weeks 0 and 3 and antibody concentration in serum was determined by ELISA.* **A)** *Anti-Gag and* **B)** *anti-Min antibody concentration in mouse sera determined by ELISA.*

6. Immune response profiling with homologous or heterologous vaccination regimens

After the formal demonstration that Gag-VLPs and our fusion-protein MinGag-VLPs were immunogenic both as a DNA vaccine and as a purified product, different vaccination regimens were tested in mice. The combination of different vaccines coding for the same immunogen was demonstrated to induce superior humoral and cellular responses (Ding *et al.*, 2011; Chea and Amara, 2017; Perdiguero *et al.*, 2019a). In this project, a homologous regimen of 4 purified VLP doses (VVVV) was tested against a heterologous regimen where the animals were primed with 2 doses of electroporated DNA and boosted with 2 doses of purified VLPs (DDVV) (Figure 16). Purified VLPs were administered at a dose of 0.1 µg of p24Gag/animal without adjuvating. Both MinGag-VLPs and Min(RA)Gag-VLPs were evaluated using both regimens. Gag-VLPs and PBS were used as controls.

6.1. Quantification of anti-Gag and anti-Min humoral responses

Vaccination with both regimens was well tolerated by animals. Mice displayed no serious adverse effects, save for the short-lived ones associated with anaesthesia and electroporation, which were mild and quickly resolved. Analysis of antibody concentration in the sera throughout the vaccination regimens demonstrated how anti-Gag and anti-Min humoral responses in both immunisation regimens were rapidly elicited (Figure 28). Anti-Gag responses reached a plateau after a single dose in both regimens and for all VLPs, except for Gag-VLPs in the VVVV regimen (Figure 28A), where the response slowly increased until the third vaccination. Furthermore, anti-Gag antibody concentration in the DDVV regimen was 1-log higher than in the VVVV regimen for Gag-VLPs ($p<0.01$), MinGag-VLPs ($p<0.01$) and Min(RA)Gag-VLPs ($p<0.001$). Anti-Min antibody response in the VVVV regimen also reached a plateau after the first immunisation (Figure 28B), but in the DDVV regimen, anti-Min titres increased until the third immunisation, yielding a 5-10-fold higher response compared to VVVV at week 12 for MinGag ($p<0.0052$). Additionally, the optimised Min(RA)Gag-VLPs in the DDVV displayed a trend towards higher antibody titres compared to MinGag-VLPs within the DDVV regimen (non-significant). Overall, the DDVV regimen reached higher antibody responses and performed better than VVVV.

Males and females within each group were compared to account for sex-based biases, but no significant differences were found at week 12 using a Kruskal-Wallis

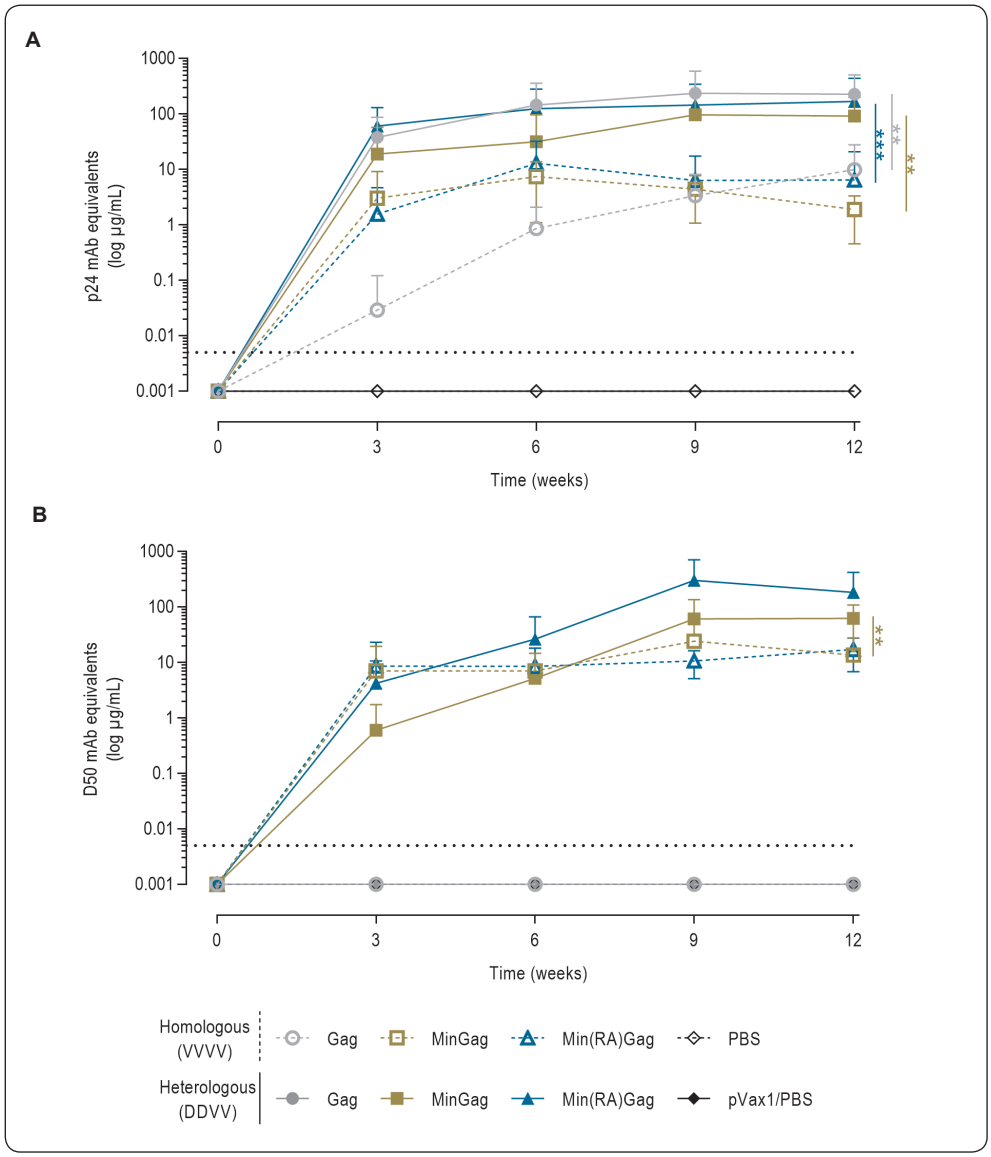

Figure 28. ***Antibody concentrations of VLP-induced humoral responses against Gag and Min using heterologous and homologous regimens****. Data represented as mean±SD of C57Bl/6JOlaHsd antibody concentration in mouse sera immunised with Gag-VLPs (n=10), Min(RA)Gag-VLPs (n=10), pVAX1/PBS control (n=4) or PBS control (n=4) using a homologous VLP regimen (VVVV; dashed lines) or a heterologous DNA/VLP regimen (DDVV; solid lines).* **A)** *Anti-Gag antibody concentration in mice serum determined by ELISA. Statistical differences at week 12 were found between Gag VVVV vs. Gag DDVV (**p=0.0054), MinGag VVVV vs. MinGag DDVV (**p=0.0073) and Min(RA)Gag VVVV vs. Min(RA)Gag DDVV (***p=0.0009) using a Kruskal-Wallis with Dunn's comparison test.* **B)** *Anti-Min antibody concentration in mice serum determined by ELISA. Statistical differences at week 12 were found between MinGag VVVV vs. MinGag DDVV (**p=0.0052) using a Kruskal-Wallis with Dunn's comparison test.*

test regardless of the vaccination regimen or the protein targeted. However, females displayed a tendency to higher antibody responses than males (Figure 29).

6.2. Epitope mapping of anti-Min antibodies

The next step was to map the anti-Min humoral response and to identify epitope specificity. Sera from animals vaccinated with the homologous and heterolo-

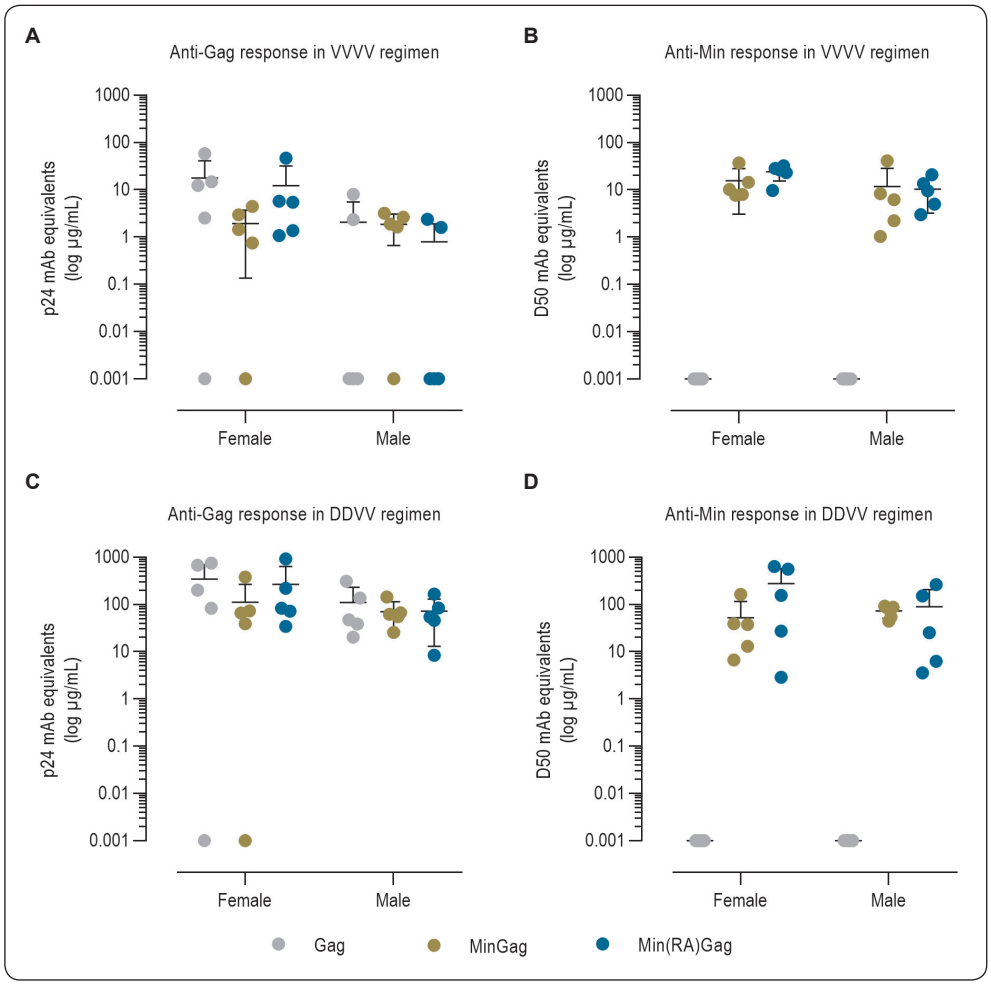

Figure 29. ***Comparison of the anti-Gag and anti-Min humoral responses between males and females.*** *Mice were immunised with Gag-VLPs (n=10), MinGag-VLPs (n=10) or Min(RA) Gag-VLPs (n=10) using either a homologous (VVVV) or a heterologous (DDVV) regimen. All groups were sex-balanced (50% females). Data represented as mean±SD.* **A)** *Anti-Gag antibody concentration in plasma using a homologous regimen.* **B)** *Anti-Min antibody concentration in plasma using a homologous regimen.* **C)** *Anti-Gag antibody concentration in plasma using a heterologous regimen.* **D)** *Anti-Min antibody concentration in plasma using a heterologous regimen. No statistically significant differences were detected using a Kruskal-Wallis test.*

gous regimens at week 12 were tested against a group of Min overlapping peptides that were 15 amino acids long and overlapped by 11 peptides (Figure 30A). Both DDVV and VVVV regimens induced humoral responses that recognised the N-terminus part of Min (Min OLP #155), meaning that they were main-

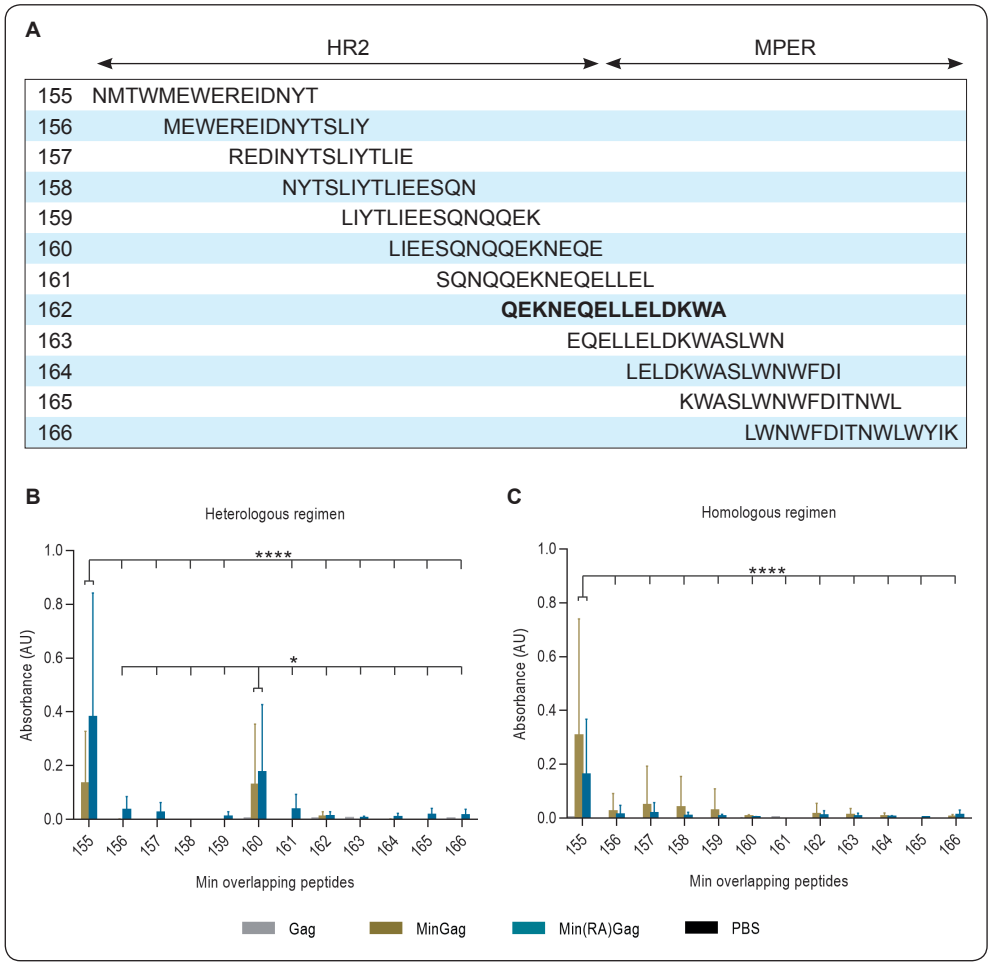

Figure 30. ***Mapping of the main Min linear epitopes targeted by VLP-induced antibody responses.*** *The reactivity of IgG antibodies present in serum samples from mice vaccinated with Gag-VLPs (n=10), MinGag-VLPs (n=10), Min(RA)Gag-VLPs (n=10) and PBS control (n=4) against 12 Min overlapping peptides (OLPs) were analysed by ELISA. Data show the mean±SD of the optical density (OD).* **A)** *Scheme of Min overlapping peptides.* **B)** *Mapping of the anti-Min humoral responses in the DDVV regimen. Significant differences in the MinGag-VLP and Min(RA) Gag-VLP vaccinated animals were found against Min OLP #155 (****p<0.0001) and #160 (*p<0.05) compared to the rest of the peptides with a Kruskal-Wallis test with Tukey's multiple comparison test.* **C)** *Mapping of the anti-Min humoral responses in the VVVV regimen. Significant differences in the MinGag-VLP and Min(RA)Gag-VLP vaccinated animals were found against Min OLP #155 (****p<0.0001) compared to the rest of the peptides with a Kruskal-Wallis test with Tukey's multiple comparison test.*

ly targeting the HR2 domain ($p<0.0001$; Figure 30B & 30C). Additionally, the antibodies induced with MinGag-VLPs and Min(RA)Gag-VLPs in the DDVV regimen also targeted the Min OLP #160, which contains the C-terminus end of the HR2 domain, closer to the MPER ($p<0.05$; Figure 30C). Anti-MPER antibodies were not successfully elicited by vaccination, probably due to the physiological characteristics of the C57Bl/6 mouse model, which mainly elicits Th1 responses and therefore it is harder to induce antibody responses in this model.

6.3. IgG subclasses profiling of anti-Gag and anti-Min antibody responses

IgG subclasses of the vaccine-induced anti-Gag and anti-Min antibodies were also determined in the mouse sera from animals vaccinated with both regimens at week 12. Determination of the IgG subclasses can help to elucidate which type of functions the antibodies may promote. C57Bl/6 IgG isotypes are IgG1, IgG2b, IgG2c and IgG3 (IgG2a and IgG2c are considered equivalents) and they arise from different stimuli and have varied functions (Collins, 2016). Both immunisation regimens (DDVV and VVVV) gave similar IgG subclasses profiles for anti-Gag and anti-Min antibodies (Table 15 and Table 16); the only difference being a lower magnitude in the VVVV regimen, which also correlated with previous results (Figure 28). In contrast, IgG subclasses signature did differ between anti-Gag and anti-Min antibodies, since anti-Min antibodies were mostly skewed towards an IgG2c subclass, while anti-Gag antibodies were more heterogeneous in both DDVV (Table 15) and VVVV (Table 16). IgG2c is considered an equivalent of human IgG1 antibodies. IgG3 subclasses were barely detected in anti-Gag and anti-Min IgGs. No differences were detected between MinGag-VLPs and Min(RA)-Gag-VLPs.

6.4. Identification of humoral responses against VLP-producing host cell proteins

Previous characterisation of MinGag-VLP composition demonstrated how host cell-derived proteins were incorporated in the VLPs during their *in vitro* production. Since VLP-producing Expi293F cells are a cell line derived from a HEK293 cell line, all the proteins incorporated into VLPs, except for the HIV-derived proteins, have a human origin. Therefore, they can be immunogenic when injected into mice.

Table 15. **IgG subclasses of anti-Gag and anti-Min humoral responses in the heterologous regimen**

DDVV	Anti-Gag response				Anti-Min response			
	IgG1	IgG2b	IgG2c	IgG3	IgG1	IgG2b	IgG2c	IgG3
Gag	0.01	0.10	0.01	0.03	0.00	0.00	0.28	0.00
	1.67	1.70	2.00	0.00	0.00	0.00	0.00	0.17
	0.88	1.00	1.82	0.06	0.00	0.00	0.00	0.00
	0.07	1.62	2.01	0.03	0.00	0.00	0.23	0.00
	1.36	2.15	2.16	0.34	0.00	0.00	0.00	0.00
	0.97	0.68	1.68	0.21	0.00	0.01	0.00	0.28
	0.00	0.62	1.34	0.05	0.00	0.00	0.42	0.00
	0.14	1.71	1.81	0.00	0.00	0.00	0.07	0.00
	1.40	1.33	1.50	0.01	0.00	0.03	0.06	0.00
	0.44	1.22	1.76	0.02	0.00	0.00	0.01	0.00
MinGag	0.07	1.99	2.21	0.69	0.00	1.66	2.05	0.00
	1.13	1.27	1.78	0.00	0.05	1.18	0.90	0.06
	0.08	0.00	0.41	0.01	0.00	0.07	0.78	0.00
	1.24	1.24	1.57	0.16	0.11	0.08	1.90	0.33
	1.14	1.52	1.78	0.38	0.02	0.43	0.90	0.00
	2.04	1.62	1.96	0.37	0.10	0.10	1.90	0.35
	0.32	0.85	1.62	0.18	0.00	1.25	2.03	0.23
	0.57	0.76	1.56	0.10	1.71	0.37	0.53	2.12
	0.05	0.94	1.93	0.06	0.08	1.44	1.74	0.02
	0.13	1.28	1.83	0.20	1.79	0.36	1.81	0.18
Min(RA)Gag	0.75	1.47	2.19	0.05	0.49	2.18	1.86	0.21
	0.00	0.68	1.85	0.00	0.05	0.04	0.29	0.00
	1.89	1.54	1.57	0.24	0.07	0.29	1.57	0.41
	0.01	0.66	1.84	0.01	0.03	0.91	1.83	0.00
	1.67	1.37	1.69	0.06	0.06	2.11	2.04	0.04
	0.47	0.60	1.78	0.28	0.00	2.01	1.92	0.07
	0.06	0.92	1.61	0.04	0.45	0.01	1.12	1.25
	0.00	0.42	0.84	0.15	0.07	0.00	0.50	0.06
	1.62	1.09	1.68	0.23	0.07	0.16	0.24	0.05
	0.60	1.13	1.84	0.02	1.13	0.04	2.06	0.28
PBS	0.00	0.00	0.00	0.00	0.00	0.00	0.00	0.00
	0.00	0.00	0.02	0.03	0.00	0.00	0.00	0.00
	0.36	0.00	0.03	0.00	0.00	0.00	0.00	0.03
	0.00	0.00	0.04	0.00	0.03	0.03	0.00	0.47

OD values are indicated.

Table 16. **IgG subclasses of anti-Gag and anti-Min humoral responses in the homologous regimen**

VVVV	Anti-Gag response				Anti-Min response			
	IgG1	IgG2b	IgG2c	IgG3	IgG1	IgG2b	IgG2c	IgG3
Gag	0.27	0.00	0.12	0.01	0.00	0.00	0.00	0.00
	0.99	0.96	0.62	0.07	0.00	0.00	0.00	0.00
	0.03	0.00	0.02	0.00	0.00	0.00	0.00	0.00
	0.88	0.14	0.29	0.02	0.00	0.01	0.00	0.00
	0.00	0.01	0.03	0.00	0.00	0.00	0.00	0.00
	0.08	0.24	0.73	0.00	0.15	0.01	0.00	0.00
	0.23	0.97	1.58	0.01	0.00	0.05	0.00	0.00
	0.54	2.55	2.11	0.21	0.00	0.06	0.00	0.00
	0.13	1.82	1.20	0.04	0.00	0.00	0.00	0.00
	0.09	0.34	0.02	0.01	0.00	0.00	0.00	0.00
MinGag	0.08	0.00	0.02	0.01	0.72	0.28	0.00	0.03
	0.29	0.00	0.47	0.07	2.19	0.15	1.19	1.91
	0.14	0.00	0.74	0.04	0.74	1.15	3.10	0.14
	1.21	0.08	0.06	0.03	0.00	0.25	1.68	0.01
	0.36	0.07	0.44	0.01	0.31	0.02	0.92	0.11
	0.06	0.01	0.02	0.00	0.00	0.17	1.97	0.01
	0.09	0.21	0.10	0.06	2.06	0.14	1.94	1.05
	0.31	0.80	0.78	0.00	1.17	0.77	2.86	0.03
	0.69	0.00	0.02	0.00	0.37	1.38	0.98	0.73
	0.68	0.23	0.06	0.06	0.00	0.11	2.38	0.04
Min(RA)Gag	0.55	0.30	0.63	0.05	0.00	0.01	2.34	0.06
	0.03	0.37	0.43	1.09	1.07	0.08	2.67	1.15
	1.25	0.00	0.34	0.00	0.67	0.14	1.02	0.45
	0.17	0.09	0.00	0.00	0.40	0.00	1.70	0.00
	0.28	0.04	0.00	0.00	2.05	0.01	2.03	0.29
	3.44	0.74	2.43	0.05	0.31	1.23	2.72	0.12
	1.00	0.77	1.00	0.02	2.35	1.69	2.12	0.73
	0.01	0.09	0.46	0.01	2.36	0.16	2.36	0.01
	0.00	0.00	0.31	0.02	0.00	0.08	2.06	0.03
	0.73	0.82	0.58	0.08	0.01	1.89	2.50	0.03
PBS	0.00	0.04	0.09	0.00	0.12	0.01	0.00	0.00
	0.00	0.00	0.07	0.00	0.00	0.00	0.00	0.00
	0.00	0.02	0.02	0.03	0.00	0.00	0.00	0.00
	0.00	0.01	0.02	0.17	0.00	0.05	0.00	0.00

OD values are indicated.

To identify anti-human specific humoral immune responses, serum from vaccinated mice was incubated with untransfected Expi293F cells and mouse antibody binding to these cells was analysed by Flow Cytometry with an anti-mouse fluorochrome-conjugated secondary antibody. This analysis demonstrated how the immune system was indeed reacting to human proteins present in the VLPs and how antibody titres elicited against these proteins increased after each immunisation (Figure 31). It is worth mentioning that antibody titres against human proteins in the VVVV regimen increased after each VLP immunisation, except for the last dose, where antibody titres did not further increase. As expected, in the DDVV regimen, a delay in the elicitation of anti-human humoral responses was detected, since the first two doses were DNA-based and VLPs were produced *in vivo* in the muscle cells of electroporated mice. At week 12, we found significant differences between the homologous and heterologous regimens in MinGag-VLP vaccinated animals (p=0.0034) and Min(RA)Gag-VLPs vaccinated animals (p=0.05).

These results could help to explain why anti-Gag and anti-Min humoral responses in the VVVV regimen reached a plateau after the first dose, since later doses were mainly boosting humoral responses against human proteins instead.

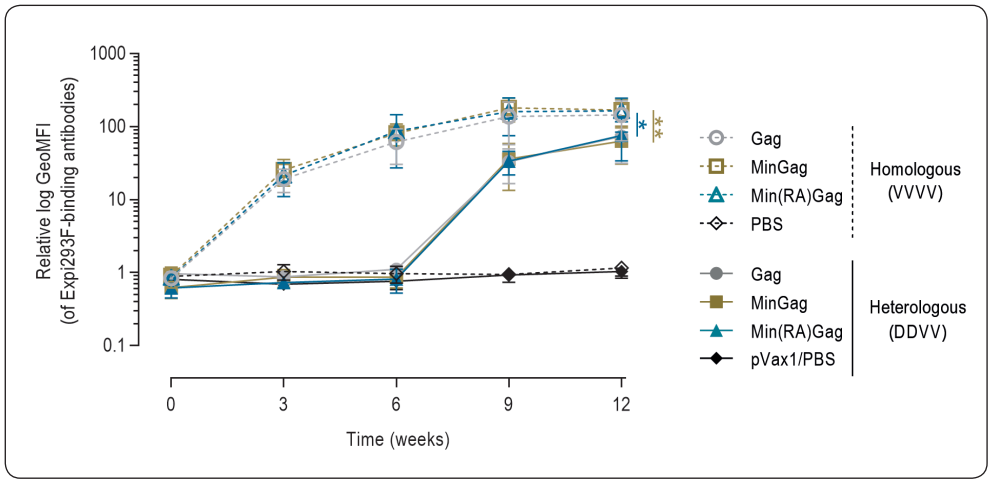

Figure 31. ***Humoral immune response against Expi293F host cell proteins.*** *The binding to Expi293F cells of IgGs present in mice immunised with Gag-VLPs (n=10), MinGag-VLPs (n=10), Min(RA)Gag-VLPs (n=10), pVAX1/PBS control (n=4) or PBS control (n=4) using a homologous VLP regimen (VVVV; dashed lines) or a heterologous DNA/VLP regimen (DDVV; solid lines), was analysed by FACS. Data presented as geometrical Mean Fluorescence Intensity (Geo-MFI)±SD. Statistical differences at week 12 were found between MinGag VVVV vs. MinGag DDVV (**p=0.0034) and Min(RA)Gag VVVV vs. Min(RA)Gag DDVV (*p=0.05) using a Kruskal-Wallis with Dunn's comparison test.*

6.5. Evaluation of antiviral functions of anti-Min antibodies

Antibody functions are diverse and range from direct neutralisation of pathogens to effector functions activated through the Fc domain of antibodies. Such effector functions are ADCC, ADCP, ADNP, opsonisation and complement activation, and they can play a major role in the protection against infectious agents, favouring the clearance of the infection (Lu *et al.*, 2018).

Neutralising antibodies are those that after binding to the virus are able to block the infection of the target cells. Therefore, elicitation of neutralising antibodies is the primary objective of most vaccine strategies, but in the case of HIV-1, is the hardest one to achieve. In our VLP strategy, MinGag-VLPs and Min(RA)Gag-VLPs were not capable of inducing a neutralisation response against a panel of 3 subtype B pseudoviruses, independently of the vaccination regimen used (Figure 32). No MPER-specific neutralising responses were detected using 7312A/C1, an HIV-2 Env chimeric pseudovirus in which the MPER domain was substituted by the HIV-1 subtype B MPER. This chimeric pseudovirus allows for the identification of anti-MPER specific neutralising antibodies.

Besides direct neutralisation, IgGs can bind to cell surface Fc Receptors via the Fc domain. Upon antigen recognition, cross-linking of multiple Fc recep-

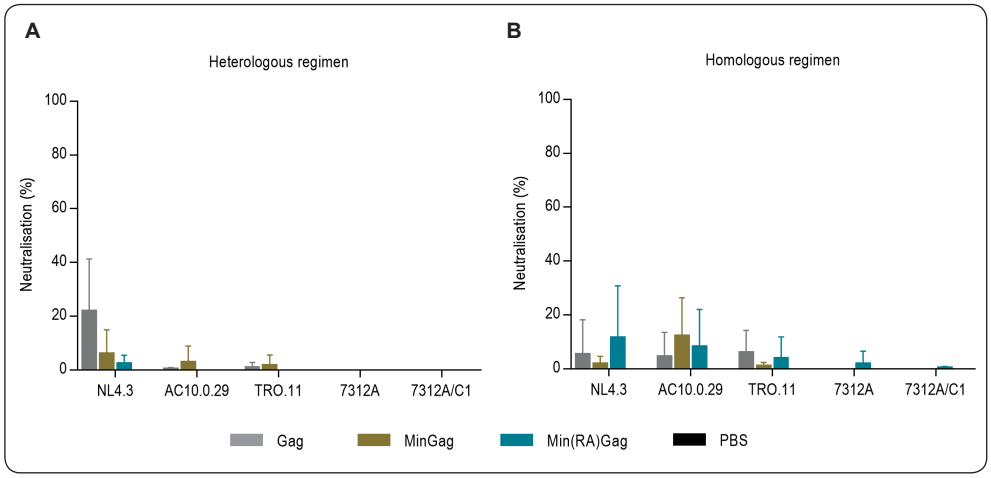

Figure 32. **In vitro *neutralisation assay of VLP-induced immune responses against a panel of 5 subtype B HIV-1 pseudoviruses***. *Serum samples from C57Bl/6JOlaHsd mice vaccinated with Gag-VLP (n=10), MinGag-VLP (n=10), Min(RA)Gag-VLP (n=10) or PBS control (n=4) were tested against a panel of 3 subtype B pseudoviruses and an HIV-2/HIV-1 subtype B MPER (7312A/C1) and its HIV-2 control (7312A). Data represented as mean±SD.* **A)** *C57Bl/6JOlaHsd mice vaccinated with a heterologous DNA/VLP regimen (DDVV).* **B)** *C57Bl/6JOlaHsd mice vaccinated with a homologous VLP regimen (VVVV). No significant differences were found between groups using a Kruskal-Wallis test.*

tors on the surface of innate immune cells, such as phagocytes, NK cells or mast cells, can trigger downstream signalling pathways that activate them to promote antibody-mediated responses. Human CD16 (FcγRIII) is one of these receptors that bind to IgG1 antibodies that have engaged their target antigen and signals NK cells to degranulate, therefore inducing ADCC against the targeted cells (Watzl and Long, 2010). The murine equivalent to human CD16 is the mouse CD16-2 (mFcγRIV), which can promote ADCC upon binding of IgG2a/IgG2c and IgG2b antibodies. Since IgG2c was the main isotype induced against Min by MinGag-VLP and Min(RA)Gag-VLP vaccination, binding to CD16-2 of VLP-induced anti-Min antibodies in mouse sera was analysed by ELISA. The results showed that anti-Min antibodies induced by MinGag-VLPs (DDVV regimen) significantly bound to CD16-2 (Figure 33A), compared to the Gag-VLP and the PBS controls ($p<0.001$ and $p<0.01$, respectively). Similar results were observed for Min(RA)Gag-VLP induced anti-Min antibodies ($p<0.05$). In contrast, in the VVVV regimen, induced antibodies only showed a higher tendency to bind to CD16-2, without achieving statistically significant differences between groups (Figure 33B), probably due to the fact that titres of anti-Min antibodies were lower in the homologous than in the heterologous regimens.

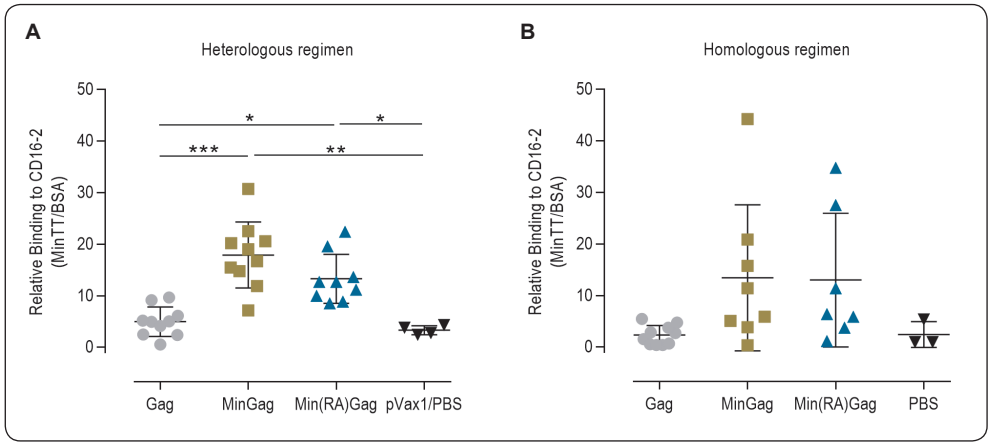

Figure 33. ***Binding of Min-specific VLP-induced IgG in serum to mFcγRIV (CD16-2)****. Data represented as mean±SD of relative binding, this being the absorbance values of each serum sample against Gp41-MinTT referred to its absorbance against BSA.* **A)** *Serum samples from Gag-VLP (n=10), MinGag-VLP (n=10), Min(RA)Gag-VLP (n=9) and pVAX1/PBS control (n=4) vaccinated animals with an heterologous DNA/VLP regimen.* **B)** *Serum samples from Gag-VLP (n=10), MinGag-VLP (n=8), Min(RA)Gag-VLP (n=7) and pVAX1/PBS control (n=3) vaccinated animals with an homologous VLP regimen. Significant differences were found in the DDVV regimen between MinGag-VLP and Min(RA)Gag-VLP vaccinated animals and the controls (*p≤0.05, **p≤0.01, ***p≤0.001, Kruskal-Wallis test).*

Even though binding to a recombinant CD16-2 receptor is not direct proof that an antibody can promote ADCC functions, these results suggest that VLP-induced anti-Min antibodies could potentially mediate protective effector functions *in vivo*.

6.6. Characterisation of cellular responses in splenocytes

Cellular immune responses are relevant not only for direct antiviral control of infected cells by $CD8^+$ Tc lymphocytes, but also $CD4^+$ Th cells play a crucial role in the activation of B cells and antibody affinity maturation in the germinal centres.

To identify IFN-γ-producing $CD8^+$ cellular responses, the splenocytes from VLP-vaccinated animals (with both homologous and heterologous regimens) were stimulated *in vitro* with a pool of 20 overlapping Gag 15-mer peptides, a pool of 12 18-mer Min peptides and the MPER peptide. Although no significant differences were found between groups, cellular immune responses were mainly generated against Gag (Figure 34). As expected, no cellular responses were

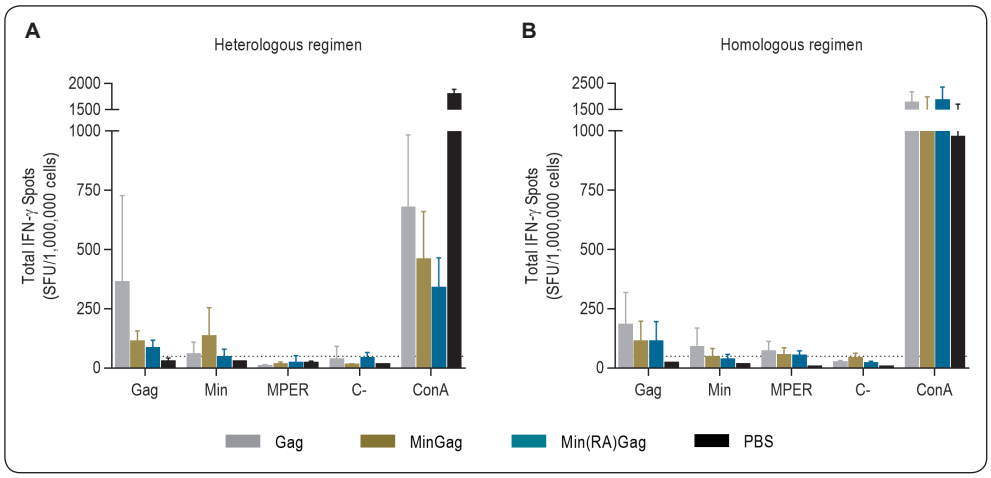

Figure 34. ***Cellular immune responses against Gag, Min and MPER****. Splenocytes from C57Bl/6JOlaHsd mice immunised with Gag-VLPs, MinGag-VLPs, Min(RA)Gag-VLPs or PBS were stimulated* in vitro *with two pools of peptides covering Gag and Min proteins, and with an MPER peptide. Unstimulated splenocytes were used as a negative control (C-) and Concanavalin A (ConA) was used as a positive control. IFN-γ-producing T cells were detected by ELISpot. Data represented as mean±SD.* **A)** *Splenocytes from mice immunised by a heterologous DNA/VLP regimen of Gag-VLPs (n=8), MinGag-VLPs (n=4), Min(RA)Gag-VLPs (n=3).* **B)** *Splenocytes from mice immunised by a homologous VLP regimen of Gag-VLPs (n=7), MinGag-VLPs (n=7), Min(RA)Gag-VLPs (n=2). No significant differences were found between groups using a Kruskal-Wallis test.*

elicited against the MPER and a modest response was elicited against Min in Min(RA)Gag-VLP immunised animals with the heterologous regimen (Figure 34A). Broadly speaking, the heterologous DDVV regimen displayed a trend for inducing superior cellular responses than the homologous regimen.

Altogether, considering the magnitude of the humoral immune response, the IgG subclass profile and the linear epitopes targeted by the vaccine-induced antibodies, the heterologous DDVV vaccination regimen induced a better immune response profile than the homologous VVVV vaccination regimen. Furthermore, the heterologous DDVV vaccination regimen also induced antibodies that had a better binding to CD16-2, while cellular responses were also superior.

SECTION 3: DEVELOPMENT OF AN *IN VIVO* EXPERIMENTAL MODEL TO IDENTIFY ANTIBODY-MEDIATED PROTECTION

Fusion-protein MinGag-VLPs demonstrated being capable of inducing potent humoral immune responses against the antigen displayed at the surface of VLPs and Gag. Moreover, anti-Min antibodies bind CD16-2, suggesting that these antibodies could mediate Fc-related functions beyond direct neutralisation. Since wild-type mice cannot get infected with HIV-1, an indirect method to assess those functions *in vivo* was developed. In this method, a melanoma tumour cell line was engineered to express Min at its surface and was inoculated into VLP-vaccinated animals to identify whether they were capable of halting tumour progression.

7. Generation of a Min-expressing melanoma (B16F10) cell line

B16F10 cells are a melanoma cell line isolated from C57Bl/6 mice. B16F10 is a well-established cell line for the evaluation of immunotherapies and different treatments against melanoma. They are characterised for being poorly immunogenic and resistant to the effect of T cell responses. In this case, stably transfected Min-expressing cells were used to functionally evaluate VLP-induced humoral responses.

B16F10 cells were transfected with a linearised pcDNA3.1-*min(tm)* plasmid, to express the Min protein with the transmembrane domain, but not Gag. Cells were selected with geneticin for 8 days (Figure 35A). After that, Min expression in transfected cells was characterised by 2F5 staining and analysed by flow cytometry (Figure 35B). 2F5-positive cells were single-cell sorted and further cultured with geneticin. Once the sorted cells started dividing, geneticin was removed and loss of Min expression in single clones was analysed (Figure 35B, right panel). Among the clones that did not display loss of Min expression, long-term culture without antibiotic was performed to analyse the stability of Min at the surface of B16F10 cells (Figure 35C). Despite a slight decrease in the initial weeks, Min expression in the sorted and antibiotic-selected B16F10Min clone was stable and well above the positivity threshold for at least two months in absence of the antibiotic.

8. *In vivo* results of tumour progression and tumour-free survival

C57Bl/6JOlaHsd mice were vaccinated with two doses (0.1 µg/dose of unadjuvanted VLPs) of Gag-VLPs or Min(RA)Gag-VLPs. Two weeks after the last

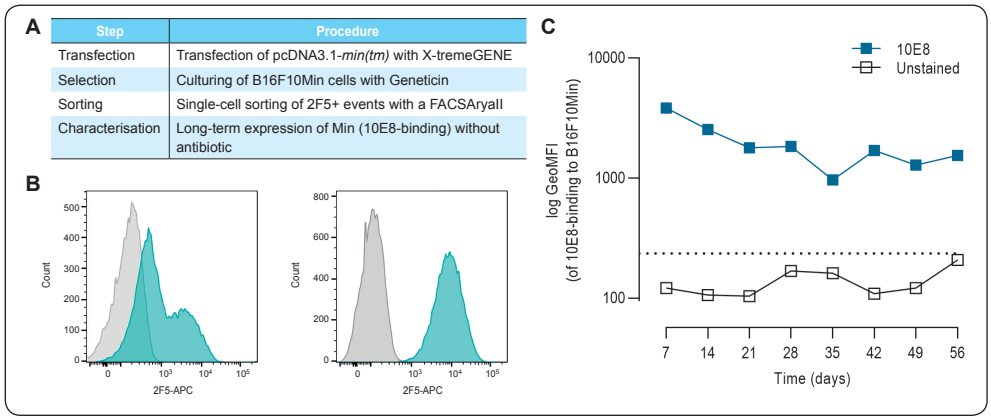

Figure 35. ***Development of a melanoma B16F10 cell line that stably expresses Min at the cell surface.*** **A)** *Pipeline for the development of B16F10Min cells.* **B)** *Histograms showing 2F5-staining of B16F10 (grey) and B16F10Min cells (blue) before sorting (left histogram) and B16F10 (grey) and a single-sorted B16F10Min clone (blue) that expresses Min in absence of antibiotic (right).* **C)** *Stability of Min at the surface of a single cell sorted B16F10Min clone in absence of eukaryotic selection antibiotic (geneticin). Data represented as geometrical mean fluorescence intensity (GeoMFI). Dotted line shows the positivity threshold determined by staining wild-type B16F10 cells.*

immunisation, vaccinated mice were inoculated with 100,000 B16F10Min cells and were monitored for 80 days after tumour inoculation. All animals injected with PBS instead of VLPs showed a rapid progression of the tumour, which was detectable as soon as 9 days after tumour-inoculation (Figure 36A). Tumour growth in VLP vaccinated animals was delayed compared to PBS animals, and it started being measurable for both Gag-VLP and Min(RA)Gag-VLP vaccinated animals 15-20 days after tumour inoculation. Tumour progression in Min(RA) Gag-VLP vaccinated animals did not start differing from Gag-VLP animals until one month after tumour inoculation. No further tumour growth was detected in any animal after day 50 post-tumour inoculation (data not shown).

Tumour-free survival results in B16F10Min-inoculated mice were similar to the tumour progression results, since the main criterion for a humane endpoint was reaching a tumour size bigger than 1,000 mm^3 and hence all animals were euthanised according to this criterion. All PBS vaccinated animals had been euthanised by day 30 post-tumour inoculation (Figure 36B) and 6 out of 9 Gag-VLP vaccinated mice were euthanised between days 30 and 50 post-tumour inoculation. In the Min(RA)Gag-VLP vaccinated group, only 1 animal out of 8 had to be euthanised. Protection against B16F10Min progression was statistically significant in Min(RA)Gag-VLP vaccinated animals compared to Gag-VLP vaccinated mice (p=0.0414), successfully demonstrating that the immune re-

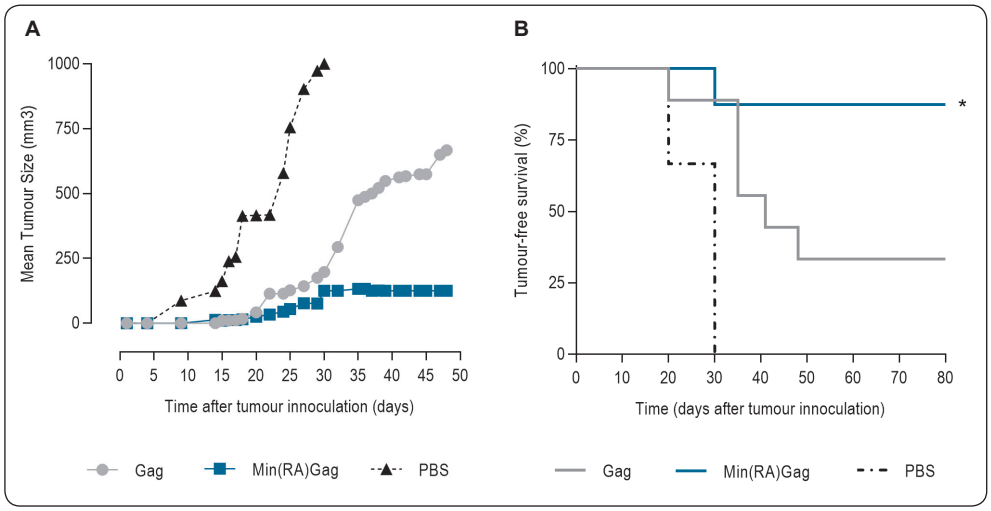

Figure 36. ***B16F10Min tumour progression in VLP-vaccinated and tumour-inoculated animals.*** **A)** *Mean Tumour growth calculated as 0.52 × length × width^2 in Gag-VLP (n=9), Min(RA) Gag-VLP (n=8) and PBS controls (n=3) vaccinated and B16F10Min-innoculated C57Bl/6JOlaHsd mice. From day 50 until day 80 post-tumour injection no further growth was detected. Animals reached a humane endpoint once tumour size was bigger than 1,000 mm^3.* **B)** *Kaplan-Meier curve and tumour-free survival of VLP-vaccinated mice. Significance was detected between Gag-VLP and Min(RA)Gag-VLP groups with a Kruskal-Wallis test (*p=0.0414).*

sponse elicited by Min(RA)Gag-VLP vaccination was capable of mediating protective immunity.

9. Characterisation of the immune response

Humoral and cellular immune responses elicited by vaccination with two doses of purified Gag-VLPs and Min(RA)Gag-VLPs were characterised in all the vaccinated and B16F10Min inoculated mice, in order to identify which elements could be contributing to the protection against B16F10Min progression.

Quantification of VLP-induced anti-Gag and anti-Min antibody concentration in mouse sera demonstrated how the second VLP dose had no major effect in the Min(RA)Gag-VLP vaccinated animals (Figure 37A & 37B), while in the Gag-VLP vaccinated group better anti-Gag antibody responses were observed after the second dose (Figure 37A). These results corresponded with the previous results in the VVVV regimen (Figure 28). Furthermore, B16F10Min inoculation at week 5 did not result in an anti-Min antibody boosting (Figure 37B), probably due to the poor immunogenicity that B16F10 cells display.

Binding to B16F10Min cells by VLP-induced anti-Min antibodies was analysed by flow cytometry. As expected, only mice vaccinated with Min(RA)Gag-VLPs displayed binding to B16F10Min (Figure 37C) compared to Gag-VLP vaccinated animals ($p<0.01$) and PBS animals ($p<0.01$), demonstrating that protection of Min(RA)Gag-VLP vaccinated animals could be associated with the humoral anti-Min response against B16F10Min cells.

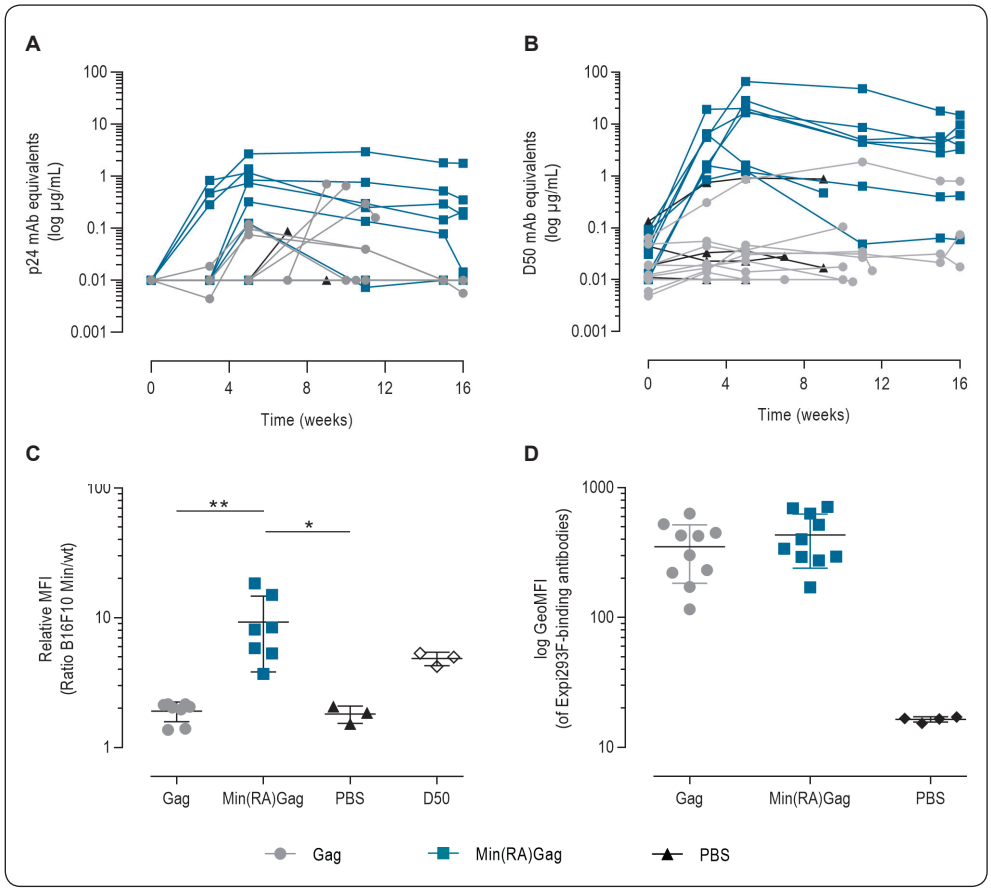

Figure 37. ***Immune response profiling of VLP-vaccinated and tumour-inoculated C57Bl/6JOlaHsd mice***. *Mice were vaccinated with 2 doses of purified Gag-VLPs (n=9), Min(RA)Gag-VLPs (n=8) and PBS (n=3) at weeks 0 and 3 and inoculated with 100,000 B16F10Min cells per animal at week 5.* **A)** *Anti-Gag humoral response follow-up determined by ELISA.* **B)** *Anti-Min humoral response follow-up determined by ELISA.* **C)** *Binding to B16F10Min cells of antibodies induced by VLP-vaccination in serum. D50 mAb was used as a positive control. Data represented as mean±SD of relative MFI of each serum sample against B16F10Min cells referred to their respective B16F10 control. Significant differences were found in the Min(RA)Gag-VLP vaccinated animals and the controls (*p≤0.05, **p≤0.01, Kruskal-Wallis test).* **D)** *Humoral response against Expi293F VLP-producing cells' host proteins determined by Flow Cytometry. Data presented as Geometrical Mean Fluorescence Intensity (Geo-MFI)±SD.*

Elicitation of antibodies against human proteins derived from VLP-producing cells was analysed by staining and analysis by flow cytometry of Expi293F cells. Both Gag-VLP and Min(RA)Gag-VLP vaccinated groups had antibodies against human Expi293F proteins and the mean between both groups was similar (Figure 37D), further demonstrating that VLP normalisation before vaccination was well performed between Gag-VLPs and Min(RA)Gag-VLPs.

IgG subclasses of anti-Gag and anti-Min antibodies of vaccinated and tumour-inoculated animals (Table 17) also matched with those previously described in section 6.3 (Tables 15 and 16). The results showed that Gag-VLPs induced a heterogeneous IgG response, encompassing mainly IgG1, IgG2b and IgG2c, while IgG2c dominate the response induce by Min(RA)Gag-VLPs (Table 17).

Table 17. IgG subclasses of anti-Gag and anti-Min humoral responses in the vaccinated and tumour inoculated C57Bl/6JOlaHsd mice at the endpoint

	Anti-Gag antibodies				Anti-Min antibodies			
	IgG1	IgG2b	IgG2c	IgG3	IgG1	IgG2b	IgG2c	IgG3
Gag	0.15	0.07	0.18	0.12	0.01	0.05	0.00	0.00
	0.00	0.00	0.00	0.04	0.00	0.06	0.00	0.00
	0.00	0.00	0.14	0.00	0.00	0.01	0.01	0.06
	0.22	0.00	0.11	0.00	0.00	0.09	0.09	0.00
	0.00	0.00	0.28	0.35	0.10	0.10	0.00	0.00
	0.04	0.00	0.10	0.04	0.05	0.45	0.12	0.00
	0.07	0.00	0.16	0.26	0.42	0.05	0.06	0.00
	0.39	0.08	0.25	0.47	0.00	0.02	0.01	0.00
	0.04	0.05	0.08	0.04	0.11	0.31	0.17	0.13
Min(RA)Gag	0.63	0.77	0.21	0.47	1.63	2.09	2.00	0.08
	0.21	0.00	0.00	0.00	0.05	0.24	0.75	0.00
	0.25	0.11	0.00	0.00	0.53	0.27	2.26	2.03
	1.27	0.00	0.59	0.00	0.09	0.45	1.08	0.12
	0.02	1.22	1.49	0.01	0.12	1.36	2.28	0.51
	1.04	1.25	0.58	0.05	0.24	1.34	2.33	0.22
	0.09	0.17	0.18	0.00	0.43	2.12	2.12	0.24
	0.14	1.01	0.51	0.00	0.00	1.36	2.05	0.22
	1.16	0.17	0.58	0.10	1.87	1.10	2.43	1.58
PBS	0.00	0.03	0.07	0.00	0.00	0.00	0.00	0.00
	0.00	0.05	0.02	0.00	0.00	0.13	0.00	0.00
	0.02	0.09	0.04	0.03	0.2	0.57	0.56	0.6

OD values are indicated.

Functional characterisation of VLP-induced antibodies demonstrated no capacity to mediate neutralisation against a subtype B tier1B Env (Bal.01) in an *in vitro* pseudovirus neutralisation assay (Figure 38A). However, anti-Min antibodies elicited by Min(RA)Gag-VLP vaccination could effectively bind mouse CD16-2 receptor (Figure 38B) compared to Gag-VLP induced humoral responses ($p \leq 0.05$), suggesting their ability to potentially induce antibody-dependent effector functions, such as ADCC.

Finally, T cell response was determined by ELISpot using splenocytes from C57Bl/6 animals immunised with VLPs and inoculated with B16F10Min cells. No significant IFN-γ-secreting T cells above the threshold (50 SFU/1,000,000 cells) were detected in any group and against any of the stimulating peptides: Gag, Min and MPER (Figure 39). This absence of cellular responses compared to the previous results of cellular responses in the DDVV and VVVV regimens (Figure 34) could be attributed to the fact that here animals received only two immunisations. Additionally, animals were euthanised between 30 and 110 days after the last immunisation, whereas in the DDVV and VVVV immunisations, all animals were euthanised 20 days after the last immunisation.

Altogether, these results showed that Min(RA)Gag-VLP elicited an immune response capable of mediating a specific protective effect in an *in vivo* model based on the inoculation of a cell line that stably expressed the Min antigen on its surface. This B16F10Min engineered melanoma cell line acted as a surrogate

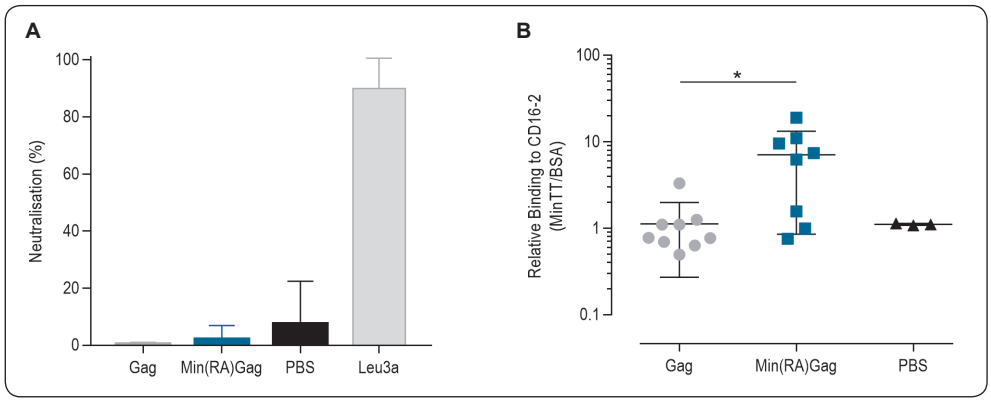

Figure 38. ***Characterisation of functional antibody responses of VLP-induced anti-Min antibodies.*** *Immune response profiling of C57Bl/6JOlaHsd Gag-VLP (n=9), Min(RA)Gag-VLP (n=8) and PBS (n=3) vaccinated and B16F10Min-inoculated mice.* **A)** In vitro *Bal.01 pseudovirus neutralisation with mouse sera collected at the endpoint.* **B)** *Relative binding to CD16-2 of anti-Min humoral responses referred to a BSA control. Significant differences in CD16-2 binding were found in the Min(RA)Gag-VLP compared to Gag-VLP vaccinated animals (*p≤0.05, Kruskal-Wallis test).*

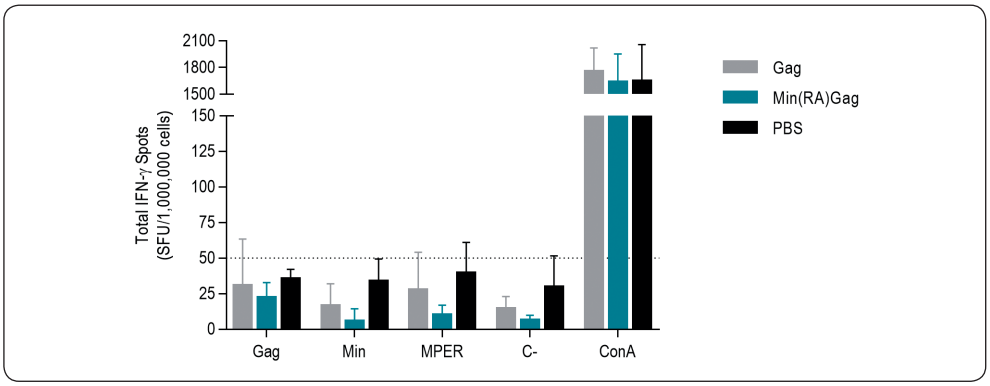

Figure 39. ***Cellular immune response against pools of Gag, Min and MPER elicited in vaccinated and tumour-inoculated mice****. The frequency of antigen-specific (Gag, Min or MPER) of IFN-γ-secreting T cells was evaluated* in vitro *using splenocytes from C57Bl/6JOlaHsd immunised with 2 doses of Gag-VLPs (n=9), Min(RA)Gag-VLPs (n=8) and PBS controls (n=3) and injected with B16F10Min cells. Data represented as mean±SD. No significant differences were found between groups using a Kruskal-Wallis test.*

of an infected cell expressing viral proteins at its surface, and hence targeted by immune responses. The characterisation of the immune response unveiled the presence of a non-neutralising anti-Min IgG2c/IgG2b antibodies, which bound to B16F10Min cells and the CD16-2 receptor. Interestingly, T cell responses were not detected. Therefore, we can hypothesise that protection mediated by antibody-dependent effector functions, such as ADCC, could have played a key role in this model.

SECTION 4. VERSATILITY OF THE VLP PLATFORM TO ACCOMMODATE OTHER ANTIGENS

In this last section, after demonstrating that the VLP platform engineered to express a high-density of antigens at the lipid surface was capable of inducing potent humoral responses that could mediate protection in an *in vivo* model, we went back to the design of the VLPs. One of the main advantages of this fusion-protein VLP platform was that it could theoretically be easily modified to express new immunogens and used both as a DNA vaccine or as VLPs produced and purified *in vitro*. Here, a formal demonstration of this platform's versatility was carried out.

10. Immunogen versatility at the surface of fusion-protein VLPs

Since fusion-protein VLP constructs were designed for rapid pseudotyping at the DNA level by genetic engineering with restriction enzymes, the Min domain in MinGag was substituted for other immunogens by digestion with *KpnI* and *BamHI* restrictions enzymes. First, we tried to replace Min with other epitopes targeted by bNAbs, such as the V1V2 loop or the Resurfaced Stabilised Core 3 (RSC3) protein. The RSC3 contains the constant regions of gp120 and result in a protein containing the CD4bs core that was designed to elicit neutralising humoral responses against the CD4bs (Wu *et al.*, 2010).

The expression of these immunogens at the surface of transfected Expi293F cells was analysed by Flow Cytometry using various Env specific bNAbs (b12, 2G12, PG9, PGT145, 2F5 and 10E8). All fusion-proteins were properly expressed at the surface of VLP-producing cells and displayed the expected antigenicity (Figure 40). In fact, the anti-CD4 binding site (CD4bs) bNAb b12 recognised the RSC3. PG9, a bNAb that targets the V1V2 N-glycosylation sites, weakly recognised the V1V2-expressing construct. A reduced MinGag construct (RedMinGag) was designed by removing the immunodominant HR2 fragment in MinGag-VLPs. This RedMinGag construct exposed the MPER to a lesser extent, as determined by staining with 10E8.

Additionally, more complex immunogens expressing multiple vulnerability sites within the same construct were cloned into a fusion-protein pcDNA3.1-*mingag* plasmid. These constructs had two or more vulnerability regions, such as the MPER, the CD4bs or the apex. The platform was also tested for its capacity to accommodate a native Env trimer at the surface of VLP-producing cells, by cloning at 5' of Gag a SOSIP trimer based on subtype B41 HIV-1 sequence and incorporating the characteristic mutations defined for the generation of soluble-stabilised SOSIP heterotrimers (Sanders *et al.*, 2015; de Taeye *et al.*, 2016;

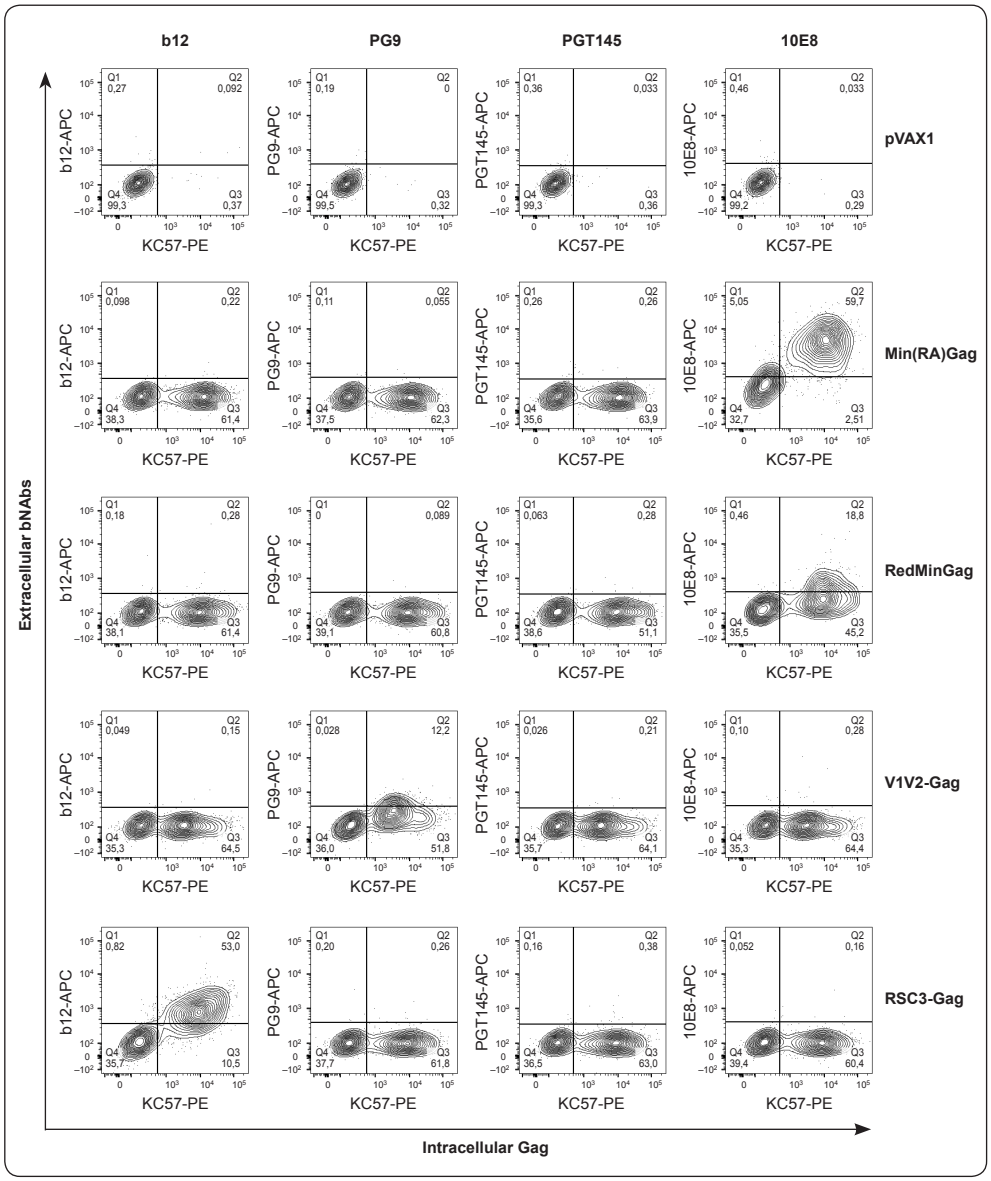

Figure 40. ***Contour plots of anti-HIV-1 bNAbs' binding to immunogen-Gag constructs expressing one immunogen.*** *VLP-producing cells expressing a single Env-derived HIV-1 immunogen (Min(RA)Gag, RedMinGag, V1V2-Gag and RSC3-Gag) were extracellularly stained with multiple bNAbs (b12, PG9, PGT145 and 10E8) and an APC-conjugated anti-human IgG antibody, and intracellularly stained with KC57-PE.*

Brouwer *et al.*, 2019). The immunogens were properly expressed on the membrane of VLP-producing cells independently of the size of the construct, and all of them properly exposed their vulnerability regions, since they were recognised by the correct bNAbs (Figure 41). Compared to constructs that expressed

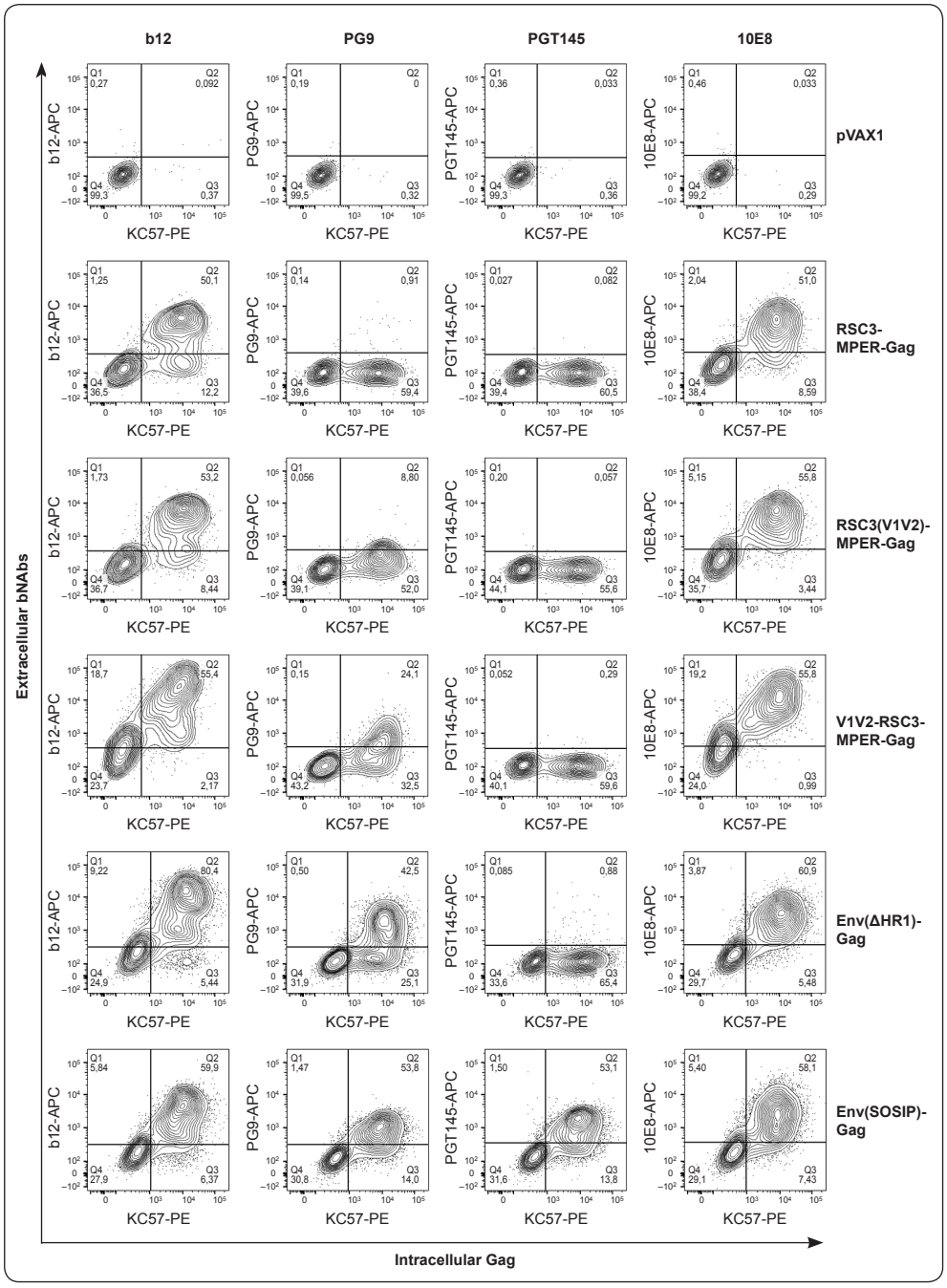

Figure 41. ***Contour plots of anti-HIV-1 bNAbs' binding to immunogen-Gag constructs expressing multiple immunogens***. *VLP-producing cells expressing multiple Env-derived HIV-1 immunogens in the same construct (RSC3-MPER-Gag, RSC3-MPER(V1V2)-MPER-Gag, V1V2-RSC3-MPER-Gag, Env(ΔHR1)-Gag and Env(SOSIP)-Gag) were extracellularly stained with multiple bNAbs (b12, PG9, PGT145 and 10E8) and an APC-conjugated anti-human IgG antibody, and intracellularly stained with KC57-PE.*

a single immunogen (Figure 40), the combination of different vulnerability regions resulted in a better recognition by neutralising antibodies (Figure 41). For instance, the V1V2-RSC3-MPER-Gag construct, which had the three immunogens one after the other from N-terminus to C-terminus, was among the constructs better recognised by b12, PG9 and 10E8. In comparison, RSC3-MPER-Gag, had a considerably lower recognition by b12 and 10E8 antibodies, indicating that their epitopes were less exposed in this immunogen (Table 18). RSC3(V1V2)-MPER-Gag, in which the V1V2 was restored at its original location, was better recognised by the bNAbs than RSC3-MPER-Gag, but not as good as V1V2-RSC3-MPER-Gag. Interestingly, none of these immunogens was recognised by the PGT145 bNAb, which targets a quaternary epitope strongly dependent on the 3D structure of the protein. In order to incorporate more complex epitopes in the platform, the Env(ΔHR1)-Gag and the Env(SOSIP)-Gag constructs were generated.

Although the binding to PG9 antibody was improved in the Env(ΔHR1)-Gag construct, only the Env(SOSIP)-Gag construct was recognised by the

Table 18. **Relative binding of anti-HIV-1 bNAbs to different immunogens presented at the surface of high-density VLP-producing cells and p24 concentration in the supernatant**

	Broadly Neutralising Antibodies (bNAbs)						p24 in s/n (ng/mL)
	CD4bs	V3 (Glycans)	V1V2 (apex)		MPER		
	IgGb12	2G12	PG9	PGT145	2F5	10E8	
Gag	1.0	1.0	1.0	1.0	1.0	1.0	1,082.7
MinGag	0.9	0.9	0.9	0.9	12.0	4.7	95.7
Min(RA)Gag	1.0	0.9	0.9	0.9	17.7	13.1	110.9
RedMinGag	1.0	1.0	1.0	1.0	4,4	2.3	89.4
V1V2-Gag	1.2	0.9	8.8	1.2	1.2	1.1	85.0
RSC3-Gag	12.4	2.5	0.9	0.9	0.8	0.9	40.2
RSC3-MPER-Gag	12.0	3.0	0.9	1.0	10.7	10.0	58.8
RSC3(V1V2)-MPER-Gag	16.3	8.2	2.1	0.9	17.3	12.6	92.0
V1V2-RSC3-MPER-Gag	21.5	16.6	3.6	0.9	25.1	18.5	141.7
Env(ΔHR1)-Gag	16.6	11.6	4.9	1.0	2.0	9.2	31.0
Env(SOSIP)-Gag	11.1	12.0	5.3	6.7	1.7	7.9	37.2

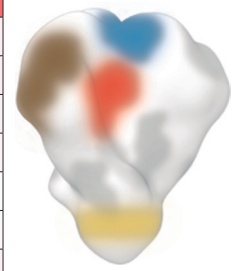

CD4bs: CD4 binding site.
MPER: Membrane Proximal External Region
s/n: supernatant
RSC3: Resurface Stabilized Core 3
Env: Envelope glycoprotein
SOSIP: soluble stabilised gp140 with I559P

PGT145 bNAb, further demonstrating that this B41 SOSIP was generating native-like trimers, while the other molecules were not able to do so (Figure 41 & Table 18).

Finally, all conditions resulted in a similar p24 amount in the supernatant, suggesting that VLPs were released to the supernatant of transiently transfected Expi293F VLP-producing cells (Table 18).

Discussion

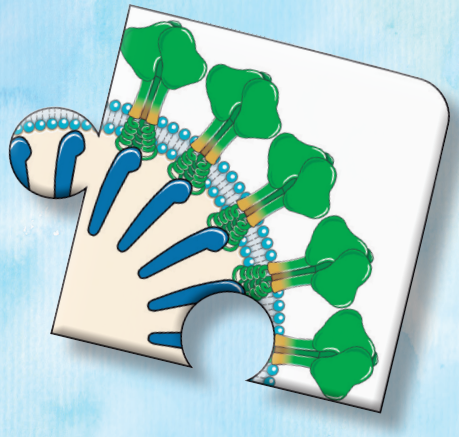

For the last 40 years, HIV-1 vaccine research has been approached from different perspectives: trying to elicit bNAbs, inducing potent effector T cells, or stimulating balanced humoral and cellular immune responses. To induce this long-sought protective immunity against HIV-1, many platforms and immunogens have been tested (Lopez Angel and Tomaras, 2020). However, the virus' diverse evasion mechanisms have hindered the success of most vaccine strategies. The virus can evade immune responses induced during natural infection and/or vaccination by concealing neutralizable functional epitopes within a dense glycan shield, by diverting the humoral response towards highly immunogenic non-neutralizable epitopes and/or by escaping effective humoral and cellular responses through new mutations (Mouquet, 2014; Olvera *et al.*, 2020). These enhanced evasion mechanisms displayed by HIV-1 have led to the discouraging fact that most of the efficacy clinical trials performed to date were stopped due to futility or counterproductive effects (Esparza, 2013).

Despite these unfruitful results, a deeper understanding of the virus and a thorough analysis of the immune correlates of protection in animal models and clinical trials, like the RV144 (Rerks-Ngarm *et al.*, 2006), has led to the development of new vaccine prototypes and strategies generated by rational vaccine design that will hopefully retrieve positive results (Burton, 2019; Thalhauser *et al.*, 2020). Currently, there is a consensus that the ideal HIV-1 vaccine should be capable of inducing balanced humoral and cellular responses with antibodies that could recognise most of the HIV-1 circulating strains and mediate a bNAb-like effect and/or other effector functions, together with a potent cellular response (Esparza, 2013). Cellular responses would help to boost antibody production and promote affinity maturation ($CD4^+$ Th), and also to rapidly clear infected cells before the virus could establish a latent reservoir ($CD8^+$ Tc).

Previous studies identified that anti-HIV-1 cellular responses are most effective when targeting Gag, Pol and Nef, while humoral responses block the virus and trigger effector responses when targeting Env (Koup and Douek, 2011). That is why most strategies currently facing clinical trials include both

Gag and Env (Table 2). A good synergism between these responses will lead to superior protection. Furthermore, the combination of different vaccine formulations can also better elicit different arms of the immune response, as recently demonstrated with the Combivac trial for SARS-CoV-2 (Borobia *et al.*, 2021; Normark *et al.*, 2021). On the one hand, nucleic acid vaccines are considered to be particularly fit to trigger cellular responses, since they will enter the target cell and produce the encoding protein while also present fragments of this protein through MHC-I molecules (Chea and Amara, 2017). On the other hand, subunit proteins and immunogens presented through multivalent platforms will directly stimulate APCs and B cells to promote an efficient generation of humoral responses (Jardine *et al.*, 2016).

The presentation of antigens at the surface of multivalent platforms, such as VLPs, notably boosts their immunogenicity (Thalhauser *et al.*, 2020). HIV-1 Gag-based VLPs are enveloped particles that mimic the structure of immature HIV-1 virions but are non-infectious and non-replicative, hence they are a good vaccine platform to induce potent immune responses by vaccination (Cervera *et al.*, 2019). HIV-1 enveloped VLPs are an especially attractive vaccine platform since they can accommodate Env proteins at their surface while containing Gag at their core, thus triggering a balanced adaptive immune response. However, a downside of this platform is that, since they mimic immature virions, they poorly incorporate Env-derived immunogens at their surface (Klein and Bjorkman, 2010). That is why many efforts have been invested in increasing antigen density at their surface (Deml *et al.*, 1997; Wang *et al.*, 2007; Vzorov *et al.*, 2016; Chapman *et al.*, 2020). Some groups have tried to incorporate mutations or to substitute the cytoplasmic tail of Env to achieve higher densities (Ingale *et al.*, 2016; Stano *et al.*, 2017). In this sense, our group devised a strategy to achieve even higher densities of antigen at the VLP surface by fusing Env-derived HIV-1 immunogens to Gag through a transmembrane domain and a linker. This process would lead to the incorporation of as many immunogens as Gag molecules are needed to assemble a VLP, which approximately is 2,500 molecules per particle (Lavado-García *et al.*, 2021).

To test our high-density fusion-protein VLP, we used a gp41-derived miniprotein ("Min"), that contained —from N- to C-terminus— a fragment of the HR2 domain, the MPER and the gp41 transmembrane domain. The C-terminus of Min and the N-terminus of Gag were fused by a short and flexible GGGS linker. After the screening of several gp41-derived proteins, the Min protein was selected because it showed a better exposure of the MPER on the surface of Min-expressing cells. MPER is a highly conserved functional epitope targeted by several bNAbs (2F5, 4E10 and 10E8). These bNAbs have efficiently protect-

ed NHP from SHIV infection (Pegu *et al.*, 2014). The presentation of the MPER can be favoured by its incorporation on a lipid membrane (Molinos-Albert *et al.*, 2017a). Molinos-Albert *et al.* previously reported that presenting Min at the surface of proteoliposomes elicited non-neutralising 2F5-like responses, which were stronger when they contained a complex membrane with lipids overrepresented in the membrane of HIV-1 virions, such as cholesterol and MPLA.

The MinGag fusion protein was designed with a signal peptide to favour its expression on the surface of the cells. The protein is synthetised at the endoplasmic reticulum. The whole protein would then migrate through Golgi to the membrane where Gag budding and VLP release would occur. This process is slightly more complex than Gag-VLP formation, which is produced directly in the cytosol where it migrates to the membrane. That could have explained the lower yields of MinGag-VLPs in the supernatant compared to Gag-VLPs. Still, the presence of Min at the surface of *mingag*-transfected cells confirmed that Min reached the plasma membrane as expected, whereas Gag was detected when performing intracellular staining. Other cell-derived elements were actively or passively incorporated into the VLPs during their production. Some of these elements were cytoskeleton and EV-associated proteins, being Hsp90 and Hsp70 complexes the most abundant ones. These proteins are associated with protein folding in the endoplasmic reticulum and are EV-markers, further suggesting that our protein was being produced as expected and was assembling into particulated VLPs. Furthermore, their production is associated with ER-stress and have been described to recruit immune cells (Asea *et al.*, 2000).

Our fusion protein MinGag construct assembled into VLPs and the MinGag protein was stable since we did not detect truncations in the supernatant. Although we did not provide direct proof that Min was expressed at a high density on the surface of MinGag-VLPs, the detection of Min on the surface of VLP-producing cells and the absence of truncations suggested that high-density antigen-displaying VLPs were being properly released. Immunogold staining electron microscopy on MinGag-VLPs using an anti-MPER conjugated antibody would provide the ultimate proof that our VLPs harbour a high density of antigens on their surface. Interestingly, MinGag-VLPs were half the size of Gag-VLPs, probably caused by the different production pathways that each VLP followed, or also due to the high accumulation of Min on the membrane surface.

Gag-VLPs and MinGag-VLPs were produced in SF and ADCF medium and purified from cell culture through methods commonly used in the industry. This is an important point that may speed up the escalation to industrial production. The gold standard technique for the purification of viral particles on a

laboratory scale is sucrose-cushion UC, which separates particles according to physical properties, mainly density. However, this method is hardly scalable. Also, VLP-producing cells released EVs that had a similar size to our VLPs, and these EV contaminants were not efficiently removed by UC. To overcome this limitation, we developed a VLP purification protocol that consisted of a three-step purification: i) clarification by centrifugation; ii) intermediate purification step by TFF, and iii) capture by LCC and AEX. This protocol allowed for the successful separation of VLPs from EVs, as previously reported by other groups (Steppert *et al.*, 2016). Our optimised, chromatography-based purification protocol further benefited from the combination of AEX with a previous LCC step [a hybrid technique between SEC and AEX (Weigel *et al.*, 2014)]. Noteworthily, MinGag-VLP purity levels were 10-fold higher with our optimised protocol compared to the gold-standard UC. Still, the advantage of our strategy was that a high purity was achieved with a technique that was based on the VLP inherent properties (electric charge), and hence, modifying the immunogen would not demand the modification of the whole protocol. Gag-VLPs and MinGag-VLPs achieved similar purity ratios with the combination of TFF + LCC + AEX, although the recovery was considerably low, meaning that there is still room for improvement. As a case in point, AEX columns could be replaced by monoliths, which have demonstrated better recoveries (Pereira Aguilar *et al.*, 2019). In addition, affinity strategies could be further pursued to achieve even higher purity yields (Reiter *et al.*, 2019). Still, our protocol allowed for the isolation of highly pure and homogeneous VLPs, enabling us to proceed to *in vivo* immunogenicity testing.

Antigen presentation on the VLP surface was optimised by the generation of Min variants containing different transmembrane and linker domains. Many groups have extensively reported how modifications in the cytoplasmic domain can modulate the extracellular antigenicity of Env (Postler and Desrosiers, 2013; Vzorov *et al.*, 2016). Therefore, we evaluated whether modifying the flexibility of the transmembrane and linker domains on the MinGag constructs also resulted in an improved presentation of Min. This was evaluated by extracellular staining of the MPER, the main Min region targeted by bNAbs, with the bNAb 10E8 on cells transfected with *mingag* constructs containing the different Min variants. The bNAb 10E8 was selected owing to its exceptional potency and breadth (Huang *et al.*, 2012). Among the four linker variants tested, none of them showed enhanced nor worsened antigen presentation. Conversely, among the four *mingag* transmembrane variants tested, two displayed an increase in 10E8 binding, while one of them had a worse antigen presentation. The construct with decreased antigenicity was *min(CD36tm)gag*, while the two

constructs with improved antigen presentation were the ones that contained the human CD44 transmembrane domain —*min(CD44tm)gag*—, and the gp41 transmembrane domain with mutation R696A —*min(RA)gag*. Since 10E8 bNAb recognises an MPER epitope embedded within the viral membrane (Molinos-Albert *et al.*, 2017b), modifications at the transmembrane level can impact the MPER exposure in the Min protein. That is the case of the R696A mutation at the gp41 transmembrane domain. Arginine 696 has been postulated to play a major role during the fusion process, helping Env to transition across different conformations that bring the cell and the viral membranes closer (Kim *et al.*, 2009). Arginine R696 could hinder the binding of the 10E8 bNAb to its epitope by embedding MPER deeper within the membrane. Therefore, the disruption of this polar amino acid could explain the better exposition of the Min/MPER region on the cell surface by *min(RA)gag* and *min(CD44)gag*. These results confirm that the transmembrane domain can drastically impact the exposure of the MPER in our MinGag protein, which was also confirmed using other anti-MPER bNAbs, such as 2F5 and 4E10.

Considering these previous results, we selected two high-density fusion-protein VLPs for immunogenicity tests: MinGag-VLPs and Min(RA)Gag-VLPs, while Gag-VLPs were used as a nude-VLP control. We chose these two constructs to assess whether a better antigen exposition at the VLP surface could also result in an enhanced immunogenicity. The rationale for choosing MinGag-VLPs and Min(RA)Gag-VLPs over the other transmembrane sequence variants was that their fusion-protein sequence was entirely derived from the HIV-1 sequence, and hence they would be more relevant for the induction of anti-HIV-1 responses.

A relevant aspect of our fusion-protein VLP platform is that MinGag-VLPs can be produced and purified *in vitro*, but they can also be delivered as a DNA-based vaccine. Considering that heterologous DNA/VLP regimens induce a more complete immune response (Excler and Kim, 2019), this would allow us to vaccinate animal models with the same immunogen but using two different strategies, achieving more complete responses. *In vivo* DNA administration, however, faces some issues like the inefficient uptake of plasmid DNA by somatic cells. Some strategies can be used to bypass this hurdle, such as *in vivo* DNA electroporation, delivery of DNA encapsulated in a liposome or a cationic polymer (Jorritsma *et al.*, 2016). *In vivo* DNA electroporation is a convenient delivery technique since purified DNA can be directly administered without the need for other processing steps like liposomal formulation and encapsulation. Furthermore, naked DNA does not contain any foreign antigen, as viral vectors do, hence anti-vector responses do not pose a problem; however, the

risk of anti-DNA antibody induction is debated (MacColl *et al.*, 2001). We further confirmed that electroporation resulted in a 3-log higher production by bioluminescence after administering a luciferase-coding plasmid delivered with and without electroporation. Moreover, the expression of luciferase was stably maintained for at least three months after electroporation, indicating that DNA vaccination has the potential to produce antigen for a long period of time, or at least until the immune system completely cleared the antigen.

Co-electroporation of plasmids coding for luciferase and Min(RA)Gag-VLPs or luciferase-only provided evidence that, first, luciferase is a highly stable poorly immunogenic protein, and second, luciferase expression was reduced in muscle cells co-electroporated with Min(RA)Gag. The luciferase expression fading in cells co-electroporated with Min(RA)Gag could be caused by either muscle cell death related to the toxicity of the Min(RA)Gag protein or by an immune-mediated cell clearance of Min(RA)Gag. The faster clearance of Min(RA)Gag:Luciferase transfected cells after a second electroporation was indicative that the immune system played a major role in this clearance. To further support that, we detected anti-Gag and anti-Min antibodies. However, the toxicity of Min(RA)Gag could still play a role since these two things were not mutually exclusive. This experiment also validated the 3-week interval as the optimal period between vaccinations since most of the antigens would have been cleared by that time. Even though we demonstrated that electroporation of the Min(RA)Gag construct resulted in the elicitation of anti-Gag and anti-Min antibodies, we did not provide direct proof that Min(RA)Gag-VLPs were being released *in vivo*, which would be worth exploring.

MinGag-VLPs and Min(RA)Gag-VLPs demonstrated to be potently immunogenic both in a homologous and a heterologous regimen. As previously detailed, combination strategies have been described to elicit superior and more complete responses (Excler and Kim, 2019; Borobia *et al.*, 2021), and our strategy also reproduced these results. The heterologous regimen induced 1-log higher anti-Gag and anti-Min antibody concentrations in the plasma of MinGag-VLP and Min(RA)Gag-VLP vaccinated animals. Interestingly, although no significant differences were found between the anti-Min antibody titres induced by MinGag-VLPs and Min(RA)Gag-VLPs independently of the vaccination regimen, the latter demonstrated a tendency to induce higher anti-Min antibody titres compared to MinGag-VLPs. Despite displaying a high heterogeneity, these results are in line with the concept that a better exposure of the Min protein on the surface of transfected cells, and probably on VLPs as well, could elicit stronger responses, justifying the use of optimised Min(RA)Gag-VLPs.

Each VLP administration consisted of 0.1 µg of p24Gag/dose, which is a notably low dosage, especially considering that subunit proteins are normally administered at a 10-100 µg/dose range and usually adjuvanted (Agwale *et al.*, 2002). This concentration was also lower compared to other studies in which HIV-1 Gag VLPs were injected in mice, where a 2-100 µg/dose was used (Buonaguro *et al.*, 2007). Still, this low concentration induced a strong humoral immune response even with a single immunisation, reaching antibody concentrations in plasma in the order of µg, which were detectable for up to half a year after the last immunisation. This finding is remarkable, especially when taking into consideration that our fusion-protein VLPs were not adjuvanted. Even if fusion-protein VLPs were not adjuvanted, we cannot discard that some components contained in our VLPs, such as Hsp70, acted like one (Asea *et al.*, 2000). Still, these results lead us to believe that our strategy can be further potentiated with adjuvating, or the immune response can be skewed using the right adjuvant (as detailed in section 3.6 of the introduction).

Considering VLP immunisations, it is worth remarking that one VLP dose elicited considerable antibody concentrations in the plasma in the homologous regimen and notably boosted DNA primed immune responses in the heterologous regimens. However, subsequent VLP doses did not further increase antibody concentrations in neither of the regimens. The absence of anti-Gag and anti-Min humoral response increase after the second VLP dose could be a consequence of the humoral immune response elicited against human proteins present within the VLP. Since VLPs are produced in Expi293F cells, which derive from HEK293 cells, human proteins from the host cell are incorporated in the VLPs, as described in results section 4. Contrary to the anti-Gag and anti-Min humoral responses, the titre of antibodies targeting Expi293F proteins increased after each purified VLP dose. This effect was not observed after DNA immunisation, confirming that it was specific to the host proteins present in the purified VLP batch. Therefore, the heterologous regimen led to a delay in the elicitation of antibodies against human proteins, thus allowing for a better boost of anti-Gag and anti-Min antibodies with the first VLP administration. In spite of second VLP boosts not leading to a higher antibody concentration, it is still possible that they played a role in the maturation of the antibody response and the maintenance of memory B cell reservoirs.

Despite detecting notable humoral responses in mice injected with VLPs, cellular responses against Min were barely detected. As expected, no anti-MPER T cell responses were detected independently of the vaccination regimen, since MPER cannot be efficiently presented by MHC-I molecules in C57Bl/6 mice, as other groups reported (Verkoczy *et al.*, 2011, 2013). Anti-Gag T cell respons-

es were detected in mice immunised with Gag-VLPs, especially in the heterologous regimen. However, these results should be interpreted with caution due to an irregular and overall low stimulation by ConA. Overall, a poor T cell response against Gag and Min proteins were detected in splenocytes. However, since mice were immunised in the hind limbs, it is possible that the specific T cells mostly accumulated in the popliteal and inguinal lymph nodes and only a minor fraction of them were localised in the spleen. Although we did not analyse the cellular immune responses against human proteins present in the VLPs, it is not farfetched to think that VLP vaccination could have elicited cellular responses mostly against these proteins. Cellular responses against Gag and the human proteins, if present, could be important to boost the production of anti-Min antibodies through the ISH effect (Elsayed *et al.*, 2018). According to this effect, Min-specific B cells would recognise their cognate epitope on VLPs, internalise the whole particle and present Gag (or human proteins when using mice or non-human animal models) through the MHC-II complex to get activated by T cells specific for these non-Min antigens. Although we did not optimise the Gag polyprotein in this project, it would be an important point to consider in the future, since properly balancing humoral and cellular responses will lead to a superior immunity.

Despite the antigenic optimisation in the Min(RA)Gag construct, a deeper characterisation of the humoral immune response demonstrated that anti-Min antibodies mainly targeted the N-terminus of Min, which contained a fragment of the HR2 peptide, but not the MPER. These results are in line with the absence of neutralising activity observed in the sera from MinGag-VLP and Min(RA)Gag-VLP vaccinated mice, since the MPER is the main target of NAbs in gp41 (Caillat *et al.*, 2020).

Complementing these findings, the main IgG subclass induced by MinGag-VLPs and Min(RA)Gag-VLPs against Min was IgG2c in both vaccination regimens, while there was no predominant IgG subclass induced by MinGag-VLPs and Min(RA)Gag-VLPs against Gag. The levels of anti-Min IgG2b antibodies were also higher than the IgG1 and IgG3 ones. The only notable difference between the homologous and heterologous regimens was that antibody titres were higher in the latter for all the IgG subclasses analysed. This finding was consistent with the fact that antibody concentration in the heterologous regimen was 1-log higher for both anti-Gag and anti-Min humoral responses.

It is worth highlighting that IgG2c and IgG2b subclasses are predominantly induced against viral infections (Collins, 2016), and hence our VLP strategies not only mimic the virus, they also induce antiviral-like responses against surface antigens, remarking the relevance of our VLP strategy in a vaccine context.

Furthermore, these two IgG subclasses in mice are mainly characterised for mediating antibody-dependent effector functions, such as ADCC and ADCP, and are considered equivalent to the human IgG1 (IgG2a/IgG2c) and IgG3 (IgG2b) isotypes (Bruhns, 2012). In this sense, the binding of anti-Min antibodies to the mFcγRIV (CD16-2) provided a proof of concept that anti-Min antibodies could prompt effector functions through their Fc portion. CD16-2 is present at the surface of NK cells and can crosslink with antibodies bound to an antigen expressed at the surface of a cell. Although other molecules can intervene in this process, this interaction is necessary and sufficient to activate the mitogen-activated protein kinase (MAPK) pathway, which will eventually promote the degranulation of NKs that will trigger the death of the target cell (Vivier *et al.*, 2004). Some groups have identified that NK degranulation and cytotoxicity was better induced by anti-gp41 antibodies, and speculated that gp41 closer proximity to the membrane of the target cell facilitated the formation of immunological synapses by NK cells (Phelps, 2021). We did not formally demonstrate that antibodies bound to the antigen could activate NK cells through binding to CD16-2 and promote degranulation and cytotoxicity to the target cell. However, the strong binding of anti-Min antibodies to CD16-2 is indicative that they could potentially mediate those types of responses, which have been associated with protection in HIV-1 vaccine efficacy clinical trials, like the RV144 (Rerks-Ngarm *et al.*, 2009).

To further characterise whether these anti-Min antibodies played a functional role *in vivo* we developed a novel animal model. In this model, since there is no murine equivalent to HIV-1 and HIV-1 has no tropism for mice, we developed a melanoma cell line engineered to express Min on its surface that acted as a surrogate of an infected cell presenting viral antigens on the surface. Other groups have pursued similar strategies, in which anti-Env responses induced by a prime-boost DNA/Fowlpox were tested against Env-bearing tumour cells (Radaelli *et al.*, 2007). Our engineered Min-expressing cell line was based on B16F10 cells, which are a poorly immunogenic and C57Bl/6-derived cell line refractory to T cell responses (Wang *et al.*, 1998). For this experiment, we performed a shorter vaccination schedule (2 doses of 0.1 µg of p24Gag/dose compared to the 4 doses administered in the previous experiment). We chose a homologous VLP regimen because our previous results showed that one VLP dose was sufficient to induce a potent immune response, and both regimens induced a similar antibody profile.

The evaluation of the humoral immune response profile corresponded with the profile identified in the homologous VVVV regimen, demonstrating that our immunisation strategy was robust across two different experiments and that re-

ducing the number of doses from 4 to 2 had no severe impact on the immunogenicity outcomes. Again, the anti-Min antibody response was not significantly boosted with the second VLP dose and anti-Min antibodies were non-neutralising, encompassed mainly IgG2c and IgG2b subclasses, which could engage the murine CD16-2 receptor. As expected, the anti-Gag humoral response was boosted in those animals that had no detectable levels of these antibodies after the first dose, and their IgG subclass profile was more heterogeneous. Gag-VLPs induced a lower anti-Gag response than Min(RA)Gag-VLPs and did not elicit anti-Min antibodies, also matching the results from the vaccination with the homologous (VVVV) regimen. Furthermore, antibody responses were stable across the duration of the experiment, up to 16 weeks after the first immunisation, as previously observed (results section 5.3). Also, similar to with the homologous and heterologous regimens, poor cellular responses against Gag nor Min were detected in VLP-immunised and tumour-injected animals. Notably, the injection of the B16F10Min tumour cell line two weeks after the second VLP dose did not boost anti-Min antibody concentration in plasma nor induce anti-Min cellular responses, corresponding with the observation that B16F10 cells are a poorly immunogenicity cell line (Wang *et al.*, 1998).

VLP-vaccinated animals displayed a delay in tumour growth of 5-10 days compared to non-immunised animals, even in the Gag-VLP control animals. This delay could be caused by two elements: i) VLP-immunisation led to a general pro-inflammatory state in the animals that helped them control the tumour, and/or ii) the humoral response induced against human proteins derived from the VLP-producing cells shared some similarities with proteins expressed by B16F10Min cells. Still, this non-specific effect was partial since most of the Gag-VLP immunised animals could not control the tumour growth. In comparison, all the Min(RA)Gag-VLP vaccinated animals but one completely halted the Min-expressing melanoma cell proliferation and did not display tumour growth during the 80 days that the experiment lasted, effectively confirming a VLP-induced Min-specific effect. Upon euthanasia, a necropsy was performed on the surviving animals and no signs of the B16F10Min-derived tumour were detected in any animal.

To shed a light on the factors that probably contributed to the protection of mice injected with B16F10Min cells, we analysed the capacity of anti-Min humoral responses to bind Min at the surface of B16F10Min cells by flow cytometry. The sera of Min(RA)Gag-VLP vaccinated animals engaged B16F10Min tumour cells, hinting at their potential effect of mediating immune clearance. Furthermore, the only animal in the Min(RA)Gag group that was not protected against B16F10Min tumour progression was the one with the lowest binding to

B16F10Min cells. This, together with the absence of anti-Min cellular responses in the spleens of vaccinated and tumour-inoculated mice, clearly indicated a prominent role of the humoral response in eliminating B16F10Min cells, probably in combination with NK cells or other innate immune cells.

Overall, all pieces of evidence derived from the immune profiling of VLP-vaccinated and tumour-inoculated mice pointed towards the fact that protection against B16F10Min tumour progression was mediated by antibodies directed against Min. These results confirm that our VLPs induce a functional response that can mediate effector functions, even if they do not display neutralising capacity. Inducing antibody-dependent effector functions such as ADCC will be crucial in the quest of eliciting protection against HIV-1, especially considering that the main correlate of protection in the RV144 phase III efficacy trial was the induction of this type of humoral response (Haynes *et al.*, 2012). Furthermore, other antibody-dependent functions like ADCP merit an especial focus since their gene signatures have been associated with protection in a few clinical trials (Andersen-Nissen *et al.*, 2021). Even if the induction of bNAb-like response will still be a relevant outcome to induce by vaccination, they will need the support of other types of functions as the ones induced by our VLPs. Exploring the role of different adjuvants to modulate the immune responses induced by our fusion-protein VLP platform could elicit broader and more robust responses that induced complementary functions, and could help to increase the magnitude of the cellular responses (Shah *et al.*, 2017).

One of the main advantages of our fusion-protein VLP platform was its versatility since it could be easily modified to express other antigens very easily and quickly. The platform was optimised and demonstrated to be potently immunogenic using gp41-Min, but the immunogen could be replaced by others through a simple and quick cloning procedure at the DNA level. Both the DNA-based vaccine strategy and the production and purification of VLPs were set up in a way that our fusion-protein VLPs could accommodate other immunogens without altering the production pipelines. VLP purification strategies were developed considering the inherent properties of the platform, such as the size of the particle or its net charge (Steppert *et al.*, 2016). Moreover, substituting the immunogen on the VLP platform would not probably impact the production and purification pipelines severely. This simple immunogen replacement could prove essential in the future if there was ever again the need for a fast development of a vaccine against an emerging pathogen (Ding *et al.*, 2018).

Our fusion-protein VLP platform demonstrated to be highly versatile and flexible. The platform could incorporate very heterogeneous immunogens, from small linear peptides containing few epitopes (RedMin or V1V2) to big and

highly glycosylated proteins (V1V2-RSC3-MPER) and even the full Env glycoprotein designed to form SOSIP trimers at the surface of our VLP platforms. The successful incorporation of a trimeric Env glycoprotein in our fusion-protein construct was remarkable since it demonstrated that the oligomerisation of Gag did not impede the formation of a complex quaternary structure (Ward and Wilson, 2017) at the VLP surface. These results demonstrate that our VLP platform could display virtually any Env-derived immunogen at their surface, which could be extremely useful for the development of improved sequential immunisation protocols with combined immunogens, leading to superior prototypes for an HIV-1 vaccine. There is a growing consensus, owing to the knowledge gathered in AMP trials, that any vaccine designed to induce protective bNAb-like responses should elicit antibodies targeting at least 2-3 different HIV-1 Env vulnerability sites (Dubrovskaya *et al.*, 2019; Zhao *et al.*, 2020). That is why developing a platform that could be easily modified to display various vulnerability sites could be crucial. A sequential immunisation strategy that would start with simpler, more restricted epitopes capable of priming the immune system and building up to more complex immunogens that helped with antibody maturation could lead to a heterogeneous response that could eventually block HIV-1.

In summary, with this work, our group has successfully designed from concept to *in vivo* testing a versatile VLP platform that overcomes one of the main hurdles faced by other multivalent platforms: displaying a high density of immunogens (Thalhauser *et al.*, 2020). This high density was achieved through a simple but conceptually elegant process of protein fusion engineering. Our group not only provided the concept but also optimised the production and purification processes, improved the antigenicity of immunogens displayed at the VLP surface and adapted the VLP concept into a DNA-based vaccine strategy. Remarkably, we propose a vaccination schedule based on a heterologous DNA/VLP regimen that was successfully tested *in vivo* in a mouse model and elicited a potent humoral response. Furthermore, we demonstrated that the humoral responses induced with our fusion-protein VLPs mediated a protective effect in a challenging *in vivo* model in which vaccination arrested the progression of a Min-expressing tumour cell line. We developed this new model trying to fill the gap left by the absence of a relevant mouse model to assess the efficacy of HIV-1 vaccines *in vivo*. Still, conclusions drawn by this model, even if they are promising, should be taken with caution, since HIV-1 is a complex virus that can still escape the pressure exerted by the immune response. The capacity of our fusion-protein VLPs to induce functional immune responses together with their high versatility could prove pivotal in the field of HIV-1 vaccines and undoubtedly merits further development.

Further research should move towards the identification of a relevant immunogen that could benefit the most from our VLP platform, and SOSIP trimers could certainly be a solid candidate (Klasse *et al.*, 2020). Additionally, owing to the platform versatility, the DNA formulation, which has proven as an invaluable asset in this project, could be adapted to the promising mRNA formulation, bypassing the risks and limitations associated with DNA immunisation (Langer *et al.*, 2013). Combining these findings with suitable immunogens into a sequential immunisation protocol would be a key point to take into consideration. Furthermore, identifying suitable adjuvants for our high-density VLP platform could further help to elicit more potent and effective responses. The high mutational rate of HIV-1 makes this virus very efficient at evading our efforts to generate a protective vaccine. Taking into consideration all the aforementioned parameters could eventually lead to the induction of a more balanced response that covered the whole spectrum of HIV-1 variants. One final aspect worth considering in the HIV-1 prevention field is to also aid in easing the burden of PLWH through therapeutic vaccination. If we want to effectively bring this stigmatising virus to its eradication, nobody can be left behind, and the global effort invested in generating a protective balanced humoral and cellular response against the virus should also balance HIV-1 prevention and cure.

Concluding Remarks

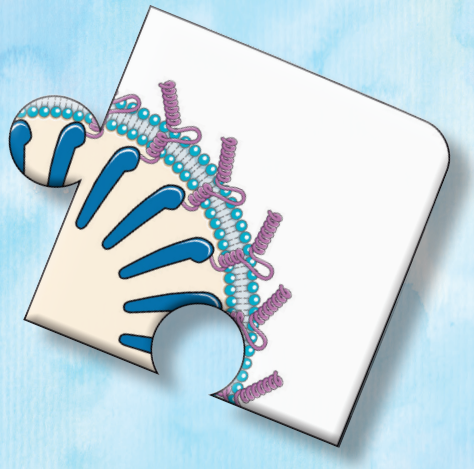

1. A novel fusion-protein Gag-based VLP platform that expressed a high density of immunogens at the VLP surface was successfully developed. These fusion-protein MinGag-VLPs were efficiently produced, characterised, and purified *in vitro* through techniques that could be easily scaled up for industrial productions. The antigen presentation at the surface of MinGag-VLPs was also improved, resulting in the optimised Min(RA)Gag-VLPs with increased antigenicity.
2. The fusion-protein MinGag-VLPs were adapted into a DNA-based vaccine strategy. This DNA-based MinGag-VLP strategy elicited a robust immune response when administered by *in vivo* electroporation.
3. The immune response induced by MinGag-VLPs and Min(RA)Gag-VLPs using either a homologous VLP or a heterologous DNA/VLP regimen was robust and significantly higher in the latter. Both vaccination regimens induced modest cellular responses, but potent humoral responses characterised by an IgG2c/IgG2b subclass profile that, despite being non-neutralising, could possibly mediate antibody-dependent effector functions.
4. The humoral immune response induced by Min(RA)Gag-VLP vaccination completely halted the progression of a poorly immunogenic tumour cell line that was engineered to stably express Min at the cell surface, effectively demonstrating that Min(RA)Gag-VLP induced humoral responses protected mice through antibody-dependent effector functions.
5. The fusion-protein VLP platform engineered to display a high density of antigens at the VLP surface could be easily modified to display other relevant immunogens, ranging from small peptides to complex and highly glycosylated native Env trimers, successfully demonstrating the versatility of the herein described vaccine platform.

Dissemination

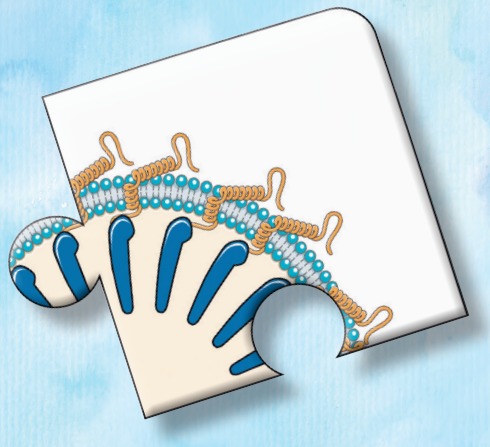

Publications related to this thesis project

- **Tarrés-Freixas, F.**; Aguilar-Gurrieri, C.; Urrea, V.; Trinité, B.; Varela, I.; Ortiz, R.; Rodríguez de la Concepción, M. L.; Blanco, P.; Pradenas, E.; Marfil, S.; Moli-nos-Albert, L. M.; Cervera, L.; Gutiérrez-Granados, S.; Segura, M. M.; Gòdia, F.; Clotet, B.; Carrillo, J.; Blanco, J. A high-density antigen-displaying HIV-1 Gag-based VLP platform induces strong antibody-dependent functional immune response. In preparation, 2021.
- Cervera, L., Gòdia, F., **Tarrés-Freixas, F.**, Aguilar-Gurrieri, C., Carrillo, J., Blanco, J., *et al.* (2019). Production of HIV-1-based virus-like particles for vaccination: achievements and limits. *Appl. Microbiol. Biotechnol.* 103(18), 7367-7384. doi:10.1007/s00253-019-10038-3.

Publications related to other projects

- Pradenas, E., Trinité, B., Urrea, V., Marfil, S., **Tarrés-Freixas, F.**, Ortiz, R., *et al.* (2021). Clinical course impacts early kinetics and long-term magnitude and amplitude of SARS-CoV-2 neutralizing antibodies beyond one year after infection. *medRxiv*, 2021.2008.2012.21261921. doi:10.1101/2021.08.12.21261921.
  —Submitted to the Cell Reports Medicine journal.
- **Tarrés-Freixas, F.**, Trinité, B., Pons-Grífols, A., Romero-Durana, M., Riveira-Muñoz, E., Ávila-Nieto, C., *et al.* (2021). SARS-CoV-2 B.1.351 (beta) variant shows enhanced infectivity in K18-hACE2 transgenic mice and expanded tropism to wildtype mice compared to B.1 variant. *bioRxiv*, 2021.2008.2003.454861. doi: 10.1101/2021.08.03.454861.
  —Under peer review in the Emerging Infectious Diseases journal.
- Trinité, B., Pradenas, E., Marfil, S., Rovirosa, C., Urrea, V., **Tarrés-Freixas, F.**, *et al.* (2021). Previous SARS-CoV-2 Infection Increases B.1.1.7 Cross-Neutralization by Vaccinated Individuals. *Viruses* 13(6). doi:10.3390/v13061135.

- Pradenas, E., Trinité, B., Urrea, V., Marfil, S., Ávila-Nieto, C., Rodríguez de la Concepción, M.L., **Tarrés-Freixas, F.**, *et al*. (2021). Stable neutralizing antibody levels 6 months after mild and severe COVID-19 episodes. *Med (N Y)* 2(3), 313-320.e314. doi:10.1016/j.medj.2021.01.005.
- Trinité, B., **Tarrés-Freixas, F.**, Rodon, J., Pradenas, E., Urrea, V., Marfil, S., *et al*. (2021). SARS-CoV-2 infection elicits a rapid neutralizing antibody response that correlates with disease severity. *Sci. Rep.* 11(1), 2608. doi:10.1038/s41598-021-81862-9.

Publications from scientific collaborations

- Perez-Zsolt, D., Muñoz-Basagoiti, J., Rodon, J., Elousa, M., Raïch-Regué, D., Risco, C., […], **Tarrés-Freixas, F.**, *et al*. (2021). Siglec-1 on dendritic cells mediates SARS-CoV-2 *trans*-infection of target cells while on macrophages triggers proinflammatory responses. *bioRxiv*, 2021.2005.2011.443572. doi:10.1101/2021.05.11.443572.
  —Submitted to the Cellular Molecular Immunology journal.
- Mitjà, O., Corbacho-Monné, M., Ubals, M., Alemany, A., Suñer, C., Tebé, C., […], **BCN-PEP-CoV2 Research Group**. (2021). A Cluster-Randomized Trial of Hydroxychloroquine for Prevention of Covid-19. *N. Engl. J. Med.* 384(5), 417-427. doi:10.1056/NEJMoa2021801.

Oral communications

- **Tarrés-Freixas, Ferran**; Aguilar-Gurrieri, Carmen; Molinos-Albert, Luis M.; Varela, Ismael; Ortiz, Raquel; Rodríguez de la Concepción, Maria Luisa; Trinité, Benjamin; Marfil, Silvia; Ávila, Carlos; Cervera, Laura; Gutiérrez-Granados, Sònia; Segura, María Mercedes; Gòdia, Francesc; Clotet, Bonaventura; Carrillo, Jorge; Blanco, Julià. An enveloped Virus-Like Particle (VLP) platform with high-density antigen display induces a strong humoral immune response. **XIIIè Congrés de la Societat Catalana d'Immunologia**. Barcelona, 14-15/11/2019.
- **Tarrés-Freixas, Ferran**; Aguilar-Gurrieri, Carmen; Molinos-Albert, Luis M.; Varela, Ismael; Ortiz, Raquel; Rodríguez de la Concepción, Maria Luisa; Trinité, Benjamin; Marfil, Silvia; Ávila, Carlos; Cervera, Laura; Gutiérrez-Granados, Sònia; Segura, María Mercedes; Gòdia, Francesc; Clotet, Bonaventura; Carrillo, Jorge; Blanco, Julià. An enveloped Virus-Like Particle (VLP) platform with high-density antigen display induces a strong humoral immune response. **XI Congreso Nacional GeSIDA**. Toledo, 10-13/12/2019.

- **Tarrés-Freixas, Ferran**; Aguilar-Gurrieri, Carmen; Molinos-Albert, Luis M.; Varela, Ismael; Ortiz, Raquel; Rodríguez de la Concepción, Maria Luisa; Trinité, Benjamin; Marfil, Silvia; Ávila, Carlos; Cervera, Laura; Gutiérrez-Granados, Sònia; Segura, María Mercedes; Gòdia, Francesc; Clotet, Bonaventura; Carrillo, Jorge; Blanco, Julià. HIV-1 enveloped Virus-Like Particles (VLP) displaying high density of HIV-1 Env derived antigens induce a functional immune response beyond neutralizing activity. **XIVè Congrés de la Societat Catalana d'Immunologia**. Virtual (Barcelona), 19-20/11/2020. Best presentation in the conference award.

Poster presentations

- **Tarrés-Freixas, Ferran**; Aguilar-Gurrieri, Carmen; Clotet, Bonaventura; Carrillo, Jorge; Blanco, Julià. A novel platform of enveloped Virus-Like Particles (VLPs) with high immunogenicity and versatility. **EMBL Course on Extracellular Vesicles**. Heidelberg, 8-14 April 2018.
- **Tarrés-Freixas, Ferran**; Aguilar-Gurrieri, Carmen; Molinos-Albert, Luis M.; Varela, Ismael; Ortiz, Raquel; Rodríguez de la Concepción, Maria Luisa; Pradenas, Edwards; Trinité, Benjamin; Marfil, Silvia; Ávila-Nieto, Carlos; Cervera, Laura; Gutiérrez-Granados, Sònia; Segura, María Mercedes; Gòdia, Francesc; Clotet, Bonaventura; Carrillo, Jorge; Blanco, Julià. A high-valency antigen displaying Gag-based VLP induces an antibody-dependent functional immune response. **Keystone eSymposia on HIV Vaccines**. Virtual (Santa Fe, NM, USA), 1-4 June 2021.

References

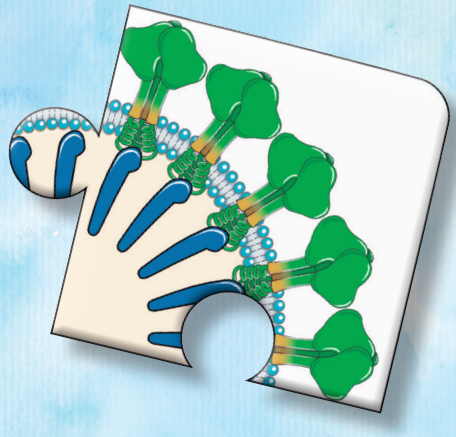

Abram, M. E., Ferris, A. L., Shao, W., Alvord, W. G., and Hughes, S. H. (2010). Nature, position, and frequency of mutations made in a single cycle of HIV-1 replication. *J. Virol.* 84, 9864-9878. doi:10.1128/JVI.00915-10.

Agwale, S. M., Shata, M. T., Reitz, M. S., Kalyanaraman, V. S., Gallo, R. C., Popovic, M., *et al.* (2002). A Tat subunit vaccine confers protective immunity against the immune-modulating activity of the human immunodeficiency virus type-1 Tat protein in mice. *Proc. Natl. Acad. Sci.* 99, 10037-10041. doi:10.1073/pnas.152313899.

Air, G. M., and West, J. T. (2008). "Antigenic Variation," in *Encyclopedia of Virology (Third Edition)*, eds. B. W. J. Mahy and M. H. V Van Regenmortel (Oxford: Academic Press), 127-136. doi:10.1016/B978-012374410-4.00582-3.

Alcamí, J., and Coiras, M. (2011). [Immunopathogenesis of HIV infection]. *Enferm. Infecc. Microbiol. Clin.* 29, 216-226. doi:10.1016/j.eimc.2011.01.006.

Almagro, J. C., Daniels-Wells, T. R., Perez-Tapia, S. M., and Penichet, M. L. (2017). Progress and Challenges in the Design and Clinical Development of Antibodies for Cancer Therapy. *Front. Immunol.* 8, 1751. doi:10.3389/fimmu.2017.01751.

Amitai, A., Chakraborty, A. K., and Kardar, M. (2018). The low spike density of HIV may have evolved because of the effects of T helper cell depletion on affinity maturation. *PLoS Comput. Biol.* 14. doi:10.1371/JOURNAL.PCBI.1006408.

Ananworanich, J., McSteen, B., and Robb, M. L. (2015). Broadly neutralizing antibody and the HIV reservoir in acute HIV infection: a strategy toward HIV remission? *Curr. Opin. HIV AIDS* 10, 198-206. doi:10.1097/COH.0000000000000144.

Andersen-Nissen, E., Fiore-Gartland, A., Ballweber Fleming, L., Carpp, L. N., Naidoo, A. F., Harper, M. S., *et al.* (2021). Innate immune signatures to a partially-efficacious HIV vaccine predict correlates of HIV-1 infection risk. *PLOS Pathog.* 17, e1009363. doi:10.1371/journal.ppat.1009363.

Antiretroviral Therapy Cohort Collaboration (2017). Survival of HIV-positive patients starting antiretroviral therapy between 1996 and 2013: a collaborative analysis of cohort studies. *Lancet. HIV* 4, e349-e356. doi:10.1016/S2352-3018(17)30066-8.

Asea, A., Kraeft, S. K., Kurt-Jones, E. A., Stevenson, M. A., Chen, L. B., Finberg, R. W., et al. (2000). HSP70 stimulates cytokine production through a CD14-dependant pathway, demonstrating its dual role as a chaperone and cytokine. *Nat. Med.* 6, 435-442. doi:10.1038/74697.

Baden, L. R., Stieh, D. J., Sarnecki, M., Walsh, S. R., Tomaras, G. D., Kublin, J. G., *et al.* (2020). Safety and immunogenicity of two heterologous HIV vaccine regimens in

healthy, HIV-uninfected adults (TRAVERSE): a randomised, parallel-group, placebo-controlled, double-blind, phase 1/2a study. *Lancet. HIV* 7, e688-e698. doi:10.1016/S2352-3018(20)30229-0.

Barouch, D. H., Mercado, N. B., Chandrashekar, A., Borducchi, E. N., Nkolola, J. P., Pau, M. G., *et al.* (2020). Combined active and passive immunization in SHIV-infected rhesus monkeys. in *CROI - Conference on Retroviruses and Opportunistic Infections* (Boston, MA). Available at: https://www.croiconference.org/abstract/combined-active-and-passive-immunization-in-shiv-infected-rhesus-monkeys/.

Barouch, D. H., O'Brien, K. L., Simmons, N. L., King, S. L., Abbink, P., Maxfield, L. F., *et al.* (2010). Mosaic HIV-1 vaccines expand the breadth and depth of cellular immune responses in rhesus monkeys. *Nat. Med.* 16, 319-323. doi:10.1038/nm.2089.

Barouch, D. H., Tomaka, F. L., Wegmann, F., Stieh, D. J., Alter, G., Robb, M. L., *et al.* (2018). Evaluation of a mosaic HIV-1 vaccine in a multicentre, randomised, double-blind, placebo-controlled, phase 1/2a clinical trial (APPROACH) and in rhesus monkeys (NHP 13-19). *Lancet (London, England)* 392, 232-243. doi:10.1016/S0140-6736(18)31364-3.

Barré-Sinoussi, F., Chermann, J. C., Rey, F., Nugeyre, M. T., Chamaret, S., Gruest, J., *et al.* (1983). Isolation of a T-lymphotropic retrovirus from a patient at risk for acquired immune deficiency syndrome (AIDS). *Science* 220, 868-871. doi:10.1126/science.6189183.

Barry, M. (2018). Single-cycle adenovirus vectors in the current vaccine landscape. *Expert Rev. Vaccines* 17, 163-173. doi:10.1080/14760584.2018.1419067.

Bekker, L.-G., Moodie, Z., Grunenberg, N., Laher, F., Tomaras, G. D., Cohen, K. W., *et al.* (2018). Subtype C ALVAC-HIV and bivalent subtype C gp120/MF59 HIV-1 vaccine in low-risk, HIV-uninfected, South African adults: a phase 1/2 trial. *Lancet. HIV* 5, e366-e378. doi:10.1016/S2352-3018(18)30071-7.

Beltran-Pavez, C., Ferreira, C. B., Merino-Mansilla, A., Fabra-Garcia, A., Casadella, M., Noguera-Julian, M., *et al.* (2018). Guiding the humoral response against HIV-1 toward a MPER adjacent region by immunization with a VLP-formulated antibody-selected envelope variant. *PLoS One* 13, e0208345. doi:10.1371/journal.pone.0208345.

Benen, T. D., Tonks, P., Kliche, A., Kapzan, R., Heeney, J. L., and Wagner, R. (2014). Development and immunological assessment of VLP-based immunogens exposing the membrane-proximal region of the HIV-1 gp41 protein. *J. Biomed. Sci.* 21, 79. doi:10.1186/s12929-014-0079-x.

Berman, P. W., Gregory, T. J., Riddle, L., Nakamura, G. R., Champe, M. A., Porter, J. P., *et al.* (1990). Protection of chimpanzees from infection by HIV-1 after vaccination with recombinant glycoprotein gp120 but not gp160. *Nature* 345, 622-625. doi:10.1038/345622a0.

Bertram, K. M., Tong, O., Royle, C., Turville, S. G., Nasr, N., Cunningham, A. L., *et al.* (2019). Manipulation of Mononuclear Phagocytes by HIV: Implications for Early Transmission Events. *Front. Immunol.* 10, 2263. doi:10.3389/fimmu.2019.02263.

Bezbaruah, R., Borah, P., Kakoti, B. B., Al-Shar'I, N. A., Chandrasekaran, B., Jaradat,

D. M. M., *et al.* (2021). Developmental Landscape of Potential Vaccine Candidates Based on Viral Vector for Prophylaxis of COVID-19. *Front. Mol. Biosci.* 8, 635337. doi:10.3389/fmolb.2021.635337.

Billich, A. (2001). AIDSVAX. VaxGen. *Curr. Opin. Investig. Drugs* 2, 1203-1208.

Biswas, P., Jiang, X., Pacchia, A. L., Dougherty, J. P., and Peltz, S. W. (2004). The human immunodeficiency virus type 1 ribosomal frameshifting site is an invariant sequence determinant and an important target for antiviral therapy. *J. Virol.* 78, 2082-2087. doi:10.1128/jvi.78.4.2082-2087.2004.

Bonsignori, M., Liao, H.-X., Gao, F., Williams, W. B., Alam, S. M., Montefiori, D. C., *et al.* (2017). Antibody-virus co-evolution in HIV infection: paths for HIV vaccine development. *Immunol. Rev.* 275, 145-160. doi:10.1111/imr.12509.

Bor, J., Fischer, C., Modi, M., Richman, B., Kinker, C., King, R., *et al.* (2021). Changing Knowledge and Attitudes Towards HIV Treatment-as-Prevention and "Undetectable=Untransmittable": A Systematic Review. *AIDS Behav.*, 1-16. doi:10.1007/s10461-021-03296-8.

Borobia, A. M., Carcas, A. J., Pérez-Olmeda, M., Castaño, L., Bertran, M. J., García-Pérez, J., *et al.* (2021). Immunogenicity and reactogenicity of BNT162b2 booster in ChAdOx1-S-primed participants (CombiVacS): a multicentre, open-label, randomised, controlled, phase 2 trial. *Lancet (London, England)* 398, 121-130. doi:10.1016/S0140-6736(21)01420-3.

Bournazos, S., Klein, F., Pietzsch, J., Seaman, M. S., Nussenzweig, M. C., and Ravetch, J. V. (2014). Broadly Neutralizing Anti-HIV-1 Antibodies Require Fc Effector Functions for In Vivo Activity. *Cell* 158, 1243-1253. doi:10.1016/j.cell.2014.08.023.

Boyer, Z., and Palmer, S. (2018). Targeting Immune Checkpoint Molecules to Eliminate Latent HIV. *Front. Immunol.* 9, 2339. doi:10.3389/fimmu.2018.02339.

Bracq, L., Xie, M., Benichou, S., and Bouchet, J. (2018). Mechanisms for Cell-to-Cell Transmission of HIV-1. *Front. Immunol.* 9, 260. doi:10.3389/fimmu.2018.00260.

Breden, F., Lepik, C., Longo, N. S., Montero, M., Lipsky, P. E., and Scott, J. K. (2011). Comparison of antibody repertoires produced by HIV-1 infection, other chronic and acute infections, and systemic autoimmune disease. *PLoS One* 6, e16857. doi:10.1371/journal.pone.0016857.

Brinkkemper, M., and Sliepen, K. (2019). Nanoparticle Vaccines for Inducing HIV-1 Neutralizing Antibodies. *Vaccines* 7. doi:10.3390/vaccines7030076.

Brouwer, P. J. M., Antanasijevic, A., Berndsen, Z., Yasmeen, A., Fiala, B., Bijl, T. P. L., *et al.* (2019). Enhancing and shaping the immunogenicity of native-like HIV-1 envelope trimers with a two-component protein nanoparticle. *Nat. Commun.* 10, 4272. doi:10.1038/s41467-019-12080-1.

Bruhns, P. (2012). Properties of mouse and human IgG receptors and their contribution to disease models. *Blood* 119, 5640-5649. doi:10.1182/blood-2012-01-380121.

Buchbinder, S. P., Grunenberg, N. A., Sanchez, B. J., Seaton, K. E., Ferrari, G., Moody, M. A., *et al.* (2017). Immunogenicity of a novel Clade B HIV-1 vaccine combination: Results of phase 1 randomized placebo controlled trial of an HIV-1 GM-CSF-expressing DNA prime with a modified vaccinia Ankara vaccine

boost in healthy HIV-1 uninfected adults. *PLoS One* 12, e0179597. doi:10.1371/journal.pone.0179597.

Buchbinder, S. P., Mehrotra, D. V, Duerr, A., Fitzgerald, D. W., Mogg, R., Li, D., *et al.* (2008). Efficacy assessment of a cell-mediated immunity HIV-1 vaccine (the Step Study): a double-blind, randomised, placebo-controlled, test-of-concept trial. *Lancet (London, England)* 372, 1881-1893. doi:10.1016/S0140-6736(08)61591-3.

Bulbake, U., Doppalapudi, S., Kommineni, N., and Khan, W. (2017). Liposomal Formulations in Clinical Use: An Updated Review. *Pharmaceutics* 9. doi:10.3390/pharmaceutics9020012.

Buonaguro, L., Devito, C., Tornesello, M. L., Schröder, U., Wahren, B., Hinkula, J., *et al.* (2007). DNA-VLP prime-boost intra-nasal immunization induces cellular and humoral anti-HIV-1 systemic and mucosal immunity with cross-clade neutralizing activity. *Vaccine* 25, 5968-77. doi:10.1016/j.vaccine.2007.05.052.

Buonaguro, L., Tagliamonte, M., Visciano, M. L., Andersen, H., Lewis, M., Pal, R., *et al.* (2012). Immunogenicity of HIV Virus-Like Particles in Rhesus Macaques by Intranasal Administration. *Clin. Vaccine Immunol.* 19, 970-973. doi:10.1128/CVI.00068-12.

Burton, D. R. (2019). Advancing an HIV vaccine; advancing vaccinology. *Nat. Rev. Immunol.* 19, 77-78. doi:10.1038/s41577-018-0103-6.

Burton, D. R., Desrosiers, R. C., Doms, R. W., Feinberg, M. B., Gallo, R. C., Hahn, B., *et al.* (2004). A Sound Rationale Needed for Phase III HIV-1 Vaccine Trials. *Science* 303, 316-316. doi:10.1126/science.1094620.

Buzón, M. J., Massanella, M., Llibre, J. M., Esteve, A., Dahl, V., Puertas, M. C., *et al.* (2010). HIV-1 replication and immune dynamics are affected by raltegravir intensification of HAART-suppressed subjects. *Nat. Med.* 16, 460-465. doi:10.1038/nm.2111.

Caillat, C., Guilligay, D., Sulbaran, G., and Weissenhorn, W. (2020). Neutralizing Antibodies Targeting HIV-1 gp41. *Viruses* 12. doi:10.3390/v12111210.

Camacho, R., and Teófilo, E. (2011). Antiretroviral therapy in treatment-naïve patients with HIV infection. *Curr. Opin. HIV AIDS* 6 Suppl 1, S3-11. doi:10.1097/01.COH.0000410239.88517.00.

Cao, L., Pauthner, M., Andrabi, R., Rantalainen, K., Berndsen, Z., Diedrich, J. K., *et al.* (2018). Differential processing of HIV envelope glycans on the virus and soluble recombinant trimer. *Nat. Commun.* 9, 3693. doi:10.1038/s41467-018-06121-4.

Casazza, J. P., Bowman, K. A., Adzaku, S., Smith, E. C., Enama, M. E., Bailer, R. T., *et al.* (2013). Therapeutic vaccination expands and improves the function of the HIV-specific memory T-cell repertoire. *J. Infect. Dis.* 207, 1829-1840. doi:10.1093/infdis/jit098.

Caskey, M. (2020). Broadly neutralizing antibodies for the treatment and prevention of HIV infection. *Curr. Opin. HIV AIDS* 15, 49-55. doi:10.1097/COH.0000000000000600.

Castro-Gonzalez, S., Colomer-Lluch, M., and Serra-Moreno, R. (2018). Barriers for HIV Cure: The Latent Reservoir. *AIDS Res. Hum. Retroviruses* 34, 739-759. doi:10.1089/AID.2018.0118.

Centlivre, M., Sala, M., Wain-Hobson, S., and Berkhout, B. (2007). In HIV-1 patho-

genesis the die is cast during primary infection. *AIDS* 21, 1-11. doi:10.1097/QAD.0b013e3280117f7f.

Centre for Disease Control (1981). Pneumocystis pneumonia—Los Angeles. *MMWR. Morb. Mortal. Wkly. Rep.* 30, 250-252.

Centre for Disease Control (1982a). Opportunistic infections and Kaposi's sarcoma among Haitians in the United States. *MMWR. Morb. Mortal. Wkly. Rep.* 31, 353-354,360-361.

Centre for Disease Control (1982b). Update on acquired immune deficiency syndrome (AIDS)—United States. *MMWR. Morb. Mortal. Wkly. Rep.* 31, 507-508,513-514.

Cervera, L., Gòdia, F., Tarrés-Freixas, F., Aguilar-Gurrieri, C., Carrillo, J., Blanco, J., *et al.* (2019). Production of HIV-1-based virus-like particles for vaccination: achievements and limits. *Appl. Microbiol. Biotechnol.* 103, 7367-7384. doi:10.1007/s00253-019-10038-3.

Chapman, R., van Diepen, M., Galant, S., Kruse, E., Margolin, E., Ximba, P., *et al.* (2020). Immunogenicity of HIV-1 Vaccines Expressing Chimeric Envelope Glycoproteins on the Surface of Pr55 Gag Virus-Like Particles. *Vaccines* 8. doi:10.3390/vaccines8010054.

Chea, L. S., and Amara, R. R. (2017). Immunogenicity and efficacy of DNA/MVA HIV vaccines in rhesus macaque models. *Expert Rev. Vaccines* 16, 973-985. doi:10.1080/14760584.2017.1371594.

Chege, G. K., Burgers, W. A., Stutz, H., Meyers, A. E., Chapman, R., Kiravu, A., *et al.* (2013). Robust immunity to an auxotrophic Mycobacterium bovis BCG-VLP prime-boost HIV vaccine candidate in a nonhuman primate model. *J. Virol.* 87, 5151-5160. doi:10.1128/JVI.03178-12.

Chen, B. (2019). Molecular Mechanism of HIV-1 Entry. *Trends Microbiol.* 27, 878-891. doi:10.1016/j.tim.2019.06.002.

Chen, H., Moussa, M., and Catalfamo, M. (2020). The Role of Immunomodulatory Receptors in the Pathogenesis of HIV Infection: A Therapeutic Opportunity for HIV Cure? *Front. Immunol.* 11, 1223. doi:10.3389/fimmu.2020.01223.

Chen, H. Y., Di Mascio, M., Perelson, A. S., Ho, D. D., and Zhang, L. (2007). Determination of virus burst size *in vivo* using a single-cycle SIV in rhesus macaques. *Proc. Natl. Acad. Sci. U. S. A.* 104, 19079-19084. doi:10.1073/pnas.0707449104.

Chen, Z. (2018). "Monkey Models and HIV Vaccine Research BT - HIV Vaccines and Cure: The Path Towards Finding an Effective Cure and Vaccine," in, eds. L. Zhang and S. R. Lewin (Singapore: Springer Singapore), 97-124. doi:10.1007/978-981-13-0484-2_5.

Chua, H. L., Serov, Y., and Brahmi, Z. (2004). Regulation of FasL expression in natural killer cells. *Hum. Immunol.* 65, 317-327. doi:10.1016/j.humimm.2004.01.004.

Climent, N., García, I., Marradi, M., Chiodo, F., Miralles, L., Maleno, M. J., *et al.* (2018). Loading dendritic cells with gold nanoparticles (GNPs) bearing HIV-peptides and mannosides enhance HIV-specific T cell responses. *Nanomedicine* 14, 339-351. doi:10.1016/j.nano.2017.11.009.

Cohen, J. (2021). Failed HIV vaccine trial marks another setback for the field. *Science*. doi:10.1126/science.abm1710.

Coiras, M., López-Huertas, M. R., Pérez-Olmeda, M., and Alcamí, J. (2009). Understanding HIV-1 latency provides clues for the eradication of long-term reservoirs. *Nat. Rev. Microbiol.* 7, 798-812. doi:10.1038/nrmicro2223.

Collins, A. M. (2016). IgG subclass co-expression brings harmony to the quartet model of murine IgG function. *Immunol. Cell Biol.* 94, 949-954. doi:10.1038/icb.2016.65.

Collins, A. M., Wang, Y., Roskin, K. M., Marquis, C. P., and Jackson, K. J. L. (2015). The mouse antibody heavy chain repertoire is germline-focused and highly variable between inbred strains. *Philos. Trans. R. Soc. London. Ser. B, Biol. Sci.* 370. doi:10.1098/rstb.2014.0236.

Coplan, P. M., Gupta, S. B., Dubey, S. A., Pitisuttithum, P., Nikas, A., Mbewe, B., *et al.* (2005). Cross-reactivity of anti-HIV-1 T cell immune responses among the major HIV-1 clades in HIV-1-positive individuals from 4 continents. *J. Infect. Dis.* 191, 1427-1434. doi:10.1086/428450.

Corey, L., Gilbert, P. B., Juraska, M., Montefiori, D. C., Morris, L., Karuna, S. T., *et al.* (2021). Two Randomized Trials of Neutralizing Antibodies to Prevent HIV-1 Acquisition. *N. Engl. J. Med.* 384, 1003-1014. doi:10.1056/NEJMoa2031738.

Corey, L., and Gray, G. E. (2017). Preventing acquisition of HIV is the only path to an AIDS-free generation. *Proc. Natl. Acad. Sci.* 114, 3798-3800. doi:10.1073/pnas.1703236114.

Cox, W. I., Tartaglia, J., and Paoletti, E. (1993). Induction of Cytotoxic T Lymphocytes by Recombinant Canarypox (ALVAC) and Attenuated Vaccinia (NYVAC) Viruses Expressing the HIV-1 Envelope Glycoprotein. *Virology* 195, 845-850. doi:10.1006/viro.1993.1442.

Crooks, E. T., Osawa, K., Tong, T., Grimley, S. L., Dai, Y. D., Whalen, R. G., *et al.* (2017). Effects of partially dismantling the CD4 binding site glycan fence of HIV-1 Envelope glycoprotein trimers on neutralizing antibody induction. *Virology* 505, 193-209. doi:10.1016/j.virol.2017.02.024.

Cunyat, F., Rainho, J. N., West, B., Swainson, L., McCune, J. M., and Stevenson, M. (2016). Colony-Stimulating Factor 1 Receptor Antagonists Sensitize Human Immunodeficiency Virus Type 1-Infected Macrophages to TRAIL-Mediated Killing. *J. Virol.* 90, 6255-6262. doi:10.1128/JVI.00231-16.

D'arc, M., Ayouba, A., Esteban, A., Learn, G. H., Boué, V., Liegeois, F., *et al.* (2015). Origin of the HIV-1 group O epidemic in western lowland gorillas. *Proc. Natl. Acad. Sci. U. S. A.* 112, E1343-52. doi:10.1073/pnas.1502022112.

Daniel, M. D., Kirchhoff, F., Czajak, S. C., Sehgal, P. K., and Desrosiers, R. C. (1992). Protective effects of a live attenuated SIV vaccine with a deletion in the nef gene. *Science* 258, 1938-1941. doi:10.1126/science.1470917.

de Sousa, J. D., Alvarez, C., Vandamme, A.-M., and Müller, V. (2012). Enhanced heterosexual transmission hypothesis for the origin of pandemic HIV-1. *Viruses* 4, 1950-1983. doi:10.3390/v4101950.

de Taeye, S. W., Moore, J. P., and Sanders, R. W. (2016). HIV-1 Envelope Trimer Design and Immunization Strategies To Induce Broadly Neutralizing Antibodies. *Trends Immunol.* 37, 221-232. doi:10.1016/j.it.2016.01.007.

Deml, L., Kratochwil, G., Osterrieder, N., Knüchel, R., Wolf, H., and Wagner, R.

(1997). Increased incorporation of chimeric human immunodeficiency virus type 1 gp120 proteins into Pr55gag virus-like particles by an Epstein-Barr virus gp220/350-derived transmembrane domain. *Virology* 235, 10-25. doi:10.1006/viro.1997.8669.

Desrosiers, R. C., Wyand, M. S., Kodama, T., Ringler, D. J., Arthur, L. O., Sehgal, P. K., *et al.* (1989). Vaccine protection against simian immunodeficiency virus infection. *Proc. Natl. Acad. Sci. U. S. A.* 86, 6353-6357. doi:10.1073/pnas.86.16.6353.

Dhesi, Z., and Stebbing, J. (2011). The HVTN 503/Phambili study: efficacy is always the issue. *Lancet. Infect. Dis.* 11, 490-491. doi:10.1016/S1473-3099(11)70103-7.

Ding, H., Tsai, C., Gutiérrez, R. A., Zhou, F., Buchy, P., Deubel, V., *et al.* (2011). Superior neutralizing antibody response and protection in mice vaccinated with heterologous DNA prime and virus like particle boost against HPAI H5N1 virus. *PLoS One* 6. doi:10.1371/journal.pone.0016563.

Ding, X., Liu, D., Booth, G., Gao, W., and Lu, Y. (2018). Virus-Like Particle Engineering: From Rational Design to Versatile Applications. *Biotechnol. J.* 13, e1700324. doi:10.1002/biot.201700324.

Dolgin, E. (2021). How COVID unlocked the power of RNA vaccines. *Nature* 589,189-191. doi:10.1038/d41586-021-00019-w.

Domingo, E., and Perales, C. (2019). Viral quasispecies. *PLOS Genet.* 15, e1008271. doi:10.1371/journal.pgen.1008271.

Douek, D. C., Brenchley, J. M., Betts, M. R., Ambrozak, D. R., Hill, B. J., Okamoto, Y., *et al.* (2002). HIV preferentially infects HIV-specific CD4+ T cells. *Nature* 417, 95-98. doi:10.1038/417095a.

Dowdle, W. (1986). The search for an AIDS vaccine. *Public Health Rep.* 101, 232-233.

Drucker, E., Alcabes, P. G., and Marx, P. A. (2001). The injection century: massive unsterile injections and the emergence of human pathogens. *Lancet (London, England)* 358, 1989-1992. doi:10.1016/S0140-6736(01)06967-7.

Dubrovskaya, V., Tran, K., Ozorowski, G., Guenaga, J., Wilson, R., Bale, S., *et al.* (2019). Vaccination with Glycan-Modified HIV NFL Envelope Trimer-Liposomes Elicits Broadly Neutralizing Antibodies to Multiple Sites of Vulnerability. *Immunity* 51, 915-929.e7. doi:10.1016/j.immuni.2019.10.008.

Ellenberger, D., Wyatt, L., Li, B., Buge, S., Lanier, N., Rodriguez, I. V., *et al.* (2005). Comparative immunogenicity in rhesus monkeys of multi-protein HIV-1 (CRF02_AG) DNA/MVA vaccines expressing mature and immature VLPs. *Virology* 340, 21-32. doi:10.1016/j.virol.2005.06.014.

Elsayed, H., Nabi, G., McKinstry, W. J., Khoo, K. K., Mak, J., Salazar, A. M., *et al.* (2018). Intrastructural Help: Harnessing T Helper Cells Induced by Licensed Vaccines for Improvement of HIV Env Antibody Responses to Virus-Like Particle Vaccines. *J. Virol.* 92. doi:10.1128/JVI.00141-18.

Emerman, M., and Malim, M. H. (1998). HIV-1 regulatory/accessory genes: keys to unraveling viral and host cell biology. *Science* 280, 1880-1884. doi:10.1126/science.280.5371.1880.

Ertl, H. C. J. (2016). Viral vectors as vaccine carriers. *Curr. Opin. Virol.* 21, 1-8. doi:10.1016/j.coviro.2016.06.001.

Esparza, J. (2013). A brief history of the global effort to develop a preventive HIV vaccine. *Vaccine* 31, 3502-3518. doi:10.1016/j.vaccine.2013.05.018.

Esteban, I., Pastor-Quiñones, C., Usero, L., Plana, M., García, F., and Leal, L. (2021). In the Era of mRNA Vaccines, Is There Any Hope for HIV Functional Cure? *Viruses* 13. doi:10.3390/v13030501.

Euler, Z., van Gils, M. J., Bunnik, E. M., Phung, P., Schweighardt, B., Wrin, T., *et al.* (2010). Cross-reactive neutralizing humoral immunity does not protect from HIV type 1 disease progression. *J. Infect. Dis.* 201, 1045-1053. doi:10.1086/651144.

Eusébio, D., Neves, A. R., Costa, D., Biswas, S., Alves, G., Cui, Z., *et al.* (2021). Methods to improve the immunogenicity of plasmid DNA vaccines. *Drug Discov. Today*. doi:10.1016/j.drudis.2021.06.008.

Excler, J.-L., and Kim, J. H. (2019). Novel prime-boost vaccine strategies against HIV-1. *Expert Rev. Vaccines* 18, 765-779. doi:10.1080/14760584.2019.1640117.

Faria, N. R., Rambaut, A., Suchard, M. A., Baele, G., Bedford, T., Ward, M. J., *et al.* (2014). HIV epidemiology. The early spread and epidemic ignition of HIV-1 in human populations. *Science* 346, 56-61. doi:10.1126/science.1256739.

Feederle, R., and Schepers, A. (2017). Antibodies specific for nucleic acid modifications. *RNA Biol.* 14, 1089-1098. doi:10.1080/15476286.2017.1295905.

Fiebig, E. W., Wright, D. J., Rawal, B. D., Garrett, P. E., Schumacher, R. T., Peddada, L., *et al.* (2003). Dynamics of HIV viremia and antibody seroconversion in plasma donors: implications for diagnosis and staging of primary HIV infection. *AIDS* 17, 1871-1879. doi:10.1097/00002030-200309050-00005.

Fischer, W., Perkins, S., Theiler, J., Bhattacharya, T., Yusim, K., Funkhouser, R., *et al.* (2007). Polyvalent vaccines for optimal coverage of potential T-cell epitopes in global HIV-1 variants. *Nat. Med.* 13, 100-106. doi:10.1038/nm1461.

Fischl, M. A. (1994). Combination antiretroviral therapy for HIV infection. *Hosp. Pract. (Off. Ed).* 29, 43-48. doi:10.1080/21548331.1994.11442959.

Fischl, M. A., Richman, D. D., Grieco, M. H., Gottlieb, M. S., Volberding, P. A., Laskin, O. L., *et al.* (1987). The efficacy of azidothymidine (AZT) in the treatment of patients with AIDS and AIDS-related complex. A double-blind, placebo-controlled trial. *N. Engl. J. Med.* 317, 185-191. doi:10.1056/NEJM198707233170401.

Flynn, N. M., Forthal, D. N., Harro, C. D., Judson, F. N., Mayer, K. H., and Para, M. F. (2005). Placebo-controlled phase 3 trial of a recombinant glycoprotein 120 vaccine to prevent HIV-1 infection. *J. Infect. Dis.* 191, 654-665. doi:10.1086/428404.

Freed, E. O. (2015). HIV-1 assembly, release and maturation. *Nat. Rev. Microbiol.* 13, 484-496. doi:10.1038/nrmicro3490.

Fuenmayor, J., Gòdia, F., and Cervera, L. (2017). Production of virus-like particles for vaccines. *N. Biotechnol.* 39, 174-180. doi:10.1016/j.nbt.2017.07.010.

Gallo, R. C. (2005). The end or the beginning of the drive to an HIV-preventive vaccine: a view from over 20 years. *Lancet* 366, 1894-1898. doi:10.1016/S0140-6736(05)67395-3.

Gao, Y., Wijewardhana, C., and Mann, J. F. S. (2018). Virus-Like Particle, Liposome, and Polymeric Particle-Based Vaccines against HIV-1. *Front. Immunol.* 9, 345. doi:10.3389/fimmu.2018.00345.

García-Arriaza, J., and Esteban, M. (2014). Enhancing poxvirus vectors vaccine immunogenicity. *Hum. Vaccin. Immunother.* 10, 2235-2244. doi:10.4161/hv.28974.

Gartner, M. J., Roche, M., Churchill, M. J., Gorry, P. R., and Flynn, J. K. (2020). Understanding the mechanisms driving the spread of subtype C HIV-1. *EBioMedicine* 53. doi:10.1016/j.ebiom.2020.102682.

Gaudinski, M. R., Coates, E. E., Houser, K. V, Chen, G. L., Yamshchikov, G., Saunders, J. G., *et al.* (2018). Safety and pharmacokinetics of the Fc-modified HIV-1 human monoclonal antibody VRC01LS: A Phase 1 open-label clinical trial in healthy adults. *PLoS Med.* 15, e1002493. doi:10.1371/journal.pmed.1002493.

Gauduin, M. C., Parren, P. W., Weir, R., Barbas, C. F., Burton, D. R., and Koup, R. A. (1997). Passive immunization with a human monoclonal antibody protects hu-PBL-SCID mice against challenge by primary isolates of HIV-1. *Nat. Med.* 3, 1389-1393. doi:10.1038/nm1297-1389.

Gilbert, P. B., Peterson, M. L., Follmann, D., Hudgens, M. G., Francis, D. P., Gurwith, M., *et al.* (2005). Correlation between immunologic responses to a recombinant glycoprotein 120 vaccine and incidence of HIV-1 infection in a phase 3 HIV-1 preventive vaccine trial. *J. Infect. Dis.* 191, 666-677. doi:10.1086/428405.

Goldstein, J. R., and Lee, R. D. (2020). Demographic perspectives on the mortality of COVID-19 and other epidemics. *Proc. Natl. Acad. Sci. U. S. A.* 117, 22035-22041. doi:10.1073/pnas.2006392117.

Gonelli, C. A., Khoury, G., Center, R. J., and Purcell, D. F. J. (2019). HIV-1-based Virus-like Particles that Morphologically Resemble Mature, Infectious HIV-1 Virions. *Viruses* 11. doi:10.3390/v11060507.

Gonelli, C. A., King, H. A. D., Mackenzie, C., Sonza, S., Center, R. J., and Purcell, D. F. J. (2021). Immunogenicity of HIV-1-Based Virus-Like Particles with Increased Incorporation and Stability of Membrane-Bound Env. *Vaccines* 9. doi:10.3390/vaccines9030239.

Gray, C. M., and Walker, B. (2008). "CHAPTER 4 - The Immune Response to HIV," in, eds. P. A. Volberding, M. A. Sande, W. C. Greene, J. M. A. Lange, J. E. Gallant, and C. C. B. T.-G. H. M. Walsh (Edinburgh: W.B. Saunders), 39-49. doi:10.1016/B978-1-4160-2882-6.50008-3.

Gray, G. E., Allen, M., Moodie, Z., Churchyard, G., Bekker, L.-G., Nchabeleng, M., *et al.* (2011). Safety and efficacy of the HVTN 503/Phambili study of a clade-B-based HIV-1 vaccine in South Africa: a double-blind, randomised, placebo-controlled test-of-concept phase 2b study. *Lancet. Infect. Dis.* 11, 507-515. doi:10.1016/S1473-3099(11)70098-6.

Gray, G. E., Bekker, L.-G., Laher, F., Malahleha, M., Allen, M., Moodie, Z., *et al.* (2021). Vaccine Efficacy of ALVAC-HIV and Bivalent Subtype C gp120-MF59 in Adults. *N. Engl. J. Med.* 384, 1089-1100. doi:10.1056/NEJMoa2031499.

Gray, G. E., Laher, F., Lazarus, E., Ensoli, B., and Corey, L. (2016). Approaches to preventative and therapeutic HIV vaccines. *Curr. Opin. Virol.* 17, 104-109. doi:10.1016/j.coviro.2016.02.010.

Graziani, G. M., and Angel, J. B. (2016). HIV-1 Immunogen: an overview of almost 30 years of clinical testing of a candidate therapeutic vaccine. *Expert Opin. Biol. Ther.* 16, 953-966. doi:10.1080/14712598.2016.1193594.

Gulick, R. M., Mellors, J. W., Havlir, D., Eron, J. J., Gonzalez, C., McMahon, D., *et al.* (1997). Treatment with indinavir, zidovudine, and lamivudine in adults with human immunodeficiency virus infection and prior antiretroviral therapy. *N. Engl. J. Med.* 337, 734-739. doi:10.1056/NEJM199709113371102.

Gurdasani, D., Iles, L., Dillon, D. G., Young, E. H., Olson, A. D., Naranbhai, V., *et al.* (2014). A systematic review of definitions of extreme phenotypes of HIV control and progression. *AIDS* 28, 149-162. doi:10.1097/QAD.0000000000000049.

Hammer, S. M., Sobieszczyk, M. E., Janes, H., Karuna, S. T., Mulligan, M. J., Grove, D., *et al.* (2013). Efficacy trial of a DNA/rAd5 HIV-1 preventive vaccine. *N. Engl. J. Med.* 369, 2083-2092. doi:10.1056/NEJMoa1310566.

Hammer, S. M., Squires, K. E., Hughes, M. D., Grimes, J. M., Demeter, L. M., Currier, J. S., *et al.* (1997). A controlled trial of two nucleoside analogues plus indinavir in persons with human immunodeficiency virus infection and CD4 cell counts of 200 per cubic millimeter or less. AIDS Clinical Trials Group 320 Study Team. *N. Engl. J. Med.* 337, 725-733. doi:10.1056/NEJM199709113371101.

Hara, Y., Tashiro, Y., Murakami, A., Nishimura, M., Shimizu, T., Kubo, M., *et al.* (2015). High affinity IgM(+) memory B cells are generated through a germinal center-dependent pathway. *Mol. Immunol.* 68, 617-627. doi:10.1016/j.molimm.2015.10.003.

Harrer, T., Harrer, E., Kalams, S. A., Elbeik, T., Staprans, S. I., Feinberg, M. B., *et al.* (1996). Strong cytotoxic T cell and weak neutralizing antibody responses in a subset of persons with stable nonprogressing HIV type 1 infection. *AIDS Res. Hum. Retroviruses* 12, 585-592. doi:10.1089/aid.1996.12.585.

Haynes, B. F., Gilbert, P. B., McElrath, M. J., Zolla-Pazner, S., Tomaras, G. D., Alam, S. M., *et al.* (2012). Immune-correlates analysis of an HIV-1 vaccine efficacy trial. *N. Engl. J. Med.* 366, 1275-1286. doi:10.1056/NEJMoa1113425.

Hemelaar, J. (2012). The origin and diversity of the HIV-1 pandemic. *Trends Mol. Med.* 18, 182-192. doi:10.1016/j.molmed.2011.12.001.

Hennig, R., Pollinger, K., Veser, A., Breunig, M., and Goepferich, A. (2014). Nanoparticle multivalency counterbalances the ligand affinity loss upon PEGylation. *J. Control. Release* 194, 20-27. doi:10.1016/j.jconrel.2014.07.062.

Hinman, A. R. (1998). Global progress in infectious disease control. *Vaccine* 16, 1116-1121. doi:10.1016/s0264-410x(98)80107-2.

HIV Database Available at: https://www.hiv.lanl.gov/content/index [Accessed July 8, 2021].

Hobernik, D., and Bros, M. (2018). DNA Vaccines-How Far From Clinical Use? *Int. J. Mol. Sci.* 19. doi:10.3390/ijms19113605.

Hodgson, S. H., Mansatta, K., Mallett, G., Harris, V., Emary, K. R. W., and Pollard, A. J. (2021). What defines an efficacious COVID-19 vaccine? A review of the challenges assessing the clinical efficacy of vaccines against SARS-CoV-2. *Lancet. Infect. Dis.* 21, e26-e35. doi:10.1016/S1473-3099(20)30773-8.

Hokello, J., Sharma, A. L., and Tyagi, M. (2021). An Update on the HIV DNA Vaccine Strategy. *Vaccines* 9. doi:10.3390/vaccines9060605.

Holmes, K. K., Bertozzi, S., Bloom, B. R., Jha, P., Gelband, H., DeMaria, L. M., *et al.* (2017). "Major Infectious Diseases: Key Messages from Disease Control Priori-

ties, Third Edition.," in, eds. K. K. Holmes, S. Bertozzi, B. R. Bloom, and P. Jha (Washington (DC). doi:10.1596/978-1-4648-0524-0_ch1.

Hosseinipour, M. C., Innes, C., Naidoo, S., Mann, P., Hutter, J., Ramjee, G., *et al.* (2021). Phase 1 Human Immunodeficiency Virus (HIV) Vaccine Trial to Evaluate the Safety and Immunogenicity of HIV Subtype C DNA and MF59-Adjuvanted Subtype C Envelope Protein. *Clin. Infect. Dis. an Off. Publ. Infect. Dis. Soc. Am.* 72, 50-60. doi:10.1093/cid/ciz1239.

Huang, C., Tang, M., Zhang, M.-Y., Majeed, S., Montabana, E., Stanfield, R. L., *et al.* (2005). Structure of a V3-containing HIV-1 gp120 core. *Science* 310, 1025-1028. doi:10.1126/science.1118398.

Huang, J., Ofek, G., Laub, L., Louder, M. K., Doria-Rose, N. A., Longo, N. S., *et al.* (2012). Broad and potent neutralization of HIV-1 by a gp41-specific human antibody. *Nature* 491, 406-412. doi:10.1038/nature11544.

Huang, X., Zhu, Q., Huang, X., Yang, L., Song, Y., Zhu, P., *et al.* (2017). *In vivo* electroporation in DNA-VLP prime-boost preferentially enhances HIV-1 envelope-specific IgG2a, neutralizing antibody and CD8 T cell responses. *Vaccine* 35, 2042-2051. doi:10.1016/j.vaccine.2017.03.006.

Ingale, J., Stano, A., Guenaga, J., Sharma, S. K., Nemazee, D., Zwick, M. B., *et al.* (2016). High-Density Array of Well-Ordered HIV-1 Spikes on Synthetic Liposomal Nanoparticles Efficiently Activate B Cells. *Cell Rep.* 15, 1986-1999. doi:10.1016/j.celrep.2016.04.078.

Ivan, B., Sun, Z., Subbaraman, H., Friedrich, N., and Trkola, A. (2019). CD4 occupancy triggers sequential pre-fusion conformational states of the HIV-1 envelope trimer with relevance for broadly neutralizing antibody activity. *PLoS Biol.* 17, e3000114. doi:10.1371/journal.pbio.3000114.

Izquierdo-Useros, N., Puertas, M. C., Borràs, F. E., Blanco, J., and Martinez-Picado, J. (2011). Exosomes and retroviruses: the chicken or the egg? *Cell. Microbiol.* 13, 10-17. doi:10.1111/j.1462-5822.2010.01542.x.

Jacobs, B. L., Langland, J. O., Kibler, K. V, Denzler, K. L., White, S. D., Holechek, S. A., *et al.* (2009). Vaccinia virus vaccines: past, present and future. *Antiviral Res.* 84, 1-13. doi:10.1016/j.antiviral.2009.06.006.

Janes, H. E., Cohen, K. W., Frahm, N., De Rosa, S. C., Sanchez, B., Hural, J., *et al.* (2017). Higher T-Cell Responses Induced by DNA/rAd5 HIV-1 Preventive Vaccine Are Associated With Lower HIV-1 Infection Risk in an Efficacy Trial. *J. Infect. Dis.* 215, 1376-1385. doi:10.1093/infdis/jix086.

Janssen Vaccines (2021). Johnson & Johnson and Global Partners Announce Results from Phase 2b Imbokodo HIV Vaccine Clinical Trial in Young Women in Sub-Saharan Africa. Available at: https://www.jnj.com/johnson-johnson-and-global-partners-announce-results-from-phase-2b-imbokodo-hiv-vaccine-clinical-trial-in-young-women-in-sub-saharan-africa [Accessed August 31, 2021].

Jardine, J. G., Kulp, D. W., Havenar-Daughton, C., Sarkar, A., Briney, B., Sok, D., *et al.* (2016). HIV-1 broadly neutralizing antibody precursor B cells revealed by germline-targeting immunogen. *Science* 351, 1458-1463. doi:10.1126/science.aad9195.

Jin, X., Bauer, D. E., Tuttleton, S. E., Lewin, S., Gettie, A., Blanchard, J., *et al.* (1999). Dramatic rise in plasma viremia after CD8(+) T cell depletion in simian immunodeficiency virus-infected macaques. *J. Exp. Med.* 189, 991-998. doi:10.1084/jem.189.6.991.

Jones, L. D., Moody, M. A., and Thompson, A. B. (2020). Innovations in HIV-1 Vaccine Design. *Clin. Ther.* 42, 499-514. doi:10.1016/j.clinthera.2020.01.009.

Jorritsma, S. H. T., Gowans, E. J., Grubor-Bauk, B., and Wijesundara, D. K. (2016). Delivery methods to increase cellular uptake and immunogenicity of DNA vaccines. *Vaccine* 34, 5488-5494. doi:10.1016/j.vaccine.2016.09.062.

Jouvenet, N., Simon, S. M., and Bieniasz, P. D. (2009). Imaging the interaction of HIV-1 genomes and Gag during assembly of individual viral particles. *Proc. Natl. Acad. Sci. U. S. A.* 106, 19114-19119. doi:10.1073/pnas.0907364106.

Julg, B., Sok, D., Schmidt, S. D., Abbink, P., Newman, R. M., Broge, T., *et al.* (2017). Protective Efficacy of Broadly Neutralizing Antibodies with Incomplete Neutralization Activity against Simian-Human Immunodeficiency Virus in Rhesus Monkeys. *J. Virol.* 91. doi:10.1128/JVI.01187-17.

Julien, J.-P., Lee, J. H., Ozorowski, G., Hua, Y., Torrents de la Peña, A., de Taeye, S. W., *et al.* (2015). Design and structure of two HIV-1 clade C SOSIP.664 trimers that increase the arsenal of native-like Env immunogens. *Proc. Natl. Acad. Sci. U. S. A.* 112, 11947-11952. doi:10.1073/pnas.1507793112.

Kalidasan, V., and Theva Das, K. (2020). Lessons Learned From Failures and Success Stories of HIV Breakthroughs: Are We Getting Closer to an HIV Cure? *Front. Microbiol.* 11, 46. doi:10.3389/fmicb.2020.00046.

Kalish, M. L., Wolfe, N. D., Ndongmo, C. B., McNicholl, J., Robbins, K. E., Aidoo, M., *et al.* (2005). Central African hunters exposed to simian immunodeficiency virus. *Emerg. Infect. Dis.* 11, 1928-1930. doi:10.3201/eid1112.050394.

Kamala, T. (2007). Hock immunization: A humane alternative to mouse footpad injections. *J. Immunol. Methods* 328, 204-214. doi:10.1016/j.jim.2007.08.004.

Karikó, K., Muramatsu, H., Welsh, F. A., Ludwig, J., Kato, H., Akira, S., *et al.* (2008). Incorporation of Pseudouridine Into mRNA Yields Superior Nonimmunogenic Vector With Increased Translational Capacity and Biological Stability. *Mol. Ther.* 16, 1833-1840. doi:10.1038/mt.2008.200.

Kasturi, S. P., Kozlowski, P. A., Nakaya, H. I., Burger, M. C., Russo, P., Pham, M., *et al.* (2017). Adjuvanting a Simian Immunodeficiency Virus Vaccine with Toll-Like Receptor Ligands Encapsulated in Nanoparticles Induces Persistent Antibody Responses and Enhanced Protection in TRIM5α Restrictive Macaques. *J. Virol.* 91. doi:10.1128/JVI.01844-16.

Kawasaki, T., and Kawai, T. (2014). Toll-Like Receptor Signaling Pathways. *Front. Immunol.* 5, 461. doi:10.3389/fimmu.2014.00461.

Keele, B. F., Van Heuverswyn, F., Li, Y., Bailes, E., Takehisa, J., Santiago, M. L., *et al.* (2006). Chimpanzee reservoirs of pandemic and nonpandemic HIV-1. *Science* 313, 523-526. doi:10.1126/science.1126531.

Kemnic, T. R., and Gulick, P. G. (2021). "HIV Antiretroviral Therapy.," in [Treasure Island (FL)].

Kesavardhana, S., and Varadarajan, R. (2014). Stabilizing the native trimer of HIV-1 Env by destabilizing the heterodimeric interface of the gp41 postfusion six-helix bundle. *J. Virol.* 88, 9590-9604. doi:10.1128/JVI.00494-14.

Kim, J. H., Excler, J.-L., and Michael, N. L. (2014). Lessons from the RV144 Thai Phase III HIV-1 Vaccine Trial and the Search for Correlates of Protection. *Annu. Rev. Med.*, 1-15. doi:10.1146/annurev-med-052912-123749.

Kim, J. H., Hartley, T. L., Curran, a. R., and Engelman, D. M. (2009). Molecular dynamics studies of the transmembrane domain of gp41 from HIV-1. *Biochim. Biophys. Acta - Biomembr.* 1788, 1804-1812. doi:10.1016/j.bbamem.2009.06.011.

Klasse, P. J., Ozorowski, G., Sanders, R. W., and Moore, J. P. (2020). Env Exceptionalism: Why Are HIV-1 Env Glycoproteins Atypical Immunogens? *Cell Host Microbe* 27, 507-518. doi:10.1016/j.chom.2020.03.018.

Klein, F., Diskin, R., Scheid, J. F., Gaebler, C., Mouquet, H., Georgiev, I. S., *et al.* (2013). Somatic mutations of the immunoglobulin framework are generally required for broad and potent HIV-1 neutralization. *Cell* 153, 126-138. doi:10.1016/j.cell.2013.03.018.

Klein, J. S., and Bjorkman, P. J. (2010). Few and far between: how HIV may be evading antibody avidity. *PLoS Pathog.* 6, e1000908. doi:10.1371/journal.ppat.1000908.

Klessing, S., Temchura, V., Tannig, P., Peter, A. S., Christensen, D., Lang, R., *et al.* (2020). CD4(+) T Cells Induced by Tuberculosis Subunit Vaccine H1 Can Improve the HIV-1 Env Humoral Response by Intrastructural Help. *Vaccines* 8. doi:10.3390/vaccines8040604.

Klinman, D. M., Klaschik, S., Tross, D., Shirota, H., and Steinhagen, F. (2010). FDA guidance on prophylactic DNA vaccines: analysis and recommendations. *Vaccine* 28, 2801-2805. doi:10.1016/j.vaccine.2009.11.025.

Ko, S.-Y., Pegu, A., Rudicell, R. S., Yang, Z., Joyce, M. G., Chen, X., *et al.* (2014). Enhanced neonatal Fc receptor function improves protection against primate SHIV infection. *Nature* 514, 642-645. doi:10.1038/nature13612.

Korber, B., Gaschen, B., Yusim, K., Thakallapally, R., Kesmir, C., and Detours, V. (2001). Evolutionary and immunological implications of contemporary HIV-1 variation. *Br. Med. Bull.* 58, 19-42. doi:10.1093/bmb/58.1.19.

Korber, B., Muldoon, M., Theiler, J., Gao, F., Gupta, R., Lapedes, A., *et al.* (2000). Timing the ancestor of the HIV-1 pandemic strains. *Science* 288, 1789-1796. doi:10.1126/science.288.5472.1789.

Koup, R. A., and Douek, D. C. (2011). Vaccine design for CD8 T lymphocyte responses. *Cold Spring Harb. Perspect. Med.* 1, a007252. doi:10.1101/cshperspect.a007252.

Kracker, S., and Radbruch, A. (2004). Immunoglobulin class switching: *in vitro* induction and analysis. *Methods Mol. Biol.* 271, 149-159. doi:10.1385/1-59259-796-3:149.

Krangel, M. S. (2009). Mechanics of T cell receptor gene rearrangement. *Curr. Opin. Immunol.* 21, 133-139. doi:10.1016/j.coi.2009.03.009.

Kula-Pacurar, A., Rodari, A., Darcis, G., and Van Lint, C. (2021). Shocking HIV-1 with immunomodulatory latency reversing agents. *Semin. Immunol.*, 101478. doi:10.1016/j.smim.2021.101478.

Kwon, Y. D., Georgiev, I. S., Ofek, G., Zhang, B., Asokan, M., Bailer, R. T., *et al.* (2016).

Optimization of the Solubility of HIV-1-Neutralizing Antibody 10E8 through Somatic Variation and Structure-Based Design. *J. Virol.* 90, 5899-5914. doi:10.1128/JVI.03246-15.

Laher, F., Bekker, L.-G., Garrett, N., Lazarus, E. M., and Gray, G. E. (2020). Review of preventative HIV vaccine clinical trials in South Africa. *Arch. Virol.* 165, 2439-2452. doi:10.1007/s00705-020-04777-2.

Laher, F., Ranasinghe, S., Porichis, F., Mewalal, N., Pretorius, K., Ismail, N., *et al.* (2017). HIV Controllers Exhibit Enhanced Frequencies of Major Histocompatibility Complex Class II Tetramer(+) Gag-Specific CD4(+) T Cells in Chronic Clade C HIV-1 Infection. *J. Virol.* 91. doi:10.1128/JVI.02477-16.

Landais, E., and Moore, P. L. (2018). Development of broadly neutralizing antibodies in HIV-1 infected elite neutralizers. *Retrovirology* 15, 61. doi:10.1186/s12977-018-0443-0.

Langer, B., Renner, M., Scherer, J., Schüle, S., and Cichutek, K. (2013). Safety assessment of biolistic DNA vaccination. *Methods Mol. Biol.* 940, 371-388. doi:10.1007/978-1-62703-110-3_27.

Lavado-García, J., Jorge, I., Boix-Besora, A., Vázquez, J., Gòdia, F., and Cervera, L. (2021). Characterization of HIV-1 virus-like particles and determination of Gag stoichiometry for different production platforms. *Biotechnol. Bioeng.* 118, 2660-2675. doi:10.1002/bit.27786.

Leal, L., Guardo, A. C., Morón-López, S., Salgado, M., Mothe, B., Heirman, C., *et al.* (2018). Phase I clinical trial of an intranodally administered mRNA-based therapeutic vaccine against HIV-1 infection. *AIDS* 32, 2533-2545. doi:10.1097/QAD.0000000000002026.

Leal, L., Lucero, C., Gatell, J. M., Gallart, T., Plana, M., and García, F. (2017). New challenges in therapeutic vaccines against HIV infection. *Expert Rev. Vaccines* 16, 587-600. doi:10.1080/14760584.2017.1322513.

LeBien, T. W., and Tedder, T. F. (2008). B lymphocytes: how they develop and function. *Blood* 112, 1570-1580. doi:10.1182/blood-2008-02-078071.

Lederman, M. M., Connick, E., Landay, A., Kuritzkes, D. R., Spritzler, J., St Clair, M., *et al.* (1998). Immunologic responses associated with 12 weeks of combination antiretroviral therapy consisting of zidovudine, lamivudine, and ritonavir: results of AIDS Clinical Trials Group Protocol 315. *J. Infect. Dis.* 178, 70-79. doi:10.1086/515591.

Lee, J., Arun Kumar, S., Jhan, Y. Y., and Bishop, C. J. (2018). Engineering DNA vaccines against infectious diseases. *Acta Biomater.* 80, 31-47. doi:10.1016/j.actbio.2018.08.033.

Lee, S. K. (2018). Sex as an important biological variable in biomedical research. *BMB Rep.* 51, 167-173. doi:10.5483/bmbrep.2018.51.4.034.

Licht, A., and Alter, G. (2016). A Drug-Free Zone—Lymph Nodes as a Safe Haven for HIV. *Cell Host Microbe* 19, 275-276. doi:10.1016/j.chom.2016.02.018.

Lifei, Y., Yufeng, S., Xiaomin, L., Xiaoxing, H., Jingjing, L., Heng, D., *et al.* (2012). HIV-1 Virus-Like Particles Produced by Stably Transfected Drosophila S2 Cells: a Desirable Vaccine Component. *J. Virol.* 86, 7662-7676. doi:10.1128/JVI.07164-11.

Liu, J., and Ostrowski, M. (2017). Development of targeted adjuvants for HIV-1 vaccines. *AIDS Res. Ther.* 14, 43. doi:10.1186/s12981-017-0165-8.

Liu, R., Simonetti, F. R., and Ho, Y.-C. (2020). The forces driving clonal expansion of the HIV-1 latent reservoir. *Virol. J.* 17, 4. doi:10.1186/s12985-019-1276-8.

Lopez-Galindez, C., Pernas, M., Casado, C., Olivares, I., and Lorenzo-Redondo, R. (2019). Elite controllers and lessons learned for HIV-1 cure. *Curr. Opin. Virol.* 38, 31-36. doi:10.1016/j.coviro.2019.05.010.

Lopez Angel, C. J., and Tomaras, G. D. (2020). Bringing the path toward an HIV-1 vaccine into focus. *PLOS Pathog.* 16, e1008663. doi:10.1371/journal.ppat.1008663.

Lu, L. L., Suscovich, T. J., Fortune, S. M., and Alter, G. (2018). Beyond binding: antibody effector functions in infectious diseases. *Nat. Rev. Immunol.* 18, 46-61. doi:10.1038/nri.2017.106.

Lynch, R. M., Wong, P., Tran, L., O'Dell, S., Nason, M. C., Li, Y., *et al.* (2015). HIV-1 fitness cost associated with escape from the VRC01 class of CD4 binding site neutralizing antibodies. *J. Virol.* 89, 4201-4213. doi:10.1128/JVI.03608-14.

MacColl, G., Bunn, C., Goldspink, G., Bouloux, P., and Górecki, D. C. (2001). Intramuscular plasmid DNA injection can accelerate autoimmune responses. *Gene Ther.* 8, 1354–1356. doi:10.1038/sj.gt.3301537.

Marsden, M. D., and Zack, J. A. (2017). Humanized Mouse Models for Human Immunodeficiency Virus Infection. *Annu. Rev. Virol.* 4, 393-412. doi:10.1146/annurev-virology-101416-041703.

Martinez-Picado, J., and Deeks, S. G. (2016). Persistent HIV-1 replication during antiretroviral therapy. *Curr. Opin. HIV AIDS* 11, 417-423. doi:10.1097/COH.0000000000000287.

Martinsen, J. T., Gunst, J. D., Højen, J. F., Tolstrup, M., and Søgaard, O. S. (2020). The Use of Toll-Like Receptor Agonists in HIV-1 Cure Strategies. *Front. Immunol.* 11, 1112. doi:10.3389/fimmu.2020.01112.

Mascola, J. R. (2002). Passive transfer studies to elucidate the role of antibody-mediated protection against HIV-1. *Vaccine* 20, 1922-1925. doi:10.1016/s0264-410x(02)00068-3.

Masemola, A., Mashishi, T., Khoury, G., Mohube, P., Mokgotho, P., Vardas, E., *et al.* (2004). Hierarchical targeting of subtype C human immunodeficiency virus type 1 proteins by CD8+ T cells: correlation with viral load. *J. Virol.* 78, 3233-3243. doi:10.1128/jvi.78.7.3233-3243.2004.

McBurney, S. P., Young, K. R., and Ross, T. M. (2007). Membrane embedded HIV-1 envelope on the surface of a virus-like particle elicits broader immune responses than soluble envelopes. *Virology* 358, 334-46. doi:10.1016/j.virol.2006.08.032.

McDermott, A. B., Mitchen, J., Piaskowski, S., Souza, I. De, Yant, L. J., Stephany, J., *et al.* (2004). Repeated Low-Dose Mucosal Simian Immunodeficiency Virus SIVmac239 Challenge Results in the Same Viral and Immunological Kinetics as High-Dose Challenge: a Model for the Evaluation of Vaccine Efficacy in Nonhuman Primates. *J. Virol.* 78, 3140-3144. doi:10.1128/JVI.78.6.3140-3144.2004.

McMichael, A. J., Borrow, P., Tomaras, G. D., Goonetilleke, N., and Haynes, B. F. (2010). The immune response during acute HIV-1 infection: clues for vaccine development. *Nat. Rev. Immunol.* 10, 11-23. doi:10.1038/nri2674.

Mei, K.-C., Bai, J., Lorrio, S., Wang, J. T.-W., and Al-Jamal, K. T. (2016). Investigating the effect of tumor vascularization on magnetic targeting *in vivo* using retrospective design of experiment. *Biomaterials* 106, 276–285. doi:10.1016/j.biomaterials.2016.08.030.

Mellins, E. D., and Kay, M. A. (2015). Viral Vectors Take On HIV Infection. *N. Engl. J. Med.* 373, 770-772. doi:10.1056/NEJMcibr1504232.

Moldt, B., Rakasz, E. G., Schultz, N., Chan-Hui, P.-Y., Swiderek, K., Weisgrau, K. L., *et al.* (2012). Highly potent HIV-specific antibody neutralization *in vitro* translates into effective protection against mucosal SHIV challenge *in vivo*. *Proc. Natl. Acad. Sci.* 109, 18921-18925. doi:10.1073/pnas.1214785109.

Molinos-Albert, L. M., Bilbao, E., Agulló, L., Marfil, S., García, E., Concepción, M. L. R. D. La, *et al.* (2017a). Proteoliposomal formulations of an HIV-1 gp41-based miniprotein elicit a lipid-dependent immunodominant response overlapping the 2F5 binding motif. *Sci. Rep.* 7, 40800. doi:10.1038/srep40800.

Molinos-Albert, L. M., Carrillo, J., Curriu, M., Rodriguez de la Concepción, M. L., Marfil, S., García, E., *et al.* (2014). Anti-MPER antibodies with heterogeneous neutralization capacity are detectable in most untreated HIV-1 infected individuals. *Retrovirology* 11, 44. doi:10.1186/1742-4690-11-44.

Molinos-Albert, L. M., Clotet, B., Blanco, J., and Carrillo, J. (2017b). Immunologic Insights on the Membrane Proximal External Region: A Major Human Immunodeficiency Virus Type-1 Vaccine Target. *Front. Immunol.* 8, 1154. doi:10.3389/fimmu.2017.01154.

Momin, T., Kansagra, K., Patel, H., Sharma, S., Sharma, B., Patel, J., *et al.* (2021). Safety and Immunogenicity of a DNA SARS-CoV-2 vaccine (ZyCoV-D): Results of an open-label, non-randomized phase I part of phase I/II clinical study by intradermal route in healthy subjects in India. *EClinicalMedicine* 38. doi:10.1016/j.eclinm.2021.101020.

Montefiori, D. C., Safrit, J.T., Lydy, S.L., Barry, A.P., Bilska, M., Vo, H.T., *et al.* (2001). Induction of Neutralizing Antibodies and Gag-Specific Cellular Immune Responses to an R5 Primary Isolate of Human Immunodeficiency Virus Type 1 in Rhesus Macaques. *J. Virol.* 75, 5879-5890. doi:10.1128/JVI.75.13.5879-5890.2001.

Montefiori, D. C. (2009). Measuring HIV neutralization in a luciferase reporter gene assay. *Methods Mol. Biol.* 485, 395-405. doi:10.1007/978-1-59745-170-3_26.

Montefiori, D. C. (2016). Bispecific Antibodies Against HIV. *Cell* 165, 1563-1564. doi:10.1016/j.cell.2016.06.004.

Moodie, Z., Walsh, S. R., Laher, F., Maganga, L., Herce, M. E., Naidoo, S., *et al.* (2020). Antibody and cellular responses to HIV vaccine regimens with DNA plasmid as compared with ALVAC priming: An analysis of two randomized controlled trials. *PLoS Med.* 17, e1003117. doi:10.1371/journal.pmed.1003117.

Moore, J. P., Kitchen, S. G., Pugach, P., and Zack, J. A. (2004). The CCR5 and CXCR4 coreceptors—central to understanding the transmission and pathogenesis of human immunodeficiency virus type 1 infection. *AIDS Res. Hum. Retroviruses* 20, 111-126. doi:10.1089/088922204322749567.

Moss, J. A. (2013). HIV/AIDS Review. *Radiol. Technol.* 84, 247-270.

Mothe, B., Hu, X., Llano, A., Rosati, M., Olvera, A., Kulkarni, V., *et al.* (2015). A human immune data-informed vaccine concept elicits strong and broad T-cell specificities associated with HIV-1 control in mice and macaques. *J. Transl. Med.* 13, 60. doi:10.1186/s12967-015-0392-5.

Mouquet, H. (2014). Antibody B cell responses in HIV-1 infection. *Trends Immunol.* 35, 549-561. doi:10.1016/j.it.2014.08.007.

Mouquet, H., Scheid, J. F., Zoller, M. J., Krogsgaard, M., Ott, R. G., Shukair, S., *et al.* (2010). Polyreactivity increases the apparent affinity of anti-HIV antibodies by heteroligation. *Nature* 467, 591-595. doi:10.1038/nature09385.

Muramatsu, M., Kinoshita, K., Fagarasan, S., Yamada, S., Shinkai, Y., and Honjo, T. (2000). Class switch recombination and hypermutation require activation-induced cytidine deaminase (AID), a potential RNA editing enzyme. *Cell* 102, 553-563. doi:10.1016/s0092-8674(00)00078-7.

Murphey-Corb, M., Martin, L. N., Davison-Fairburn, B., Montelaro, R. C., Miller, M., West, M., *et al.* (1989). A formalin-inactivated whole SIV vaccine confers protection in macaques. *Science* 246, 1293-1297. doi:10.1126/science.2555923.

Murphy, K., Weaver, C., and Janeway, C. (2017). *Janeway's immunobiology*. New York: Garland Science.

Nabi, G., Genannt Bonsmann, M. S., Tenbusch, M., Gardt, O., Barouch, D. H., Temchura, V., *et al.* (2013). GagPol-specific CD4+T-cells increase the antibody response to Env by intrastructural help. *Retrovirology* 10, 117. doi:10.1186/1742-4690-10-117.

Naranjo-Gomez, M., and Pelegrin, M. (2019). Vaccinal effect of HIV-1 antibody therapy. *Curr. Opin. HIV AIDS* 14, 325-333. doi:10.1097/COH.0000000000000555.

Nemazee, D. (2017). Mechanisms of central tolerance for B cells. *Nat. Rev. Immunol.* 17, 281-294. doi:10.1038/nri.2017.19.

Nielsen, C. M., Ogbe, A., Pedroza-Pacheco, I., Doeleman, S. E., Chen, Y., Silk, S. E., *et al.* (2021). Protein/AS01B vaccination elicits stronger, more Th2-skewed antigen-specific human T follicular helper cell responses than heterologous viral vectors. *Cell Reports Med.* 2, 100207. doi:10.1016/j.xcrm.2021.100207.

Normark, J., Vikström, L., Gwon, Y.-D., Persson, I.-L., Edin, A., Björsell, T., *et al.* (2021). Heterologous ChAdOx1 nCoV-19 and mRNA-1273 Vaccination. *N. Engl. J. Med.* doi:10.1056/NEJMc2110716.

Notka, F., Stahl-Hennig, C., Dittmer, U., Wolf, H., and Wagner, R. (1999). Accelerated clearance of SHIV in rhesus monkeys by virus-like particle vaccines is dependent on induction of neutralizing antibodies. *Vaccine* 18, 291-301. doi:10.1016/S0264-410X(99)00200-5.

Olvera, A., Cedeño, S., Llano, A., Mothe, B., Sanchez, J., Arsequell, G., *et al.* (2020). Does Antigen Glycosylation Impact the HIV-Specific T Cell Immunity? *Front. Immunol.* 11, 573928. doi:10.3389/fimmu.2020.573928.

Ondondo, B., Murakoshi, H., Clutton, G., Abdul-Jawad, S., Wee, E. G.-T., Gatanaga, H., *et al.* (2016). Novel Conserved-region T-cell Mosaic Vaccine With High Global HIV-1 Coverage Is Recognized by Protective Responses in Untreated Infection. *Mol. Ther.* 24, 832-842. doi:10.1038/mt.2016.3.

Oriol-Tordera, B., Llano, A., Ganoza, C., Cate, S., Hildebrand, W., Sanchez, J., *et al.*

(2017). Impact of HLA-DRB1 allele polymorphisms on control of HIV infection in a Peruvian MSM cohort. *HLA* 90, 234-237. doi:10.1111/tan.13085.

Paliard, X., Liu, Y., Wagner, R., Wolf, H., Baenziger, J., and Walker, C. M. (2000). Priming of Strong, Broad, and Long-Lived HIV Type 1 p55gag-Specific CD8+ Cytotoxic T Cells after Administration of a Virus-Like Particle Vaccine in Rhesus Macaques. *AIDS Res. Hum. Retroviruses* 16, 273-282. doi:10.1089/088922200309368.

Pardi, N., Hogan, M. J., Porter, F. W., and Weissman, D. (2018). mRNA vaccines — a new era in vaccinology. *Nat. Rev. Drug Discov.* 17, 261-279. doi:10.1038/nrd.2017.243.

Patterson, L. J., and Robert-Guroff, M. (2008). Replicating adenovirus vector prime/protein boost strategies for HIV vaccine development. *Expert Opin. Biol. Ther.* 8, 1347-1363. doi:10.1517/14712598.8.9.1347.

Pau, A. K., and George, J. M. (2014). Antiretroviral therapy: current drugs. *Infect. Dis. Clin. North Am.* 28, 371-402. doi:10.1016/j.idc.2014.06.001.

Pauthner, M. G., Nkolola, J. P., Havenar-Daughton, C., Murrell, B., Reiss, S. M., Bastidas, R., *et al.* (2019). Vaccine-Induced Protection from Homologous Tier 2 SHIV Challenge in Nonhuman Primates Depends on Serum-Neutralizing Antibody Titers. *Immunity* 50, 241-252.e6. doi:10.1016/j.immuni.2018.11.011.

Pauthner, M., Havenar-Daughton, C., Sok, D., Nkolola, J. P., Bastidas, R., Boopathy, A. V, *et al.* (2017). Elicitation of Robust Tier 2 Neutralizing Antibody Responses in Nonhuman Primates by HIV Envelope Trimer Immunization Using Optimized Approaches. *Immunity* 46, 1073-1088.e6. doi:10.1016/j.immuni.2017.05.007.

Payne, R. P., Kløverpris, H., Sacha, J. B., Brumme, Z., Brumme, C., Buus, S., *et al.* (2010). Efficacious early antiviral activity of HIV Gag- and Pol-specific HLA-B 2705-restricted CD8+ T cells. *J. Virol.* 84, 10543-10557. doi:10.1128/JVI.00793-10.

Pegu, A., Yang, Z., Boyington, J. C., Wu, L., Ko, S.-Y., Schmidt, S. D., *et al.* (2014). Neutralizing antibodies to HIV-1 envelope protect more effectively in vivo than those to the CD4 receptor. *Sci. Transl. Med.* 6, 243ra88. doi:10.1126/scitranslmed.3008992.

Pejawar-Gaddy, S., Kovacs, J. M., Barouch, D. H., Chen, B., and Irvine, D. J. (2014). Design of Lipid Nanocapsule Delivery Vehicles for Multivalent Display of Recombinant Env Trimers in HIV Vaccination. *Bioconjug. Chem.* 25, 1470-1478. doi:10.1021/bc5002246.

Perdiguero, B., Gómez, C. E., García-Arriaza, J., Sánchez-Corzo, C., Sorzano, C. Ó. S., Wilmschen, S., *et al.* (2019a). Heterologous Combination of VSV-GP and NYVAC Vectors Expressing HIV-1 Trimeric gp145 Env as Vaccination Strategy to Induce Balanced B and T Cell Immune Responses. *Front. Immunol.* 10, 2941. doi:10.3389/fimmu.2019.02941.

Perdiguero, B., Sánchez-Corzo, C., Sorzano, C. O. S., Saiz, L., Mediavilla, P., Esteban, M., *et al.* (2019b). A Novel MVA-Based HIV Vaccine Candidate (MVA-gp145-GPN) Co-Expressing Clade C Membrane-Bound Trimeric gp145 Env and Gag-Induced Virus-Like Particles (VLPs) Triggered Broad and Multifunctional HIV-1-Specific T Cell and Antibody Responses. *Viruses* 11. doi:10.3390/v11020160.

Pereira Aguilar, P., González-Domínguez, I., Schneider, T. A., Gòdia, F., Cervera, L., and Jungbauer, A. (2019). At-line multi-angle light scattering detector for faster

process development in enveloped virus-like particle purification. *J. Sep. Sci.* 42, 2640–2649. doi:10.1002/jssc.201900441.

Perez-Zsolt, D., Cantero-Pérez, J., Erkizia, I., Benet, S., Pino, M., Serra-Peinado, C., *et al.* (2019a). Dendritic Cells From the Cervical Mucosa Capture and Transfer HIV-1 via Siglec-1. *Front. Immunol.* 10, 825. doi:10.3389/fimmu.2019.00825.

Perez-Zsolt, D., Martinez-Picado, J., and Izquierdo-Useros, N. (2019b). When Dendritic Cells Go Viral: The Role of Siglec-1 in Host Defense and Dissemination of Enveloped Viruses. *Viruses* 12. doi:10.3390/v12010008.

Perkus, M. E., Tartaglia, J., and Paoletti, E. (1995). Poxvirus-based vaccine candidates for cancer, AIDS, and other infectious diseases. *J. Leukoc. Biol.* 58, 1-13. doi:10.1002/jlb.58.1.1.

Pernas, M., Tarancón-Diez, L., Rodríguez-Gallego, E., Gómez, J., Prado, J. G., Casado, C., *et al.* (2018). Factors Leading to the Loss of Natural Elite Control of HIV-1 Infection. *J. Virol.* 92, e01805-17. doi:10.1128/JVI.01805-17.

Phelps, M. (2021). Short Talk: Broadly Neutralizing Antibody Recognition of HIV Envelope Epitopes Modulates Effector Function. *Keystone Symposia on HIV Vaccines* (Virtual), June 1st-4th 2021.

Picard, O., Lebas, J., Imbert, J. C., Bigel, P., and Zagury, D. (1991). Complication of intramuscular/subcutaneous immune therapy in severely immune-compromised individuals. *J. Acquir. Immune Defic. Syndr.* 4, 641-643.

Pilkington, E. H., Suys, E. J. A., Trevaskis, N. L., Wheatley, A. K., Zukancic, D., Algarni, A., *et al.* (2021). From influenza to COVID-19: Lipid nanoparticle mRNA vaccines at the frontiers of infectious diseases. *Acta Biomater.* doi:10.1016/j.actbio.2021.06.023.

Pitisuttithum, P., Gilbert, P., Gurwith, M., Heyward, W., Martin, M., van Griensven, F., *et al.* (2006). Randomized, double-blind, placebo-controlled efficacy trial of a bivalent recombinant glycoprotein 120 HIV-1 vaccine among injection drug users in Bangkok, Thailand. *J. Infect. Dis.* 194, 1661-1671. doi:10.1086/508748.

Pitisuttithum, P., Nitayaphan, S., Chariyalertsak, S., Kaewkungwal, J., Dawson, P., Dhitavat, J., *et al.* (2020). Late boosting of the RV144 regimen with AIDSVAX B/E and ALVAC-HIV in HIV-uninfected Thai volunteers: a double-blind, randomised controlled trial. *Lancet. HIV* 7, e238-e248. doi:10.1016/S2352-3018(19)30406-0.

Plana, M., García, F., Gallart, T., Tortajada, C., Soriano, A., Palou, E., *et al.* (2000). Immunological benefits of antiretroviral therapy in very early stages of asymptomatic chronic HIV-1 infection. *AIDS* 14, 1921-1933. doi:10.1097/00002030-200009080-00007.

Postler, T. S., and Desrosiers, R. C. (2013). The tale of the long tail: the cytoplasmic domain of HIV-1 gp41. *J. Virol.* 87, 2–15. doi:10.1128/JVI.02053-12.

Poteet, E., Lewis, P., Chen, C., Ho, S. O., Do, T., Chiang, S., *et al.* (2016). Toll-like receptor 3 adjuvant in combination with virus-like particles elicit a humoral response against HIV. *Vaccine* 34, 5886-5894. doi:10.1016/j.vaccine.2016.10.036.

Prado, J. G., and Frater, J. (2020). Editorial: Immune Surveillance of the HIV Reservoir: Mechanisms, Therapeutic Targeting and New Avenues for HIV Cure. *Front. Immunol.* 11, 70. doi:10.3389/fimmu.2020.00070.

Qin, F., Xia, F., Chen, H., Cui, B., Feng, Y., Zhang, P., *et al.* (2021). A Guide to Nucleic Acid Vaccines in the Prevention and Treatment of Infectious Diseases and Can-

cers: From Basic Principles to Current Applications. *Front. cell Dev. Biol.* 9, 633776. doi:10.3389/fcell.2021.633776.

Radaelli, A., Bonduelle, O., Beggio, P., Mahe, B., Pozzi, E., Elli, V., *et al.* (2007). Prime-boost immunization with DNA, recombinant fowlpox virus and VLPSHIV elicit both neutralizing antibodies and IFNγ-producing T cells against the HIV-envelope protein in mice that control env-bearing tumour cells. *Vaccine* 25, 2128-2138. doi:10.1016/j.vaccine.2006.11.009.

Radaelli, A., Zanotto, C., Perletti, G., Elli, V., Vicenzi, E., Poli, G., *et al.* (2003). Comparative analysis of immune responses and cytokine profiles elicited in rabbits by the combined use of recombinant fowlpox viruses, plasmids and virus-like particles in prime-boost vaccination protocols against SHIV. *Vaccine* 21, 2052-2064. doi:10.1016/S0264-410X(02)00773-9.

Rainone, V., Dubois, G., Temchura, V., Überla, K., Clivio, A., Nebuloni, M., *et al.* (2011). CCL28 Induces Mucosal Homing of HIV-1-Specific IgA-Secreting Plasma Cells in Mice Immunized with HIV-1 Virus-Like Particles. *PLoS One* 6, e26979. doi:10.1371/journal.pone.0026979.

Rao, M., and Alving, C. R. (2016). Adjuvants for HIV vaccines. *Curr. Opin. HIV AIDS* 11, 585-592. doi:10.1097/COH.0000000000000315.

Rappuoli, R., Pizza, M., Del Giudice, G., and De Gregorio, E. (2014). Vaccines, new opportunities for a new society. *Proc. Natl. Acad. Sci. U. S. A.* 111, 12288-12293. doi:10.1073/pnas.1402981111.

Ratnapriya, S., Perez-Greene, E., Schifanella, L., and Herschhorn, A. (2021). Adjuvant-mediated enhancement of the immune response to HIV vaccines. *FEBS J.* n/a. doi:10.1111/febs.15814.

Redd, A. D., Quinn, T. C., and Tobian, A. A. R. (2013). Frequency and implications of HIV superinfection. *Lancet Infect. Dis.* 13, 622-628. doi:10.1016/S1473-3099(13)70066-5.

Reddy, S. T., Rehor, A., Schmoekel, H. G., Hubbell, J. A., and Swartz, M. A. (2006). *In vivo* targeting of dendritic cells in lymph nodes with poly(propylene sulfide) nanoparticles. *J. Control. Release* 112, 26-34. doi:10.1016/j.jconrel.2006.01.006.

Reichmuth, A. M., Oberli, M. A., Jaklenec, A., Langer, R., and Blankschtein, D. (2016). mRNA vaccine delivery using lipid nanoparticles. *Ther. Deliv.* 7, 319-334. doi:10.4155/tde-2016-0006.

Rerks-Ngarm, S., Brown, A. E., Khamboonruang, C., Thongcharoen, P., and Kunasol, P. (2006). HIV/AIDS preventive vaccine 'prime-boost' phase III trial: foundations and initial lessons learned from Thailand. *AIDS* 20. doi:10.1097/01.aids.0000237362.26370.f8

Rerks-Ngarm, S., Pitisuttithum, P., Excler, J.-L., Nitayaphan, S., Kaewkungwal, J., Premsri, N., *et al.* (2017). Randomized, Double-Blind Evaluation of Late Boost Strategies for HIV-Uninfected Vaccine Recipients in the RV144 HIV Vaccine Efficacy Trial. *J. Infect. Dis.* 215, 1255-1263. doi:10.1093/infdis/jix099.

Rerks-Ngarm, S., Pitisuttithum, P., Nitayaphan, S., Kaewkungwal, J., Chiu, J., Paris, R., *et al.* (2009). Vaccination with ALVAC and AIDSVAX to prevent HIV-1 infection in Thailand. *N. Engl. J. Med.* 361, 2209-2220. doi:10.1056/NEJMoa0908492.

Rhee, S.-Y., and Shafer, R. W. (2018). Geographically-stratified HIV-1 group M pol subtype and circulating recombinant form sequences. *Sci. data* 5, 180148. doi:10.1038/sdata.2018.148.

Riddell IV, J., Amico, K. R., and Mayer, K. H. (2018). HIV Preexposure Prophylaxis: A Review. *JAMA* 319, 1261-1268. doi:10.1001/jama.2018.1917.

Robey, W. G., Arthur, L. O., Matthews, T. J., Langlois, A., Copeland, T. D., Lerche, N. W., *et al.* (1986). Prospect for prevention of human immunodeficiency virus infection: purified 120-kDa envelope glycoprotein induces neutralizing antibody. *Proc. Natl. Acad. Sci. U. S. A.* 83, 7023-7027. doi:10.1073/pnas.83.18.7023.

Robinson, H. L. (2002). New hope for an AIDS vaccine. *Nat. Rev. Immunol.* 2, 239-250. doi:10.1038/nri776.

Rodriguez-Fernandez, S., Almenara-Fuentes, L., Perna-Barrull, D., Barneda, B., and Vives-Pi, M. (2021). A century later, still fighting back: antigen-specific immunotherapies for type 1 diabetes. *Immunol. Cell Biol.* 99, 461-474. doi:10.1111/imcb.12439.

Rols, M.-P. (2008). Mechanism by which electroporation mediates DNA migration and entry into cells and targeted tissues. *Methods Mol. Biol.* 423, 19-33. doi:10.1007/978-1-59745-194-9_2.

Rosás-Umbert, M., Llano, A., Bellido, R., Olvera, A., Ruiz-Riol, M., Rocafort, M., *et al.* (2019). Mechanisms of Abrupt Loss of Virus Control in a Cohort of Previous HIV Controllers. *J. Virol.* 93. doi:10.1128/JVI.01436-18.

Ross, T. M., Pereira, L. E., Luckay, A., McNicholl, J. M., García-Lerma, J. G., Heneine, W., *et al.* (2014). A Polyvalent Clade B Virus-Like Particle HIV Vaccine Combined with Partially Protective Oral Preexposure Prophylaxis Prevents Simian-Human Immunodeficiency Virus Infection in Macaques and Primes for Virus-Amplified Immunity. *AIDS Res. Hum. Retroviruses* 30, 1072-1081. doi:10.1089/aid.2014.0030.

Rusche, J. R., Lynn, D. L., Robert-Guroff, M., Langlois, A. J., Lyerly, H. K., Carson, H., *et al.* (1987). Humoral immune response to the entire human immunodeficiency virus envelope glycoprotein made in insect cells. *Proc. Natl. Acad. Sci. U. S. A.* 84, 6924-6928. doi:10.1073/pnas.84.19.6924.

Rusert, P., Kouyos, R. D., Kadelka, C., Ebner, H., Schanz, M., Huber, M., *et al.* (2016). Determinants of HIV-1 broadly neutralizing antibody induction. *Nat. Med.* 22, 1260-1267. doi:10.1038/nm.4187.

Russell, N. D., and Marovich, M. A. (2016). Pox-Protein Public Private Partnership program and upcoming HIV vaccine efficacy trials. *Curr. Opin. HIV AIDS* 11, 614-619. doi:10.1097/COH.0000000000000322.

Saag, M. S., Gandhi, R. T., Hoy, J. F., Landovitz, R. J., Thompson, M. A., Sax, P. E., *et al.* (2020). Antiretroviral Drugs for Treatment and Prevention of HIV Infection in Adults: 2020 Recommendations of the International Antiviral Society-USA Panel. *JAMA* 324, 1651-1669. doi:10.1001/jama.2020.17025.

Sabin, C. A., and Lundgren, J. D. (2013). The natural history of HIV infection. *Curr. Opin. HIV AIDS* 8, 311-317. doi:10.1097/COH.0b013e328361fa66.

Sadanand, S., Suscovich, T. J., and Alter, G. (2016). Broadly Neutralizing Antibodies

Against HIV: New Insights to Inform Vaccine Design. *Annu. Rev. Med.* 67, 185-200. doi:10.1146/annurev-med-091014-090749.

Sällberg, M., Frelin, L., Ahlén, G., and Sällberg-Chen, M. (2015). Electroporation for therapeutic DNA vaccination in patients. *Med. Microbiol. Immunol.* 204, 131-135. doi:10.1007/s00430-014-0384-8.

Sánchez-Palomino, S., Massanella, M., Carrillo, J., García, A., García, F., González, N., *et al.* (2011). A cell-to-cell HIV transfer assay identifies humoral responses with broad neutralization activity. *Vaccine* 29, 5250-5259. doi:10.1016/j.vaccine.2011.05.016.

Sanders, R. W., and Moore, J. P. (2021). Virus vaccines: proteins prefer prolines. *Cell Host Microbe* 29, 327-333. doi:10.1016/j.chom.2021.02.002.

Sanders, R. W., van Gils, M. J., Derking, R., Sok, D., Ketas, T. J., Burger, J. A., *et al.* (2015). HIV-1 VACCINES. HIV-1 neutralizing antibodies induced by native-like envelope trimers. *Science* 349, aac4223. doi:10.1126/science.aac4223.

Sanders, R. W., Vesanen, M., Schuelke, N., Master, A., Schiffner, L., Kalyanaraman, R., *et al.* (2002). Stabilization of the soluble, cleaved, trimeric form of the envelope glycoprotein complex of human immunodeficiency virus type 1. *J. Virol.* 76, 8875-8889. doi:10.1128/jvi.76.17.8875-8889.2002.

Sasso, E., D'Alise, A. M., Zambrano, N., Scarselli, E., Folgori, A., and Nicosia, A. (2020). New viral vectors for infectious diseases and cancer. *Semin. Immunol.* 50, 101430. doi:10.1016/j.smim.2020.101430.

Satkauskas, S., Bureau, M. F., Puc, M., Mahfoudi, A., Scherman, D., Miklavcic, D., *et al.* (2002). Mechanisms of *in vivo* DNA electrotransfer: respective contributions of cell electropermeabilization and DNA electrophoresis. *Mol. Ther.* 5, 133-140. doi:10.1006/mthe.2002.0526.

Sauter, D., and Kirchhoff, F. (2019). Key Viral Adaptations Preceding the AIDS Pandemic. *Cell Host Microbe* 25, 27-38. doi:10.1016/j.chom.2018.12.002.

Sauter, D., Schindler, M., Specht, A., Landford, W. N., Münch, J., Kim, K.-A., *et al.* (2009). Tetherin-driven adaptation of Vpu and Nef function and the evolution of pandemic and nonpandemic HIV-1 strains. *Cell Host Microbe* 6, 409-421. doi:10.1016/j.chom.2009.10.004.

Sauter, D., Specht, A., and Kirchhoff, F. (2010). Tetherin: holding on and letting go. *Cell* 141, 392-398. doi:10.1016/j.cell.2010.04.022.

Schaefer, R., Schmidt, H. A., Ravasi, G., Mozalevskis, A., Rewari, B. B., Lule, F., *et al.* (2021). Articles Adoption of guidelines on and use of oral pre-exposure prophylaxis : a global summary and forecasting study. *Lancet HIV* 3018, 1-9. doi:10.1016/S2352-3018(21)00127-2.

Schatz, D. G., Oettinger, M. A., and Baltimore, D. (1989). The V(D)J recombination activating gene, RAG-1. *Cell* 59, 1035-1048. doi:10.1016/0092-8674(89)90760-5.

Scheid, J. F., Mouquet, H., Feldhahn, N., Seaman, M. S., Velinzon, K., Pietzsch, J., *et al.* (2009). Broad diversity of neutralizing antibodies isolated from memory B cells in HIV-infected individuals. *Nature* 458, 636-640. doi:10.1038/nature07930.

Schild, G. C., and Stott, E. J. (1993). Where are we now with vaccines against AIDS? *BMJ* 306, 947-948. doi:10.1136/bmj.306.6883.947.

Sekaly, R.-P. (2008). The failed HIV Merck vaccine study: a step back or a launching point for future vaccine development? *J. Exp. Med.* 205, 7-12. doi:10.1084/jem.20072681.

Serra, P., and Santamaria, P. (2019). Antigen-specific therapeutic approaches for autoimmunity. *Nat. Biotechnol.* 37, 238-251. doi:10.1038/s41587-019-0015-4.

Shah, R. R., Hassett, K. J., and Brito, L. A. (2017). "Overview of Vaccine Adjuvants: Introduction, History, and Current Status BT - Vaccine Adjuvants: Methods and Protocols," in, ed. C. B. Fox (New York, NY: Springer New York), 1-13. doi:10.1007/978-1-4939-6445-1_1.

Sharp, P. M., and Hahn, B. H. (2008). AIDS: prehistory of HIV-1. *Nature* 455, 605-606. doi:10.1038/455605a.

Shehu-Xhilaga, M., Crowe, S. M., and Mak, J. (2001). Maintenance of the Gag/Gag-Pol ratio is important for human immunodeficiency virus type 1 RNA dimerization and viral infectivity. *J. Virol.* 75, 1834-1841. doi:10.1128/JVI.75.4.1834-1841.2001.

Shibata, R., Igarashi, T., Haigwood, N., Buckler-White, A., Ogert, R., Ross, W., *et al.* (1999). Neutralizing antibody directed against the HIV-1 envelope glycoprotein can completely block HIV-1/SIV chimeric virus infections of macaque monkeys. *Nat. Med.* 5, 204-210. doi:10.1038/5568.

Shibata, R., Sakai, H., Kiyomasu, T., Ishimoto, A., Hayami, M., and Adachi, A. (1990). Generation and characterization of infectious chimeric clones between human immunodeficiency virus type 1 and simian immunodeficiency virus from an African green monkey. *J. Virol.* 64, 5861-5868. doi:10.1128/jvi.64.12.5861-5868.1990.

Simek, M. D., Rida, W., Priddy, F. H., Pung, P., Carrow, E., Laufer, D. S., *et al.* (2009). Human immunodeficiency virus type 1 elite neutralizers: individuals with broad and potent neutralizing activity identified by using a high-throughput neutralization assay together with an analytical selection algorithm. *J. Virol.* 83, 7337-7348. doi:10.1128/JVI.00110-09.

Sliepen, K., Han, B. W., Bontjer, I., Mooij, P., Garces, F., Behrens, A.-J., *et al.* (2019). Structure and immunogenicity of a stabilized HIV-1 envelope trimer based on a group-M consensus sequence. *Nat. Commun.* 10, 2355. doi:10.1038/s41467-019-10262-5.

Sliepen, K., Ozorowski, G., Burger, J. A., van Montfort, T., Stunnenberg, M., LaBranche, C., *et al.* (2015). Presenting native-like HIV-1 envelope trimers on ferritin nanoparticles improves their immunogenicity. *Retrovirology* 12, 82. doi:10.1186/s12977-015-0210-4.

Smith, J. M., Rao Amara, R., Campbell, D., Xu, Y., Patel, M., Sharma, S., *et al.* (2004). DNA/MVA Vaccine for HIV Type 1: Effects of Codon-Optimization and the Expression of Aggregates or Virus-Like Particles on the Immunogenicity of the DNA Prime. *AIDS Res. Hum. Retroviruses* 20, 1335-1347. doi:10.1089/aid.2004.20.1335.

Sohail, M., Levitan, E. B., Rana, A. I., Heath, S. L., Rastegar, J., Kempf, M.-C., *et al.* (2020). Estimating the First 90 of the UNAIDS 90-90-90 Goal: A Review. *J. Int. Assoc. Provid. AIDS Care* 19, 2325958220919290. doi:10.1177/2325958220919290.

Stanfield, R. L., and Wilson, I. A. (2014). Antibody Structure. *Microbiol. Spectr.* 2. doi:10.1128/microbiolspec.AID-0012-2013.

Stano, A., Leaman, D. P., Kim, A. S., Zhang, L., Autin, L., Ingale, J., *et al.* (2017). Dense Array of Spikes on HIV-1 Virion Particles. *J. Virol.* 91. doi:10.1128/JVI.00415-17.

Steichen, J. M., Lin, Y.-C., Havenar-Daughton, C., Pecetta, S., Ozorowski, G., Willis, J. R., *et al.* (2019). A generalized HIV vaccine design strategy for priming of broadly neutralizing antibody responses. *Science* 366. doi:10.1126/science.aax4380.

Steimer, K. S., Scandella, C. J., Skiles, P. V, and Haigwood, N. L. (1991). Neutralization of divergent HIV-1 isolates by conformation-dependent human antibodies to Gp120. *Science* 254, 105-108. doi:10.1126/science.1718036.

Steppert, P., Burgstaller, D., Klausberger, M., Berger, E., Aguilar, P. P., Schneider, T. A., *et al.* (2016). Purification of HIV-1 gag virus-like particles and separation of other extracellular particles. *J. Chromatogr. A* 1455, 93-101. doi:10.1016/j.chroma.2016.05.053.

Storcksdieck genannt Bonsmann, M., Niezold, T., Hannaman, D., Überla, K., and Tenbusch, M. (2016). The improved antibody response against HIV-1 after a vaccination based on intrastructural help is complemented by functional CD8+ T cell responses. *Vaccine* 34, 1744-1751. doi:10.1016/j.vaccine.2016.02.059.

Subbaraman, H., Schanz, M., and Trkola, A. (2018). Broadly neutralizing antibodies: What is needed to move from a rare event in HIV-1 infection to vaccine efficacy? *Retrovirology* 15, 52. doi:10.1186/s12977-018-0433-2.

Sun, X., Zhang, H., Xu, S., Shi, L., Dong, J., Gao, D., *et al.* (2017). Membrane-anchored CCL20 augments HIV Env-specific mucosal immune responses. *Virol. J.* 14, 163. doi:10.1186/s12985-017-0831-4.

Sundaramurthi, J. C., Ashokkumar, M., Swaminathan, S., and Hanna, L. E. (2017). HLA based selection of epitopes offers a potential window of opportunity for vaccine design against HIV. *Vaccine* 35, 5568-5575. doi:10.1016/j.vaccine.2017.08.070.

Sundquist, W. I., and Kräusslich, H.-G. (2012). HIV-1 assembly, budding, and maturation. *Cold Spring Harb. Perspect. Med.* 2, a006924. doi:10.1101/cshperspect.a006924.

Tebit, D. M., and Arts, E. J. (2011). Tracking a century of global expansion and evolution of HIV to drive understanding and to combat disease. *Lancet Infect. Dis.* 11, 45-56. doi:10.1016/S1473-3099(10)70186-9.

Thalhauser, S., Peterhoff, D., Wagner, R., and Breunig, M. (2020). Critical design criteria for engineering a nanoparticulate HIV-1 vaccine. *J. Control. Release* 317, 322-335. doi:10.1016/j.jconrel.2019.11.035.

Tohidi, F., Sadat, S. M., Bolhassani, A., Yaghobi, R., and Larijani, M. S. (2019). Induction of a Robust Humoral Response using HIV-1 VLP(MPER-V3) as a Novel Candidate Vaccine in BALB/c Mice. *Curr. HIV Res.* 17, 33-41. doi:10.2174/1570162X17666190306124218.

Tokatlian, T., Kulp, D. W., Mutafyan, A. A., Jones, C. A., Menis, S., Georgeson, E., *et al.* (2018). Enhancing Humoral Responses Against HIV Envelope Trimers via Nanoparticle Delivery with Stabilized Synthetic Liposomes. *Sci. Rep.* 8, 16527. doi:10.1038/s41598-018-34853-2.

Toukam, D. K., Tenbusch, M., Stang, A., Temchura, V., Storcksdieck genannt Bons-

mann, M., Grewe, B., *et al.* (2012). Targeting antibody responses to the membrane proximal external region of the envelope glycoprotein of human immunodeficiency virus. *PLoS One* 7, 1-10. doi:10.1371/journal.pone.0038068.

Truong, C., Brand, D., Mallet, F., Roingeard, P., Brunet, S., and Barin, F. (1996). Assembly and Immunogenicity of Chimeric Gag-Env Proteins Derived from the Human Immunodeficiency Virus Type 1. *AIDS Res. Hum. Retroviruses* 12, 291-301. doi:10.1089/aid.1996.12.291.

UNAIDS (2021). Fact sheet - Latest global and regional statistics on the status of the AIDS epidemic. Available at: https://www.unaids.org/en/resources/documents/2021/UNAIDS_FactSheet.

Valenzuela, P., Medina, A., Rutter, W. J., Ammerer, G., and Hall, B. D. (1982). Synthesis and assembly of hepatitis B virus surface antigen particles in yeast. *Nature* 298, 347-350. doi:10.1038/298347a0.

Vanderslott, S., Dadonaite, B., Roser, M. (2013). Vaccination. *Published online at OurWorldInData.org.* Retrieved from: 'https://ourworldindata.org/vaccination'

Van der Sluis, R. M., Kumar, N. A., Pascoe, R. D., Zerbato, J. M., Evans, V. A., Dantanarayana, A. I., *et al.* (2020). Combination Immune Checkpoint Blockade to Reverse HIV Latency. *J. Immunol.* 204, 1242-1254. doi:10.4049/jimmunol.1901191.

Van Heuverswyn, F., Li, Y., Bailes, E., Neel, C., Lafay, B., Keele, B. F., *et al.* (2007). Genetic diversity and phylogeographic clustering of SIVcpzPtt in wild chimpanzees in Cameroon. *Virology* 368, 155-171. doi:10.1016/j.virol.2007.06.018.

Verkoczy, L., Chen, Y., Bouton-Verville, H., Zhang, J., Diaz, M., Hutchinson, J., *et al.* (2011). Rescue of HIV-1 broad neutralizing antibody-expressing B cells in 2F5 VH x VL knockin mice reveals multiple tolerance controls. *J. Immunol.* 187, 3785-3797. doi:10.4049/jimmunol.1101633.

Verkoczy, L., Chen, Y., Zhang, J., Bouton-Verville, H., Newman, A., Lockwood, B., *et al.* (2013). Induction of HIV-1 broad neutralizing antibodies in 2F5 knock-in mice: selection against membrane proximal external region-associated autoreactivity limits T-dependent responses. *J. Immunol.* 191, 2538-2550. doi:10.4049/jimmunol.1300971.

Viant, C., Weymar, G. H. J., Escolano, A., Chen, S., Hartweger, H., Cipolla, M., *et al.* (2020). Antibody Affinity Shapes the Choice between Memory and Germinal Center B Cell Fates. *Cell* 183, 1298-1311.e11. doi:10.1016/j.cell.2020.09.063.

Victora, G. D., and Nussenzweig, M. C. (2012). Germinal Centers. *Annu. Rev. Immunol.* 30, 429-457. doi:10.1146/annurev-immunol-020711-075032.

Vidarsson, G., Dekkers, G., and Rispens, T. (2014). IgG subclasses and allotypes: from structure to effector functions. *Front. Immunol.* 5, 520. doi:10.3389/fimmu.2014.00520.

Vidya Vijayan, K. K., Karthigeyan, K. P., Tripathi, S. P., and Hanna, L. E. (2017). Pathophysiology of CD4+ T-Cell Depletion in HIV-1 and HIV-2 Infections. *Front. Immunol.* 8, 580. doi:10.3389/fimmu.2017.00580.

Visseaux, B., Damond, F., Matheron, S., Descamps, D., and Charpentier, C. (2016). HIV-2 molecular epidemiology. *Infect. Genet. Evol. J. Mol. Epidemiol. Evol. Genet. Infect. Dis.* 46, 233-240. doi:10.1016/j.meegid.2016.08.010.

Vivier, E., Nunès, J. A., and Vély, F. (2004). Natural Killer Cell Signaling Pathways. *Science* 306, 1517-1519. doi:10.1126/science.1103478.

Vos, Q., Lees, A., Wu, Z. Q., Snapper, C. M., and Mond, J. J. (2000). B-cell activation by T-cell-independent type 2 antigens as an integral part of the humoral immune response to pathogenic microorganisms. *Immunol. Rev.* 176, 154-170. doi:10.1034/j.1600-065x.2000.00607.x.

Vzorov, A. N., Wang, L., Chen, J., Wang, B.-Z., and Compans, R. W. (2016). Effects of modification of the HIV-1 Env cytoplasmic tail on immunogenicity of VLP vaccines. *Virology* 489, 141-150. doi:10.1016/j.virol.2015.09.015.

Wabl, M., and Steinberg, C. (1996). Affinity maturation and class switching. *Curr. Opin. Immunol.* 8, 89-92. doi:10.1016/s0952-7915(96)80110-5.

Wagner, R., Deml, L., Notka, F., Wolf, H., Schirmbeck, R., Reimann, J., *et al.* (1996). Safety and Immunogenicity of Recombinant Human Immunodeficiency Virus-Like Particles in Rodents and Rhesus Macaques. *Intervirology* 39, 93-103. doi:10.1159/000150480.

Wagner, R., Teeuwsen, V. J. P., Deml, L., Notka, F., Haaksma, A. G. M., Jhagjhoorsingh, S. S., *et al.* (1998). Cytotoxic T Cells and Neutralizing Antibodies Induced in Rhesus Monkeys by Virus-like Particle HIV Vaccines in the Absence of Protection from SHIV Infection. *Virology* 245, 65-74. doi:10.1006/viro.1998.9104.

Walker, L. M., Huber, M., Doores, K. J., Falkowska, E., Pejchal, R., Julien, J.-P., *et al.* (2011). Broad neutralization coverage of HIV by multiple highly potent antibodies. *Nature* 477, 466-470. doi:10.1038/nature10373.

Wandeler, G., Johnson, L. F., and Egger, M. (2016). Trends in life expectancy of HIV-positive adults on antiretroviral therapy across the globe: comparisons with general population. *Curr. Opin. HIV AIDS* 11, 492-500. doi:10.1097/COH.0000000000000298.

Wang, B.-Z., Liu, W., Kang, S.-M., Alam, M., Huang, C., Ye, L., *et al.* (2007). Incorporation of high levels of chimeric human immunodeficiency virus envelope glycoproteins into virus-like particles. *J. Virol.* 81, 10869-10878. doi:10.1128/JVI.00542-07.

Wang, J., Saffold, S., Cao, X., Krauss, J., and Chen, W. (1998). Eliciting T Cell Immunity Against Poorly Immunogenic Tumors by Immunization with Dendritic Cell-Tumor Fusion Vaccines. *J. Immunol.* 161, 5516-5524.

Wang, N., Chen, M., and Wang, T. (2019). Liposomes used as a vaccine adjuvant-delivery system: From basics to clinical immunization. *J. Control. Release* 303, 130-150. doi:10.1016/j.jconrel.2019.04.025.

Wang, Q., and Zhang, L. (2020). Broadly neutralizing antibodies and vaccine design against HIV-1 infection. *Front. Med.* 14, 30-42. doi:10.1007/s11684-019-0721-9.

Ward, A. B., and Wilson, I. A. (2017). The HIV-1 envelope glycoprotein structure: nailing down a moving target. *Immunol. Rev.* 275, 21-32. doi:10.1111/imr.12507.

Watanabe, H., Numata, K., Ito, T., Takagi, K., and Matsukawa, A. (2004). Innate immune response in Th1- and Th2-dominant mouse strains. *Shock* 22, 460-466. doi:10.1097/01.shk.0000142249.08135.e9.

Watzl, C., and Long, E. O. (2010). Signal Transduction During Activation and Inhibition of Natural Killer Cells. *Curr. Protoc. Immunol.* 90, 11.9B.1-11.9B.17. doi:10.1002/0471142735.im1109bs90.

Weichseldorfer, M., Heredia, A., Reitz, M., Bryant, J. L., and Latinovic, O. S. (2020). Use of Humanized Mouse Models for Studying HIV-1 Infection, Pathogenesis and Persistence. *J. AIDS HIV Treat.* 2, 23-29.

Weigel, T., Solomaier, T., Peuker, A., Pathapati, T., Wolff, M. W., and Reichl, U. (2014). A flow-through chromatography process for influenza A and B virus purification. *J. Virol. Methods* 207, 45-53. doi:10.1016/j.jviromet.2014.06.019.

West, A. P. J., Scharf, L., Scheid, J. F., Klein, F., Bjorkman, P. J., and Nussenzweig, M. C. (2014). Structural insights on the role of antibodies in HIV-1 vaccine and therapy. *Cell* 156, 633-648. doi:10.1016/j.cell.2014.01.052.

Whitaker, N., Hickey, J. M., Kaur, K., Xiong, J., Sawant, N., Cupo, A., *et al.* (2019). Developability Assessment of Physicochemical Properties and Stability Profiles of HIV-1 BG505 SOSIP.664 and BG505 SOSIP.v4.1-GT1.1 gp140 Envelope Glycoprotein Trimers as Candidate Vaccine Antigens. *J. Pharm. Sci.* 108, 2264-2277. doi:10.1016/j.xphs.2019.01.033.

Wibmer, C. K., Moore, P. L., and Morris, L. (2015). HIV broadly neutralizing antibody targets. *Curr. Opin. HIV AIDS* 10, 135-143. doi:10.1097/COH.0000000000000153.

Worobey, M., Gemmel, M., Teuwen, D. E., Haselkorn, T., Kunstman, K., Bunce, M., *et al.* (2008). Direct evidence of extensive diversity of HIV-1 in Kinshasa by 1960. *Nature* 455, 661-664. doi:10.1038/nature07390.

Wren, L., and Kent, S. J. (2011). HIV Vaccine efficacy trial: Glimmers of hope and the potential role of antibody-dependent cellular cytotoxicity. *Hum. Vaccin.* 7, 466-473. doi:10.4161/hv.7.4.14123.

Wu, X., Yang, Z.-Y., Li, Y., Hogerkorp, C.-M., Schief, W. R., Seaman, M. S., *et al.* (2010). Rational design of envelope identifies broadly neutralizing human monoclonal antibodies to HIV-1. *Science* 329, 856-861. doi:10.1126/science.1187659.

Xiao, P., Dienger-Stambaugh, K., Chen, X., Wei, H., Phan, S., Beavis, A. C., *et al.* (2021). Parainfluenza Virus 5 Priming Followed by SIV/HIV Virus-Like-Particle Boosting Induces Potent and Durable Immune Responses in Nonhuman Primates. *Front. Immunol.* 12, 162. doi:10.3389/fimmu.2021.623996.

Xu, L., Pegu, A., Rao, E., Doria-Rose, N., Beninga, J., McKee, K., *et al.* (2017). Trispecific broadly neutralizing HIV antibodies mediate potent SHIV protection in macaques. *Science* 358, 85-90. doi:10.1126/science.aan8630.

Yang, L., Song, Y., Li, X., Huang X., Liu, J., Ding H., *et al.* (2012). HIV-1 Virus-Like Particles Produced by Stably Transfected Drosophila S2 Cells: a Desirable Vaccine Component. *J. Virol.* 86, 7662-7676. doi:10.1128/JVI.07164-11.

Yang, B., Jeang, J., Yang, A., Wu, T. C., and Hung, C.-F. (2014). DNA vaccine for cancer immunotherapy. *Hum. Vaccin. Immunother.* 10, 3153-3164. doi:10.4161/21645515.2014.980686.

Ye, L., Wen, Z., Dong, K., Wang, X., Bu, Z., Zhang, H., *et al.* (2011). Induction of HIV Neutralizing Antibodies against the MPER of the HIV Envelope Protein by HA/

gp41 Chimeric Protein-Based DNA and VLP Vaccines. *PLoS One* 6, e14813. doi:10.1371/journal.pone.0014813.

Yoshimura, K. (2017). Current status of HIV/AIDS in the ART era. *J. Infect. Chemother. Off. J. Japan Soc. Chemother.* 23, 12-16. doi:10.1016/j.jiac.2016.10.002.

Zhao, F., Joyce, C., Burns, A., Nogal, B., Cottrell, C. A., Ramos, A., *et al.* (2020). Mapping Neutralizing Antibody Epitope Specificities to an HIV Env Trimer in Immunized and in Infected Rhesus Macaques. *Cell Rep.* 32, 108122. doi:10.1016/j.celrep.2020.108122.

Zhou, T., Doria-Rose, N. A., Cheng, C., Stewart-Jones, G. B. E., Chuang, G.-Y., Chambers, M., *et al.* (2017). Quantification of the Impact of the HIV-1-Glycan Shield on Antibody Elicitation. *Cell Rep.* 19, 719-732. doi:10.1016/j.celrep.2017.04.013.

Zolla-Pazner, S., Michael, N. L., and Kim, J. H. (2021). A tale of four studies: HIV vaccine immunogenicity and efficacy in clinical trials. *Lancet. HIV* 8, e449-e452. doi:10.1016/S2352-3018(21)00073-4.

Acknowledgements

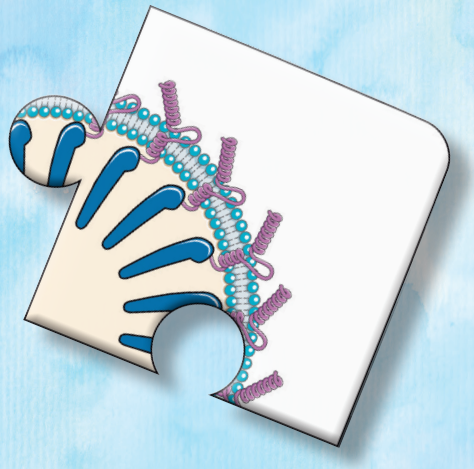

"In every job that must be done, there is an element of fun. You find the fun and snap! The job's a game. […] Just **a spoonful of sugar helps the medicine go down** in a most delightful way!". Un dels avenços cientificomèdics més importants del segle xx va servir d'inspiració per aquesta cançó de la pel·lícula "Mary Poppins": la vacuna oral de Sabin, la qual s'administrava als nens amb un terròs de sucre. Tal i com diu la cançó, tot treball té alguna cosa divertida per fer-lo passar millor, i en el meu cas, tots els que m'heu acompanyat en el trajecte heu estat aquesta "mica de sucre".

Primer de tot, gràcies infinites a en **Julià** i en **Jorge**, per haver-me donat l'oportunitat i el privilegi de formar part d'aquest gran equip que és IrsiCaixa, i de treballar en un projecte que no ha estat senzill però del que em sento molt orgullós d'haver-hi participat. I no només estic agraït per l'oportunitat i la confiança, sinó també per totes les eines a nivell científic que m'heu anat facilitant al llarg del camí i de tot el coneixement que m'heu transmès, juntament amb la passió per la recerca, que és sens dubte el títol més gran que m'enduc d'aquests 5 anys.

Aquest projecte no hauria avançat com ho ha fet sense el suport i la col·laboració d'un gran equip i que cada dia es va fent més gran, que és la família de VIC/AJ/IgG. A tota la gent del(s) grup(s) i a tots els que en algun moment hi heu passat, gràcies pel suport. A en **Luís**, per supervisar els meus primers baby steps a p3 i a ensenyar-me a que els hibridomes no se'm quedessin "moñecos". A la **Sílvia M** per totes les tècniques i tot el suport continu. A la **Marisa**, per resoldre incansablement la infinitat de dubtes que m'han anat sorgint al llarg del camí, sobretot al "taller de MARISAs". A en **Víctor U.**, per aportar l'anàlisi crítica i realista dels resultats, sempre acompanyat d'un bon cafè. A **Edwards**, máster Neutras, gracias por compartir horas de cabina en p3 y a enseñarme todos los intríngulis de las neutralizaciones. A la **Carmen**, que amb la seva arribada el "Team VLPs" va fer un salt endavant. A la **Raquel**, gràcies pel suport i pels punts de vista i comentaris sense filtre que subratllaven a cada pas el caràcter més humà de la ciència. Merci beaucoup à **Ben**, ta tutelle et ton éxpérience m'ont permis de voir l'un des meilleurs côtés de la science. Tu êtes un modèle à suivre, pas juste

dans mai aussi dehors le laboratoire. Honestly, a *million thanks, Ben*! A l'**Ana,** que va voltar el món i va tornar al Born, gràcies per tota l'ajuda i en especial amb els ELISpots. A en **Carlos**, ex-VIC, gracias por los ratos en ELISAs y los torreznos "pick-me up". A la **Montse**, que vam començar i acabem alhora el doctorat, hem sobreviscut. També gràcies a l'**Isma**. A en **Pau** per ajudar-me a copsar la complexitat de les electroporacions i optimitzar un protocol bàsic per aquest treball. A **Laura** y a **Silvia P.** de La Laguna. A la **Lucía P**. A l'**Erola,** també, per compartir els seus punts de vista i l'experiència americana. A la **Carla**, perquè des de que ens vam conèixer compartint escenari fins ara compartint laboratori em vas demostrar realment què és l'esperit de superació i quina és la raó per la qual hem de remar tots junts per tirar això endavant, moltes gràcies. A l'**Anna**, perquè espero que la feina que li deixo entre mans li sigui tan enriquidora com ho ha estat per mi. També als AlbaJunos, gràcies a en **Víctor C.**, Alba gu bràth ;). A la **Cris L.**, també. I a l'*isleña* **Cris V**. Als globetrotters *IrsiVoley* i *IrsiRaners* AlbaJunos, que sempre esteu disposats a entrar a tots els *fregaos*: **Ester A.**, il·lustre santandreuenca, gràcies per ensenyar-me a posar ordre al caos (una mica) i en **Francesc** per aportar sempre la seva experiència i inestimable punt de vista en qualsevol protocol o discussió i ajudar-me a sortir del pou dels ADCCs.

Moltes gràcies a la gent de VITI, **Ceci**, **Eli Ga**, **Jordi**, **Eli Go** i la *IrsiVoley* **Sònia** per aguantar-me a tot arreu on coincidíem (que realment és a tot arreu): a mòduls esquena contra esquena, a p3 robant-vos temps de cabina, al laboratori de bacteris, a NCB3 del CMCiB i un llarg etcètera.

A la gent de GREC, moltes gràcies a tots. **Xavi**, **Mª Carmen P.**, **María S.**, **Judith**, **Pat**, **Jakub**, **Cris G**, **Sara, Ángel,** la *irsiraner* **Sílvia B, Maria P., Maria F**. También a **Itziar** por cuidar de los citómetros y por lo tanto cuidarnos a todo Irsi, eskerrik asko. A la *isleña* **Mari**, que esperem que tornis aviat! También a **Xabi**, por todas las teorías científicas pero en especial por las teorías *geeks* sobre Marvel, DC, Star Wars... y lo que se venga.

A la gent de PISTA, muchas gracias **Nuria I.** por estar siempre dispuesta a aportar tu punto de vista y enriquecer cualquier debate. Gràcies **Dani** que, com un kolog, sempre acabes fent somriure a la gent (yahaha!). Gràcies **Jordana** i **Dàlia** per estar sempre predisposades a donar un cop de mà a NCB3 del CMCiB.

Al grup de VIRIEVAC, gràcies **Julia**, per sempre pensar com fomentar activitats per a pre-docs i en general a tot Can Ruti. Gràcies a la **Ruth**, la **Julieta**, l'**Òscar**, l'**Athina**, en **Dan**, l'**Eudald,** l'**Alba** la *IrsiVoley* **Esther** (el nucli dur de l'IrsiVoley) i l'*isleño* **Miguel**.

A la gent de Immunitat Cel·lular i Genètica de l'Hoste (aka Branders), thanks to **Christian** i també a la **Sandra**, la **Bea**, l'**Anuska**, la **Marta** i en **Pep**. Gràcies a l'*irsiraner* **Àlex**, pels entrenaments i les converses *on the run* (ja pots

anar entrenant que sinó els Gratanúvols del Montseny us passarem la mà per la cara als Perduts de Begur al proper Oncotrail). Gràcies a la **Míriam**, en **Luís**, la **Clara**, la **Tuixent**, la **Cris P**. A la *IrsiVoley* **Samandhy** por su alegría y por amenizar cualquier jornada en p3 con música. També a la **Bruna**, veïna del Montseny, que també tanca aquesta etapa aviat.

Al grup de ViHIT, gràcies a l'**Ester B.**, l'**Eva** i a l'*irsiraner* **Roger B.**, a qui li dedico una cançó d'un grup que sé que t'agrada: https://bit.ly/3AWOBHdh. Gràcies a la Hufflepuff **Edurne** (algun dia aprendràs que la millor casa de Hogwarts és Ravenclaw), thanks to **Ifeanyi**, also an *isleño* y a la ex-*isleña* **Lucía**, al gironí **Eudald** i a la cambrilenca **Maria P**. (del Cambrils de veritat). Gràcies a tots per aguantar-nos tantes hores al lab de Westerns, i deixar-nos que us robem puntes de pipetes per carregar gels, PBS, etc.

A la gent de GEM, moltíssimes gràcies a tots. Gràcies **Roger P.**, en especial per cuidar, junt amb tot el personal hospitalari, a la societat durant aquesta pandèmia. Gràcies també a en **Marc**, no només per l'esforç seqüenciant VIH i SARS-CoV-2, sinó també per ser el cervell darrere les Irsi-calçotades! Gràcies a la **Maria C.**, l'**Aleix**, la *isleña* **Mariona** per escoltar les penes a la "isla", l'**Alessandra**, en **Francesc C.**, la **Carmen F.** y **Carlos B.**, la **Muntsa** i la **Yolanda**.

Al jove grup de TRIA, els hi vull donar les gràcies a la **Marta M.**, la *irsiraner* **Maria N**. i la *isleña* **Mace**. A totes tres gràcies per estar sempre de bon humor i per tenir algun somriure o alguna broma entre tanta i tanta feina.

Al grup de Variabilitat Genètica i Fenotípica del VIH i del VHC, gràcies **Miguel Ángel**, a la ex-*isleña* **Ana J.** i a la *isleña* **Sandra**, sempre predisposada a qualsevol conversa i a ajudar amb el que sigui.

Al grup de NeoVaCan, gràcies **Leticia**, **Juan**, **Carla** i la *isleña* **Núria**. Merci per aguantar-me quan venia a ocupar la webcam d'en Ben i la Carmen per a reunions virtuals.

Al Living Lab, **Rosina**, **Marina** i **Aina**, moltes gràcies sempre per enfocar la ciència des d'un altra punt de vista, tan i tan necessari per la societat, i gràcies per la confiança comptant amb mi per xerrades de divulgació. Tocar de peus a terra i apropar-se a la societat és una obligació de tot científic.

Moltes gràcies a les Project Managers i *isleñas*, **Eli**, **Natàlia**, **Diana**, **Anna**, i en especial, **Chiara** i **Laura** (illenca per partida doble), que feu un treball dur i a vegades poc agraït però indispensable; sense vosaltres la isla no seria la isla.

Infinites gràcies a Comunicació, gràcies a les *isleñas* **Rita** i **Elena** i també a la **Júlia**. Mil gràcies per la confiança que m'heu donat i per fer una feina àrdua. Gràcies pels comentaris divertits i per les discussions, i per veure fins a quin punt és d'important trobar la paraula adequada per la situació corresponent, feu una gran feina!

Gràcies a la **Penélope**, la **Cris** i l'*irsiVoley* **Arnau** (per cert, has vist la peli *Luca*?). Gràcies per tenir sempre un bon dia a la nostra disposició i a ajudar-nos amb el que faci falta.

Gràcies al grup de Serveis, aka "chicas de muestras", l'ànima d'IrsiCaixa. Gràcies a l'**Eulàlia**, la **Rafi**, la **Luci**, la **Mireia**, la **Susana** (santa paciència que tens amb tots nosaltres). També en especial a la **Cris R.** i la **Teresa** pels milers de mostres que vau seqüenciar per aquest projecte. Moltíssimes gràcies a la **Lidia**, que a part de coordinar un grup, té la responsabilitat de fer funcionar IrsiCaixa com un rellotge i que, junt amb la Ceci, creeu un càlid ambient al lab de bacteris ;).

També agrair la feinada a la **Lourdes** i sobretot a en **Bonaventura**, ja que crear i sobretot dirigir i fomentar un centre pioner com IrsiCaixa té tot el mèrit del món, i sense els quals aquests agraïments s'acabarien molt abans.

Menció especial a tots els isleños de la "**Illa**", amb qui fa dos anys que comparteixo oficina. Ningú a part de vosaltres és capaç d'idear un "calaix de la felicitat" o d'inventar milers de sinònims o dir en diferents idiomes "tanqueu la p... porta!". Només me'n penedeixo d'haver estat tan a dins del lab de p3 per no compartir més temps amb vosaltres! També "shoutout" especial a **Irsivoley** i al torn de matí dels **Irsiraners** (perquè el torn de tarda mai ha funcionat), per tots els moments extra-curriculars que m'heu regalat.

A tota el personal de **FLS** i **infeccioses**, que formeu part d'aquesta gran família en la que hem compartit feina, espai i moments. Els vasos comunicants entre tots són els que han permès crear un entorn veritablement únic i especial.

Un fort agraïment també a la gent de l'IGTP, des del servei de citometria (**Marco** i **Gerard**) per ajudar-me amb el sorting i ensenyar-me a copsar la versatilitat de la citometria de flux, i el servei de genòmica (**Pilar**). Gràcies sobretot al departament d'Immuno (**Irma**, **Laia**, **David**, **Adri**, **Lidia**, **Mª Jose**, **Eva**) i en especial a la **Marta** per creure en mi i apropar-me a IrsiCaixa.

Moltes gràcies al personal del CMCiB, des de la seva fase com a SE a les catacumbes de l'Hospital (**Yaiza**, **Rosa**, **Jorge**, **Lino**), fins a la fase actual (**Sara**, **David**, **Patricia**, **Jennifer**, **Vego**, **Montse**) al cim més alt de la serralada de Marina (o això sembla vist cada matí des d'IrsiCaixa abans de pujar). Gràcies a tots per la paciència i la facilitat per a trobar solucions, facilitant molt un treball molt complicat amb models animals que comporta molta responsabilitat.

Al grup de bioenginyeria de processos de la UAB, a la **Laura**, la **Sònia**, la **Maria Mercedes** i a en **Francesc Gòdia**, part també d'aquest gran projecte de les VLPs.

En aquest últim any i mig, amb la pandèmia del SARS-CoV-2 per desgràcia ha canviat moltes coses, també d'aquesta tesi. Per fortuna, però, ens ha donat la oportunitat d'envoltar-nos de gewnt dels quals he pogut aprendre molt. Gràcies

a la gent del CReSA (**Joaquim**, **Júlia**, **Jordi** i **Mónica**) i del BSC (**Víctor G.**, **Alba**, **Miguel** i **Alfonso**).

No em voldria oblidar tampoc dels Biomeds i B'n'Ds (**Xavi**, **Tiffany**, **Mireia**, **Marina**, **Manu**, **Fátima**, **Maite**) i sobretot en **Roger**, ara et toca a tu encarar aquest privilegi i malson d'escriure la tesi, danke schön! A la gent del grup de **Farmaco** de la UAB, als amics **d'Edinburgh** i a l'**Arnau L.**, la **Rosalía**. En especial gràcies a en **Narcís** amb qui hem compartit anys d'Uni i penes i alegries al voltant de la tesi, ànims en aquest esprint final! Tots vosaltres m'heu ajudat a veure la meva passió per la ciència i m'heu ajudat a pensar-hi i oblidar-ho (quan era necessari) a parts iguals.

Agrair també als amics de tota la vida del poble, l'**Arnau** i l'**Ester**, l'**Egea** i l'**Anna** i la petita **Mia**, en **Bernat**, en **Martínez**, en **Quico** i la **Lucía**, en **Pau**, en **Campde** i en **Molist**. Pels viatges, sopars, sortides i caminades. Perquè tornar d'un cap de setmana del poble després de veure-us em recarregava les piles per tota la setmana d'experiments.

Finalment, només em queda agrair des del més profund del cor a la meva família, pel suport incondicional, als meus pares **Jaume** i **Marina**, a la meva germana **Laura** i en **Joan** i la petita **Dana**, la iaia **Maria**. También a **Carmen** y **Vicente**, que sin él esta tesis luciría mucho menos. I sobretot a tu **Silvia RF**, per creure en mi i per estar al meu costat a les verdes i a les madures, i perquè el final d'aquesta tesi també significa el principi d'una nova etapa al teu costat.

A tots, gràcies per fer que d'aquesta etapa no només en surti millor científic, sinó també millor persona. I també a tu que has arribat fins a la última pàgina d'un projecte que ha durat 5 anys però que obre la porta a un ventall de possibilitats futures, només em queda dir: **Salut i ciència!!!**

Ferran Tarrés i Freixas

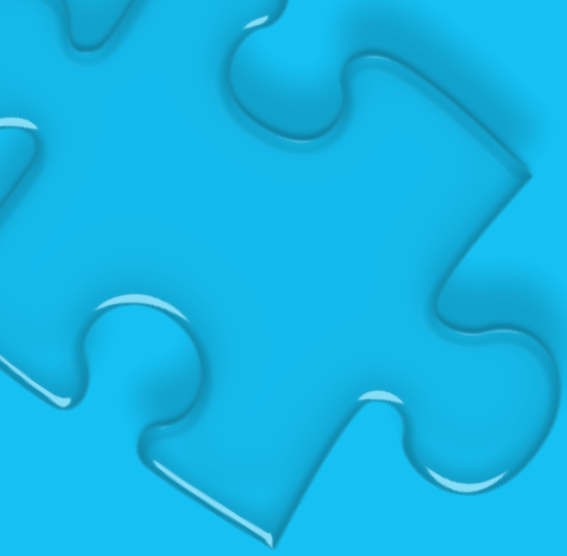

A preventive vaccine against the Human Immunodeficiency Virus (HIV-1) has eluded science and societies' efforts for nearly 40 years, and to date HIV-1 remains a chronic, non-curable infection. The identification of new vaccine platforms could prove key for tackling such an evasive virus as HIV-1. In this doctoral thesis project, our group develop a novel HIV-1 based virus-like particle (VLP) that mimics the structure of the virus and presents a high density of antigens that induce a robust and protective immune response. Furthermore, this vaccine platform can be easily adapted to express other relevant antigens on its surface, aiming at the generation of better fit vaccine strategies against HIV-1. Hopefully, this vaccine platform will show its potential, not only as a promising HIV-1 vaccine prototype, but also as a vehicle against other infectious agents and diseases.

IrsiCaixa
Institut de Recerca de la Sida

UAB
Universitat Autònoma de Barcelona